



SMART GREEN AND INTEGRATED TRANSPORT

Integrity improvement of rotorcraft main gear box



An Agency of the European Union



Disclaimer

This study has been carried out for the European Aviation Safety Agency by an external organization and expresses the opinion of the organization undertaking the study. It is provided for information purposes only and the views expressed in the study have not been adopted, endorsed or in any way approved by the European Aviation Safety Agency. Consequently it should not be relied upon as a statement, as any form of warranty, representation, undertaking, contractual, or other commitment binding in law upon the European Aviation Safety Agency.

Ownership of all copyright and other intellectual property rights in this material including any documentation, data and technical information, remains vested to the European Aviation Safety Agency. All logo, copyrights, trademarks, and registered trademarks that may be contained within are the property of their respective owners.

Reproduction of this study, in whole or in part, is permitted under the condition that the full body of this Disclaimer remains clearly and visibly affixed at all times with such reproduced part.

No part of this report may be reproduced and/or disclosed, in any form or by any means without the prior written permission of the owner.

REPORT NUMBER:	D1-1
REPORT CLASSIFICATION:	UNCLASSIFIED
DATE:	14 January 2022
KNOWLEDGE AREA(S):	Research, rotorcraft MGB, configuration and component design
DESCRIPTOR(S):	Potential weaknesses, single point of failure, failure flow analysis
CUSTOMER:	European Aviation Safety Agency
CONTRACT NUMBER:	EASA.2019.C15
OWNER:	European Aviation Safety Agency
DISTRIBUTION:	Limited
CLASSIFICATION OF TITLE:	UNCLASSIFIED
Author(s):	W. Riesen, S. Hilleke

APPROVED BY:	AUTHOR	REVIEWER	MANAGING DEPARTMENT
Robert Stürzer	Waldemar Riesen	Jörg Litzba	ZFL Drive Train Transmission

DATE: 14 January 2022

EVALUATE AND DEFINE ROTOR AND ROTOR DRIVE SYSTEM DESIGN
OPTIONS TO PREVENT SINGLE POINTS OF CATASTROPHIC FAILURE

Review of the state-of-the-art rotorcraft gearbox configurations and component designs

ZF Luftfahrttechnik GmbH

ZF Luftfahrttechnik GmbH is a worldwide company known for its helicopter transmission systems. With our EASA and FAA privileges we are active for design and development, manufacturing and maintenance of helicopter transmission systems and geared applications for fix wing aircrafts and engines. Our service activities are not only keeping transmission system components airworthy, also mission support for a broad range of customers are conducted. For nearly all helicopter manufacturers around the world, ZF Luftfahrttechnik GmbH designs and supplies worldwide turn-key solutions for gearbox and rotor test stands.

Flugplatzstrasse | 34379 Calden, Germany | + 49 5674 701 0 | + 49 5674 701 606 | GIFT-MGB.aviation@zf.com |
<https://www.zf.com/products/en/aviation/home/aviation.html>

SUMMARY

Problem area

The aim of this report is to evaluate state-of-the-art rotor and rotor drive system configurations as well as potential alternative configurations and to determine system architecture and individual component design means to prevent single point of catastrophic failure based on the contract between EASA and ZFL [2] according the EASA tender [1] based on the Horizon 2020 Work Program Societal Challenge 4, 'Smart, green and integrated transport'.

Description of work

The frame of stream 1 of the project will be achieved via analysis of potential weaknesses of several MGB architectures, their principal function (scheme of architecture) and their criticality in terms of single point of failure using failure flow diagrams.

Results and Application

Different applications were studied with regards to their weaknesses and criticality. By reviewing the described generic cases, the factors which contribute to designs experiencing breakage and/or cracking can be summarized by the following issues:

- Ejection of fragments from gear mesh not possible, which could further lead to additional damage
- Release of fragments and damaging of other gear stages by overrolling
- No sufficient support from e.g. bearing and hub of parts after breakage, which further contributes noises, high vibrations, and jamming due to deflection/movement of fragments/parts.
- Incorrect gear re-engaging due to loss of single tooth or multiple teeth leading to jamming of the gear or the loss of transmitting power
- Total wear of spline leading to loss of transmitting power to the main rotor or tail rotor
- Radial, circumferential or longitudinal cracks leading to a disconnect in the power transmission path or a jamming due to increased deflection or deformation of the components

As a result of the assessment, it was shown that circumferential and radial cracks or tooth breakages could lead to jamming or disconnection within the load path. Mainly for shafts, longitudinal cracks lead to a stiffness reduction rather than a disconnection or jamming and therefore, they do not lead to catastrophic events as often as circumferential or radial cracks. Longitudinal cracks at the rotor mast are an exception. It is also assumed, that a stiff bolted connection could reduce the risk of catastrophic failures due to radial cracks. Additionally, it is shown that tooth breakage does not automatically lead to a disconnection of load transmission but rather contributes to jamming if the broken parts cannot be ejected.

Nevertheless, there are many other cases, which could potentially lead to catastrophic events, which were not part of the evaluation of the failure flow diagrams as they are not part of the main transmission path from input stages to output stages of a MGB.

However, the given results will be used as a basis for the following D1-2 Report.

CONTENTS

SUMMARY	5
Problem area	5
Description of work	5
Results and Application	5
CONTENTS	6
ABBREVIATIONS	7
1. Introduction	8
2. Drive system configurations	9
2.1 Epicyclic architectures	13
2.2 Collector architectures	20
2.3 Summary	24
3. Failure mode and mechanism overview	27
3.1 General	27
3.2 Corrosion	27
3.3 Wear	30
3.4 Rolling contact fatigue	33
3.5 Permanent deformation	39
3.6 Fracture/Breakage/Cracking	43
3.7 Compilation of observed in-service damages	47
4. In-service and MRO experience.....	52
4.1 In-service experience	52
4.2 MRO experience	66
4.3 Windmill industry	68
5. Catastrophic failure modes on drive system configurations.....	70
5.1 General	70
5.2 Failure flow diagram and criticality analysis	71
5.3 Summary	80
6. Conclusion	102
7. References	104
Bibliography	106
Annex A Flow diagram of examples.....	107

ABBREVIATIONS

ACRONYM	DESCRIPTION
AAIB	Air Accidents Investigation Branch
ARIS	Anti-Resonant Isolated System
AGB	Auxiliary/Accessory Gearbox
AW	AgustaWestland
CHD	Case Hardness Depth
CS	Certification Specification
EASA	European Union Aviation Safety Agency
FAA	Federal Aviation Administration
H/C	Helicopter
HUMS	Health and usage monitoring systems
IGB	Intermediate Gearbox
IHUMS	Integrated health and usage monitoring systems
IR	Inner Race
LH	Left Hand
LOL	Loss of Lubrication
MBB	Messerschmitt-Bölkow-Blohm
MCP	Maximum Continuous Power
MGB	Main Gearbox
MR	Main Rotor
MRO	Maintenance, Repair and Overhaul
NDT	Non-Destructive Test
NOTAR	No Tail Rotor-System
PMA	Permanent magnet alternator
OEI	One Engine Inoperative
OR	Outer Race
RB	Rotor Brake
RH	Right Hand
RPM	Round Per Minute
SKF	Svenska Kugellagerfabrik
SPoCF	Single Point of Catastrophic Failure
SPoF	Single Point of Failure
SRB	Spherical Roller Bearing
TEMP	Temperature
TGB	Tail rotor Gearbox
TR	Tail Rotor
ZFL	ZF Luftfahrttechnik GmbH

1. Introduction

The aim of this report is to evaluate state-of-the-art rotor and rotor drive system configurations, describe typical failure mechanisms affecting these systems and evaluate the consequences of these based on the actual design characteristics of a number of existing designs. The objective is to then use the outcome of this activity to determine system architecture and individual component design means to prevent single point of catastrophic failure as described in the contract between EASA and ZFL [2] according the EASA tender [1] based on the Horizon 2020 Work Programme Societal Challenge 4, 'Smart, green and integrated transport'.

In the frame of stream 1 of the project, this will be achieved via analysis of the weaknesses of several MGB architectures, their principal function (scheme of architecture), and their criticality in terms of single point of failure using failure flow diagrams.

Subsequently, as part of the next steps of this stream of the project, proposals of alternative solutions will be made wherever possible, limiting the consequences of any failure mode resulting from the failure of single components of the rotor and rotor drive system to loss of drive, or at least minimizing the number of catastrophic failures.

As the first deliverable, this report (D1-1) contains the analysis of weaknesses of several MGB architectures, their principal function (scheme of architecture), and their criticality regarding single point of failure using failure flow analysis, and is subdivided into the following chapters.

- Chapter 2** provides an analysis of existing kinds of MGB architecture based on open sources
- Chapter 3** describes general failure modes and their mechanisms based on open sources, as well as experiences of ZFL and its partners within this project
- Chapter 4** considers experiences from service, maintenance, repair and overhaul, as well as summarized incidents based on open sources
- Chapter 5** provides generic analysis of existing catastrophic failure modes on main drive train configurations
- Chapter 6** gives a conclusion based on the analyzed failures

2. Drive system configurations

Several studies have been conducted to evaluate different configurations present in existing rotorcraft for splitting the reduction ratio across the various transmission components and achieving a design for maximum transmission reliability while fulfilling weight and configuration requirements. [11]

In conventional H/C (those with main and rear rotors), heavy helicopters typically require a higher rotor diameter to lift the H/C than do light H/Cs. As a result and due to the maximum speed that can be reached on blade extremities, heavy helicopters typically use a lower rotation speed than light helicopters. The reduction ratio required between engines and main rotors of heavy helicopters is then often higher than on light helicopters. The overall reduction could have a ratio up to ~100:1 to reduce the speed from the engine to the main rotor. This ratio is achieved using several stages of gearing (e.g. reduction stages, main gearbox). [11]

Normally there are at least four gearboxes in helicopters for the transmission of motion and power:

- Main gearbox (MGB)
- Auxiliary/Accessory gearbox (AGB)
- Intermediate gearbox (IGB); not applicable for Fenestron and Coaxial configurations
- Tail gearbox (TGB); not applicable for Coaxial and NOTAR configurations

As an example, Figure 1 shows the gearboxes of an advanced light helicopter. The MGB receives the motion from the engine and transfers it to the main rotor in order to rotate the main rotor blades. The speed from the engine is very high and with low torque, thus MGB increases the torque by reducing the speed, and simultaneously transmits the motion to the tail gearbox via the auxiliary and intermediate gearboxes, if existing. [4]

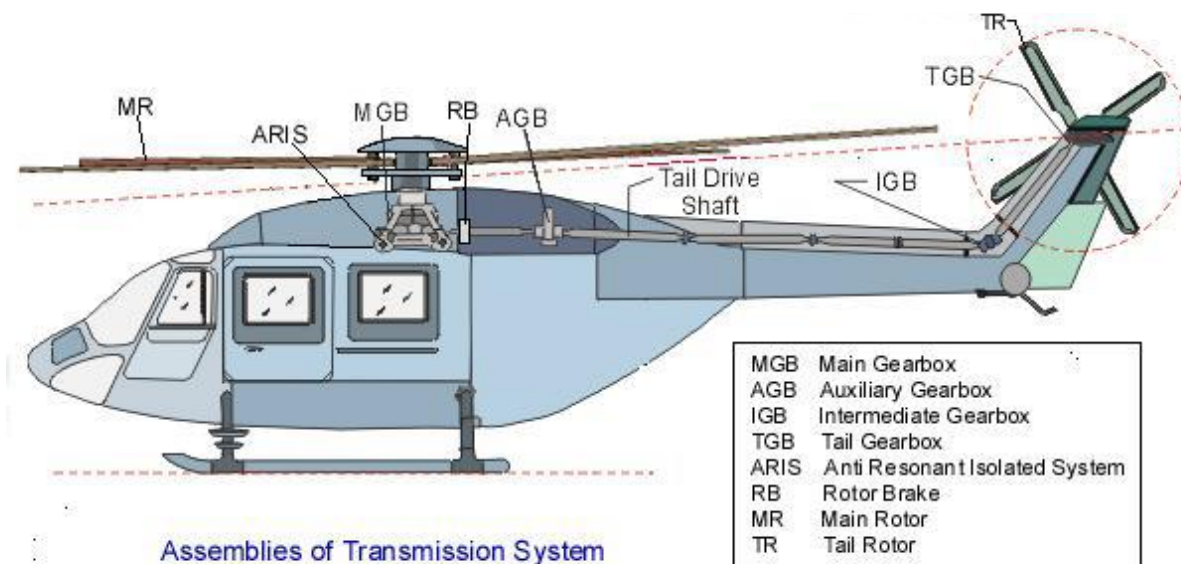


Figure 1: Gearboxes of an advanced light H/C [4]

This investigation shows first that there are two ways of transmitting the power of an engine to the main rotor using the MGB. On the one hand, the power will be transmitted by one or more input and intermediate stages, collected by a bull gear and further transmitted to the rotor mast (collector architecture). On the other hand, one or more epicyclic/planetary stages additionally reduce the ratio (epicyclic architecture).

In [12], two advanced geared transmission concepts are investigated. Firstly, a single engine configuration (1). Secondly, a conceptual sketch of a split torque transmission, which is a subgroup of collector architectures (2).

- 1) Four-gear planetary transmission exemplarily for an epicyclic gear train transmission: The concept in Figure 2 is a high contact-ratio four-gear planetary transmission for improved load capacity and longevity driven by a input stage, intermediate stage and a sun gear and transfers the loads to the rotor mast as well as the tail rotor. The high-contact ratio gears are expected to result in lower noise and reduced dynamic loads. The main bevel gear has been straddle mounted to improve deflection of the gear mounting, thereby improving load sharing in the gear mesh. The planetary ring gear has been cantilever-mounted to relieve problems inherent in the ring-gear-to-case-spline interface.

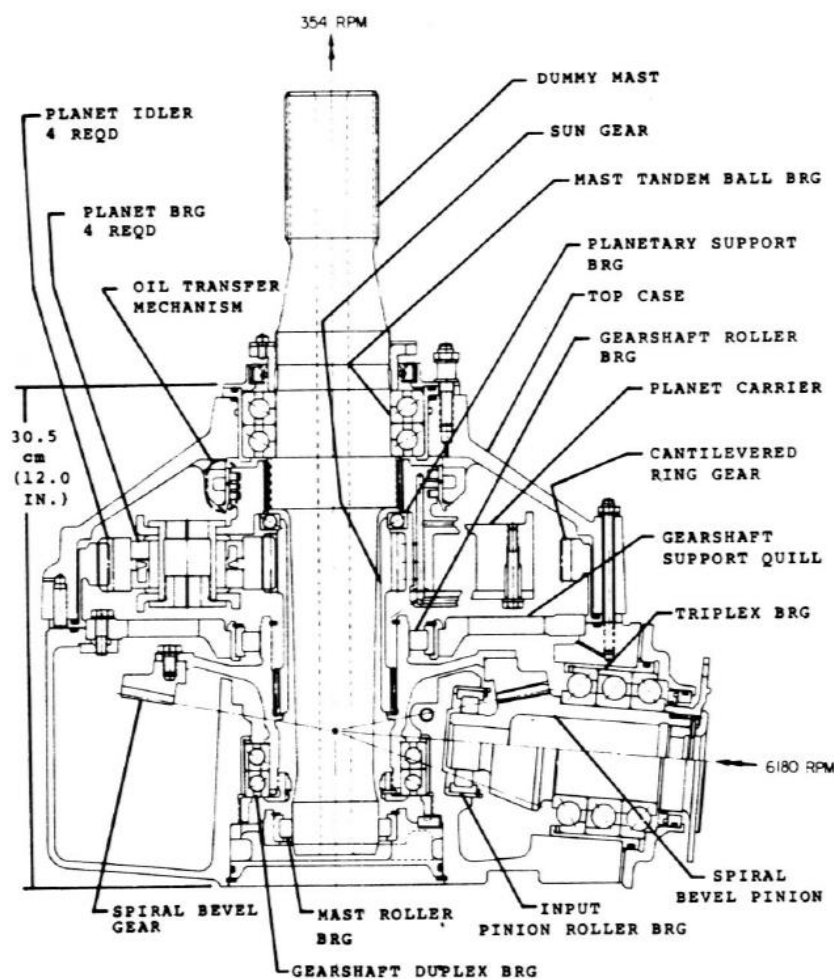


Figure 2: Advanced components transmission with ball bearings for Bell OH-58 MGB [12]

- 2) Split-torque transmission exemplarily for a collector architecture: A means of decreasing the weight-to-power ratio of a transmission or decreasing the unit stress of gear teeth is by load sharing through one or more stand alone or multiple power paths. The concept in Figure 3 is referred to as the split-torque transmission (multiple power path), which is a variant of a collector architecture with only one load path per engine.

Instead of a planetary-gear arrangement, the input power is split into two or more power paths and recombined in a bull gear to the output power (rotor) shaft. This concept appears to offer weight advantages over conventional planetary concepts without high-contact-ratio gearing. Incorporating high-contact-ratio gearing into the split torque concept is expected to further reduce transmission weight.

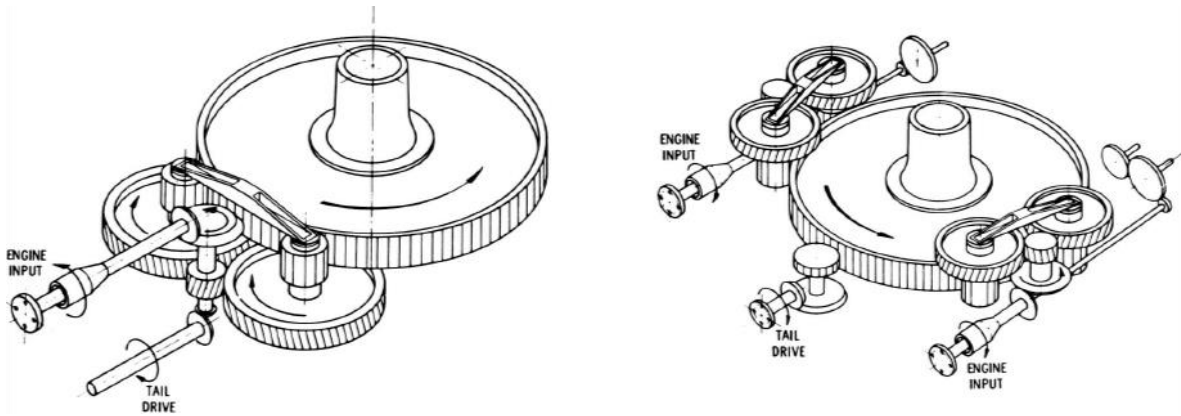


Figure 3: Conceptual sketch of a split torque transmission (left: single input; right: dual input) [12]

Table 1 shows some examples of the H/C configuration with illustration and MGB configuration. More detailed description of the main gearboxes considered in Table 1 is given in chapters 2.1 and 2.2.

Designation and MGB configuration	Illustration [23]
Airbus Helicopters H225 SuperPuma	
MGB: Epicyclic configuration	
AgustaWestland AW189 MGB: Epicyclic configuration	
Bell 212 MGB: Epicyclic configuration	
MBB BO 105 MGB: Epicyclic configuration	

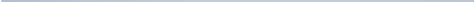
Designation and MGB configuration	Illustration [23]
Bell 525	
MGB: Epicyclic configuration	
Mil MI-24	
MGB: Epicyclic configuration	
Airbus Helicopters H-135	
MGB: Collector configuration	
TR: Fenestron	
Sikorsky CH-53K	
MGB: Collector configuration (split torque variant)	
Kawasaki BK117	
MGB: Collector configuration	
TR: Fenestron	
Mil MI-26	
MGB: Collector configuration (split torque variant)	
Coaxial configuration (e.g. Kamov Ka-226)	
MGB: Collector configuration (coaxial-rotor)	

Table 1: Overview of gearboxes in considered in this report

2.1 Epicyclic architectures

One configuration in current designs is the planetary gear train using one or more planetary gears powered by one to three engines. It provides high torque density in a lightweight and compact gear reduction configuration.

A possible configuration, common in older helicopter designs, involves a 2-stage planetary main gearbox where the sun gear of the first stage is the input and the carrier of the second stage is the output and transfers torque to the main rotor shaft. [5]

In the following, several example configurations are described:

Airbus Helicopters H225 SuperPuma gearbox and transmission [18], [19], [39]

Each engine power turbine is connected to the MGB via a high speed shaft. The high speed shaft runs inside a coupling tube, which is also the aft engine attachment.

The MGB consists of two main sections. The lower section, referred to as the main module, reduces the input shaft speed from the two engines. The second section is the epicyclic reduction gearbox module bolted on top of the main module (Figure 4). This reduces the rotational speed of the output from the main module to 265 [rpm] during cruise and 275 [rpm] when the airspeed is below 40 kt.

A conical housing made from aluminum is bolted on top of the epicyclic gearbox (Figure 4). A lift housing made from titanium is bolted on the top of the conical housing. The lift housing holds the lift bearing, the main rotor drive shaft, and the main rotor head.

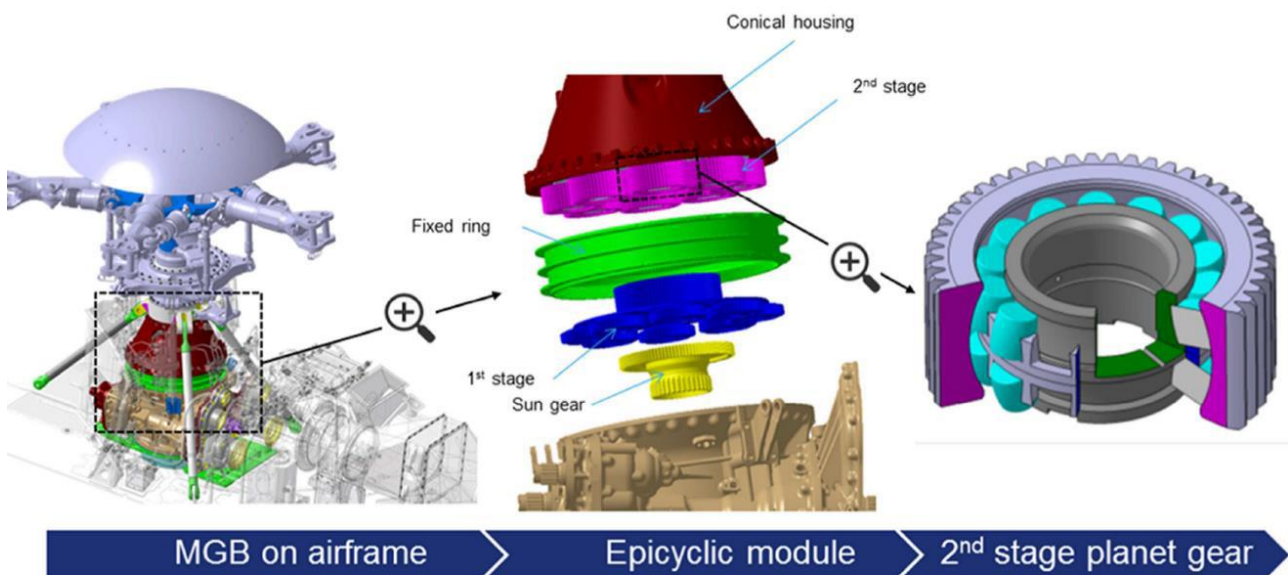


Figure 4: Illustration of the MGB installation, exploded view of epicyclic module and one second stage planet gear. Main module shown in light brown. Source: Airbus Helicopters [19]

Power output from both engines is transmitted to the main module of the MGB through the left and right reduction gearboxes, mounted on the front of the main module. These reduce the rotational speed of the input drive from 23,000 [rpm] to 8,011 [rpm]. The output from the left and right reduction gearboxes provides power to the left and right accessory modules respectively and is combined by the combiner gear within the main module (Figure 5). This combined drive provides power to the tail rotor drive shaft and the bevel gear. The bevel gear reduces the rotational speed of the input drive to 2,405 [rpm] and changes the combined input to the vertical plane to drive the epicyclic reduction gearbox module.

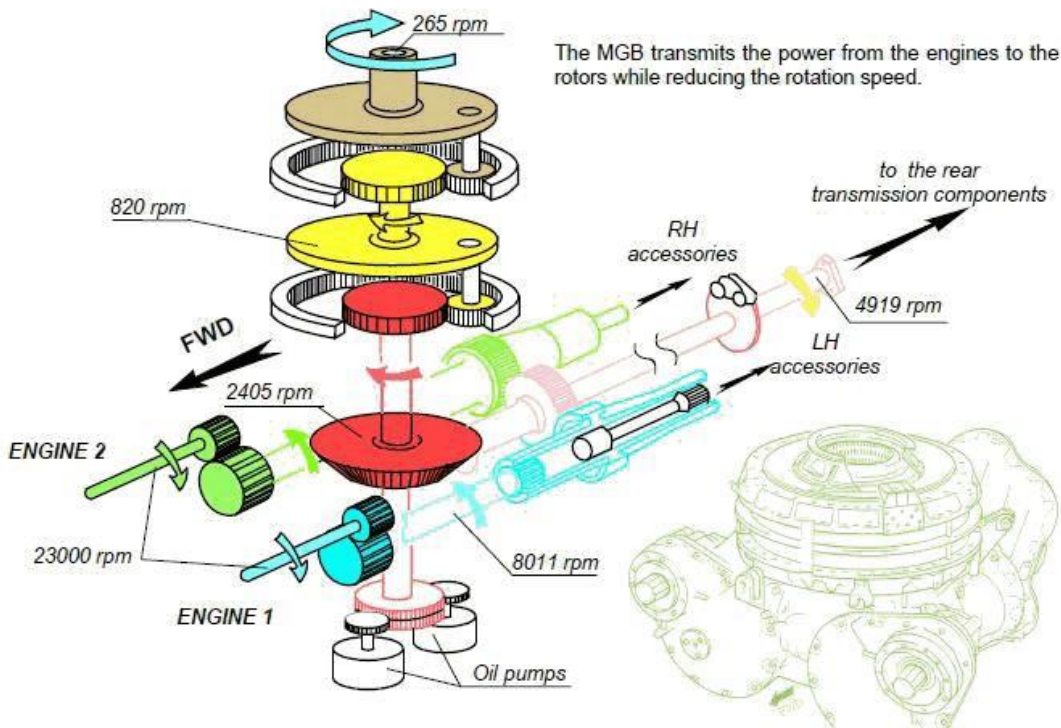


Figure 5: Main rotor gearbox dynamic components [19]

Drive from the main module is transmitted via the first stage sun gear (Figure 5). This drives eight first stage planet gears, contained by the epicyclic (fixed) ring gear and mounted on stub shafts on the first stage planet carrier (Figure 6). The upper section of the first stage planet carrier consists of the second stage sun gear. This drives eight second stage planet gears, contained by the same epicyclic ring gear and mounted on stub shafts on the second stage planet carrier, which then turns the main rotor drive shaft through a splined coupling.

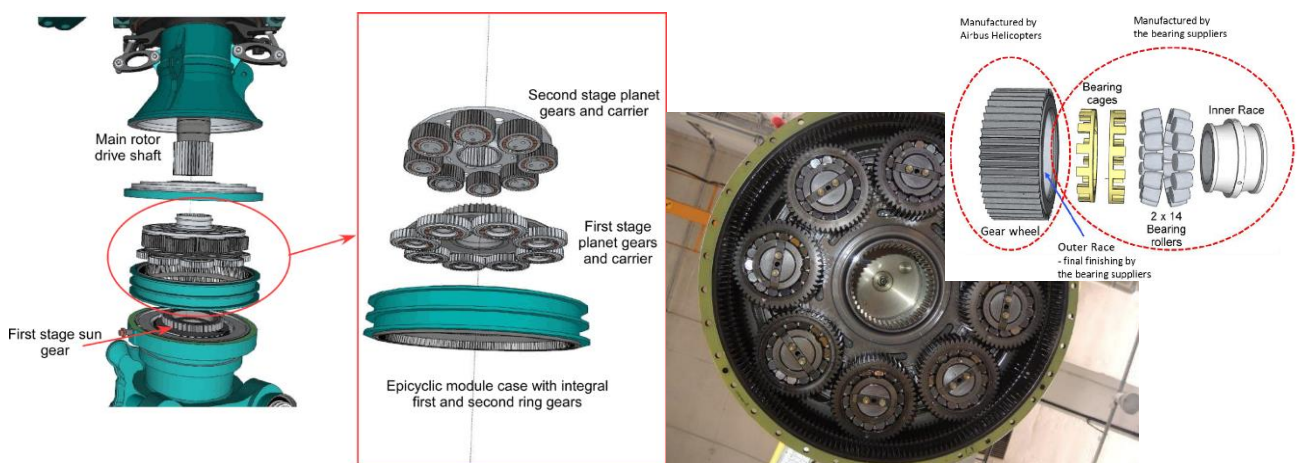


Figure 6: Layout of the epicyclic reduction gearbox and its second stage on the carrier inside the ring gear [18], [19]

AgustaWestland AW189 [20]

The MGB is a twin engine configuration gearbox. The input shafts run at about 21000 [rpm] and the MGB reduces the engine output speed to the main rotor speed (approximately 290 [rpm]) by means of three reduction stages: the first two stages are of the spiral bevel type, the third reduction stage is an epicyclic planetary stage (see Figure 11). Accessories are directly driven from the second stage collector gear.

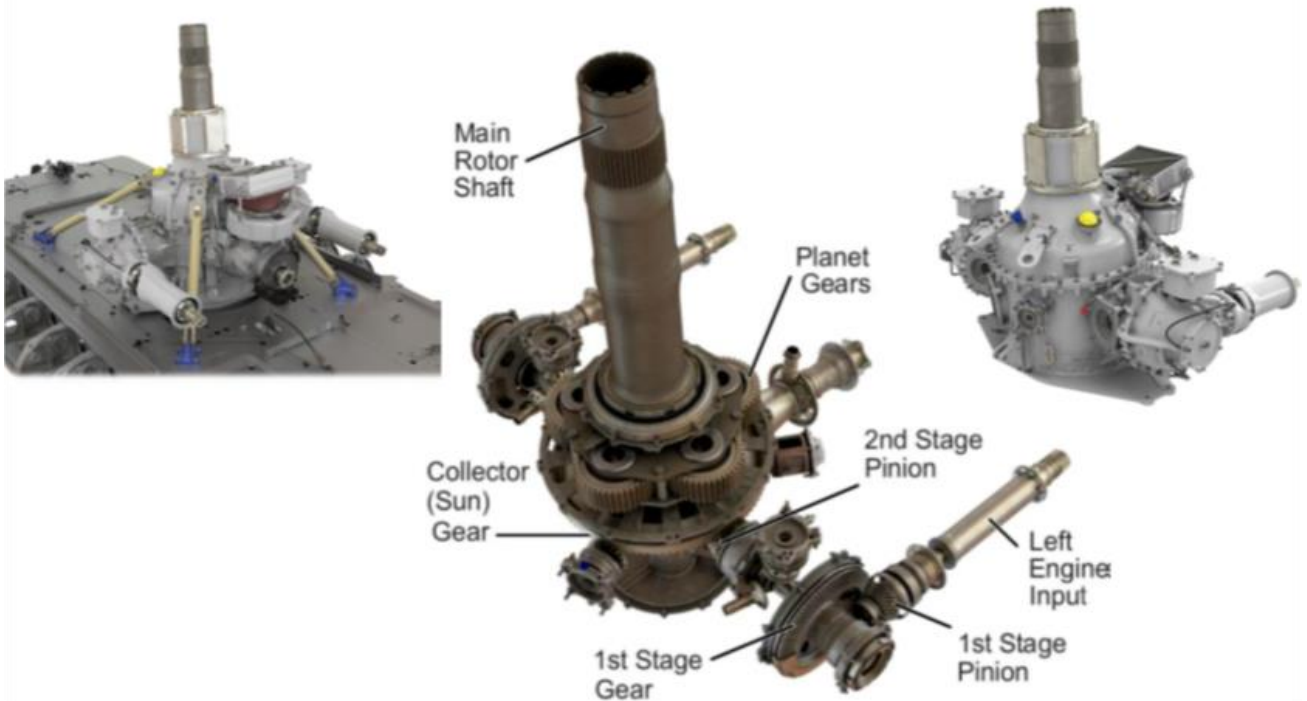


Figure 7: AW189 MGB on airframe and its layout [20]

The high input speed of the AW189 MGB is another aspect common to most AW designs and deviates from the previous projects in which the turbine engines are fitted with their own reduction gearbox. The direct coupling of the turbine engines to the MGB involves an increase of the MGB input speed, from the previous values of 6000-8000 [rpm] up to 20000-30000 [rpm]. This large jump in input speed provides some overall benefit in terms of weight reduction, a smaller number of parts, and a few other advantages for MGB architecture and power plant installation. However, this design choice poses more challenges to extended endurance after loss of oil and it directs our attention and efforts toward the first reduction stages (high speed) of the MGB.

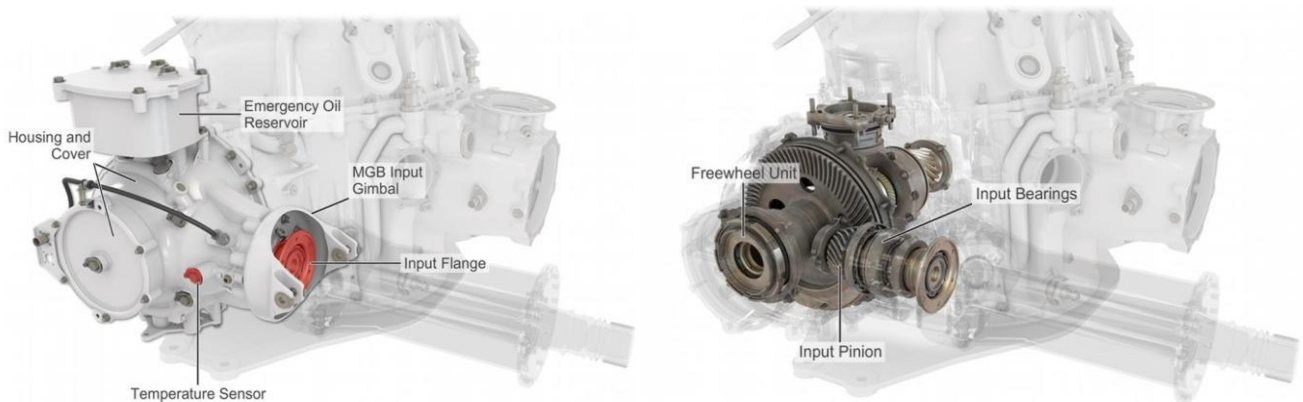


Figure 8: Input module of the AW189 MGB [20]

Bell 212 gearbox and transmission [3]

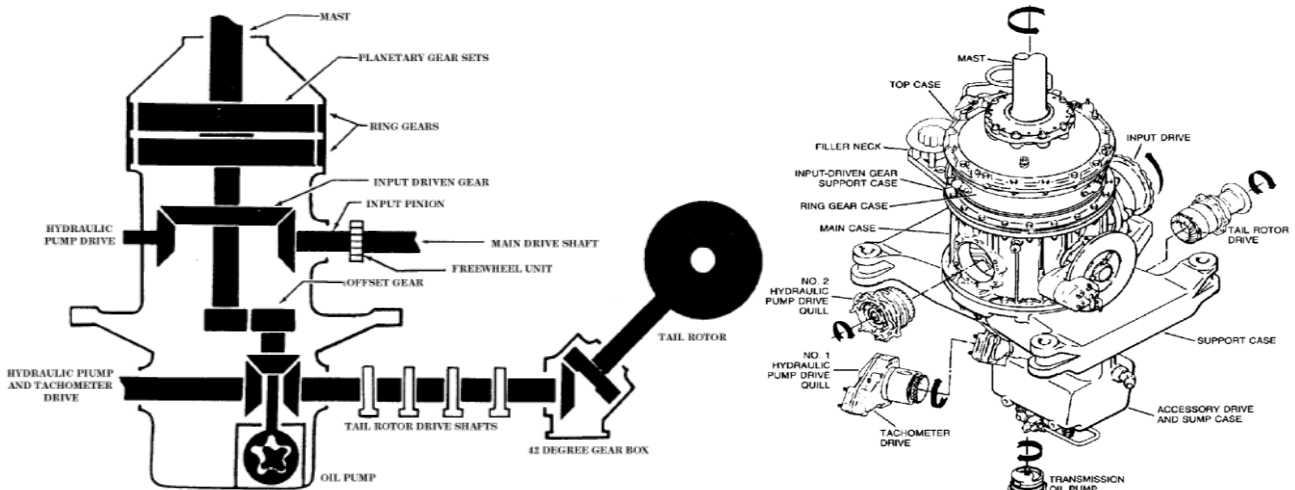


Figure 9: Power train and main transmission of the Bell 212 [3]

The powertrain of the Bell 212 distributes engine power to drive the H/C main and tail rotor systems and other required subsystems. The powertrain includes the main drive shaft, main transmission, main rotor mast and tail rotor drive system.

The main transmission, mounted on the transmission pylon of the airframe, changes the angle of drive and reduces the speed of the power plant drive to power the rotor mast and main rotor. It also powers the tail rotor drive system, its own lubrication system, both hydraulic systems, and provides for operation of the rotor brake.

The main drive shaft torque is transmitted through an input drive quill at the rear of the transmission case to the input pinion gear. The pinion gear drives the input-driven gear, which in turn drives the rotor mast through two stages of planetary gears. This sequence results in an approximate 20:1 reduction in speed. The input-driven gear also drives the No. 2 hydraulic pump and the rotor brake disk. A gear assembly, powered by a splined sleeve from the input-driven gear, drives an offset gear, which in turn drives a geared shaft that drives two pinion gear shafts. One shaft drives the No. 1 hydraulic pump and the main rotor tachometer generator, and the other drives the tail rotor drive system. The offset gear shaft also drives the main transmission lubrication pump at the bottom (sump) of the transmission case.

MBB BO105 gearbox and transmission [8]

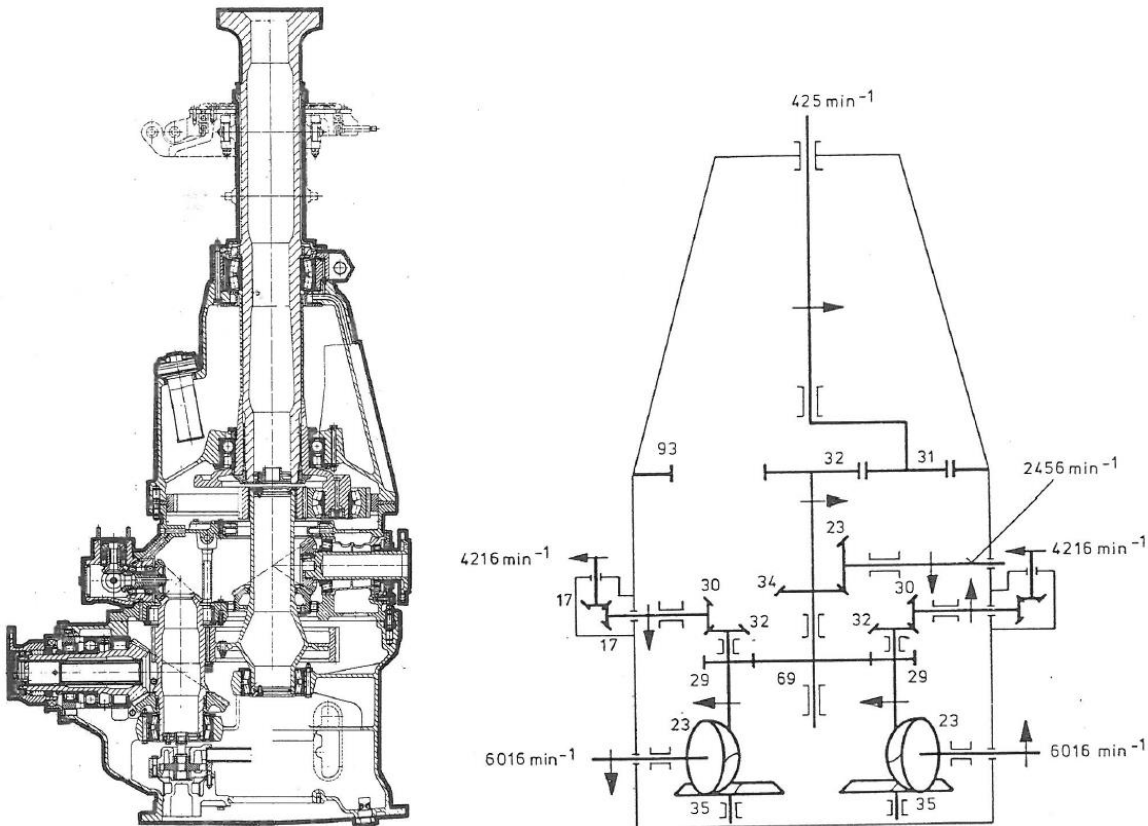


Figure 10: Example of epicyclic transmission of power from input to rotor of the BO105[8]

The main rotor transmission contains all necessary reduction gear stages for transmitting engine power to the main rotor head, tail rotor output, blower assembly, and accessory drive unit and consists of several major subassemblies such as lower, central, and upper housing. The two bevel gear input stages with freewheeling clutches, a spur gear collector stage, and a planetary reduction stage are located there. The power input is via input pinions, which are bevel geared to the intermediate gears to change the power flow from horizontal to vertical. The intermediate shafts are coupled to the collector gear with a spur gear in the collector stage. A splintered vertical shaft connects the collector gear to the sun gear in the planetary stage. The output drive for the tail rotor is also included in this stage. The sun gear drives against the five planetary gears, which are contained in the planetary gear carrier in the upper housing. The planetary gears react against the ring gear fixed to the upper housing of transmission, causing the planetary carrier connected to the rotor mast to rotate.

Bell 525 gearbox and transmission [24]

The aim of the 525 “Relentless” drive system configuration was to minimize the number of single load path components, to provide maximum system separation and redundancy, and to minimize maintenance incidents and the possibility of loss of lubrication events. Furthermore, the MGB loss of lubrication capability should be maximized. For these purposes, a dual gearbox path was incorporated into the design of the overall transmission (Figure 11), as well as separate dual engine reduction gearboxes to isolate failures from the rest of the drive system (freewheeling clutches in the MGB) and the removal of high speed gears and bearings from the MGB, which includes its own fuzz burning chip detector, oil pump, and lubrication system. Separate, dual accessory gearboxes isolate failures from the MGB and gearbox driven accessories are distributed among the separate systems.

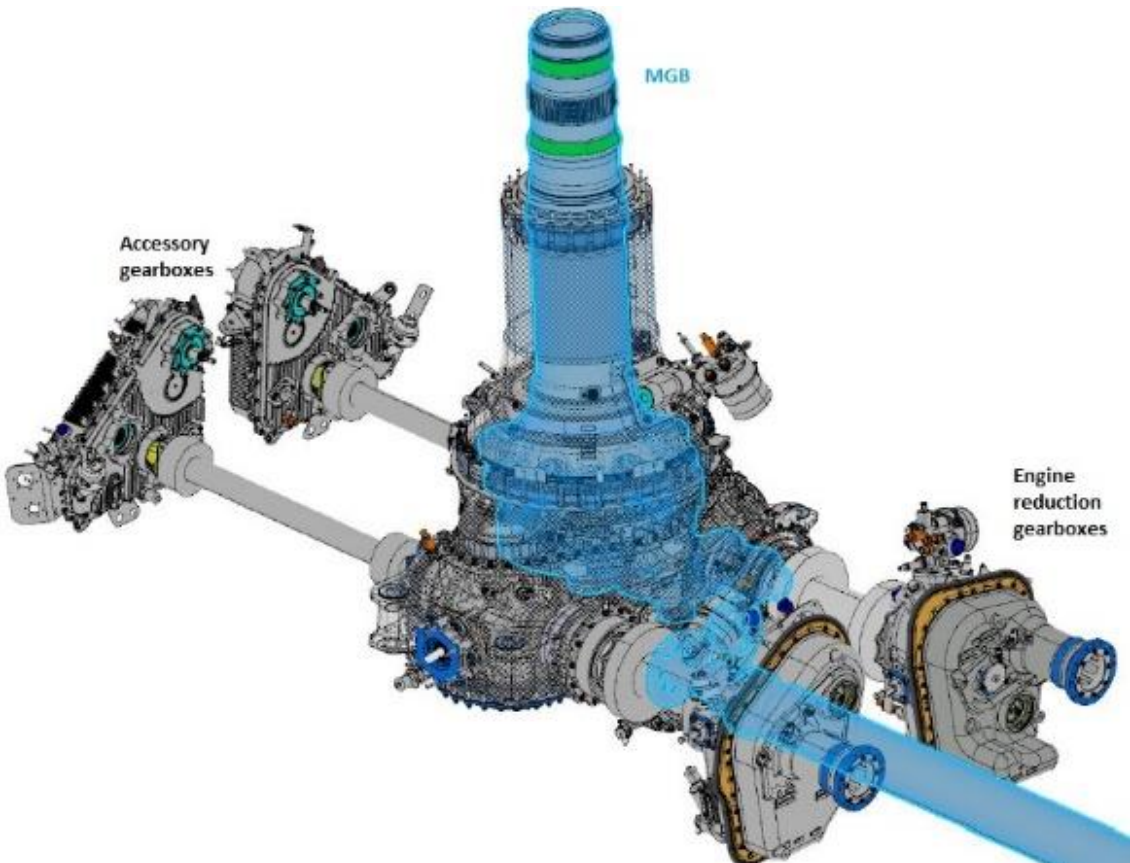


Figure 11: Drive paths of Bell 525 [24]

Each reduction gearbox transmits torque from the engine to the MGB by a two-mesh reduction while reducing speed from 21,000 to 6,000 [rpm]. In the following, the power of each engine is transmitted via a bevel gear stage to a helical gear stage where both are collected and follow a planet gear stage with six pinions to the rotor mast (Figure 12) within the MGB.

Due to the redundancy of the dual paths, a safe flight can continue via OEI operation in the case of a failure in one of the paths. In addition, the relentless drive system incorporates an innovative arrangement and construction of components that collectively minimizes the possibility of a loss of lubrication event and ensures that the maximum flight time is achieved if such an event does occur.

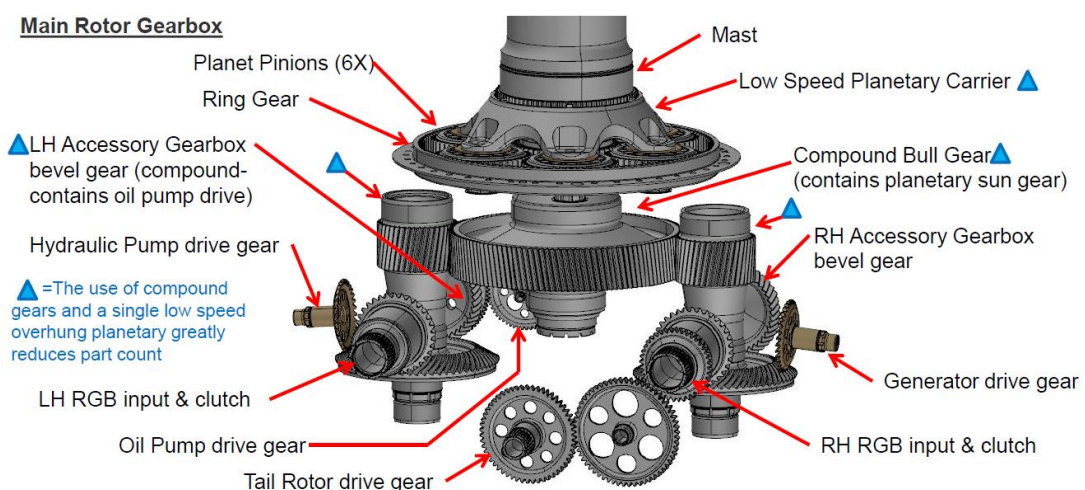
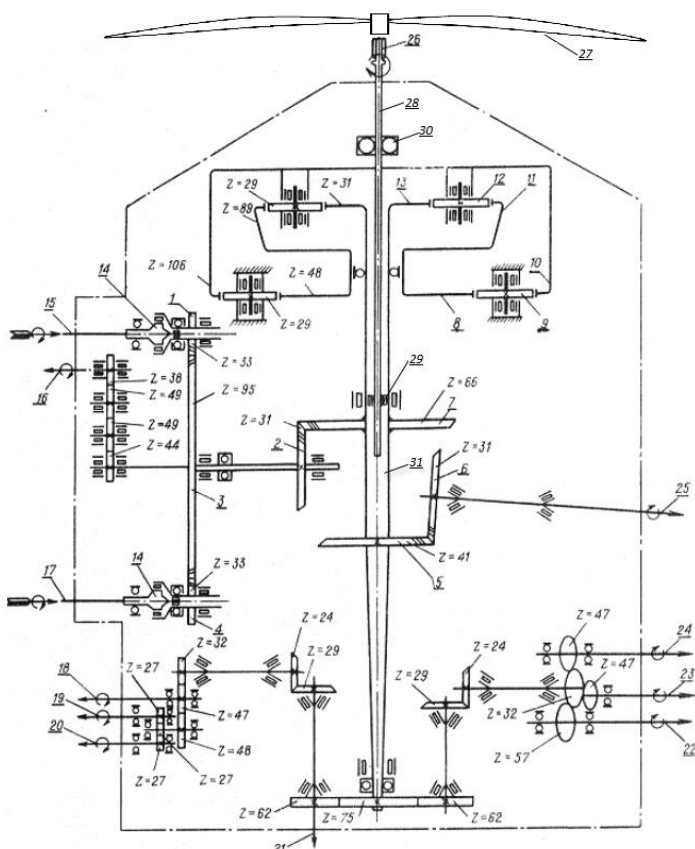


Figure 12: MGB gear chain of Bell 525 [24]

Mil MI-24 gearbox and transmission [7]

The main gearbox WR-24 is a separate assembly in the Mi-24 propulsion system. The main power plant of the helicopter is composed of the main gearbox along with two turbo-shaft engines TW3-117. The main gearbox is intended to combine power from both engines and transmit it to the main and tail rotor shafts, proportional to the required engine ranges. The first stage is a spur gear train, which combines the torques from the two turboshaft engines. The second stage is a bevel gear train, and the third and fourth stages are the compound planetary stages, with final power take-off to the main rotor shaft.

The gearbox is furnished with two freewheeling clutches that automatically disengage the output shafts of either one or both of the engines as soon as their rotational speed is lower than that of the input shaft of the gearbox.



- 1 – Cylindrical spur gear
 - 2 – Spiral bevel gear
 - 3 – Cylindrical helical gears
 - 4 – Cylindrical helical gears
 - 5 – Spiral bevel gears
 - 6 – Spiral bevel gears
 - 7 – Spiral bevel gears
 - 8 – Planetary (epicyclic) gear
 - 9 – Planetary (epicyclic) gear
 - 10 – Planetary (epicyclic) gear
 - 11 – Planetary (epicyclic) gear
 - 12 – Planetary (epicyclic) gear
 - 13 – Planetary (epicyclic) gear
 - 14 – One-way clutch
 - 15 – Engine providing power (15 000 rpm)
 - 16 – Main mechanical fan drive
 - 17 – Engine providing power (15 000 rpm)
 - 18 – Hydraulic pump No. 1 drive ($n=2436$ rpm)
 - 19 – Power drives for tacho generators No. 1 ($n=2384$ rpm)
 - 20 – Power drives for tacho generators No. 1 ($n=2384$ rpm)
 - 21 – Oil-pump drive ($n=2960$ rpm),
 - 22 – Air compressor drive ($n=2008$ rpm)
 - 23 – Hydraulic pump No. 2 drive ($n=2436$ rpm)
 - 24 – Hydraulic pump No. 3 drive ($n=2436$ rpm)
 - 25 – Accessory gearbox/ rear shaft drive ($n=3236$ rpm)
 - 26 – Main rotor shaft ($n=240$ rpm)
 - 27 – Main rotor
 - 28 – Main rotor shaft ($n=240$ rpm)
 - 29 – Lower supporting bearing of main shaft,
 - 30 – Upper bearing of the main shaft
 - 31 – Tubular axle of the planetary gear

Figure 13: Kinematic diagram of MGB WR-24 [7]

2.2 Collector architectures

A collector architecture does have a combining gear (alternative description: e.g. bull gear) at the axis of the rotor shaft, which is supported by at least one power stage and one load path per power stage through input and intermediate stages. A variant of this is the split torque configuration, where the power of the engine is split in at least two load paths.

A split-torque drive also offers great potential for saving on weight and design space powered by one to three engines. In [5] the benefit of the split torque model is summed up as follows:

"Gear volume is proportional to the square of gear diameter, while torque-carrying capacity of gearing is proportional to lower order determinants of gear diameter (depending on whether bending or compressive stress evaluations are being used). Therefore, if torque is reduced by approximately one-half (based on the actual percentage of torque split between gears) for a load carrying gear, the weight of the gear can be reduced by more than one-half, due to the square relationship of weight to gear diameter."

In the following, several example configurations (partly split torque variant) are described:

Airbus Helicopters H135 gearbox and transmission [6]

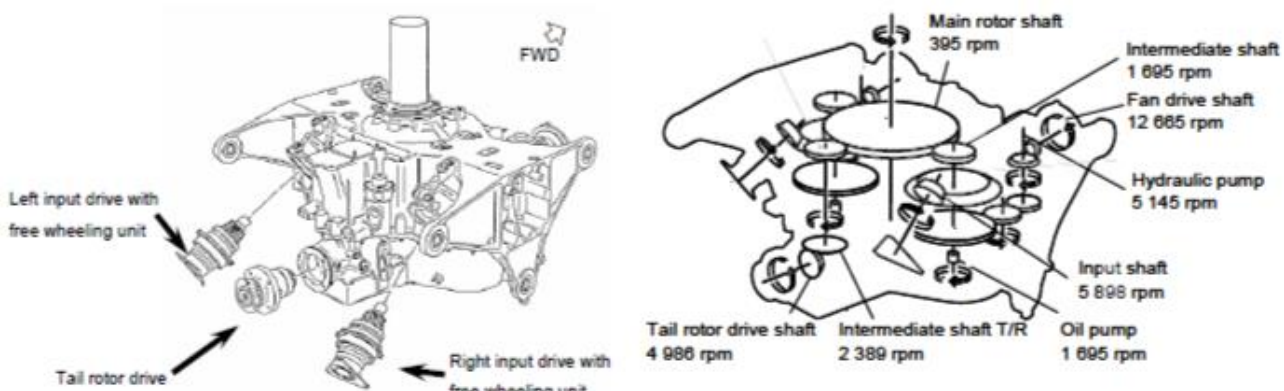


Figure 14: EC/H 135 MGB drive train layout overview and schematic view with speeds of each shaft [6]

The H135 MGB is a modern, lightweight design in which the power transmission flow is designed as one-way power flow from the turbines to the main transmission.

The main transmission of the power is achieved by two shaft turbines that drives two input and intermediate speed decrease stages resulting in a collector wheel that drives the main rotor. Additionally, the transmission to the tail rotor and to the auxiliary drive units of the helicopter. Free wheel units are implemented to ensure that the turbines cannot be driven by the transmission.

The housing is a structural component of the helicopter and transmits all static and dynamic loads between the main rotor system and the fuselage. All mounting points, attachment fittings and oil lines are integrated in the transmission casing. It contains input stages, intermediate stages, collector stage, tail rotor output stage, accessory unit, housing, lubrication and cooling system.

Sikorsky CH-53K gearbox and transmission [15]

The transmission includes two engine reduction gearboxes, one main gearbox assembly, intermediate and tail gearboxes, all of which interconnected via drive shafts and flexible diaphragm couplings. The left-hand (No. 1) and right-hand (No. 3) input accessory modules, located at the front of the main gearbox, receive input torque from two high speed input shafts that are driven by nose gearboxes which are attached to engines No. 1 and No. 3. The No. 2 engine is supported by the rear module housing and provides torque through a sprag clutch

assembly in the rear module where torque is redirected to the main module, rear accessories (oil cooler fan and one hydraulic pump), and the tail take off. The forward accessory modules drive two generators, two permanent magnet alternators (PMAs), and two hydraulic pumps.

The CH-53K main gearbox (MGB), shown in Figure 15, is rated for 13,000 horsepower maximum continuous power (MCP). However, transient power level may reach almost 20,000 horsepower. The split torque MGB is designed based on torsional compliant quill shaft architecture with modular structure, dry sump, and pressurized oil lubrication system.

The main gearbox is mounted directly on the airframe upper deck and transfers rotor head thrust, shear, torque, and torsion loads directly to the airframe. The multiple path drive train transfers the torque from the three engine inputs to the bull gear/main rotor shaft assembly. The compliant quill shafts allow precise load sharing between highly loaded gearbox components. The gears of the second and the third stage of reduction are not axially constrained. This minimizes any impact on the gear train from gearbox deformation caused by loading.

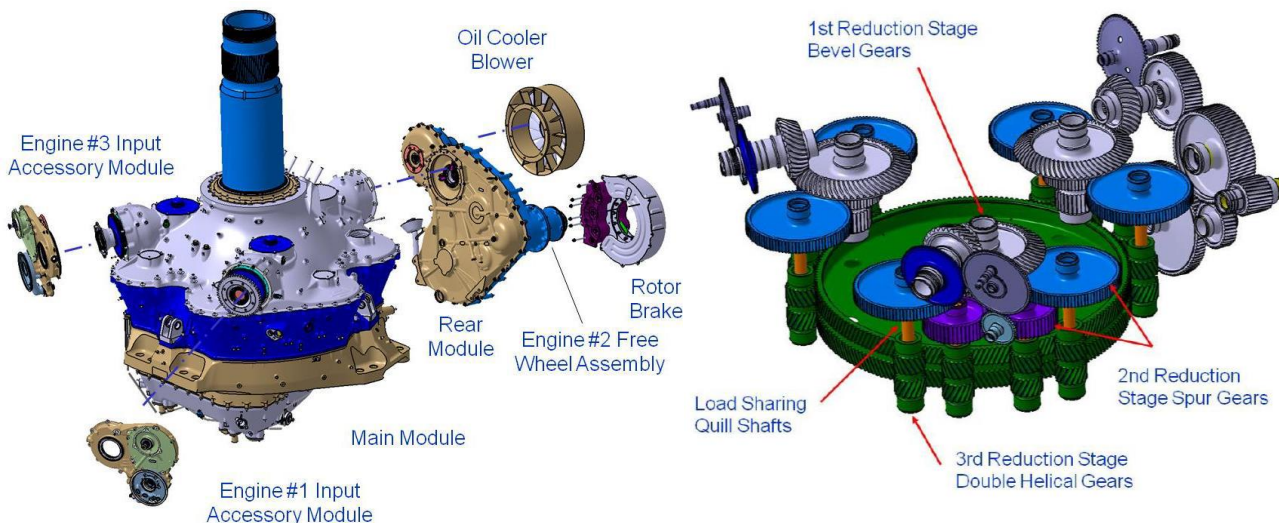


Figure 15: Example of collector transmission of power from input to rotor [15]

Kawasaki BK117 gearbox and transmission [21], [22]

The helicopter transmission is installed on top of the cabin and performs the following operations. Firstly, it transfers power from the engine to the main rotor (rotor blade) and the tail rotor after stepping down the speed. Secondly, it drives accessories. Thirdly, it transfers the lift generated by the main rotor to the helicopter body and receives the thrust force as well as the drag force that acts in opposition to the direction of movement.

In the BK117 D-2, the transmission reduces an engine speed of 6,000 [rpm] to 380 [rpm] (reduction ratio of about 16:1), and at the same time increases the torque to 19,600 [Nm] to drive the main rotor. This is a remarkable torque capacity, sufficient to lift two passenger cars attached to the end of a 1 meter long bar.

To be more specific, the rotary shafts from a pair of engines that generate a total of 1,000 horsepower are coupled to spiral bevel gears that change the direction of rotary motion by 90 degrees, and simultaneously reduce the engine output speed. After the directional change, the rotational speed is reduced by a helical gear on the second stage, resulting in an optimal rotor speed.

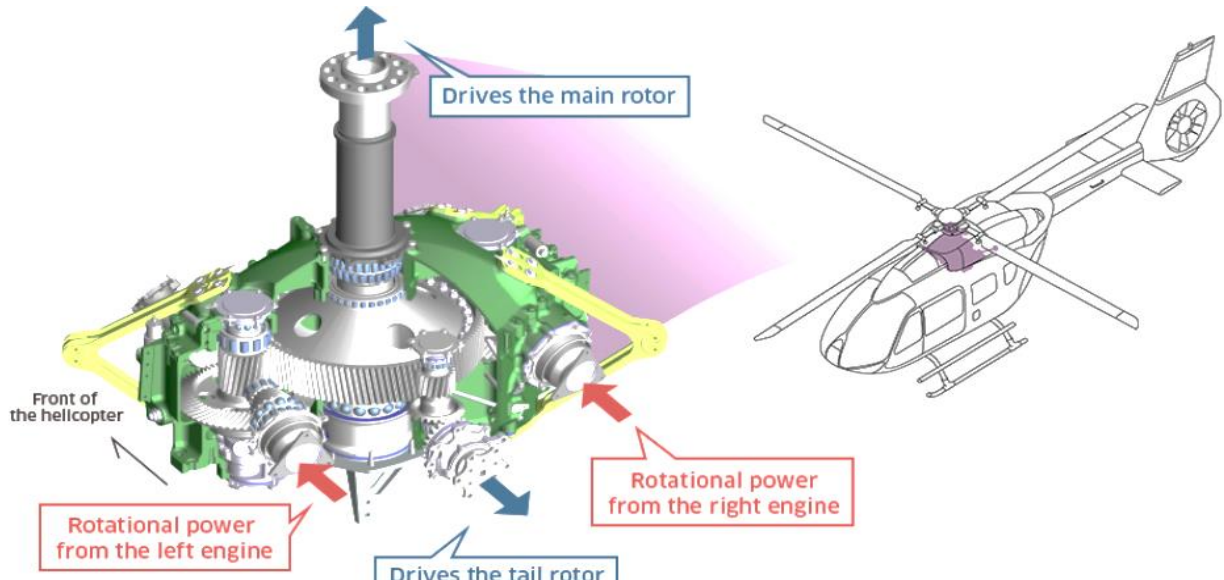


Figure 16: BK117 drive train arrangement [22]

Mil Mi-26 gearbox and transmission [9]

Another MGB design is the split torque gearbox of the helicopter Mi-26 (Figure 17). In this gearbox, the torque from each engine shaft is distributed to two spiral bevel reduction gears and to the power take-off gear train to the tail shaft. The torque is delivered from four spiral bevel reduction gears to four spur gear trains of the second stage. From these second-stage spur gears, the torque is transmitted via eight trains to eight gear pairs, which are meshed with two central gears on the main shaft. The gear trains of all three stages are connected by torsional flexible splined quill shafts that ensure uniform distribution of the torque along the trains.

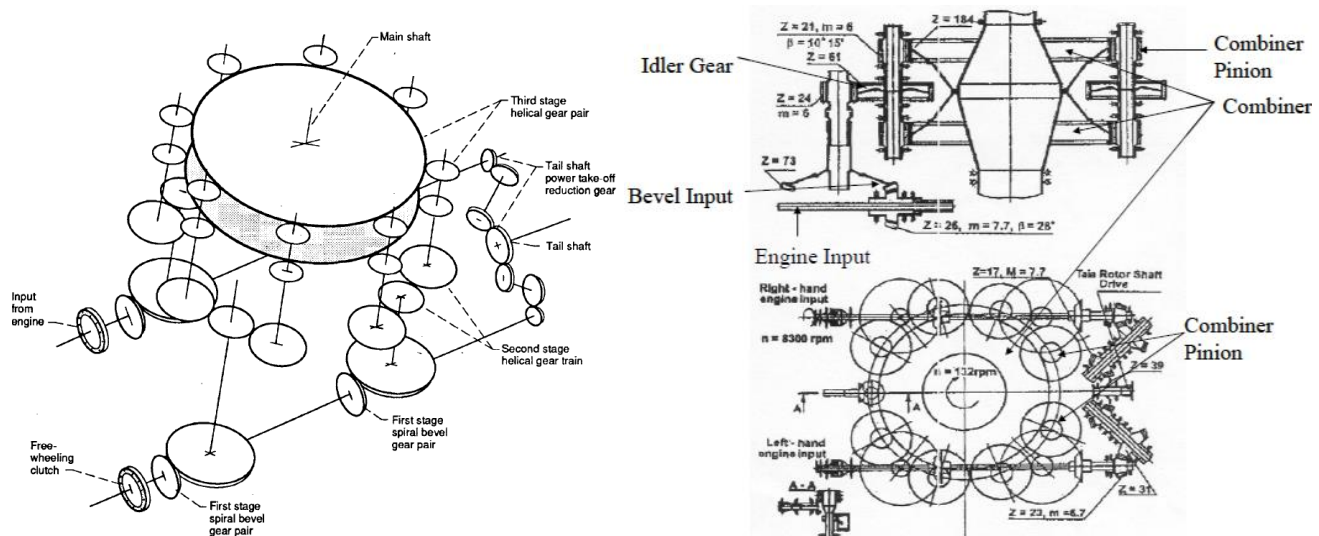


Figure 17: Mi-26 drive train arrangement [5], [9]

Coaxial configuration gearbox and transmission (e.g. Kamov Ka-226) [10]

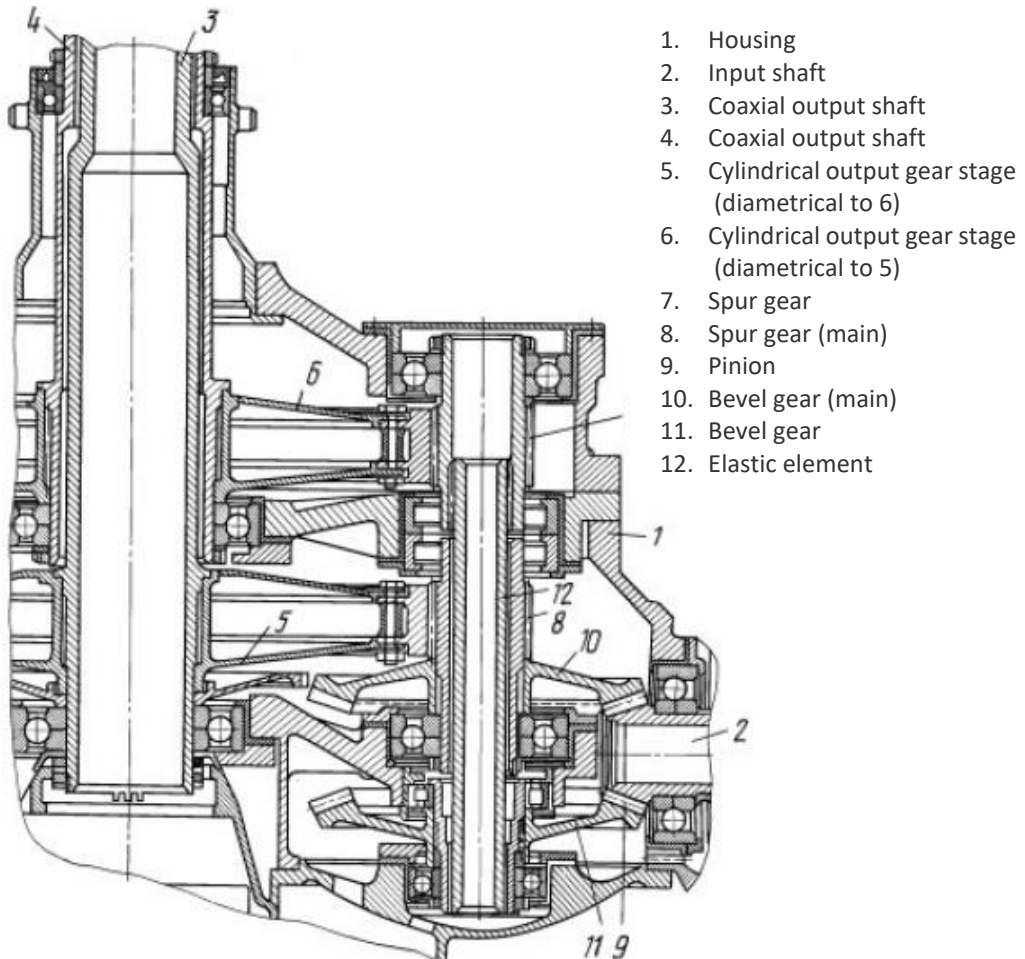


Figure 18: Spur MGB coaxial configuration [10]

Figure 18 relates in particular to transmissions of coaxial-rotor helicopters comprised of a housing element, an input shaft with input pinion, two coaxial output shafts and the main gear output stage comprised of two diametrical cylindrical wheels with the same number of teeth as on the coaxial output shafts. It also includes two spur gear stages with the same number of teeth, as well as two driven bevel gears with the same number of teeth (primary and secondary). The lower spur gear is connected with the upper spur gear via the elastic element, which torsional stiffness is less than the torsional rigidity of the upper driven bevel gear connection. By rotating the input shaft its pinion engages with the two driven bevel gears, then with the spur gears and their diametrical output stage connected to the output shafts.

Finally, the output shafts have the same speed, which is characteristic for modern coaxial helicopters and which means the dynamic influence of the main rotors, engines and elements of the main transmission can mean that the main gearbox needs equal bevel and spur gears, which simplifies the design of the gearbox and its manufacture and repair.

2.3 Summary

Table 2 summarizes the different concepts from 2.1 and 2.2 insofar as data is available.

H/C	MTOW	MGB configuration and licensing regulation acc. CS	Ratio, Stages and used gear technology	Bearing configurations
Aérospatiale AS332 L2 / Airbus Helicopters H-225 Super Puma	8,600 - 11,000 kg	Epicyclic configuration CS 29	<p>Ratio: 86.792 Input speed: 23000 rpm MR speed: 265 rpm</p> <p>1. Spur gears 2. Spur gears 3. Bevel gears 4. 1st epicyclic module 5. 2nd epicyclic module</p>	<ul style="list-style-type: none"> - The rotor carries the weight of the helicopter via the lift bearing attached to the main rotor shaft. The lift bearing is located inside the lift housing which is attached to the conical housing on top of the MGB. - Bevel gear vertical shaft supported by two upper bearings (one roller/one ball) and lower roller bearing - Epicyclic modules: Combined gear and bearing assembly. The OR of the bearing and the gear wheel are one single component. Other elements are IR, two sets of 14 bearing rollers (upper and lower), and two bearing cages. Each planet gear is 'self-aligning' thanks to the use of spherical outer races and asymmetric barrel-shaped bearing rollers
Augusta Westland AW189	8,300 – 8,600 kg	Epicyclic configuration CS 29	<p>Ratio: 75.224 Input speed: 21420 rpm MR speed: 284.75 rpm</p> <p>1. Spiral bevel gears 2. Spiral bevel gears 3. Epicyclic module</p>	<ul style="list-style-type: none"> - Ball bearing: Conventional, split IR, integrated IR - Roller bearing: Conventional, integrated IR + OR - Type of planet bearing not identified - Type of lift bearing not identified
Bell 212	5,080 kg	Epicyclic configuration CS 29	<p>Ratio: 20.370 Input speed: 6600 rpm (combining gbx output) MR speed: 324 rpm (max. power on)</p> <p>1. Bevel gears 2. Epicyclic module 3. Epicyclic module</p>	<ul style="list-style-type: none"> - Type of planet bearing not identified - Type of lift bearing not identified

H/C	MTOW	MGB configuration and licensing regulation acc. CS	Ratio, Stages and used gear technology	Bearing configurations
MBB BO-105	2,500 - 2,600 kg	Epicyclic configuration CS 27	Ratio: 14.151 Input speed: 6000 rpm MR speed: 424 rpm 1. Bevel gears 2. Spur collector gear stage 3. Epicyclic module	- Ball bearing: Conventional, split IR (input) - Roller bearing: Conventional, integrated IR (input) - Type of planet bearing: roller, tapered (redesign) - MR upper bearing: Roller + four point bearing/ spherical (redesign) bearing not identified - MR lower bearing: roller bearing/ ball + roller bearing (redesign)
Bell 525	9,300 kg	Epicyclic configuration CS 29	Ratio: unknown Input speed: 6000 rpm (reduction gearbox output) MR speed: unknown 1. Bevel gears 2. Helical gears (bull gear contains planetary sun gear) 3. Epicyclic module	- Type of planet bearing not identified - Type of lift bearing not identified
Mil Mi-24	11,000 kg	Epicyclic configuration CS 29	Ratio: 62.5 Input speed: 15000 rpm MR speed: 240 rpm 1. Helical gears 2. Spiral bevel gears 3. Epicyclic module 4. Epicyclic module	Integrated ball and roller bearings, plus ball bearing with IR + OR - Type of planet bearing: roller - MR upper bearing: ball bearing (probably integrated) - MR bottom thrust bearing for support of the main shaft (an intermediate bearing between the main shaft and the output shaft of the planetary transmission: roller bearing (probably integrated))
Airbus Helicopters H-135	2,910 kg	Collector configuration CS 27	Ratio: 14.932 Input speed: 5898 rpm MR speed: 395 rpm 1. Bevel gears 2. Helical gears	- Ball bearing: Conventional, split IR (input) - Roller bearing: Conventional, integrated IR (input), special OR - MR upper bearing: Roller bearing - MR lower bearing: Four point bearing + roller bearing

H/C	MTOW	MGB configuration and licensing regulation acc. CS	Ratio, Stages and used gear technology	Bearing configurations
Sikorsky CH-53K King Stallion	38,400 kg	Collector configuration Split torque arrangement CS 29	Ratio: 82.629 Input speed: 14708 rpm MR speed: 178 rpm 1. Bevel gears 2. Spur gears 3. Helical gears	- Type of lift bearing not identified
Kawasaki BK117	3,400 - 3,800 Kg	Collector configuration CS 27	Ratio: 15.649 Input speed: 6000 rpm MR speed: 383.4 rpm 1. Bevel gears 2. Helical gears	- Ball bearings - Roller bearings: Conventional, integrated - MR upper bearing: Spherical roller bearing - MR lower bearing: Roller bearing + four point bearing
Mil Mi-26 Halo	56,000 kg	Collector configuration CS 29	Ratio: 62.879 Input speed: 8300 rpm MR speed: 132 rpm 1. Spiral bevel gears 2. Helical gears 3. Helical gears	- Type of lift bearing not identified
Kamov Ka-226T	3,600 kg	Collector configuration with two coaxial rotors CS 29	Ratio: 20.979 Input speed: 6000 rpm MR speed: 286 rpm 1. Bevel gears 2. Spur gears 3. Spur gears	- Conventional and integrated rolling bearings - Inner rotor mast: upper roller bearing + lower four point bearing - Outer rotor mast: upper four point bearing + lower roller bearing

Table 2: Summary of the different analyzed H/C MGB concepts

3. Failure mode and mechanism overview

This chapter describes main failure modes from damage catalogues based on the structure of [28] and on the information available in different public literature, e.g. [13], as well as on experience from ZF [16] and SKF [17]. It deals with a wide range of failure modes and their varied range of mechanisms. With the help of suitable illustrations and descriptions of causes, it is expected that all damage can be interpreted accurately.

3.1 General

Each different cause of failure produces its own characteristic damage. Such damage, known as primary damage, gives rise to secondary, failure-inducing damage, flaking, and cracks. Even the primary damage may necessitate scrapping parts because of e.g. excessive clearance/backlash, vibrations and noise.

A failed bearing frequently displays a combination of primary and secondary damage. A gear has failed when it can no longer efficiently do the job for which it was designed.

The consequence of the failure may lead to catastrophic breakage if it remains unnoticed. Failure in a drive train can be prevented in many cases. When it occurs, a proper re-design of the part will ensure a trouble-free unit. Regardless of when the trouble is rectified – in the design or redesign stage – the most important aid to the designer is the ability to recognize the exact type of incipient failure, how far it has progressed, and the cause and cure of the problem.

3.2 Corrosion

3.2.1 General corrosion

General corrosion is indicated by rust scours on the surface, which may be caused by the ingress of water, by condensation forming under unfavourable operating conditions, or by oil ageing in such quantities that the lubricant cannot provide protection for the steel surfaces, as well as by storage conditions. Figure 19 shows corrosion spots on a helical gear and on a raceway. Figure 20 show chemical attacked bearing raceway, Figure 21 gives an example on a light corrosion.

According to [17] the usual consequence in bearings is increased vibration followed by wear, with subsequent increase in radial clearance or loss of preload. In extreme cases, corrosion can initiate early fatigue failures, but not to the scope of the initiation of critical bearing failure based on SKF investigation.

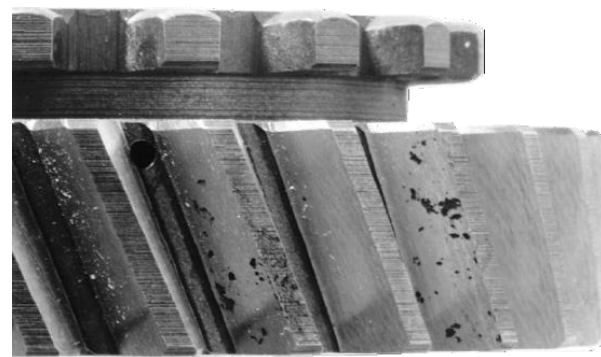


Figure 19: General corrosion [16]



Figure 20: Corrosion results from a chemical attack on the metal by hostile fluids or atmospheres [14]

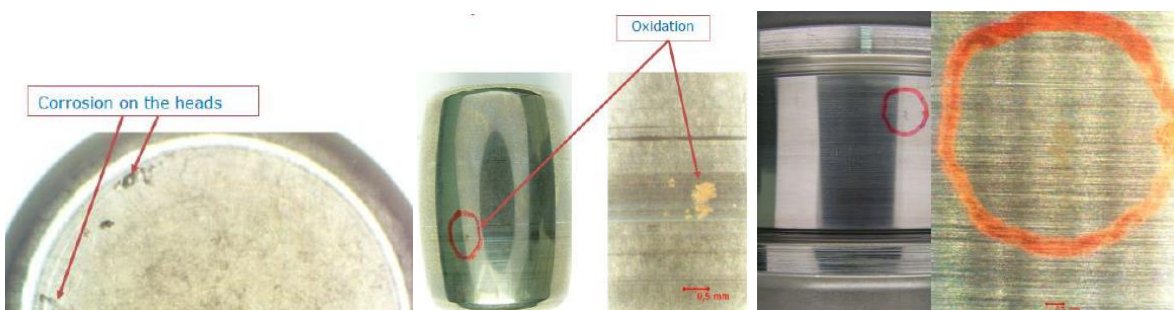


Figure 21: Example of observed light corrosion damages [17]

3.2.2 Friction-induced corrosion

Figure 22 (left) shows friction corrosion produced by the micro movement of contacting metal surfaces, which transmit force without rolling motion and lead to local oxides of varied structures, microscopic metal particles, and decomposition products from oils and their additives, which accelerate the wear process.

False brinelling as shown on a bearing in Figure 22 (right) can be categorized as a type of friction corrosion, which indicates excessive external vibration.



Figure 22: Friction induced corrosion [16] and false brinell marks are bright and surrounded by debris [14]

3.2.3 Fretting corrosion

Fretting is commonly combined with corrosion. Initial fretting corrosion is either black or reddish-brown. When this is accelerated by poor lubricant supply, this kind of damage occurs within a brief period.

Figure 23 shows areas of rust on the outside surface of a gearing and the outer ring or in the bore of the inner ring. The raceway path pattern is heavily marked at corresponding positions. If the thin oxide film is penetrated, oxidation will proceed deeper into the material. An instance of this is the corrosion that occurs when there is a small relative movement between bearing ring and shaft or housing, on account of the fit being too loose. The relative movement may also cause small particles of material to become detached from the surface. These particles oxidize quickly when exposed to the oxygen in the atmosphere.

As a result of the fretting corrosion, the bearing rings may not be evenly supported and this has a detrimental effect on the load distribution in the bearings. Rusted areas also act as fracture notches. [17]



Figure 23: Fretting on gearing (left) [16] and inner ring bore diameter (middle/right) [17]

3.2.3.1 Tribological oxidation/ininitely brinelled surface

Figure 24 shows tribological oxidation, also referred to as infinitely brinelled surface, which occurs as a result of fretting corrosion in the shaft bearing races (gear/shaft) and takes the form of uniform radial wear (gear wear) by several vibrations.

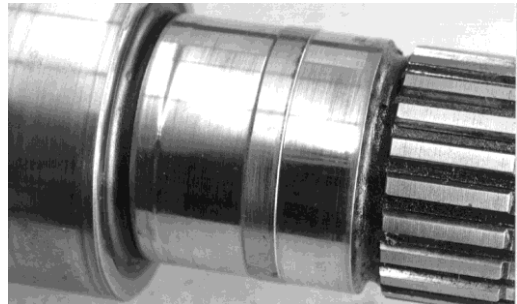


Figure 24: Highly polished race surface by tribological oxidation [16]

3.2.4 Corrosive wear

This is a deterioration of the surface due to chemical action, as shown in Figure 25, and is often caused by active ingredients in the lubricating oil such as acid, moisture and extreme-pressure additives. The oil breaks down so that corrosive chemicals present in the oil attack contacting surfaces. Often this affects the grain boundaries, causing fine pitting more or less uniformly over the tooth surfaces. At high temperatures, extreme-pressure additives sometimes from very active corrosive agents.

Lubricants can also become contaminated from absorption of foreign material from external sources. In such cases, the gear unit should be isolated from its environment. Because they are chemically active, lubricants with high anti-scoring, anti-wear additive content must be kept under careful observation to ensure that they are not attacking working surfaces, which should be managed by regular inspection of the gearbox.

At times, surfaces can be affected chemically during processing in the factory, e.g. when copper plate is stripped from the gear after carburizing or when nital-etch is used to detect grinding burns. Proper processing procedures must be set up and carefully followed. [13]

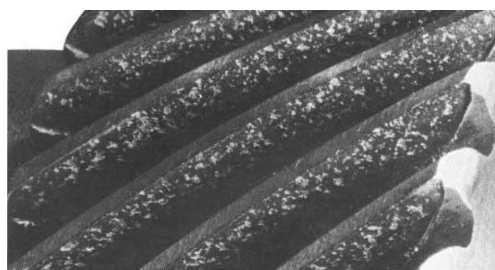


Figure 25: Example: Corrosive wear on gear tooth [13]

3.3 Wear

3.3.1 General

Wear is a surface phenomenon in which layers of metal are more or less uniformly removed, or “worn away” from the contacting surfaces due to operating influences such as high speed combined with reduced loading, high loading, and high usage as well as by oil quality, e.g. contamination by particles or thermal ageing or external factors. As peaks of roughness worn away and wear progresses, visible, slightly full areas appear on the material, which are often defined as “grey staining” and which constitute the initial stage of pitting as shown in Figure 26. This typically becomes noticeable over time in the form of increased noise and/or temperature.



Figure 26: Worn on roller and races like axial protrusion (left) and grey staining (right) [16]

Cage wear in the cage-roller contact or cage-ring landing area may be caused by inadequate lubrication, by excessive roller skew, by high temperature, or by abrasive particles (Figure 27). The idea with rolling bearings is of course to avoid sliding friction. However, where the cages are concerned, sliding cannot be eliminated in the contacts with the other components of the bearing. This explains why the cages are the first components to be affected when the lubrication becomes inadequate.

The cages are always made of softer material than the other components of the bearing and consequently wear comparatively quickly. As the cage pockets increase in size due to wear, the roller guidance deteriorates. This also applies in cases where the cages are centered on the rollers. Cage wear is also very often a consequence of major damage to roller or raceway resulting in higher loads and vibration on the cage contact area. [17]

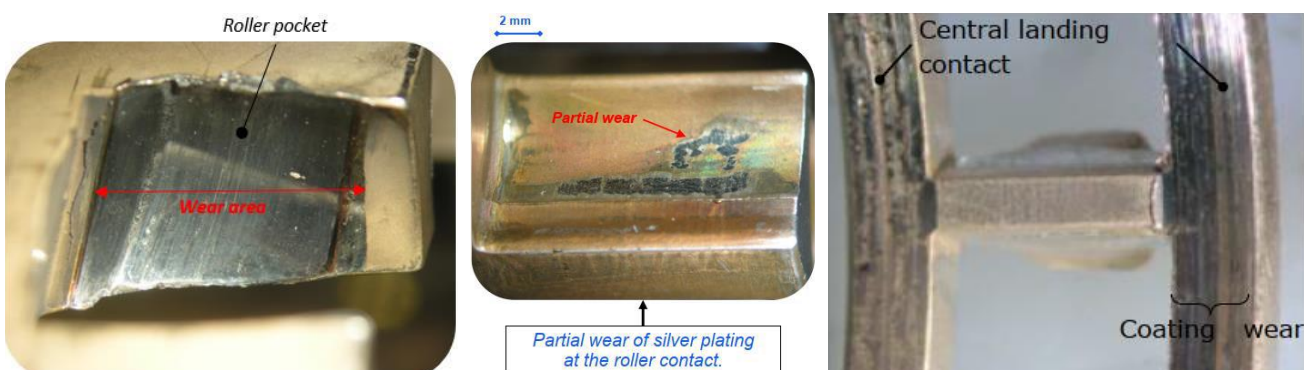


Figure 27: Example of cage wear, various wear level and cage area [17]

3.3.1.1 Polishing

Polishing is a very slow wearing-in process in which the asperities of the contacting surfaces are gradually worn off until a very fine and smooth surface develops. This condition is usually caused by metal-to-metal contact during operation and generally occurs on slow-speed applications where the elastic-hydrodynamic lubrication film is not sufficiently thick and operation is near the boundary-lubrication range.

Since it usually provides for good conformity of surfaces, often this condition need not be avoided unless the design life of the equipment is much longer than the predicted wear life due to polishing. After the gear is well polished, the surface can be protected by substituting a lubricant with a higher viscosity and by reducing the transmitted load operating speed to obtain a better elastic-hydrodynamic oil film. [13]



Figure 28: Example: Polishing wear [13]

3.3.1.2 Moderate wear

The type of wear classified as moderate takes place over a relatively long period. On gears the contact pattern indicates that metal has been removed in the addendum and dedendum area (Figure 29). In addition, the pitch line begins to show as an unbroken line.

Moderate wear is most commonly caused by an inadequate lubrication film or dirt in the system, with the film thickness being too thin for the load, which can be solved by specification of a lubricant with a greater film strength or one with a higher viscosity and general operation at a greater speed to build up the lubricating film, or by using a material with a higher wear resistance.

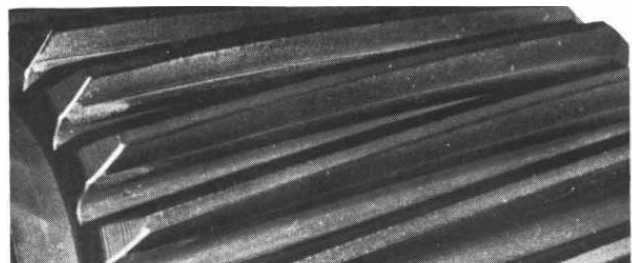


Figure 29: Example: Moderate Wear [13]

3.3.1.3 Excessive wear

This is simply normal wear which has progressed to the point where a considerable amount of material has been removed from the surfaces, usually caused by the failure to notice early enough that wear is occurring (Figure 30). On gears, the pitch line is very prominent and shows signs of pitting. When enough material has been worn from the tooth surface, the involute profiles are destroyed and the gears begin to run roughly.

The situation is aggravated by the rough running, causing still greater wear. Eventually the surface is such that the gears are no longer fit for reliable service.

This condition might be avoided by using the same methods given for moderate wear. If the gear unit is splashed-fed, changing to a positive spray lubrication system with a filter will help keep wear particles out of the gear mesh and ensure that adequate lubricating oil is delivered to the working surfaces. [13]

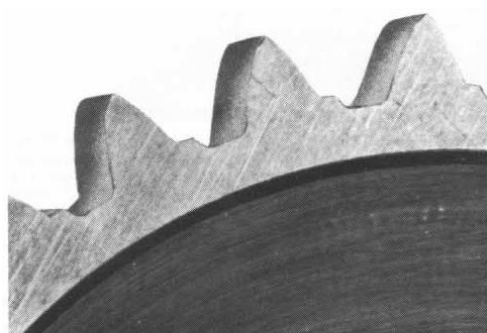


Figure 30: Example: Excessive Wear [13]

3.3.1.4 Abrasive wear

When abrasive wear has taken place, contact surfaces show signs of a lapped finish, radial scratch marks or grooves, or some other unmistakable indication that contact has occurred (Figure 31) caused by foreign material in the lubrication system. Apart from a clean system, a finer grade of filter can be implemented, if a filter is already being used, or as higher-viscosity lubricant that develop a thicker oil film which will pass fine particles without scratching for prevention of abrasive wear.

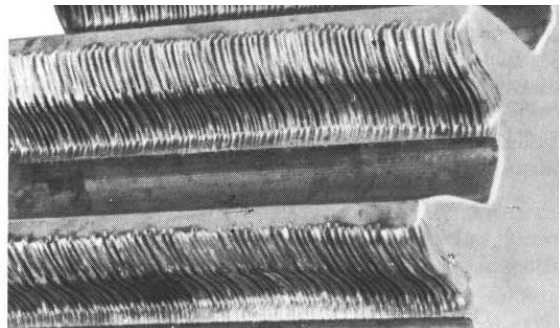


Figure 31: Example: Abrasive wear on a gear [13]

On the races of bearing components, grinding burrs undergo plastic deformation and some chip off. The metallic particles this process creates give rise to abrasive wear. Further consequences include the development of scoring and scratches and micro pitting. The wear process develops rapidly as the bearing play continues to increase. Finally, this leads to powder rubbing or peeling of the surface layers and severe subsequent damage caused by oil quality, e.g. particles, contamination, time and thermal ageing or high loading (Figure 32).



Figure 32: Peeling of the surface layers [16]

3.3.2 Scoring

Scoring is a rapid wear resulting from a failure of the oil film due to overheating of the mesh, permitting metal-to-metal contact. This contact produces alternate welding and tearing which removes metal rapidly from the surfaces. In general, reduced oil temperatures or better control of temperature fluctuations will tend to keep the heat level within safe limits. A mild extreme-pressure oil may be helpful but may not be necessary.

In the early stages of scoring frosting occurs, that is caused by heat in the mesh, which results in only marginal lubrication as shown in Figure 33. The heat of the mesh and the bulk temperature of the rotating gears combine to break down the lubrication film.

Often where frosting appears, subsequent operation of the unit will slowly polish away the frosted areas if all operating conditions remain constant. [13]

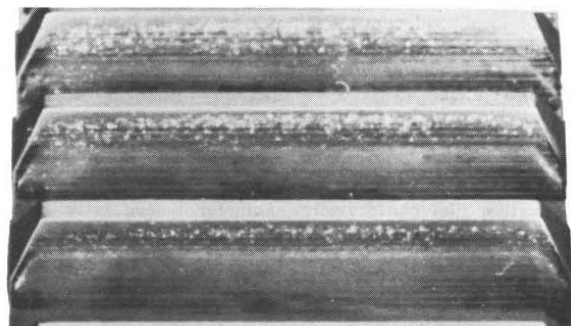


Figure 33: Example: Frosting [13]

Following frosting a moderate scoring occur, a characteristic wear pattern becomes visible across the full face or only local as shown in Figure 34, often in patches and sometimes with indications of radial tear marks. In some cases, a solid lubricant placed on the contact surface helps prevent the scoring from progressing. Honing has also found increased use when guarding against scoring. [13]

Definite indications of radial scratch and tear marks in the directions of sliding are called destructive scoring or scuffing. Often material has been displaced radially over the tips of the gears. In addition, there are indications that considerable material has been removed from above and below the pitch line and the pitch line itself stands out prominently. When the lubricant breaks down, the welding and tearing destroys the profile in minutes (Figure 35).

Another kind of scoring is visible by definite signs of metal removal on the deep-dedendum section of the gear and may often show destructive radial scratch marks, but undamaged other sections of the contacting face as shown Figure 36. The heavy loading at the tip or root of the mating pair, or the interference caused by a tight mesh, prematurely breaks down the lubricant film and causes rapid metal removal at the tips and roots and general abrasion of the teeth.

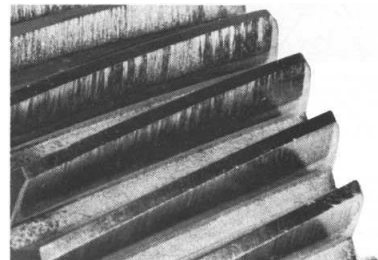


Figure 34: Example: Light to moderate scoring [13]

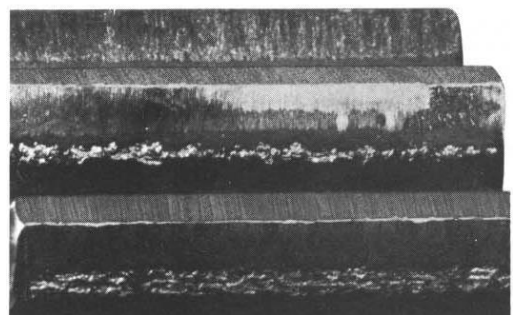


Figure 35: Example: Destructive Scoring [13]

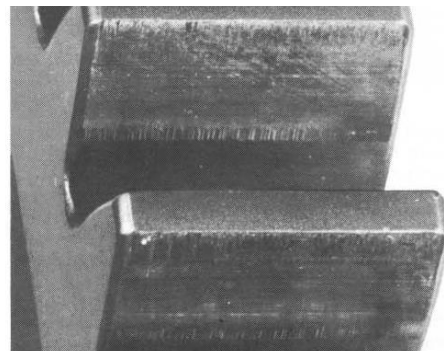


Figure 36: Example: Tip and root interference [13]

3.4 Rolling contact fatigue

The change in the structure, which is caused by repeated stresses developed in the contacts between the parts, is described as fatigue. Rolling contact fatigue is a form of fatigue that occurs due to the cyclic strains arising from loading present during rolling contact between two parts of an assembly and is manifested visibly as flaking of the surface.

3.4.1 Subsurface initiated fatigue

Under the influence of loads in rolling contacts as described by the Hertzian Theory, structural changes will occur and micro cracks will be initiated at a certain depth under the surface, i.e. subsurface. The micro cracks are often initiated by inclusions in the steel. The micro cracks will normally cluster at the rolling contact surface producing flaking, spalling (pitting), and then peeling [28].

Starting with matt gray spots with microscopic hair-line cracks (Figure 37; left), the damaged surface is considerably brighter than the surface of an undamaged part, leading to individual or connected shell-shaped

chips (Figure 37; middle). There is micro-fracture formation in zones close to the surface also subject to load. Breakage cracks proceed obliquely towards the surface starting from these micro-fractures. As a result, pieces of the material break off and the consequential pitting continues to spread. The broken material shards are over rolled and lead to local overloads (Figure 37; right).



Figure 37: Gray spots (left), pitting formation (middle) and initial pitting (right) [13], [16]

In destructive pitting, the surface pits are usually considerably larger in diameter than those associated with initial pitting. For instance, the dedendum section of the drive gear is often the first to experience serious pitting damage. As operation continues, however, pitting usually progresses to the point where a considerable portion of all surfaces have developed pitting craters of various shapes and sizes, as can be seen in Figure 38.

Destructive pitting usually results from surface overload, which cannot be alleviated by corrective (initial) pitting. Once enough stress cycles have been built up, pitting continues until the contact profile is completely destroyed, leading to extremely rough operation and considerable noise. Often a bending fatigue crack will originate from a pit, causing a premature breakage failure.

Destructive pitting can be avoided by maintaining the load on the material. In addition, hardness of the material can be increased so that the endurance limit will rise to a point where pitting does not take place.

On gears, pitting can sometimes be arrested by increasing the hardness level of only the driving member. [13]

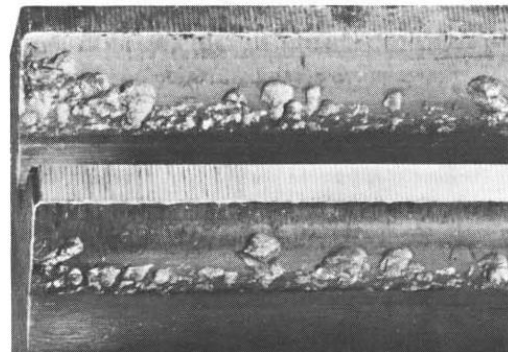


Figure 38: Example: Destructive pitting [13]

Spalling is similar to destructive pitting except that the pits are usually larger in diameter and quite shallow. Often the spalled area does not have a uniform diameter and frequently occurs in medium-hard material, as well as in highly loaded fully hardened material. Spalling of this kind should not be confused with "case crushing", which is associated with case-hardened material. Spalling is usually caused by excessively high contact stresses that typically result in premature fatigue. Usually, large pits are formed. Because stress levels are high, the edges of the initial pits break away rapidly, resulting in large irregular voids. Often these voids join together.

Contact stress on the gear surface can be reduced below the endurance limit of the material if the gear material has increased surface strength. A complete redesign of the gear elements is often the best option since destructive pitting and spalling are evidence that the gears do not have sufficient surface capacity. [13]

The fractures of the running surfaces of bearings and subsequent removal of small, discrete particles of material occur progressively on the inner ring, outer ring, or balls. Once initiated it will spread as a result of further operation and be consistently accompanied by a marked increase in vibration, indicating an abnormality. The remedy is to replace the bearing or consider a redesign using a bearing with a greater calculated fatigue life and capacity. [14]

Although not considered a pitting failure, case crushing may appear similar in that damage has occurred on the contacting surface. It occurs on heavily loaded case-hardened parts, such as those which are case-carburized or nitrided. For example, failure often occurs on only one or two teeth of a pinion or gear. The other teeth appear to be undamaged. Often, longitudinal cracks appear on the surface and large, long pieces of the tooth surface break away. The general appearance suggests that the case material has chipped away in large flakes at a parting line just below the case-to-core junction.

Cracks originate at the subsurface when stresses exceed the strength of the subsurface material. The cracks propagate along the case-to-core boundary and to the surface of the gear tooth. When several cracks reach the tooth surface, large chunks of material are removed (Figure 39). Failures are caused by insufficient case depth or by very high residual stresses. Failures most often can be overcome by increasing the effective depth of the case material. A change in basic material can also be considered.

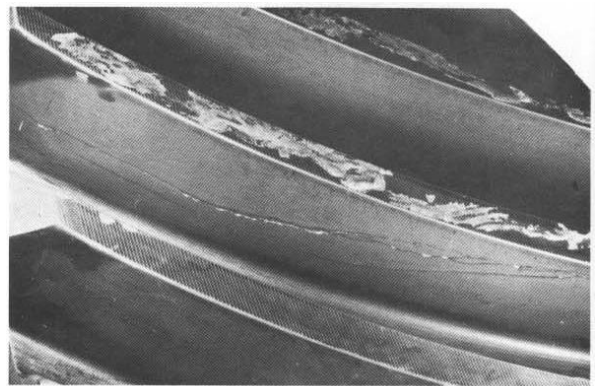


Figure 39: Example: Case crushing [13]

A phase after spalling is a peeled surface, as shown in Figure 40, produced by broken off pieces which may have been over rolled after pitting. This only occurs when lubrication is sufficient. Otherwise, fretting or seizure damage takes place.



Figure 40: Peeling [16]

3.4.2 Surface initiated fatigue

Surface initiated fatigue failure is a collective terms for all the cases where the secondary and major damage is due to surface distress. For satellite SRB of helicopter gearbox, this represents more than 60% of the observed damages at SKF. Various primary damages, such as wearing, bands, indentations, and micro-spall can be identified as the origin of surface initiated fatigue mode to subsequently cause a macro-spall due to insufficient lubrication.

It can be highlighted that the common root cause is the poor lubrication due to inappropriate running conditions not creating a sufficient oil film and surface separation. As a consequence, parts running in mixed or boundary lubrication conditions lead to micro-spalling followed by unavoidable indentations due to the polluted oil.

In its initial phase, the wear that then results has roughly the same effect as lapping. The peaks of the microscopic asperities that remain after the production processes are torn off. At the same time, a certain rolling-out effect is obtained. This gives the surfaces concerned a varying degree of mirror-like finish. At this stage, surface distress can also arise. If the lubrication is overly poor, the temperature will rise rapidly and the surfaces then show blue to brown discolouration bands. The coloured worn bands are not detrimental until this surface distress generates a primary surface initiated damage, as shown in Figure 41.



Figure 41: Example of worn and coloured bands on inner ring and outer rings [17]

The initial micro-spalling damage is not visible to the naked eye. A more advanced stage is marked by small, shallow craters with crystalline fracture surfaces. In later stages, micro-spalling is characterized by low depth material removal and high roughness area. Small cracks then form in the surfaces, known as surface distress. These cracks must not be confused with the fatigue cracks that originate beneath the surface and lead to flaking. The surface distress cracks are microscopically small and increase very gradually to such a size that they interfere with the smooth running of the part, as shown in Figure 42.

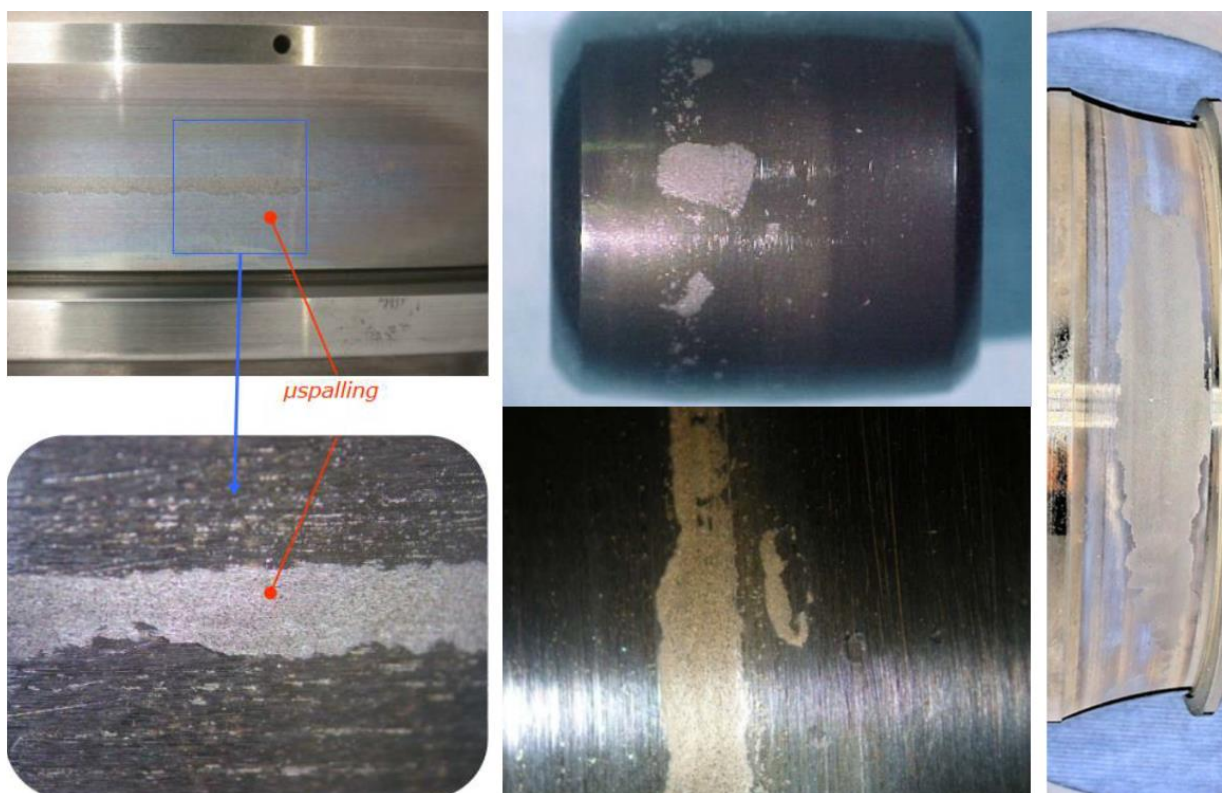


Figure 42: Micro-spalling and discolouration [17]

Another case is the small indentations as shown in Figure 43, which may be distributed around the raceways of both rings and on the rollers by foreign particles, and not necessarily hard ones.

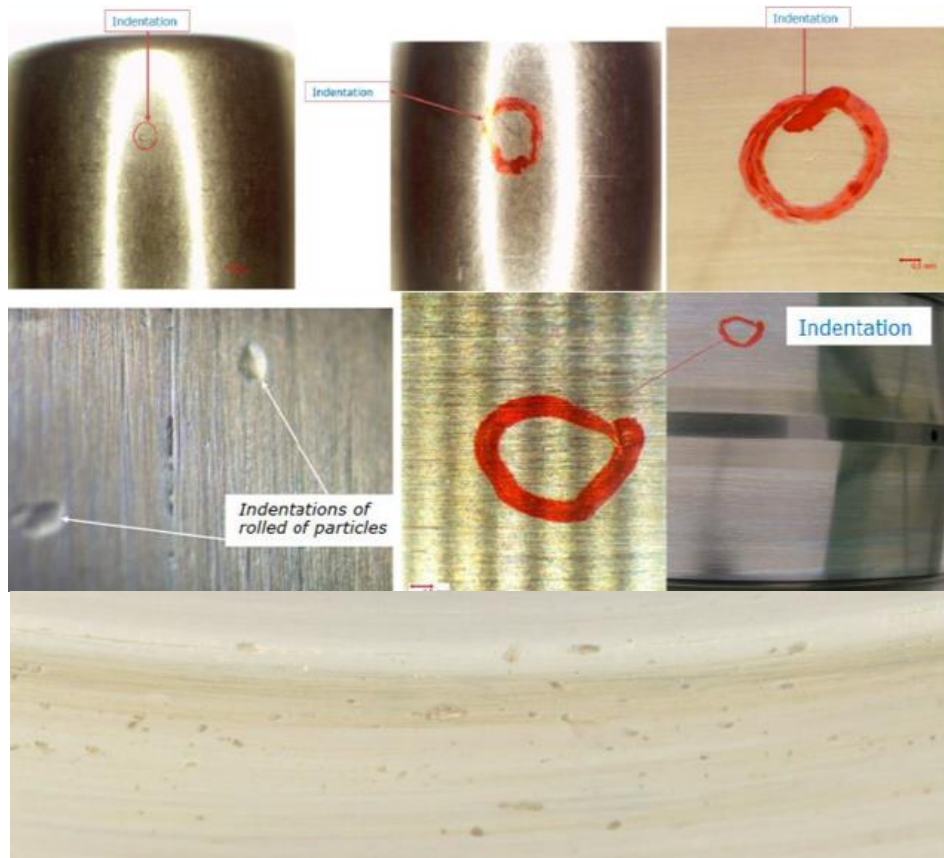


Figure 43: Indentation on raceway and roller due to foreign particles [17]

All these preliminary damages can lead to major defects. Several cases of severe spalling have been observed due to surface distress. Major flaking created from surface are characterized by the typical “V shape” at the initiation location as shown in Figure 44.

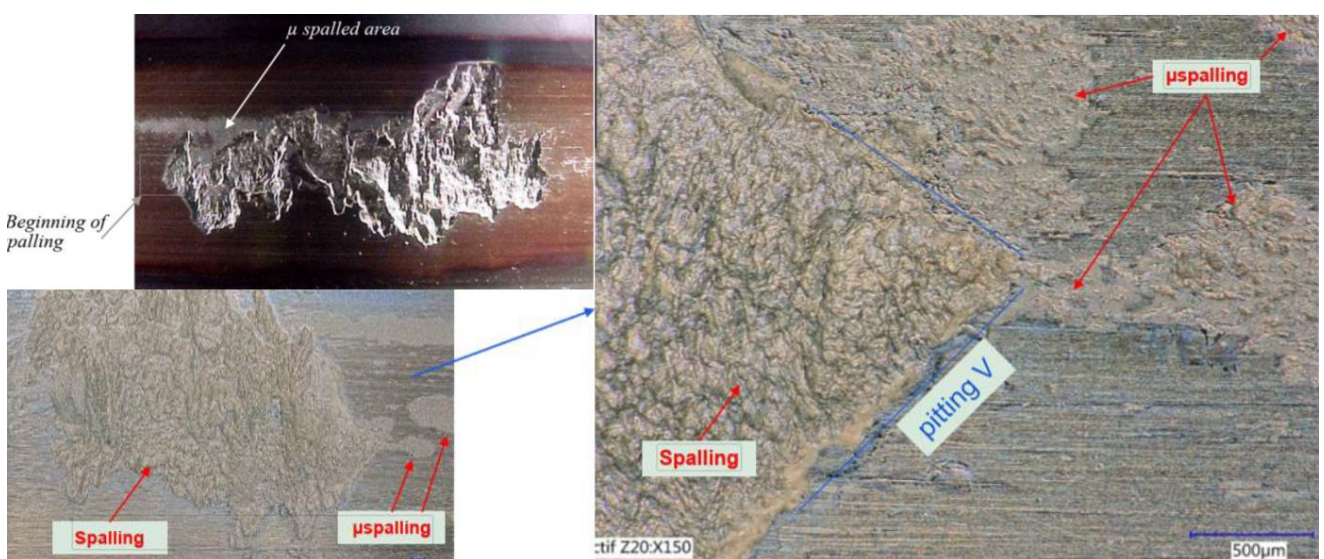


Figure 44: Massive spalling initiated by micro-spalling [17]

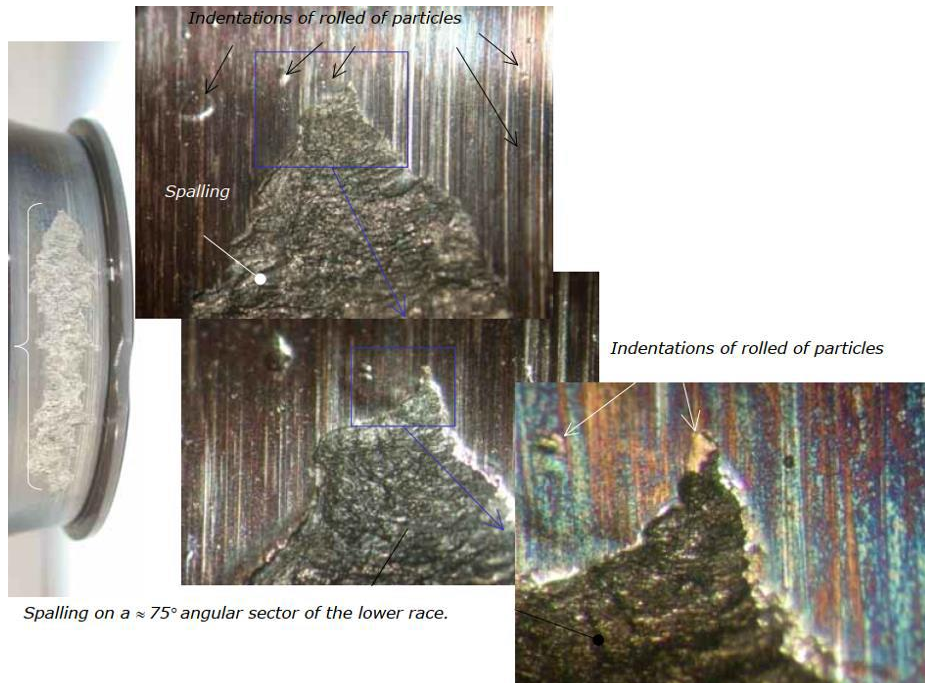


Figure 45: Massive spalling initiated by surface indentation [17]

It can also be noted that even if both inner and outer rings are running in poor lubrication conditions, the major failures mainly occur on the inner ring (~90% of SKF cases), more precisely on the upper row in cases of double row spherical roller bearing. Indeed, as already mentioned, the inner ring contact pressure is generally higher than that of the outer ring and the upper row's poor lubrication condition is worsened by the effect of gravity. Another issue is the management of the axial clearance as one of the key parameters in the design of the spherical roller bearings. Roller spalling could start from the roller-edge contact zone or from the roller edge/corner as shown in Figure 46. Indeed, the contact between the rollers and ring shoulders can induce very high stress and significant friction wear, rapidly leading to spalling. On the other hand, an overly large clearance can lead to excessive roller skewing and can induce ring surfaces to wear. This kind of interference could occur due to not adapting the design, so that the clearance between inner ring shoulders and rollers is not ensured. [17]

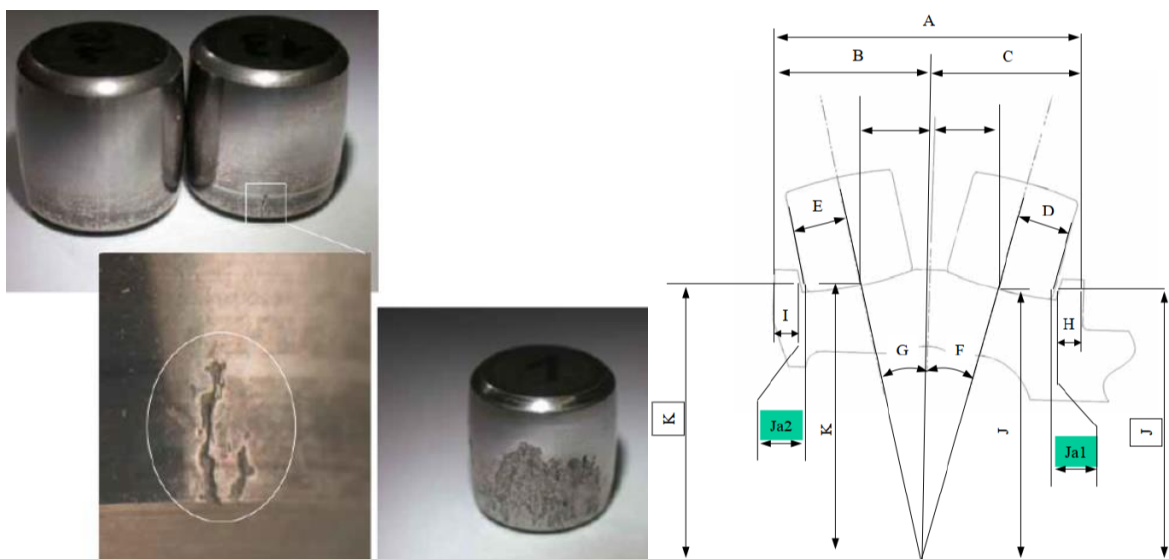


Figure 46: Example of roller spalling due to interference with the inner ring shoulder (left); Ja = Negative interference of the rollers with the inner ring shoulder (right) [17]

3.5 Permanent deformation

3.5.1 General

Generally, permanent deformation occurs whenever the yield strength of the material is exceeded, based on the contact load over a substantial portion of the contact or a foreign object rolled over by only a small part of the contact. [28]

3.5.2 Overload/True brinelling

Brinelling occurs when loads exceed the elastic limit of the ring material. Brinell marks appear as indentations in the raceways, which increase bearing vibration. Severe brinell marks can cause premature fatigue failure as well as any static overload, for example due to the assembly or disassembly of the part as is shown in Figure 47.



Figure 47: Careful handling and installation practices can minimize or eliminate true brinelling problems [14]

3.5.2.1 Brinelling

This kind of damage is critical due to the very high increase in radial play on helically cut gears. This can result in contact pattern displacement on the mating gears and can even ultimately lead to tooth failure caused by several vibrations. Figure 48 (left) shows clearly detectable recesses in the circumferential face, spaced identically to and caused by the roller bodies of the bearing. Another case is closely grouped rows of indentations, which can be seen and felt as shown in the middle of Figure 48. The right picture in Figure 48 shows brinelling in the bore of a helical gear mounted on a needle bearing. If the bearing only performs a supporting function over a longer period, i.e. there is no relative movement between the gear and the supporting shaft, the bearing contact areas may show signs of fretting corrosion.

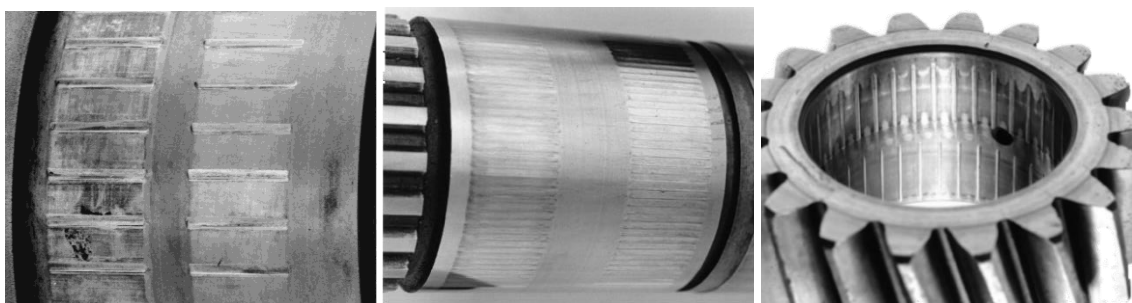


Figure 48: Recesses in the circumferential face (left); Fine brinelling marks (middle); Brinelling in the bore of a helical gear (right) [16]

3.5.3 Plastic flow

Plastic flow can be understood as a cold working of contact surfaces caused by high contact stresses and the rolling and sliding action of the parts. It is a surface deformation resulting from the yielding of the surface and subsurface material and is usually associated with the softer materials – although it often occurs in heavily loaded case-hardened and through-hardened gears. [13]

3.5.3.1 Cold flow

In this type of failure, the surface and subsurface material show evidence of metal flow, where surface material has been worked over the tips of the gear teeth giving a finned appearance, or the tooth tips are heavily rounded-over and a depression appears on the contacting surface as the contact stress is too high or the hardness of the material is too low. Under heavy load, the rolling and peening action of the mesh cold-works the surface and subsurface material. If the contact stresses are high enough, the sliding action tends to push or pull the material in the direction of sliding. The dents and battered appearance of the surface are the result of dynamic loading caused by errors produced during the manufacturing process, or by continuous operation while the profile is in the process of deteriorating from a combination of cold-working and wear as is illustrated in Figure 49.

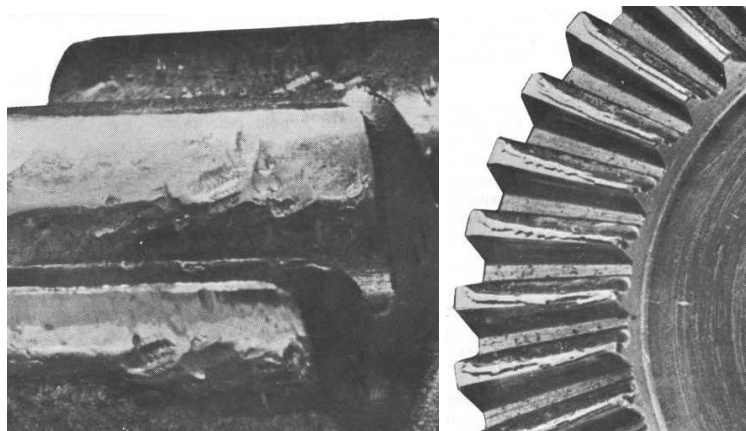


Figure 49: Examples: Cold flow [13]

3.5.3.2 Rippling

Rippling is a periodic wave-like formation at right angles to the direction of sliding or motion and is not always considered a surface failure unless it has progressed to an advanced stage. High contact stresses under cyclic operation tend to roll and knead the surface, causing the immediate subsurface material to flow. Slow-speed operation is usually associated with this type of failure because it does not build up adequate elastic-hydrodynamic film thickness. This combination of high contact stress, repeated cycles, and an inadequate lubrication film will produce a rippled surface with a fish-scale appearance is usually observed on hardened gear surfaces under certain conditions, as can be seen in Figure 50.

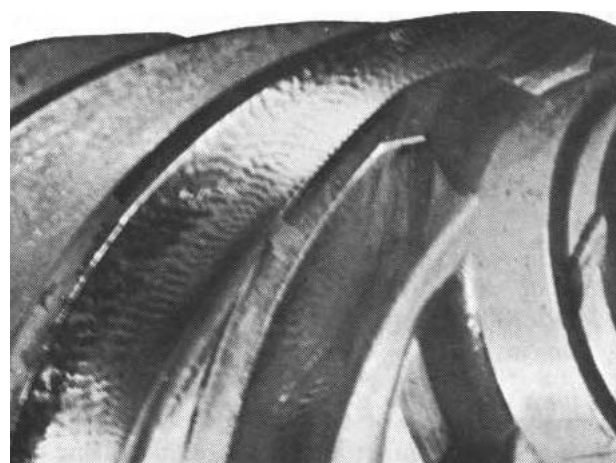


Figure 50: Example: Rippling [13]

3.5.3.3 Ridging

Ridging is caused by the plastic flow of surface and subsurface material due to high contact compressive stresses and high relative sliding velocities. It is often present on heavily loaded worm and worm wheel drives and on hypoid pinions and gear drives. Often, ridging exists on low-hardness materials but may also be present in high-hardness materials if the contact stresses are high, such as in case-hardened hypoid rear axles. The formation of deep ridges due to plastic flow of surface and subsurface material show definite peaks and valleys or ridges across the surface in the direction of sliding as seen in Figure 51.

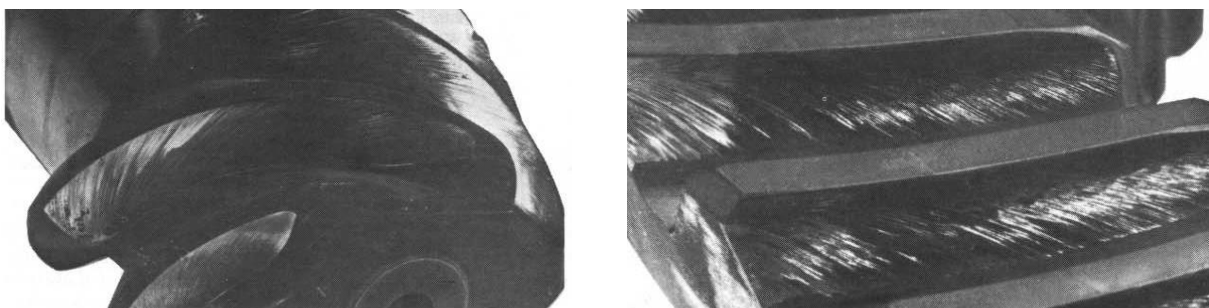


Figure 51: Examples: Ridging [13]

3.5.3.4 Polygon damage

Polygon profiles have more favourable loading properties than other profiles, but also have the disadvantage that they are susceptible to damage from high surface pressures at the contact points between shaft and hub. If overloading occurs, tremendous spreading forces are exerted. Figure 52 shows a spalled countershaft hub caused by overloading of the torque level. Considerable quantities of deposited material can be seen on the shaft.

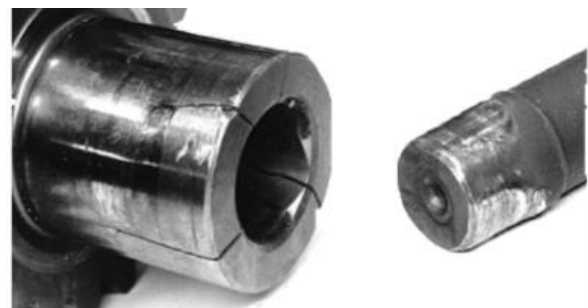


Figure 52: Polygon damage/hub breakage [16]

3.5.3.5 Overheating and thermal deformation

Insufficient or inadequate lubrication is primarily the basis for overheating, which causes a reduction in hardness and a greyish to bluish-black discoloration of the part and therefore scored or grooved flank wear in the direction of sliding. More extreme overheating causes greater distortion of the part, up to deformation as shown in Figure 53.

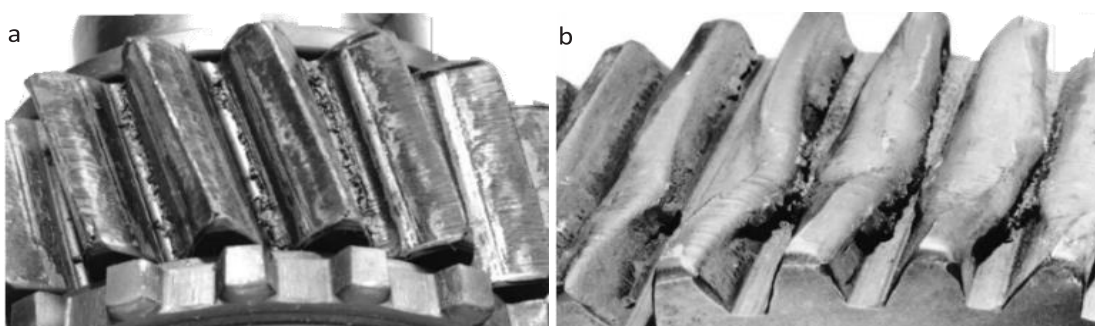


Figure 53: a) Gear, which has overheated as the result of a lack of oil. In this failure mode, there is blue or grey-black discoloration of the teeth. b) Thermal deformation of a gear caused by a lack of oil [16]

Ball bearings depend on the continuous presence of a very thin film of lubricant between the contact surfaces as well. If this is not the case, overheating and subsequent catastrophic failures may occur as shown by the discoloured example in Figure 54. The temperature rise can also degrade or destroy lubricant. Common influences are heavy electrical heat loads, inadequate heat paths, and insufficient cooling or lubrication when loads and speeds are excessive.



Figure 54: Lubricant failure will lead to excessive wear, overheating, and subsequent bearing failure [14]

3.5.4 Electrical power damage

In most cases, the initial cause of the craters due to electrical power damage is usually obscured or erased by subsequent relative flank movement and cannot therefore be identified. Similar damage may also occur on splines, caused by distinct relative flank movement in conjunction with dry friction. If several similar faults with these characteristics occur in a gearbox/assembly, this is a sure sign of electrical power damage. Figure 55 shows electrical power damage on the flank of a spur gear (left), flank damage on a spline caused by electrical power and subsequent relative movement (middle), and small craters on the contact surfaces due to electrical power (right).

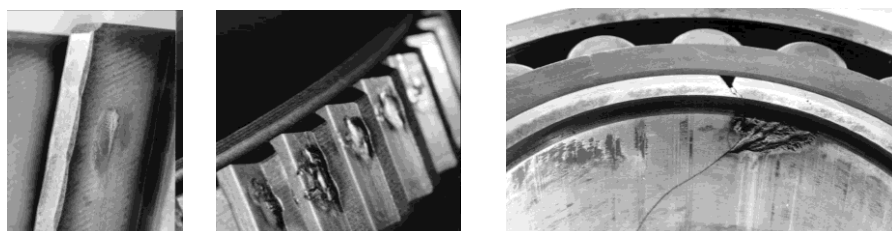


Figure 55: Electrical power damage [16]

In cases of lightning strikes, the sharp edges and corners on the rotors are primarily affected. Lightning enters and exits through the rotors. However, this can also lead to increasing vibrations, leakage, and failure of moving parts, especially various bearings. It leaves craters of various sizes as shown in Figure 56 (left) as well as metal wear such as pitting in the bearing tracks and on the faces of transmission gear teeth (Figure 56, right).

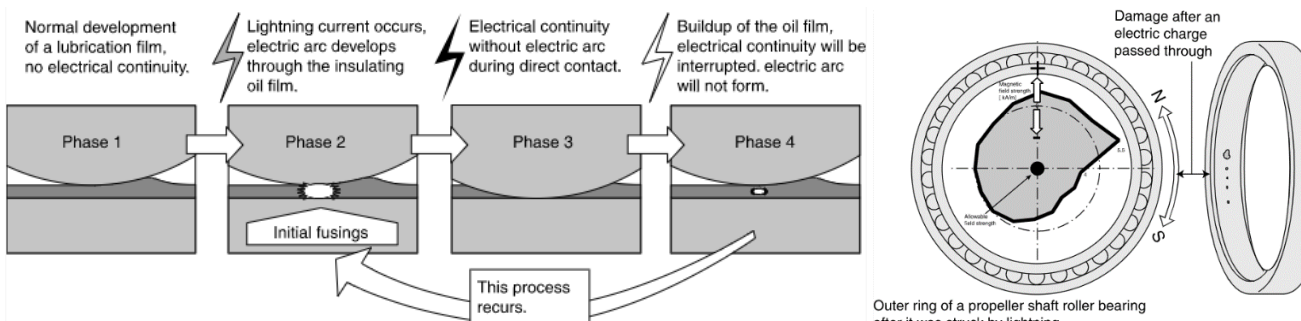


Figure 56: Initial fusions and positioning at the races of anti-friction bearings during electrical continuity (left) and characteristic traces (right) by lightning strike [31]

3.6 Fracture/Breakage/Cracking

Overload breakage occurs when stress is applied and increased continuously until failure occurs, which typically happens at the point of applied stress reaching material's ultimate strength. This breakage pattern can be identified on most materials by means of the rough, fine to coarse-grained, irregular and partially striated failure surface.

The majority of fatigue breakages on machine components are due to stress concentrations at the failure points. Repeated excessive loadings at these stress concentration points can gradually lead to "fatigue" of the material, leading in turn to vibration-induced or fatigue breakage. In this instance, the load is reciprocating in nature, i.e. the stress alters periodically or non-periodically in accordance with size and direction over time. Cracking propagates with each new stress peak. Failure culminates in an overload breakage of the residual cross section. In contrast to overload breakage, a fatigue breakage can usually be identified by the flat, smooth, shiny breakage surface, frequently also covered with fine lines.

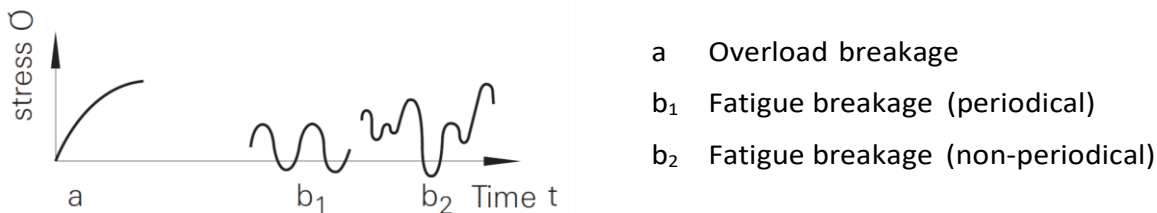


Figure 57: Chronological sequence of stress pattern under differing types of stress [16]

3.6.1 Fatigue breakage

As visible in Figure 58, the surface of a bending broken part consists of two different zones. One has a finely structured velvety or powdery fatigue breakage surface while the other has a grainy, rough residual breakage surface. The fatigue breakage surface is located on the side with the highest load. The proportion of the fatigue breakage surface area to the entire breakage surface area is influenced by the load condition. A large fatigue breakage surface area points to an overall low load level, with individual peak loads causing the fracture. On the other hand, the fatigue breakage surface area is small if the overall load level is high.

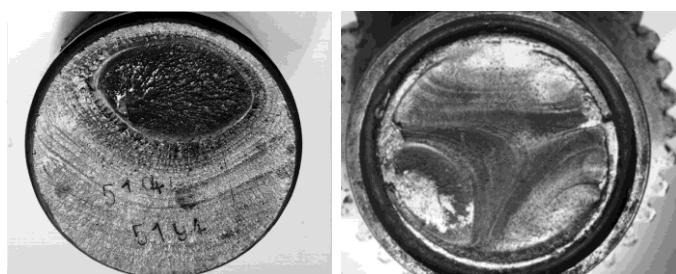


Figure 58: Bending breakage and cyclic bending breakage [16]

Figure 59 (left) shows a gear-tooth failure from bending fatigue, which generally results from an origin point in the root section of the gear tooth. The break shows signs of fretting and conventional smooth beach marks in the break area that may be caused by various impacts such as excessive loads, which result in stresses higher than the endurance limit of the material. Additionally, stress risers (notches in the root fillet, hob tears, inclusions, small heat-treat cracks, grinding burns and residual stresses) help aggravate this condition and subject a gear to higher root stress levels than would normally be predicted. This failure can be prevented by means of the design and the material, but also with manufacturing processes such as heat treatment to achieve

the best structure and to minimize detrimental residual stresses. An adjustment to the root fillet area is helpful as well, to prevent such cracks as shown in Figure 59 (right).

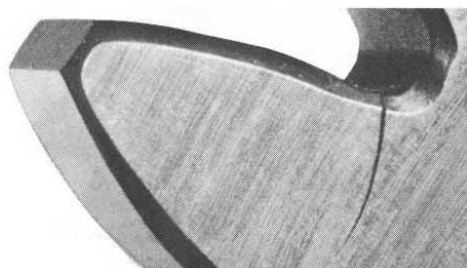
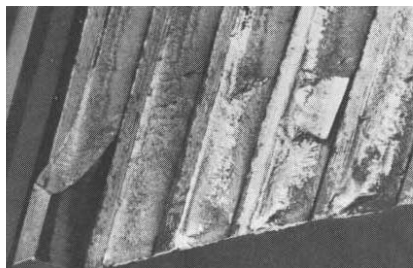


Figure 59: Example: Bending fatigue [13]

The rim of a gear usually fails between two adjacent teeth, and the crack propagates through the rim and into the web as shown in Figure 60, often caused by flexure stresses in the gear teeth and highly loaded thin rims and webs. Sometimes cracks appear in the web near the rim and web junction without disturbing the rim itself. Web cracks may be caused by stress risers, from holes in the web or web vibrations. If vibration is not the cause or the cause cannot be eliminated, both scenarios can be prevented by increasing its thickness in order to eliminate the stress level.

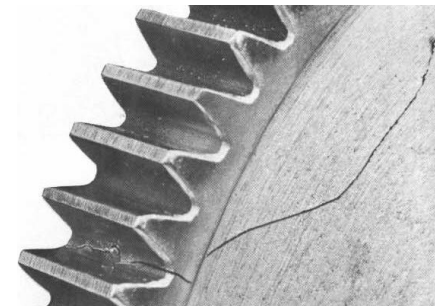


Figure 60: Example: Rim and web failure [13]

Torsional bending fatigue breakages, which are caused by high loading conditions such as failure of other components in the transmission or driveline, accident, operating faults, and functional errors. The breakage works towards the center of the shaft cross-section. Eventually, the breakage proceeds to such an extent that the remaining sound cross-section can no longer withstand the torque to be transmitted and fails as shown in Figure 61.

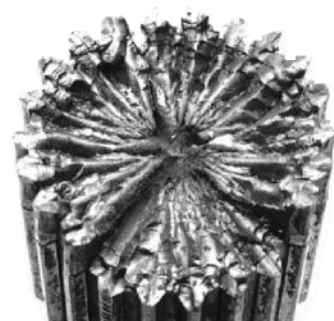


Figure 61: Bending breakage through torsion [16]

Other example of fatigue failure is the failure of bearing cages as a result of vibrations, which may be cause by different issues, e.g. imbalance on the shaft. The damage is not induced by the bearing itself and leads to failure of the bearing due to hairline cracks which propagate until the cage cracks fully through as shown in Figure 62.



Figure 62: Cage breakage [16]

3.6.2 Overload breakage

An overload fracture results in a stringy, fibrous break showing evidence of having been pulled or torn apart. In harder materials, the break has a finer stringy appearance but still shows evidence of being pulled apart abruptly. An example of tooth breakage caused by overload which exceeds the tensile strength of the gear material is shown in Figure 63 and may result from a bearing seizure, failure of driven equipment, foreign material passing through the mesh, or a sudden misalignment from a failed or wiped gear bearing.

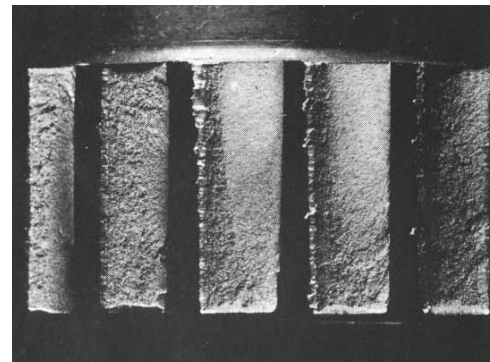


Figure 63: Example: Overload breakage [13]

An example of a broken bearing collar is shown in Figure 64 (left) and caused by excessive load or torque peaks based on seizure, breakage of other transmission or driveline components, accident, operating errors or influence of shaft. [16]

Another example where a breakage occurs in the area under highest stress on a housings (bearing points, idler gear, transmission mountings, webs, hubs), is visible in Figure 64 (right), caused by shaft imbalance, excessive deflection strains in driveline, vibrations, shock loads, and/or alternating loads.



Figure 64: Example of an overloaded/broken bearing collar (left) and housing (right) [16]

In the case of breakage due to bending the surface is finely grained in the edge zone. Beneath this zone, the surface is rough and striated (Figure 65). Classical bending overload failures seldom occur in practice, failure is frequently a combination of the features described above.

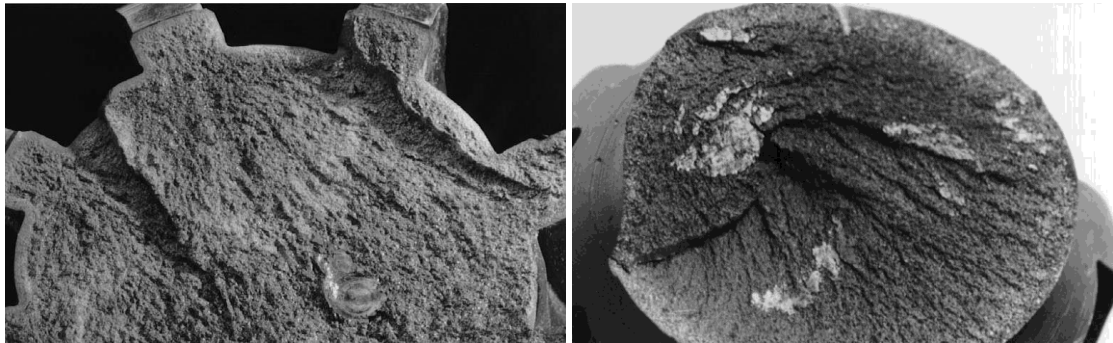


Figure 65: Bending overload failure [16]

In the case of breakage due to torsion the surface is rough and frequently fibrous. In the edge zone the breakage structure is finer as shown in Figure 66.

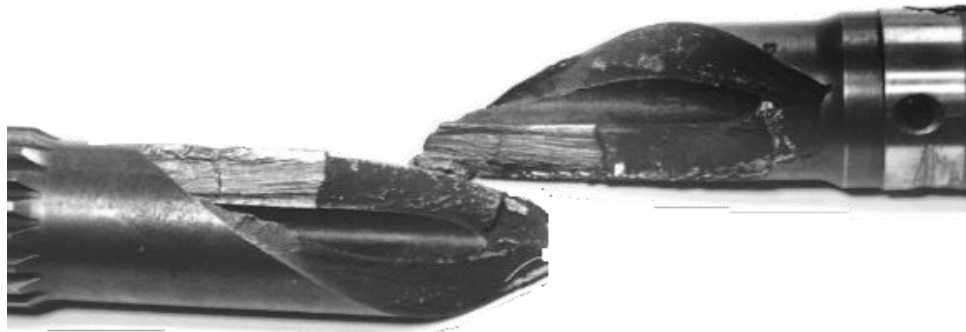


Figure 66: Breakage through torsion [16]

Gear-tooth breakage is usually associated with the root-fillet section of the gear tooth. Failures of this kind are often caused by deficiencies in the gear tooth, which result in a high stress concentration at a particular area that cause local fractures as shown in Figure 67.

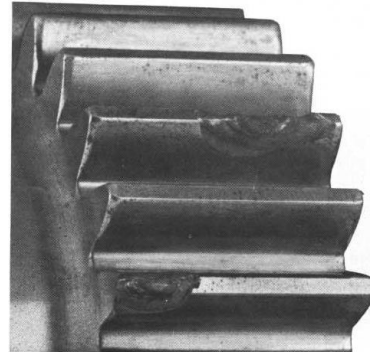


Figure 67: Example: Tooth tip Breakage [13]

3.6.3 Contributing manufacturing defects

In most cases of material flaws and linear slag inclusion, there is a single crack right through the cross section of a gear tooth and occasionally penetrating into the gear body. This fault commonly affects several adjacent teeth at once. Figure 68 shows a) tooth breakage on a spur gear as a result of forging wrinkles and b) cracks in the flank resulting from an accumulation of non-metallic impurities, linear slag inclusions, or other non-metallic impurities or forging wrinkles.

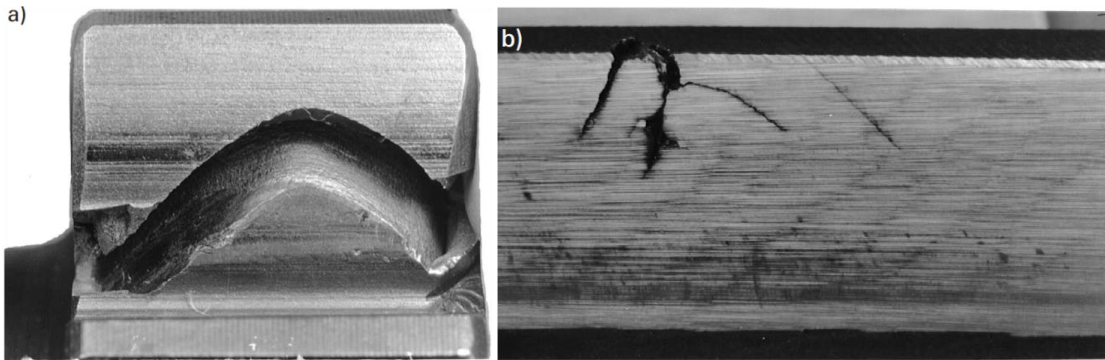


Figure 68: a) tooth breakage; b) cracks in the flank [16]

Another contributing defect is hardening cracks which occasionally occur as transformation stress cracks on case-hardened steels with a high alloy content, where linear cracks frequently covering large areas. Figure 69 (left) shows hardening cracks on a Cr-Ni-Mo steel with a higher alloy content caused by transformation stresses produced during the air cooling process following carburization. In case-hardening steels with a high alloy content, structural transformations which take place in the core during the air cooling process following carburization may cause substantial tensile stresses in the rim zone. Hardening cracks occur if these stresses exceed the tensile strength.

Grinding burns may be regarded as a preliminary stage leading to grinding cracks. These can only be detected by means of special test methods. The surface hardness is usually reduced around the grinding burn zones. Grinding cracks are cracks in the ground flanks which, as a rule, form a pattern and are so fine that in most cases they can only be detected by means of crack testing methods. They will be followed by premature pitting or cracks if not observed. Figure 69 (middle) shows grinding burns made visible by nital etching and grinding cracks (right) in a network configuration, which are a result of an incorrect grinding technique.



Figure 69: Hardening cracks (left), grinding burns (middle) and cracks (right) [16]

Spot-like elevations on the tooth flank are called scaling. Under load conditions in a transmission, these local elevations are smoothed down and soon develop a metallic polish.

3.7 Compilation of observed in-service damages

3.7.1 Compilation of gear damage occurring during operational service and the observed causes

Table 3 and Table 4 distinguish between major causes (◆) and minor causes (✗) based on ZF experience regarding gearing. This distinction is based on the significance of the role played by the cause. Excessive load, incorrect heat treatment, or material may cause almost all these types of damage. However, they are only specified as a cause of damage if they constitute the primary cause. [16]

Possible cause	Damage in Service	Overload breakage	Fatigue breakage	Tooth tip breakage	Hub breakage	Scratches (no damage)	Scoring	Abrasive wear	Plastic flow
Overload (once or infrequent)		◆							
Overload (frequent or continuous)			◆						
Low peripheral speeds									◆
High peripheral speeds									
Micro movement									
Specific sliding action						X	X	X	
Flank damage (pitting, spalling)				X					
Contact pattern displacement ¹⁾	X	X	◆						
Inadequate backlash							X		
Notches (e.g. oil ducts)		X			X				
Shrinkage stress (e.g. close hub fit)		X			◆				
Inadequate root radius		X			X				
Grinding burns		X	X						
Grinding notches		X							
Flank roughness						X	X		
Incorrect heat treatment	X	X							
Forging folds, inclusions, etc.	X		X						
Unsuitable viscosity						X	◆	X	X
High oil temperature							X		
Oil ageing									
Unsuitable oil additives							X		X
Inadequate lubrication							X		
Impurities (solids)						◆		◆	
Water in the gearbox									

1) caused by tilting of the idler gear, shaft deflection, interference, tooth correction or geometry defects

Table 3: Summary of gear damage analysis by ZF occurring during operational service (1/2) [16]

Possible cause	Damage in service	Friction Corrosion	Brinelling (rippling)	Destructive Scoring (Scuffing)	Grey staining (frosted area)	Pitting	Spalling	Overheating, thermal deformation	Corrosion
Overload (once or infrequent)				X					
Overload (frequent or continuous)						◆	◆		
Low peripheral speeds			X			X			
High peripheral speeds				X					
Micro movement	◆								
Specific sliding action			X	X	X	X	X		
Flank damage (pitting, spalling)									
Contact pattern displacement ¹⁾						X	X		
Inadequate backlash				X					X
Notches (e.g. oil ducts)									
Shrinkage stress (e.g. close hub fit)									
Inadequate root radius									
Grinding burns				X		X	X		
Grinding notches									
Flank roughness				X	◆	X	X		
Incorrect heat treatment						X	X		
Forging folds, inclusions, etc.									
Unsuitable viscosity		X	X	◆	X	X			
High oil temperature			X	X	X	X	◆		
Oil ageing				X		X	X		X
Unsuitable oil additives		◆	◆	◆	X	X			X
Inadequate lubrication	X	X							
Impurities (solids)								◆	
Water in the gearbox									◆

1) caused by tilting of the idler gear, shaft deflection, interference, tooth correction or geometry defects

Table 4: Summary of gear damage analysis by ZF occurring during operational service (2/2). [16]

3.7.2 Compilation of bearing damage occurring during operational service and the observed causes

In addition to the observed gear damages in 3.7.1, Table 5 gives an overview of the observed damages of failure modes at SKF aerospace on planet bearings. Table 6 shows an analysis of rolling bearings in general [28]. Insufficient lubricant, manufacture processes, design and adjacent parts, as well as operating conditions and maintenance may cause these types of damage.

Failure mode		% of observed damages	Possible causes according to ISO 15243							Oil of test
			Lubricant		Bearing Manufacture		Design and adjacent parts	Operating conditions and maintenance		
			Not enough lubricant	Solid contamination	Liquid contamination	Material, heat treatment	Machining and assembly	Inappropriate fits and tolerances	Inappropriate storing condition	Vibration excitation
Rolling contact fatigue	Subsurface initiated fatigue	3					Spall due to grinding burn			
	Surface initiated fatigue	43	Worn surfaces + discoloration					Roller edge spalling		
		0	Microspalling							
Wear	Abrasive wear	17	Cage wear	Cage wear						
	Adhesive wear		Cage wear	Cage wear		Coating failure or early wear				
Corrosion	Moisture corrosion	3			Corrosion			Corrosion		
	Frictional corrosion: Fretting	3						Fretting (not clearly identified)		Fretting (not clearly identified)
Electrical erosion	Frictional corrosion: False brinelling	0								
Plastic deformation	Overload deformation	0								
	Indentation from particles	27		Surface dents / indentation						
Cracking and fracture	Forced fracture	3								Roller breakage
	Fatigue fracture									
	Thermal cracking									

Table 5: Planet bearing failure mode analysis from SKF aerospace [17]

Table 6: ISO 15243 bearing failure mode analysis [28].

4. In-service and MRO experience

4.1 In-service experience

During literature survey and analysis of public available data and documentation, some relevant examples of incidents and accidents were found involving MGB failures which led or may have led, under different circumstances, to catastrophic failure. All the events found correspond to design with epicyclic architectures. In contrast to that, no catastrophic failure coming from the MGB used within collector architectures, were noticed. All summarized events and their assessment that are presented in the following part of this report are only taken over from above mentioned public sources. No rating of these events, linked root cause analysis or assessment performed has been rated by ZFL additionally. The given experience has been taken into account and used as valuable input for further described analysis in chapter 5.

However, the most studied catastrophic incidents are a result of), environmental conditions (e.g. weather) and/or human error (e.g. loss of awareness [36], lack of experience [37]) or happened during training ([38].

In [35] an accident is described involving a news H/C during a repositioning flight back to the home base after the original traffic surveillance mission had to be aborted due to a camera malfunction. The H/C crashed into the front yard of a house in a Buenos Aires residential area and was destroyed on impact, which was vertical with no or very low forward speed, and by the resulting fire. The statement that the main rotor speed was very low is based on the failure signature of the MR blades as well as witness statements and a slap mark on the roof. Impact and scratch marks on the tail rotor blades reveal that the tail rotor was turning at substantial speed. Finally, it was found that the sun gear of the planetary stage of the transmission has lost all its teeth, which could be found deposited in the ring gear, having been shifted there by the planetary gears. Therefore the MR drive was able to disconnect.

Furthermore, all components of the planetary gear stage showed heavy corrosion. Turning over the bottom of the main transmission revealed that only water and practically no oil was trickling out. The chip detector and its housing had accumulated an excessive amount of debris. All nozzles of the oil spray ring, which supplies the planetary stage, were found to be blocked. The oil filter contained an excessive amount of debris, as did the oil pump. It was assessed that the excessive amount of debris and deposits had accumulated in the oil system over time and finally interrupted the lubrication of the planetary stage. Without proper lubrication on the sun gear, it finally failed, depriving the main rotor of drive from the engines.

Similar damage on the sun gear was observed in [34], where an offshore H/C of the type of BO 105 DBS-4 crashed into the water of the Gulf of Mexico. The sun gear was completely damaged, without any gear teeth residue and showing signs of high temperature. The other gears of the planetary stage had signs of high temperature as well, although none of the teeth were broken but rather heavily deformed. Dark deposit and blocked nozzles were additionally found. Finally, the large metallic parts in the ring gear teeth had affected the gear mesh between the ring gear and planetary gears as well as the free rotating of the rotor mast. So, the lack of gear mesh between sun gear and planetary gears interrupted/disconnected the main rotor drive.

In [33] an H/C made an emergency landing due to a bang followed by a jolting sensation and a loud, grinding, "metal on metal" sound accompanied by vibration. Upon disassembly of the upper housing of the main transmission it was quickly found that the cause of the grinding sound was an interruption of the main rotor drive train due to the failing of the planetary stage of the main transmission. The sun gear in particular was found to be damaged beyond recognition and had no more teeth.

The root cause of the transmission failure was detected to be the production of fine abrasion and particles on at least one of the planetary axles, which had deteriorated over time and subsequently polluted the lubrication system with (ferro-magnetic) debris. It is assumed that originally the deterioration of one (or more) of the

planetary axles was initiated and/or aggravated by the influence of corrosion, which was the result of a very long period of non-operation/storage of the helicopter (nearly 4 years) without the necessary preservation as mandated by the maintenance manual. Transmission “health monitoring” is carried out by periodic inspection of a magnetic plug. This is a method widely used in aviation and well proven for the BO 105 helicopter fleet which has accumulated more than 6 million flight hours. Especially after a long time period of non-operation it is of utmost importance to adhere to the correct procedure of magnetic plug inspection. Taking the nature and amount of the particles into account, which have to be assumed of being produced by wear and deterioration of the affected parts, it is fair to state that the chip detector system would have indicated unusual wear and imminent failure well in advance. So in summary, incorrect maintenance and disregard or lack of knowledge of aviation practices have to be seen as the root cause of this main transmission malfunction.

The most prominent catastrophic failure in-service is described in [19]. The LN-OJF failure scenario has been identified as the structural degradation of a second stage planet gear, a critical part in which subsurface cracks developed undetected to the point of catastrophic fatigue failure. The fatigue fracture initiated from a surface micro-pit in the upper outer race of the bearing, spreading to the subsurface while producing a limited quantity of particles from spalling before turning towards the gear teeth and fracturing the rim of the gear. The investigation has shown that the combination of material properties, surface treatment, design, operational loading environment, and debris gave rise to a failure mode which was not previously anticipated or assessed.

The LN-OJF accident has clear similarities to the G-REDL accident [18] off the coast of Scotland in 2009. But there are some differences between the two accidents and the subsequent investigations. Both MGBs had identical epicyclic modules and second stage planet gears, and in both accidents one of the eight second stage planet gears in the epicyclic module fractured as a result of fatigue. For G-REDL, only around two thirds of the failed planet gear was recovered and the origin of the crack was in a section of the failed gear which was not found. Consequently the precise origin and nature of the fracture could not be determined. For LN-OJF, there was more background information available both from the previous incidents and because the part of the planet gear in which the fracture initiated was recovered.

G-REDL was an AS 332 L2 helicopter and LN-OJF was an EC 225 LP helicopter. Each EC 225 LP planet gear takes 12 to 14% more load than each of the AS 332 L2 planet gears. The helicopters had nearly identical main rotor gearboxes, with the significant exception that the AS 332 L2 at that time had a different MGB configuration with the ring of magnets installed on a particle collector between epicyclic module and main module. The G-REDL investigation concluded that the ring of magnets probably trapped released debris from the epicyclic module and reduced the likelihood of detection. The ring of magnets was removed from AS 332 L2 and EC 225 LP helicopters as a direct result of the G-REDL accident. Another difference was that LN-OJF had a magnetic particle detector in the conical housing connected to the cockpit warning system, whereas the corresponding detector in G-REDL was connected to the HUMS and, therefore, accessible only after the flights.

In contrast to LN-OJF, there was indication of impending failure of the second stage planet gear in G-REDL. Some 36 flying hours prior to the G-REDL accident, a magnetic particle had been discovered on the epicyclic chip detector during maintenance. Unfortunately, due to misunderstanding or miscommunication between the operator and Airbus Helicopters, the chip was misinterpreted and the MGB was not opened following the discovery of the particle. The particle was not recognized as an indication of degradation of the second stage planet gear, the same gear that subsequently failed. After this single chip detection, the detection methods existing at the time did not provide any further indication of degradation of the second stage planet gear.

Because the parts of the planet gear in which the fracture initiated were recovered from LN-OJF, the AIBN/QinetiQ investigation was able to document the full extent of the crack, i.e. the initial micro-pit and subsurface crack formation. In the G-REDL, AAIB UK/QinetiQ did not have the initial part of the crack and could only make assumptions regarding crack initiation and propagation.

The G-REDL report included a stress model prediction for crack growth in the section of the planet gear which was not recovered. The crack propagation underneath the depth of the carburized layer in the retrieved second stage planet gear from the LN-OJF accident appears to be very similar to the G-REDL stress model prediction of

crack growth (Figure 70). The LN-OJF gear segment closely resembles the estimated states of the missing gear part from G-REDL. Figure 71 shows the FTA of the G-REDL accident prepared in [43].

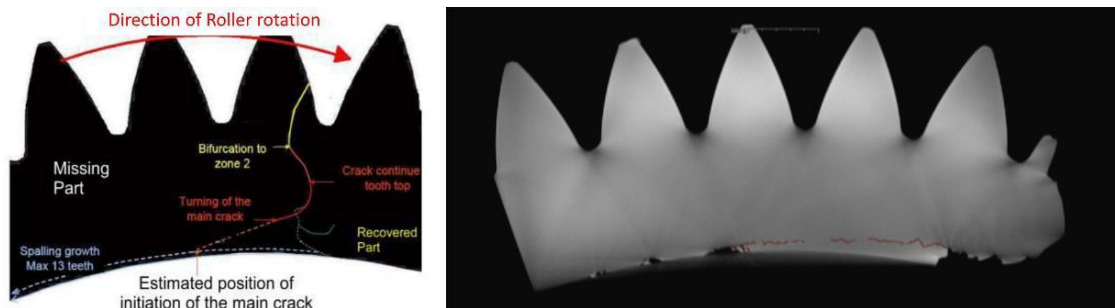


Figure 70: Stress model estimation of crack growth from the G-REDL accident at left, compared with the CT scan from the LN-OJF gear with the crack in red

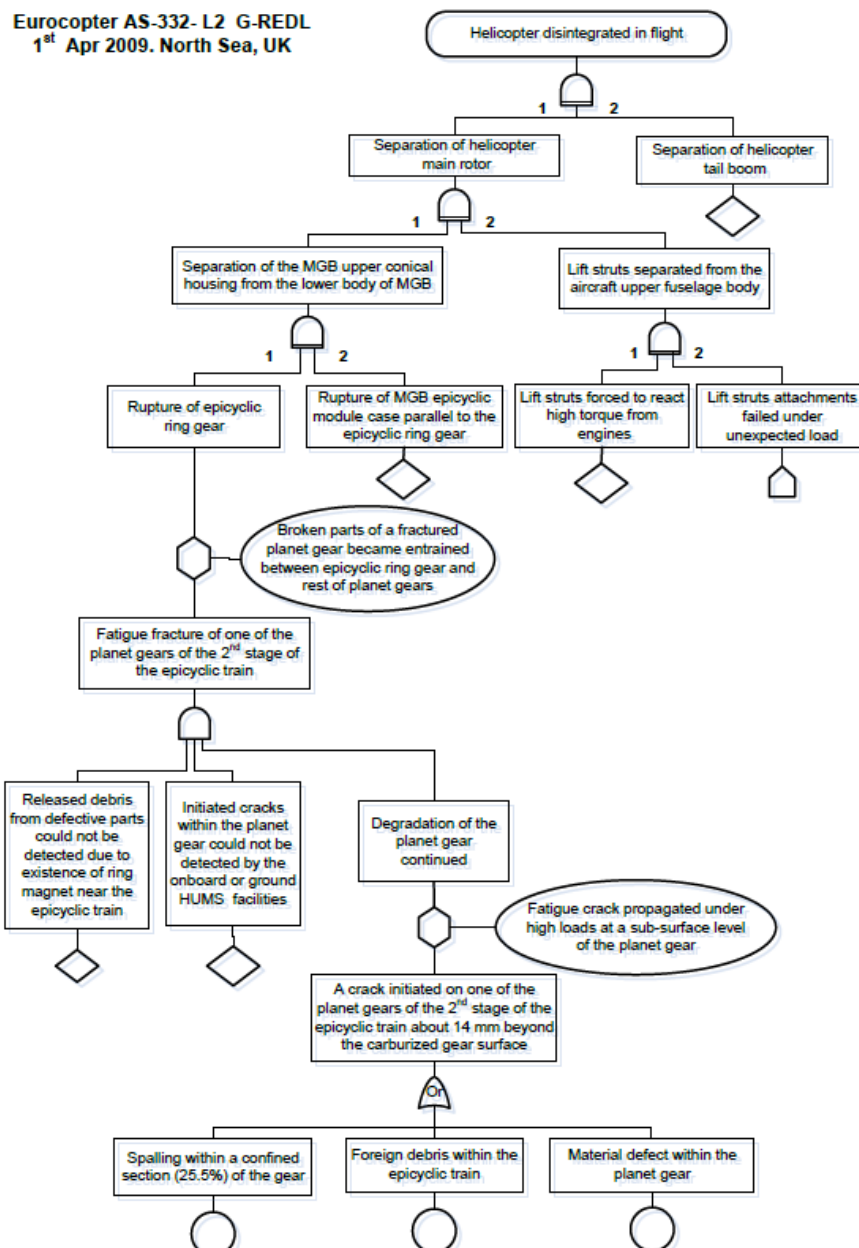


Figure 71: FTA of the G-REDL [43]

As described in [39], while operating over the North Sea in daylight, the crews of G-REDW and G-CHCN describe experiencing a loss of main rotor gearbox oil pressure, which required them to activate the emergency lubrication system, and shortly afterwards it became necessary to ditch their helicopters immediately in the North Sea.

The loss of oil pressure on both helicopters was caused by a failure of the bevel gear vertical shaft in the main rotor gearbox, a component which drives the oil pumps. The shafts had failed as a result of a circumferential fatigue crack in the area where the two parts of the shaft are welded together.

On G-REDW, the crack originated from a small corrosion pit on the countersink of the 4 mm manufacturing hole in the weld. The corrosion probably resulted from the presence of moisture within the gap between the PTFE plug and the countersink. The shaft on G-REDW had accumulated 167 flying hours since new.

On G-CHCN, the crack originated from a small corrosion pit located on a feature on the shaft described as the inner radius. Debris that contained iron oxide and moisture had become trapped on the inner radius, which led to the formation of corrosion pits. The shaft fitted to G-CHCN had accumulated 3,845 flying hours.

The stress in the areas where the cracks originated was found to be higher than that predicted during the certification of the shaft. However, the safety factor of the shaft was still adequate, providing there were no surface defects such as corrosion.

The emergency lubrication system operated in both cases, but the system warning light illuminated as a result of an incompatibility between the helicopter wiring and the pressure switches.

The following causal factors were identified in the ditching of both helicopters:

- a. A 360° circumferential high-cycle fatigue crack led to the failure of the main gearbox bevel gear vertical shaft and the loss of drive to the oil pumps.
- b. The incompatibility between the aircraft wiring and the internal configuration of the pressure switches in both the bleed-air and water/ glycol (Hydrosafe 620) supplies resulted in the illumination of the MGB EMLUB warning.

The following factors contributed to the failure of the EC225 LP main gearbox bevel gear vertical shafts:

- a. The helicopter manufacturer's Finite Element Model underestimated the maximum stress in the area of the weld.
- b. Residual stresses introduced during the welding operation were not fully taken into account during the design of the shaft.
- c. Corrosion pits were present on both shafts from which fatigue cracks originated:
 - I. On G-REDW the corrosion pit was located at the inner countersink in the 4.2 mm hole and probably resulted from the presence of moisture within the gap between the PTFE plug and the countersink.
 - II. On G-CHCN the corrosion pit was located at the inner radius and probably resulted from moisture trapped within an iron oxide deposit that had collected in this area.

[32] describes an accident of a Wessex Mark 31B H/C. After recovery of the aircraft from the sea, the cause of the crash was attributed to the catastrophic failure of the input spiral bevel pinion in the main rotor gearbox. Metallurgical investigations revealed that the pinion failed because of a fatigue crack, which started at a subsurface inclusion near the root of one of the teeth. The crack progressed radially into the gear before growing axially fore and aft (Figure 72), probably over a period of several hundred flying hours. When the crack reached the neck of the gear, it changed direction and moved circumferentially around the gear. During this phase, growth was much more rapid and it is believed that the crack may have travelled around a large part of the gear in as little as 20 minutes until final overload failure occurred.

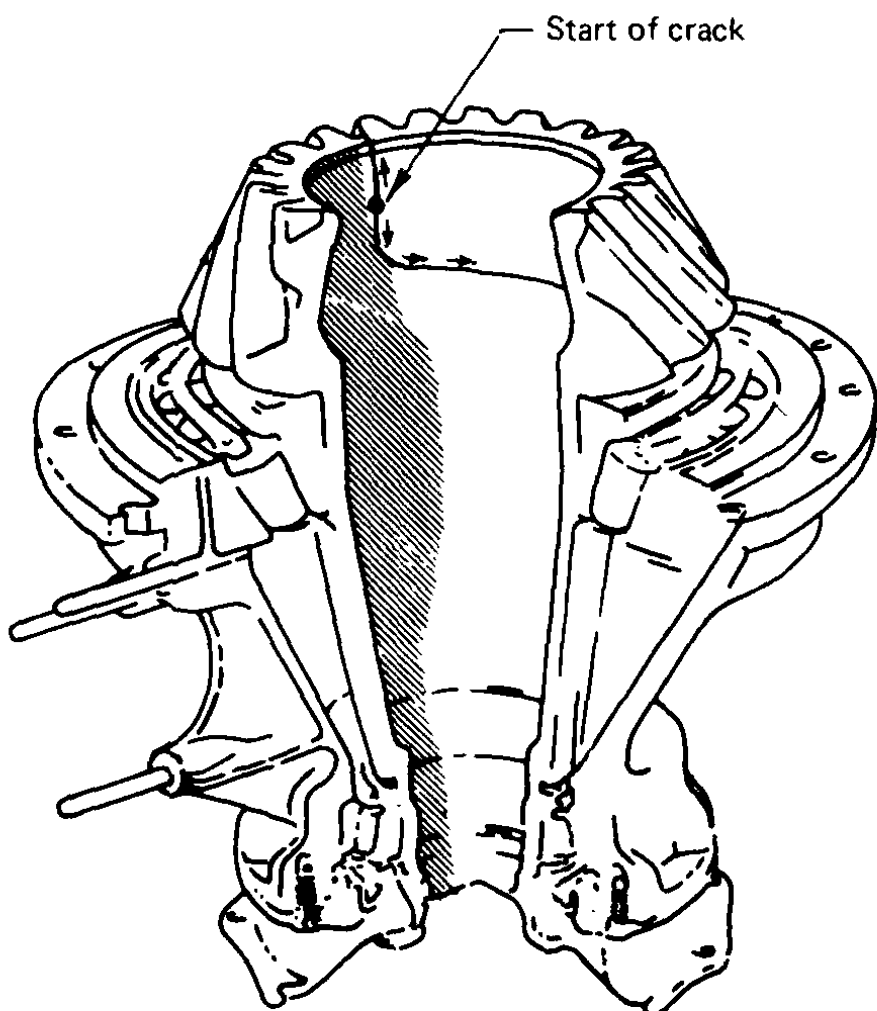


Figure 72: Path of the fatigue crack in the pinion

In [40] an accident of a Sikorsky S-92A is described. On the helicopter involved, the nuts and studs supporting the filter bowl of the MGB lubrication system had accumulated sufficient galling damage to prevent the correct preload from being applied during installation.

Titanium alloy surfaces are susceptible to galling under conditions such as the removal or installation of a nut. Every time this operation is repeated, the damage becomes more severe. The presence of grey paint found on the MGB oil filter bowl attachment nuts inspected after the accident demonstrates that the original nuts were in use, although according to an AMM revision, new nuts should have been installed.

When galling occurs, friction increases. As a result of this increased friction, the torque was not converted into bolt preload. The reduced preload lead to an increase of the cyclic load experienced by the studs during operation and to the generation and propagation of fatigue cracks. Fatigue cracking then developed in a second stud due to increased loading resulting from the initial stud failure. The two studs broke during cruise flight, resulting in a sudden loss of oil in the MGB.

The disassembly of the MGB led investigators to conclude that the loss of lubrication oil caused a catastrophic failure of the tail take-off pinion, which resulted in the loss of drive to the tail rotor shafts.

The helicopter's MGB operated for approximately 11 minutes after the total loss of lubricating oil pressure. Examination of the MGB components showed damage due to frictional heating caused by continued operation without oil. This frictional heating led to the plastic collapse of the tail take-off pinion's teeth, eventually causing the loss of drive to the tail rotor shafts (Figure 73).



Figure 73: Damaged tail take-off pinion (right) in comparison to a new one (left)

There was no indication of component seizure that would have prevented the main rotor from free-turning at the time of impact. The tail take-off pinion shaft is held in position in the radial and axial directions by two tapered roller bearings and these bearings had damage consistent with operation under inadequate lubrication conditions.

This is a different failure than the one experienced during the initial certification test, where the loss of lubrication oil caused a catastrophic failure of the sun gear resulting in the loss of drive to the main rotor. However, the MGB was not being operated under the same parameters as those used during the initial certification test. Therefore, it would be reasonable to expect a different mode of failure. Since the MGB was operated at a higher torque and airspeed than the minimum required in the RFM, it would require more tail rotor thrust to maintain its heading. The higher thrust requirement would result in a higher load on the tail take-off pinion. Sikorsky has indicated that a loss of drive, which could occur in either the main or tail drive sections, is more likely to occur if the MGB is operated at a high power and if rapid or frequent power changes are made.

Further accidents and incidents involving H/C transmission systems, as well as some of those already described, are listed in Table 7.

#	Date	Aircraft type	Registration	Country	Reference/ Report	Description
1	10 May 12	EC225 LP Super Puma	G-REDW	UK	UK AAIB Bulletin: S3/2012 EW/C2012/05/01	Loss of drive to MGB main lubricating system oil pumps due to 360° circumferential crack, in the bevel gear vertical shaft in the helicopter's main gearbox, and later failure of the emergency MGB lubrication system.
2	01 Apr 09	Aerospatiale AS 332 L2	G-REDL	UK	UK AAIB Report 2/2011 EW/C2009/04/01	Loss of MGB oil due to MGB case rupture (failed 2 nd stage epicyclic planet gear).
3	12 Mar 09	Sikorsky S-92A	C-GZCH	Canada	TSB Canada A09A0016	Total loss of MGB oil due to fracture of oil filter bowl fixing titanium studs
4	20 Nov 07	Aerospatiale AS 332 L2	G-CHCF	UK	UK AAIB Bulletin 2/2009 EW/C2007/11/03	The right engine freewheel unit had failed causing that engine to overspeed, this was contained by the overspeed protection system shutting down the engine.
5	13 Oct 06	Aerospatiale AS 332 L	G-PUMI	UK	UK AAIB Report 7/2010 EW/C2006/10/06	One main rotor blade spindle had fractured, through the lower section of its attachment yoke on the leading side of the spindle. Post-fracture plastic deformation of the lug had stretched open the fracture, separating the faces by some 12 mm.
6	22 Feb 03	Eurocopter AS332-L2	G-JSAR	UK	UK AAIB Bulletin: 8/2004 EW/C2003/02/06	Oil cooler drive shaft and gear wheel fractured. Bearing housing fractured.
7	16 Dec 02	Sikorsky S-61N	C-FHHD	Canada	TSB – Canada A02P0320	The plain bearing in the main gearbox cover for the number 1 input pinion failed, lost lubrication, and disintegrated
8	16 Jul 02	Sikorsky S-76A+	G-BJYX	UK	UK AAIB Report 1/2005 EW/C2002/07/04	Aircraft suffered a catastrophic structural failure. One main rotor blade fractured in flight. The helicopter's main rotor assembly separated almost immediately and the fuselage fell to the sea surface.
9	15 Jul 02	Sikorsky S-61N	G-BBHM	UK	UK AAIB Report 2/2004 EW/C2002/7/3	The No 2 engine suffered rapid deterioration of the No 5 (location) bearing of the free turbine, causing failure of the adjacent carbon oil seal and mechanical interference between the Main Drive Shaft Thomas coupling and the Engine Mounting Rear Support Assembly tube, which completely severed the support tube.
10	11 Mar 83	Sikorsky S-61N	G-ASNL	UK	UK AIB Report 4/85 EW/C815	Loss of MGB oil due to MGB case rupture due to failure of the 1st stage of No. 1 spur gear.
11	16 Dec 80	Aerospatiale SA 330 J	9M-SSC	Brunei	In: UK AAIB Report 2/2011 EW/C2009/04/01	The break-up of the second stage planet gear of the MGB.
12	8 Sep 97	Eurocopter AS 332 L1	LN-OPG	Norway	AIBN report 47/2001	Fatigue cracks in the splined sleeve of the R/H shaft input of the MGB, led to series of mechanical failures that caused the power turbine section of the R/H engine to burst, thus disintegrating the aircraft in flight. Whole sequence of the incident continued for only 3.9 seconds

Table 7: Accidents and incidents involving helicopter transmission systems [43]

On the following pages, Table 8 shows the primary (or initiating) and secondary (or subsequent) failures and faults found in more detail, using failure analysis of only the helicopter MGB and main transmission accidents and incidents in Table 7. The primary failure can be interpreted as initiating failure, the secondary as subsequent failure, as well.

#	Case	Description	Primary failure/fault	Secondary failure/fault	External qualifiers	HUMS / IHUMS Involvement
1	G-REDW	Loss of drive to MGB main lubricating system oil pumps due to 360° circumferential crack, in the bevel gear vertical shaft in the helicopter's main gearbox, and later failure of the emergency MGB lubrication system.	Small corrosion pit 60 µm deep in the inner countersink of the 4.2 mm hole on the bevel shaft's joining weld end point. Small machining defect in the internal part of the 4.2 mm hole. Other failures suspected as well.	Fatigue crack 'A' around 250° of the shaft circumferential weld joining upper and lower parts of the shaft.	Manufacturing defect suspected – investigation ongoing.	HUMS data indicated higher vibration of the vertical bevel shaft of MGB at 6 flying hours before start of the accident flight. Prior to these 6 hours, the vibration levels on indicators associated with the bevel gear vertical shaft were below the main level established from data collected from 23 other helicopters of the same type. During the last 6 flying hours the collected vibration indications increased. An amber alert was generated after the last flight the day before the accident, and after the first flight of the accident day. Required maintenance actions were conducted as per the maintenance manual. Aircraft was placed on a 10 hourly close monitoring cycle and released for flight.
				Fatigue crack 'B' around 80° of the shaft circumferential weld.	Manufacturing defect suspected – investigation ongoing.	
				Crack 'C' around 30° of the shaft circumferential weld starting from crack 'A' and going under crack 'B'	Undetermined - investigation ongoing.	
				Total circumferential failure of vertical bevel gear shaft at the circumferential weld.	None	
				Vertical down movement of the lower vertical bevel gear.	None	
				Damage of outer race of bevel shaft lower roller bearing.	None	
				Pinion partially disengaged from oil pump drive gear.	None	
				Damage of teeth of pump drive gear.	None	
				Failure of drive to main and standby oil pumps.	None	
				MGB emergency lubrication system failed (MGB EMLUB caption) came on	Undetermined - investigation ongoing.	

#	Case	Description	Primary failure/fault	Secondary failure/fault	External qualifiers	HUMS / IHUMS Involvement
2	G-REDL	Failure of one of the eight second stage planet gears in the epicyclic module as a result of a fatigue crack, the precise origin of which could not be determined. This led to the MGB outer case fracture and main rotor separation.	A crack had initiated from a point at or close to the surface of a highly loaded section of the bearing outer race in one of the second stage epicyclic planet gears of the MGB. A particle had been released from a position approximately 14 mm from the edge of the outer race of the failed gear Spalling of the planet gear. Material defect within the gear (suspected).	<p>Crack propagated under fatigue until the gear failed and broke into several sections.</p> <p>A section of the failed second stage epicyclic planet gear becomes entrained between the remaining second stage planet gears and the ring gear.</p> <p>Rupture of the MGB epicyclic module case due to overload. This case is integral with the epicyclic ring gear.</p> <p>Loss of MGB oil pressure.</p> <p>Extensive leak (loss) of MGB oil.</p> <p>MGB conical housing separated from the remainder of the MGB.</p> <p>Lift struts reacted engine torque, thus fractured under load.</p> <p>Separation of the main rotor</p>	<p>The AS332 L2 does not provide an alert to the flight crew when the epicyclic module magnetic chip detector detects a particle.</p> <p>The ring of magnets introduced on EC225 MGBs reduced the possibility of metallic debris generated in the epicyclic module being detected by the main module magnetic chip detector or during inspection of the oil filter.</p> <p>Many other external technical and human inputs</p> <p>None</p> <p>None</p> <p>None</p> <p>None</p> <p>Lift struts were not designed to react to engine torque</p> <p>None</p>	<p>HUMS recorded 667 epicyclic magnetic chip detection warnings 6 days prior to accident. These were not investigated due to the absence of an alert generated by the HUMS ground station.</p> <p>Alerts will not be displayed on the HUMS ground station summary screens if the HUMS data card is not closed down correctly.</p> <p>HUMS recorded 76 chip detection warnings for the first operation of the day 6 days prior to accident, and 94 for the second operation. For both operations, the first recorded detection was during engine start.</p> <p>Three minutes and three seconds prior to the loss of MGB oil pressure, HUMS recorded an epicyclic chip detection warning.</p> <p>Three further detections were recorded over the next minute and 43 seconds.</p> <p>Review of HUMS vibration data available at the time of the accident revealed no unusual trends related to the epicyclic module.</p> <p>HUMS vibration monitoring capability of detecting degradation in epicyclic stage planet gear bearings is limited.</p>

#	Case	Description	Primary failure/fault	Secondary failure/fault	External qualifiers	HUMS / IHUMS Involvement
3	C-GZCH	Total loss of MGB oil due to fracture of titanium studs securing the MGB oil filter bowl. This led to the failure of the MGB.	Galling of the titanium studs	<p>Fracture of first stud.</p> <p>Fracture of second stud.</p> <p>Loss of MGB oil from oil filter bowl.</p> <p>Plastic collapse of teeth of the tail take-off pinion (to tail rotor shaft).</p> <p>Damage to two tapered roller bearings of the tail take-off pinion shaft.</p> <p>Loss of axial and radial constraints of the main rotor brake disk.</p>	<p>Increased removal/installation cycles of studs.</p> <p>Improper pre-load installation of studs during maintenance.</p> <p>Increased cyclic loads on studs during flight.</p> <p>Increased load on the 2nd stud after failure of 1st.</p> <p>Increased removal/installation cycles of studs.</p> <p>Improper pre-load installation of studs.</p> <p>Increased cyclic loads on studs during flight.</p> <p>None</p> <p>Continued MGB operation after loss of oil.</p> <p>Continued MGB operation after loss of oil.</p> <p>Continued MGB operation after loss of oil.</p>	<p>HUMS data from the helicopter is downloaded every day and used to monitor the helicopter's systems for faults or to detect trends that could lead to faults.</p> <p>However, the accident final formal report doesn't list any specific HUMS data that could have helped indicate pending failures of oil filter bowl studs prior to accident flight. This could be attributed to the non-rotating nature of the filter assembly.</p>

#	Case	Description	Primary failure/fault	Secondary failure/fault	External qualifiers	HUMS / IHUMS Involvement
6	G-JSAR	Oil cooler drive shaft and gear wheel fractured, as well as the fracture of its bearing housing.	Transient torsional loads arising from 'snatching' in the gear train within the gearbox module.	The intermediate gear wheel fractured from the bearing at the center to the outer edge of the gear. Its bearing housing was also fractured through one of the three attachment lugs. Oil cooler drive shaft fractured at the coupling flange on the MGB output drive.	None None None	Prior to the accident, HUMS detected a potential problem in the main gearbox left hand accessory module. A decision had thus been made to monitor closely the relevant parameters (manufacturer advised to continue flying but with close monitoring for a further 50 flight hours), and the failure occurred during this monitoring period. The report notes that a similar incident occurred to G-PUMS.
7	C-FHHD	The plain bearing in the main gearbox cover for the number 1 input pinion failed, lost lubrication, and disintegrated. Engine 1 thus lost power.	The plain bearing in the main gearbox cover for the number 1 input pinion failed	The bearing adjacent to the carbon seal broke down. Bearing lost lubrication (grease) and disintegrated. The carbon seal for the failed plain bearing disintegrated Oil spray out from the MGB on to the pinion shaft The number 1 pinion rapidly overheated and weakened. Local fire started within the area (base of transmission) Fracture of the No 1 pinion. Malfunction of the No. 1 free wheel unit, Engine 1 lost power	None None None None Continued MGB operation after loss of oil. Rotational imbalance due to bearing fracture. None None None None	Not reported

#	Case	Description	Primary failure/fault	Secondary failure/fault	External qualifiers	HUMS / IHUMS Involvement
10	G-ASNL	MGB case rupture due to failure of the 1st stage of No. 1 spur gear.	Permanent distortion (creep) of gear input casing that occurred in service Error during re-machining of the bearing location sleeves during input casing refurbishment	Static dimensional inaccuracies in the spur gear shaft support bearings locations. Gear tooth misalignment, uneven tooth contact of failed spur gear. Initiation of root (flank) fatigue crack in the spur gear teeth. Growth of radial fatigue crack through the rim and web of the spur gear. Circumferential cracking of the spur gear. Rupture of the web and separation of the rim of the gear wheel. A segment of 60% of the outer web and rim of the spur gear was ejected through the MGB input casing. MGB input casing fracture. Loss of drive to the No 1 transmission Engine 1 over speeded and automatically shut down. Loss of MGB oil pressure. Extensive leak (loss) of MGB oil.	Many external technical and human inputs None None None None None None None None None None None None None	Not reported

#	Case	Description	Primary failure/fault	Secondary failure/fault	External qualifiers	HUMS / IHUMS Involvement
11	9M-SSC (written off)	The break-up of the second stage planet gear of the MGB and break out of tail boom.	Seizure of roller bearing associated with secondary stage planet pinion (gear).	Widespread contamination of the main gearbox magnetic plug and filter had occurred during the six weeks preceding the accident.	Mistaken health monitoring of the gearbox leading to a deterioration of the mechanical condition of the gearbox components. Maintenance personnel had wrongly interpreted the amount of allowable debris as defined in the Aérospatiale Standard Practices Manual, due to the mistaken interpretation of an unfamiliar metric term.	The epicyclic module was not equipped with a detector.
				Disintegration of a secondary stage planet pinion [gear] within the gearbox.	None	
				The associated metal debris caused jamming within the rotating assemblies, generating forces which fractured the common epicyclic ring gear and the main gearbox.	None	
				Circumferential failures of the ring gear casing, above and below the epicyclic stages, together with a vertical rupture.	None	
				Loss of the main rotor assembly, together with the attached bell housing containing the second stage gears of the epicyclic gearbox.	None	
				This resulted in overall instability in the rotor system, which caused blades to strike the fuselage.	None	
				Almost simultaneously, the entire tail boom section parted from the aircraft.	None	

#	Case	Description	Primary failure/fault	Secondary failure/fault	External qualifiers	HUMS / IHUMS Involvement
12	LN-OPG	Fatigue cracks in the splined sleeve of the RH shaft input of the MGB, led to series of mechanical failures that caused the power turbine section of the RH engine to burst, thus disintegrating the aircraft in flight. Whole sequence of the incident lasted for only 3.9 seconds.	The hard metal coating of the splined sleeve containment was of larger carbide grains than the thickness of coating. Thickness of coating is less than the design requirements in some parts. Porosity of the coating is significantly larger than required by design. Local lamination of the hard metal coating. Defective bonding between hard metal and coating	Several fatigue cracks on splined sleeve of RH shaft input of MGB started 121 62 Fh prior to accident. Failure of the splined sleeve Loosen locking washer slipped into the power transmission Bendix shaft of RH engine. Failure of the Bendix shaft under large imbalance loads Increased onset of vibrations on RH engine Failure of engine speed regulating controls RH engine overspeed out of control Engine power turbine burst 2 flight-rod-controls-fracture to MR Fracture of one rod control to TR Destruction of power turbine section of the LH engine Front suspension bar of the MGB failed in overload MR head damaged & disintegrated	None Missing O-ring on splined sleeve increased freedom of movement between sleeve and flange, thus hastened crack propagation on splined sleeve. Design shortcoming of shaft. Inadequate maintenance procedures. Significant maintenance errors (missing O ring, inaccurate pre-flight checks, inadequate documents updates and signatures, etc.). Inaccurate and incomplete inspections None None Engine was freed of load due to Bendix shaft failure None None None None None	An IHUMS accelerometer with an 'alarm' that monitored the problem area was out of operation at time of accident (since 2 months before). It is concluded that adequate operation of this accelerometer would have given enough warning prior to the accident. The working parts of the IHUMS indicated a problem within the RH engine and MGB connection area few days before the accident. This information remained saved in the associated database and had to be manually decoded to expose the trend of the problem. This was not conducted. The installation of IHUMS was on voluntary basis, thus some parts of it were occasionally left out of use.

Table 8: Primary and secondary failures and faults found using failure analysis of the helicopter MGB and main transmission accidents and incidents in Table 7 [43]

4.2 MRO experience

During SKF internal investigations, ZFL was asked to provide analysis on planet gear bearings (roller bearing 649550A) that have been returned from service [42]. This also includes an investigation on the outer raceway concerning sub-surface cracks (destructive testing and metallurgical analysis).

The planetary gear shows two raceways at the inner diameter. On each raceway a spalling is visible. A band of micro-pitting is located near one of the spellings. The indentations of metal particles on the raceway are the secondary damage of the peeling at the bearing (Figure 74).

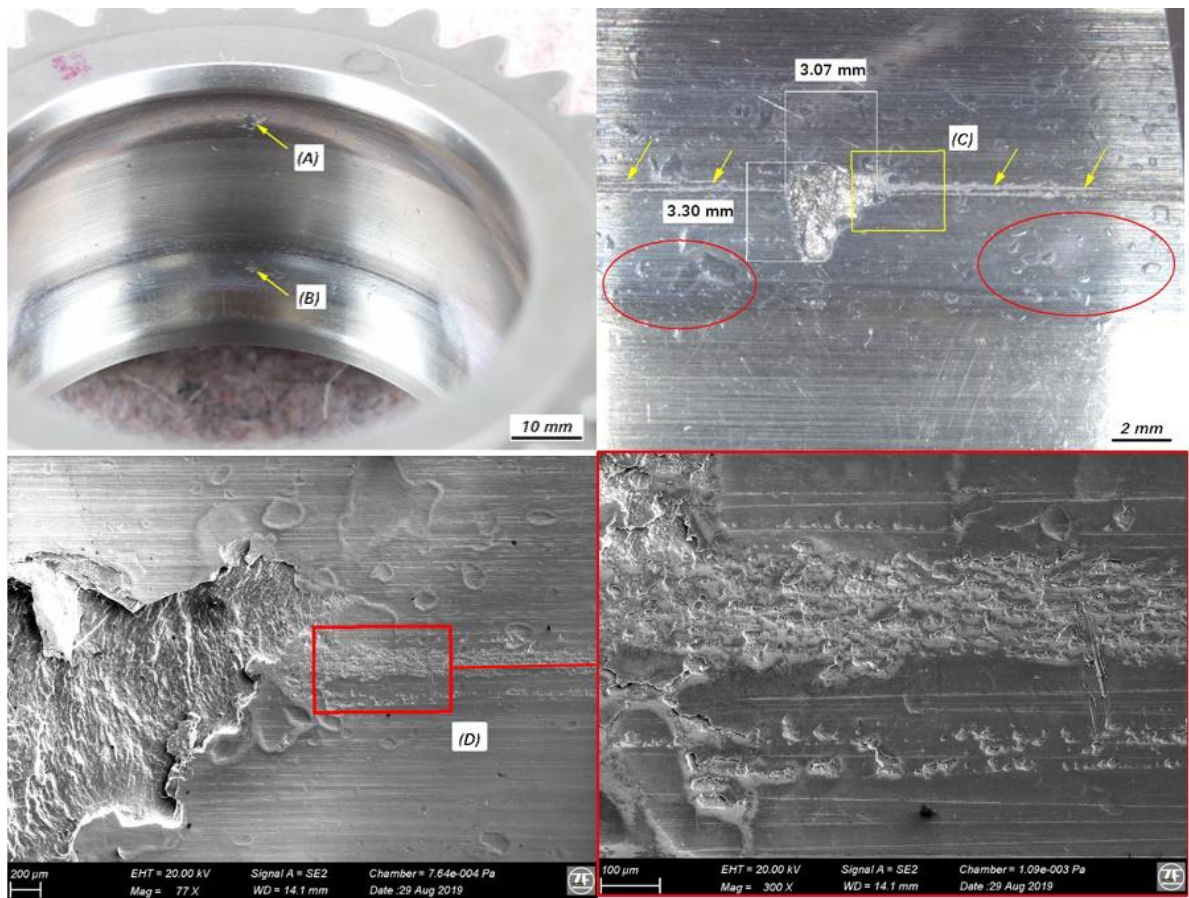


Figure 74: Spalling on raceways and band of micro-pitting and indentations from metal particles

After a cross-section was made, cracks were visible under the raceway surface in a predominantly longitudinal direction. The beginnings of the cracks lay directly on the spallings. The cracks show both inter- and trans-crystalline propagations (Figure 75)

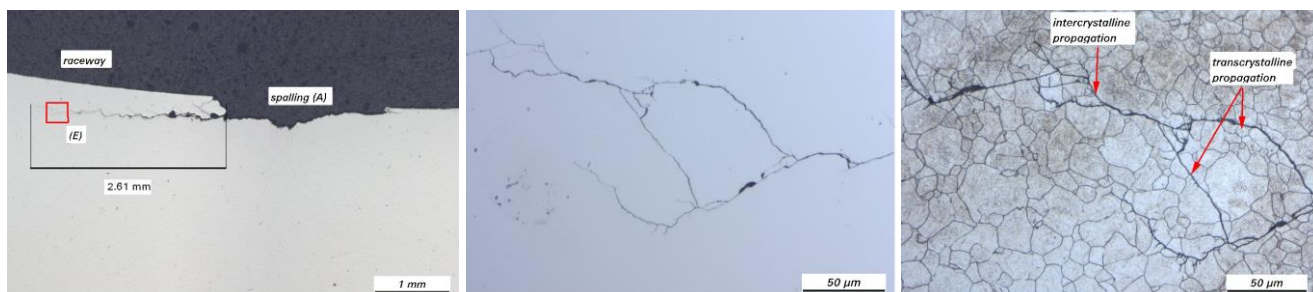


Figure 75: Beginning of the crack (left); detailed crack propagation (middle); inter- and trans-crystalline propagations (right)

The material and heat treatment conditions of the planetary gear meet the specifications with the exception of the Case Hardened Depth (CHD) of the raceway. The slight underrun of the CHD is not relevant to the damage. Cracks are detected under the inner raceway of the planetary gear, starting on both spallings. The formation of the spallings was due to fatigue on the raceway surface.

In the frame of an inspection [41], some indications were found in the axial direction on the integrated bearing race of an intermediate shaft. The shaft shows fine axial cracks over the entire circumference of the bearing raceway. In addition, crossed and curved machining marks are visible on the surface. There is no classic fatigue to be seen (Figure 76).

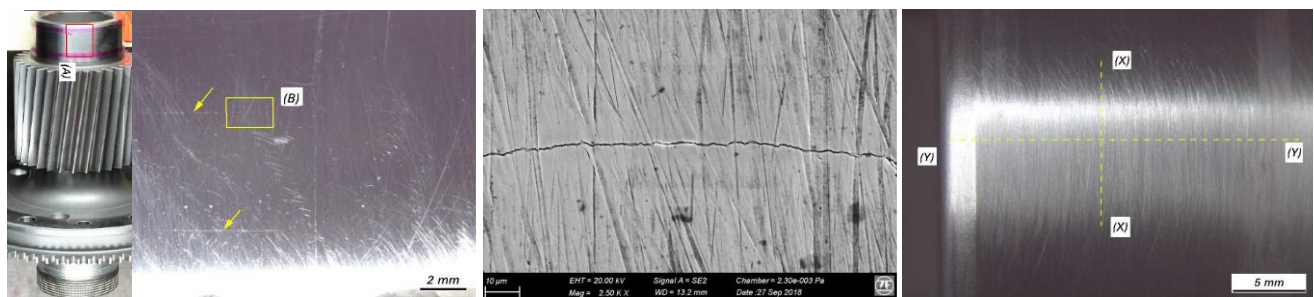


Figure 76: Fine axial cracks (left/middle) and crossed and curved machining marks (right)

The crack starts on the surface. The crack depth is approx. 200 μm and is within the case hardening layer. Tempered martensite, signs of grinding burn, can be seen on the edge of the cross-section (Figure 77).

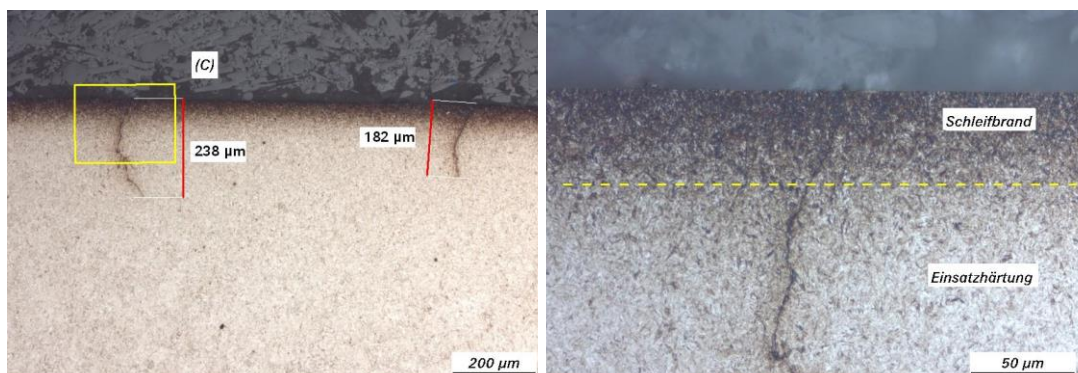


Figure 77: Initial cracks in the surface (left), Tempered martensite visible on the surface (right)

The formation of grinding burn is distributed unevenly in the axial direction (Figure 78). The material, the CHD, and the core strength correspond to specifications. The surface hardness in the grinding burn area is below specification.

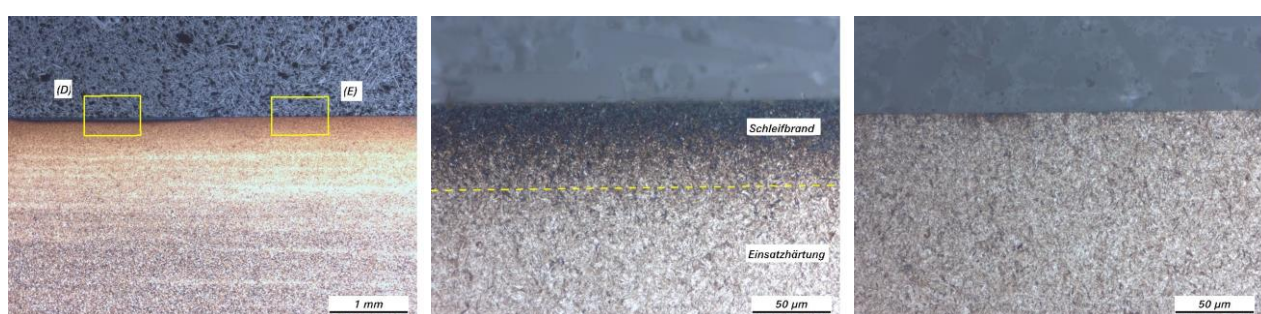


Figure 78: Grinding burn: Non-uniform (left); Tempered martensite visible on the surface (middle); None (right)

4.3 Windmill industry

The overview in [17] on the windmill industry is not intended to provide an exhaustive comparison between this sector and rotorcraft in terms of planet bearings. But because planetary gearboxes are also widely deployed and the bearing concepts are similar in the windmill industry, the description of some main designs and failure mode characteristics in the planet bearings can be highlighted to display some similarities or differences in approach.

Windmills are designed for a service life of 20 years. Gearboxes with 1, 2, or 3 stages are possible. One stage can have from 3 to 8 planet gears.

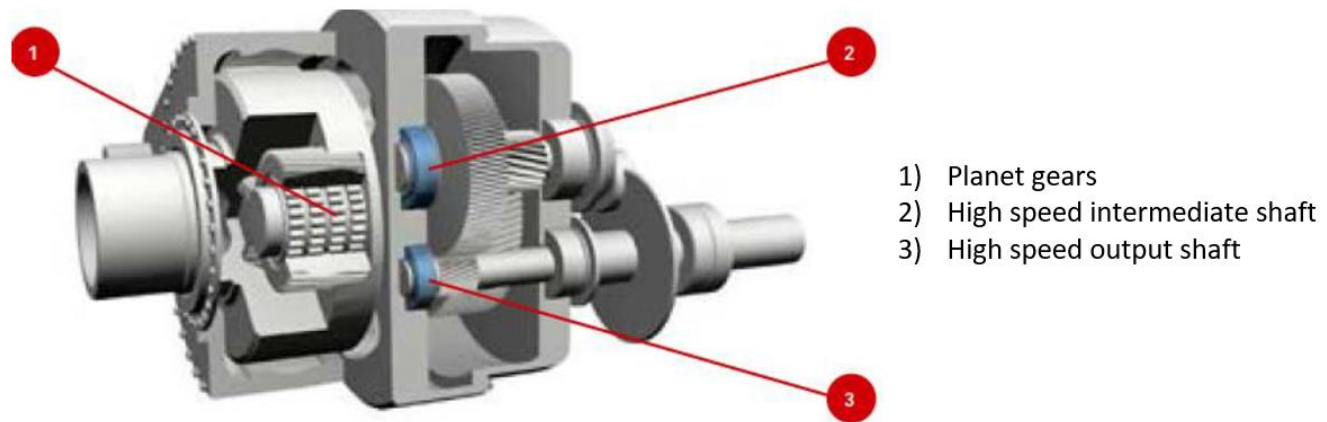


Figure 79: Windmill gearbox [17]

The planet bearings are also oil lubricated and can be mainly multi-row Cylindrical Roller Bearings (CRB) or Tapered Roller Bearings (TRB), 2, 3 or 4 rows. For low speed stages CRB can also have full complement configuration without cages.

Typical bore diameters are between 240mm and 400mm.

It is also important to underline that SRB bearing types were also considered in the past but are no longer used for planet gear applications. Some reliability issues were the cause of their market decline.

In most modern applications, the bearing outer ring and the planet gear are integrated for reasons of power density and also to avoid the 2 component tight-fit configuration.

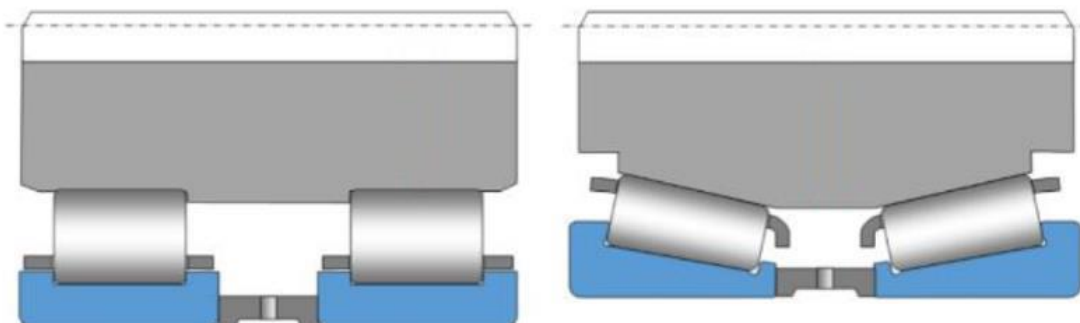


Figure 80: Example of planet bearing design [17]

On the material side, their rings are mainly through-hardened steel (martensitic or bainitic). Some innovations have been recently introduced with case-carbonitrided steel.

For windmill gearbox application, 5 typical types of failure can be considered, as are illustrated below. They do not solely or specifically concern the planet bearings.

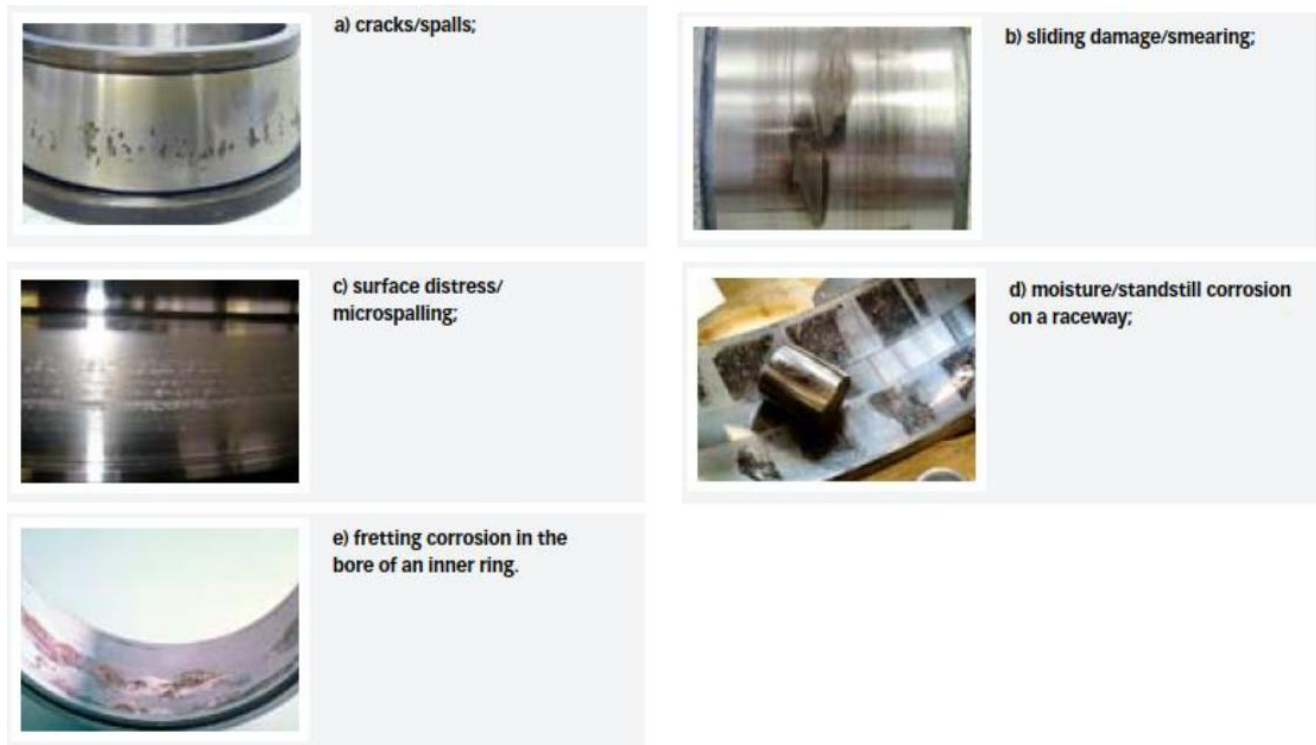


Figure 81: Wind gearbox bearing damages [17]

For the planet bearings, especially for the 1st planetary stage (the one rotating at the lowest speed), white etching cracks (Figure 81, case a) can be highlighted as a failure mode for premature damages. This corresponds to the alteration of the microstructure when polishing and etching a micro section. The corresponding area consists of ultra-fine, nano-recrystallized, carbide-free ferrite. This phenomena is mainly observed on inner rings.

The root causes are still a point of debate in the windmill industry, but most probably a result of mixed lubrication conditions and high surface frictions.

The second failure mode to underline for these planet bearings is micro spalling (Figure 81, case c), which essentially occurs due to poor lubrication conditions in application. As a solution for this and several other failure modes, SKF developed a Black Oxide treatment (Figure 80), which shall reduce premature failure due to cracks/white etching cracks.



Figure 82: Planet multi rows CRB with SKF Black Oxide treatment [17]

5. Catastrophic failure modes on drive system configurations

5.1 General

The objective of this chapter is to identify single points of failure (SPOF) that could lead to catastrophic failure at the rotorcraft level. The analyses described in 5.2 below will be used to identify these single points of failure and the possible causes and failure mechanisms leading to them on some specific examples from existing designs.

SPOFs are undesirable in any system with a goal of high availability or reliability, be it a business practice, software application, or other industrial system, such as the MGB for H/C.

By reviewing the described failure modes in chapter 3 with regards to their effect on catastrophic failures modes, the causes can be summarized as

- Inappropriate design assumptions
- Lubrication issues such as loss of oil and/or oil pressure
- Material defects
- Manufacturing defects
- Lightning/electrical power damage
- Excessive wear
- Assembly failures

The following chapter will apply some of this causes to several of the architectures described in chapter 2 within a failure flow analysis, pointing out the catastrophic paths on the basis of Table 9. The analysis was done based on several assumptions due to a lack of detailed design information. Therefore, some causes were not or only partly considered (e.g. seizure of bearings, excessive wear, inappropriate design assumptions, etc.).

Effect on rotorcraft	No effect on operational capabilities or safety	Slight reduction in functional capabilities or safety margins	Significant reduction in functional capabilities or safety margin	Large reduction in functional capabilities or safety margins (Note 4)	Loss of rotorcraft
Effect on occupants excluding flight crew	Inconvenience	Physical discomfort	Physical distress, possibly including injuries	Serious or fatal injury to a passenger or a cabin crew member (NOTE 2)	Multiple Fatalities
Effect on flight crew	No effect on flight crew	Slight increase in work load which involve crew actions well within crew capabilities such as routine flight plan changes	Physical discomfort or a significant increase in workload or in conditions impairing crew efficiency	Physical distress or excessive workload impairs ability to perform tasks accurately or completely	Fatalities or incapacitation
DO-178C Software Level (Note 3)	E	D	C	B	A
Failure Condition Category	No Effect	Minor	Major	Hazardous or Severe-Major	Catastrophic
Qualitative Probability	Frequent	Reasonably Probable	Remote	Extremely Remote	Extremely Improbable
Quantitative Probability :	No probability requirement	$\leq 10^{-3}$ (Note 1)	$\leq 10^{-5}$	$\leq 10^{-7}$	$\leq 10^{-9}$

Table 9: Table of categories and definitions according AC29-2C

5.2 Failure flow diagram and criticality analysis

Failure criticality analysis is a main aspect of gearbox development, and not only in the aviation industry. Particularly for products with a high safety level requirement, it is becoming increasingly important to make sure that the design is reliable and meets the safety requirement. Within this project, failure criticality analysis shall be used for predefined gearbox architectures in order to detect critical load paths with a risk of single point of failures (SPOF's). The models were chosen as a good representation of current helicopter models with different technical solutions for gearbox architecture. The BO105 MGB and the Bell 525 MGB were selected to include a gearbox architecture with planetary gear stages. The BK117 was selected to include a gearbox architecture with a collector gear stage. The Bell OH58 represents a helicopter type with a single engine system and the CH53-K from Sikorsky is a variant with split torque load paths and a double collector stage.

To detect SPOF's within the aforementioned architectures, a top-down methodology was chosen. This methodology is described in Figure 83.

The top-down methodology starts with a generic failure flow diagram (see also Figure 86), that could be used and implemented for each gearbox architecture, giving an overview about general gearbox failure mechanisms and their respective root cause. This generic approach can be seen as a starting point and was used to discover critical load paths, their causes, and their effects regarding the safe flight and landing capability of the H/C.

In the second step within the top-down methodology (see Figure 83), more specific work was done. Diagrams of the gearbox architectures were made to get an overview of the different components inside the gearbox, their connections, and the load path. The gearbox architectures show the system and gear stages inside the MGB (coloured in blue) and the components/systems outside the gearbox (coloured in white) on assembly level. Moreover, components with integrated bearings or standard bearings are marked and redundant load paths are highlighted. In addition to the generic failure flow diagram (e.g. Figure 86), which is identical for each helicopter type, a specific part was introduced (e.g. Figure 88), which is able to detect redundancies inside the gearbox drive train and evaluate the failures according to the criticality and effects on the safety of the helicopter. In this case, the two main failure results ("loss of transmitting power" and "loss of integrity of the component/stage") are used to show what will happen if one of these failure mode arises.

As a final step and based on this generic and specific pre-work, failure flow diagrams were made for all main components of the gearboxes with the potential for catastrophic failures (Figure 83, right).

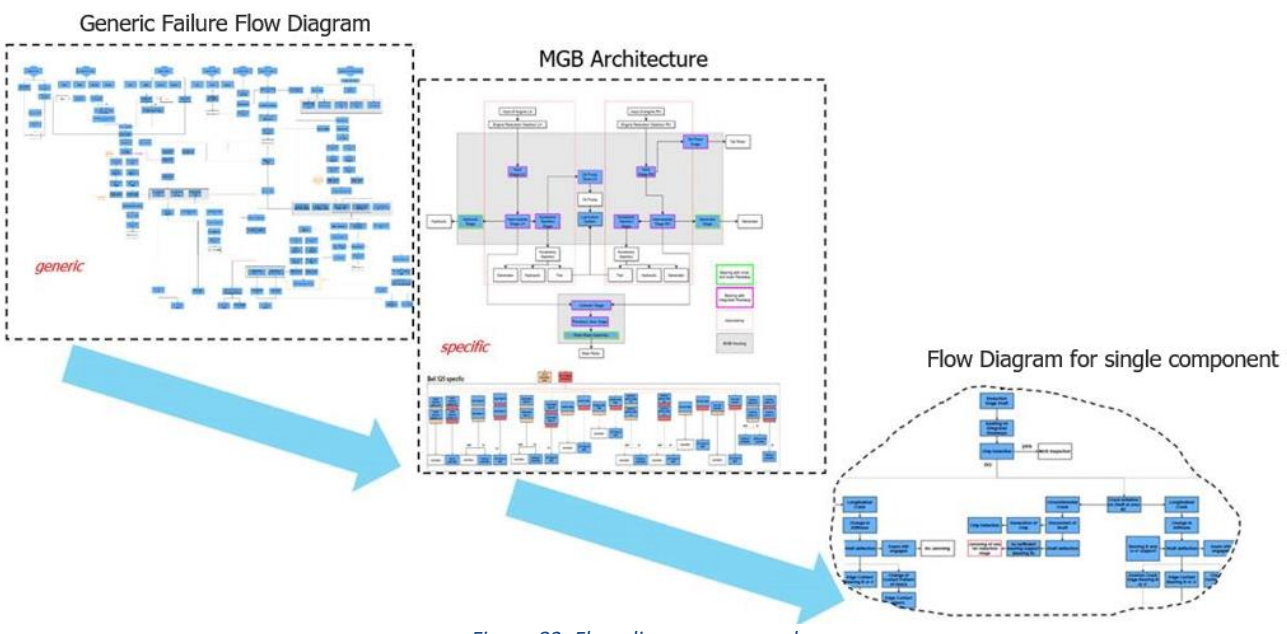


Figure 83: Flow diagram approach

The single component flow diagrams are structured as presented in Figure 84. The component and the corresponding failure mechanism is given at the top level. As a result, the different failure causes are shown, ending in final events (white background). The final events are divided in non-catastrophic (black frame) and catastrophic events (red frame). Catastrophic events will lead to a catastrophic failure of the MGB if there is no redundancy or other safety barrier interrupting the failure progression. A catastrophic failure does not strictly lead to loss of the rotorcraft and a safe landing may be possible depending on the flight conditions. This flow diagram of the single components will later on be used to define the single point of failures (SPOF) and define adequate design implementations to avoid catastrophic failures.

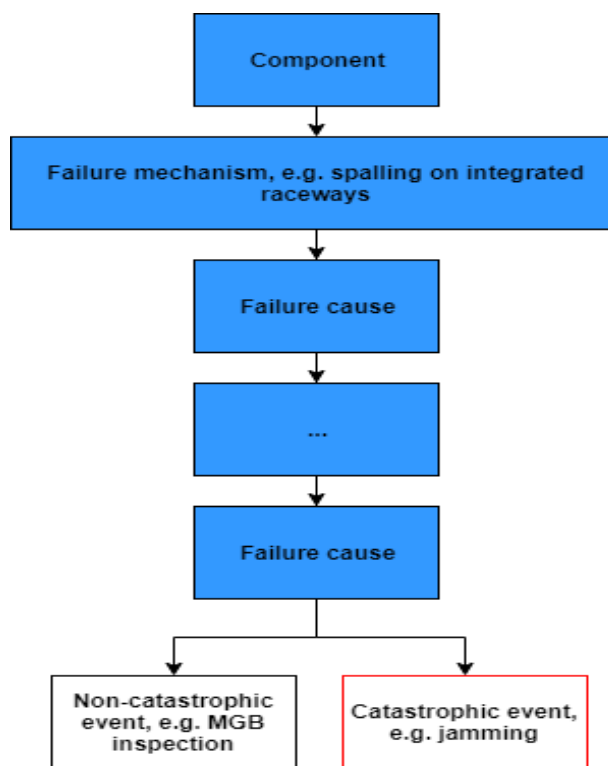


Figure 84: Structure of failure flow diagrams

Subchapters 5.2.1 to 5.2.5 show the results of the investigations for the mentioned helicopter gearboxes based on the approach represented in Figure 83 and Figure 84.

Some assumptions were made for all failure flow diagrams due to the lack of detailed design information. As fundamental design information are not known to ZFL (e.g. safety margins, detailed design characteristics, etc.), the drawing of conclusions for the failure criticality is difficult. In general, the most conservative failure classification was used. As a general and simplified approach, circumferential, radial and longitudinal cracks were taken into account for all components due to the lack of design information, even if in reality a combination of these types could occur. It can be seen as a generic approach to identify possible sources of failures within this research project. An overview for clarification of the use of longitudinal, radial or circumferential cracks is given in Figure 85.

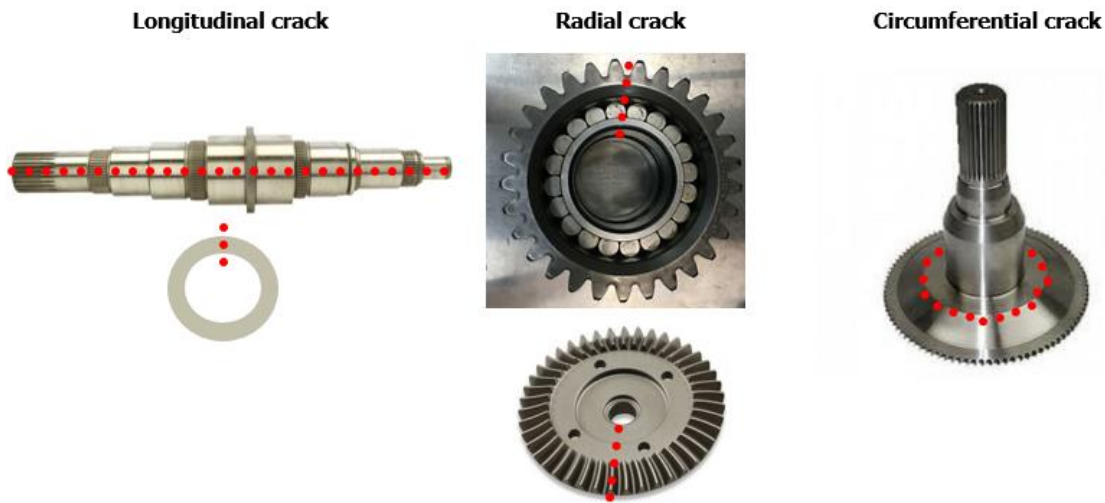


Figure 85: Overview of simplified crack types

Additionally, no seizure of any bearings is considered, as it is assumed that rolling element bearings are not prone to this failure mode under normal conditions (e.g. sufficient lubrication, standard load condition). The least information are available for the Bell 525 and the CH53-K. As a result, for these designs the detailed bearings used and their specific positions were not available for this study. In these cases, conservative assumptions were made based on ZFL experience and similar in-house solutions (e.g. H135 MGB). Therefore, a deviation between reality and the given flow diagram/gearbox architecture for the Bell 525 and the CH53-K is possible. The general intention to show possible critical load paths and SPOF's is not affected by this.

The given flow diagrams for the MGB of the Bell 525, MBB BO105, Kawasaki BK117, and Sikorsky CH53K and Bell OH-58 are based on [24] and [26]-[27] and were analyzed because they represent an architecture well. Moreover, the output of the generic flow diagram was used as an input for the specific failure flow diagram in the examples. In that specific flow diagram, the influence of the failure modes at a certain MGB stage/component and their final impact on the safety of the helicopter flight were evaluated. The critical components and all other components of the main load path were further analyzed by detailed component diagrams to underline the statements made for the specific examples.

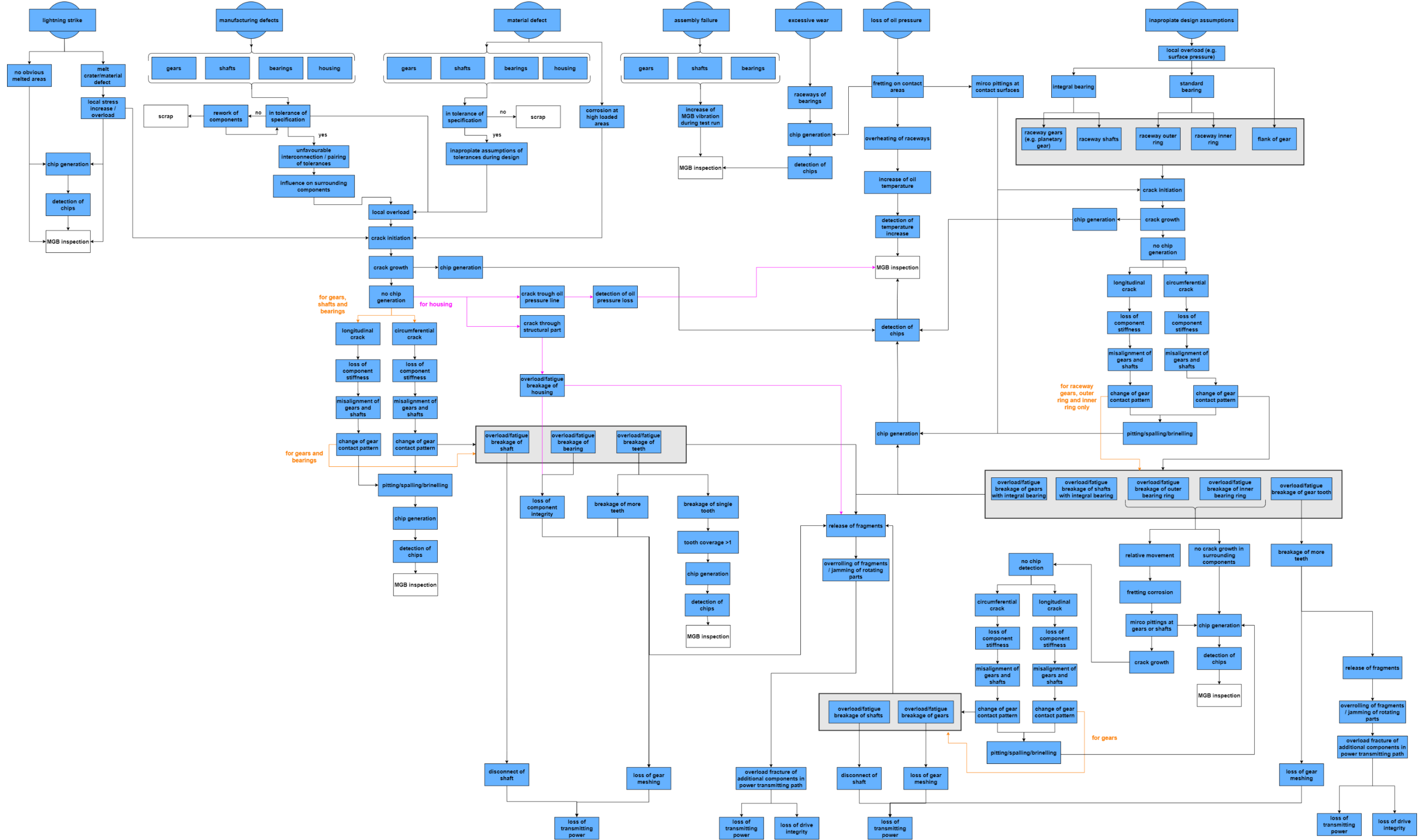
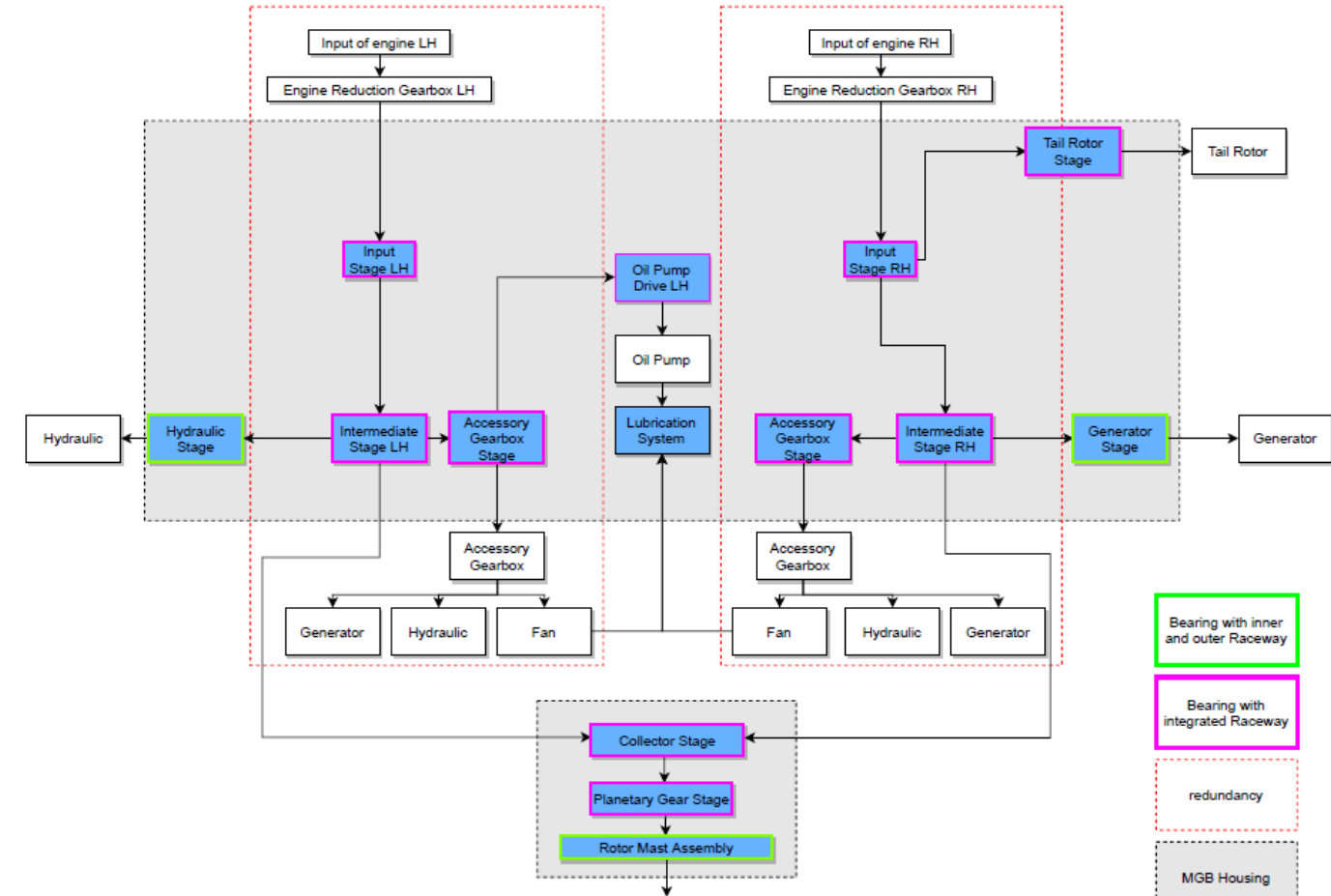


Figure 86: General flow diagram, leading to loss of transmitting power and loss of drive

5.2.1 Example 1: Bell 525 MGB

The Bell 525 MGB was chosen due to the good representation of a recently designed MGB with a collector wheel and planetary gear stage and two redundant intermediate and input stages. Based on available information [24], Figure 87 was created to get an initial overview of the Bell 525 MGB layout (Figure 12), its redundancies and possible load paths. The specific failure flow diagram for the Bell 525 MGB is shown in Figure 88 with the following stages/components that were identified as having the potential for catastrophic failure. The detailed analysis is given in Annex A.1 (Figure 98 to Figure 115).

- Collector stage
- Planetary gear stage
- Tail rotor stage
- Rotor mast assembly



loss of transmitting power
disconnect in the load path. No torque can be transmitted, but surrounding components are still free to turn. Rotormast Assembly is mechanically working and able to do autorotation

loss of integrity of the component/stage
jamming and overrolling of fragments lead to breakage of several surrounding components. There is an overload through the whole load path in a way, that integrity of the component is lost and surrounding components are damaged/broken. The autorotation function of the system is lost.

Bell 525 specific

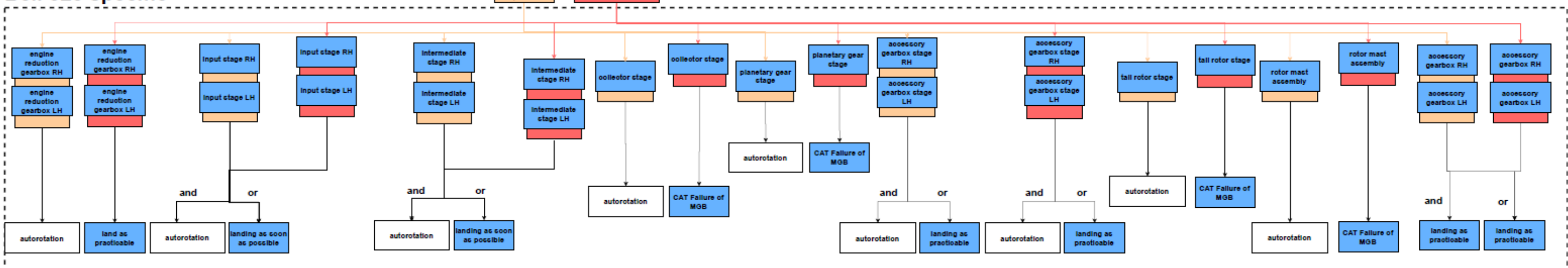


Figure 88: Bell 525 specific flow diagram

5.2.2 Example 2: Bell OH-58 MGB

The Bell OH-58 MGB was chosen due to the good representation of a single engine MGB with a planetary gear stage. Based on available information (Figure 89), Figure 90 was created to get an initial overview of the Bell OH-58 MGB layout and its single load paths.

The specific failure flow diagram for the Bell OH-58 MGB is shown in Figure 89 with the following stages/components that were identified as having the potential for catastrophic failure. The detailed analysis is given in A.2 (Figure 116 to Figure 122).

- First reduction stage
- Second reduction stage
- Rotor mast assembly

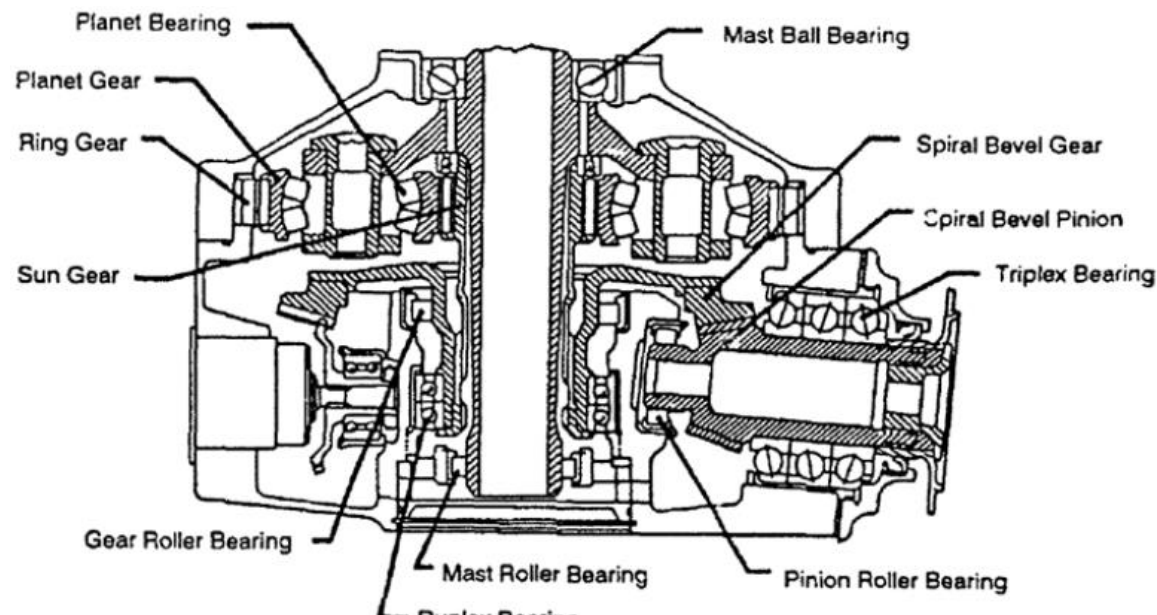


Figure 89: Bell OH-58 Design

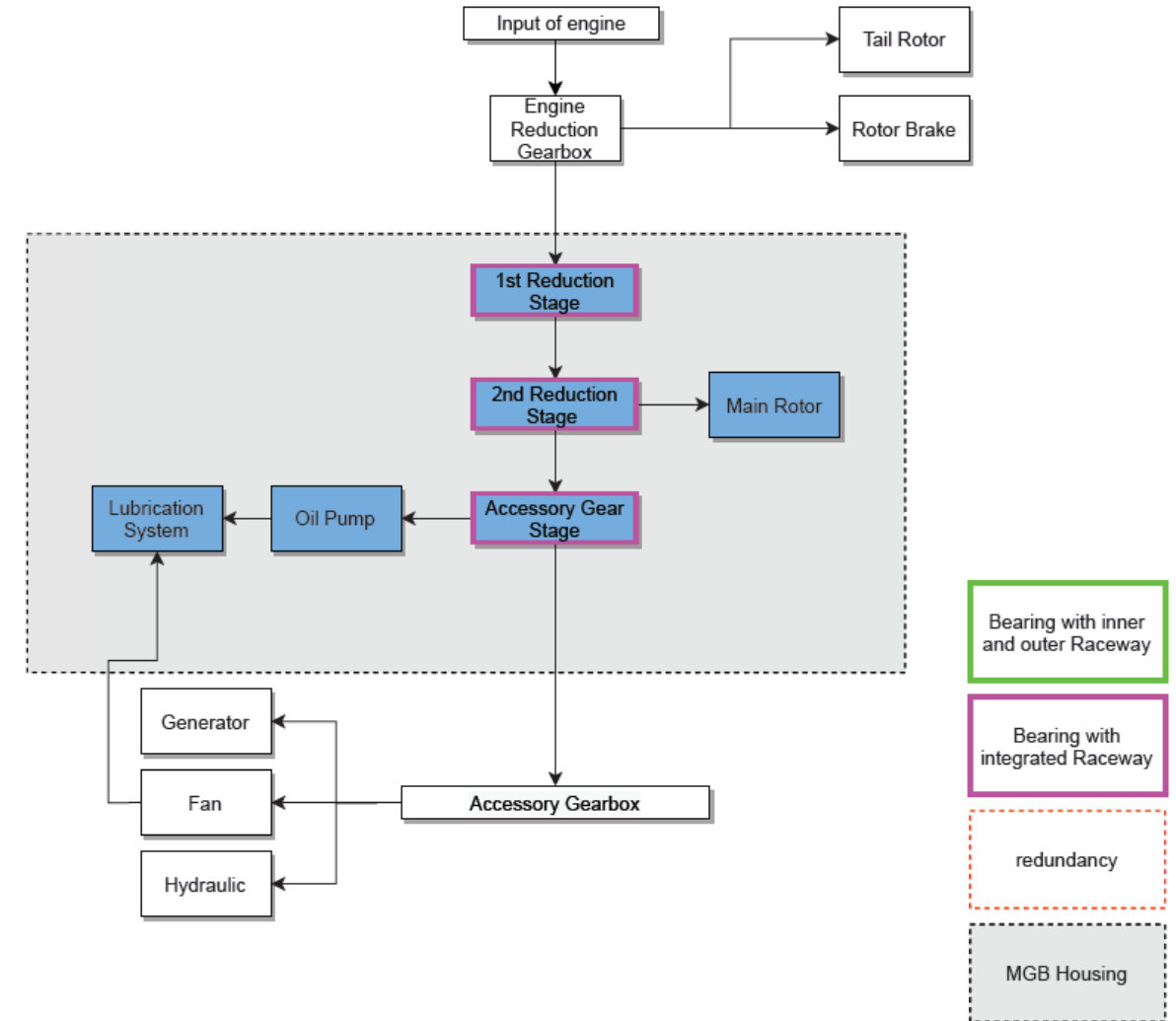


Figure 90: Bell OH-58 layout

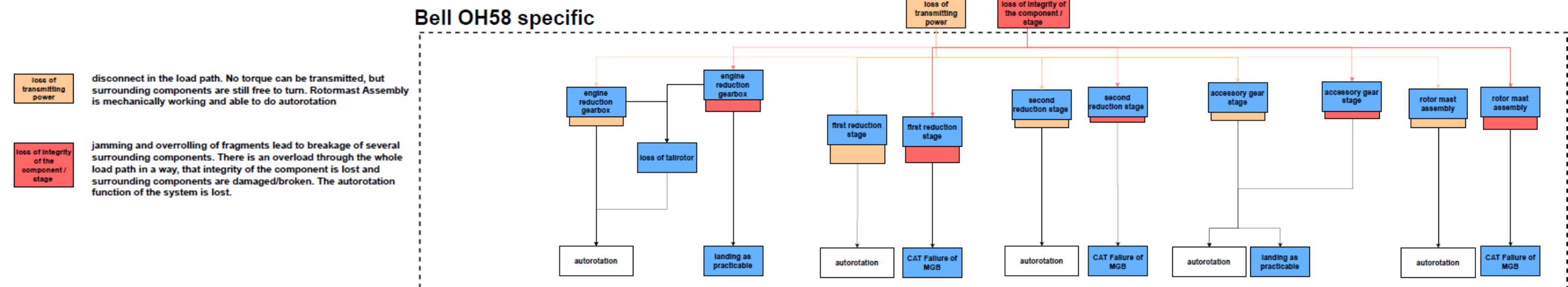


Figure 91: Bell OH-58 specific flow diagram

5.2.3 Example 3: BO105 MGB

The BO105 MGB was chosen due to the good representation of twin engine MGB with a planetary gear stage. Based on available information Figure 92 was created to get an initial overview of the BO105 MGB layout (Figure 10), its redundancies and possible load paths.

The specific failure flow diagram for the BO105 MGB is shown in Figure 93 with the following stages/components that were identified as having the potential for catastrophic failure. The detailed analysis is given in Annex A.3 (Figure 123 to Figure 136).

- Intermediate stage
- Collector stage
- Planetary gear stage
- Rotor mast assembly
- Tail rotor stage

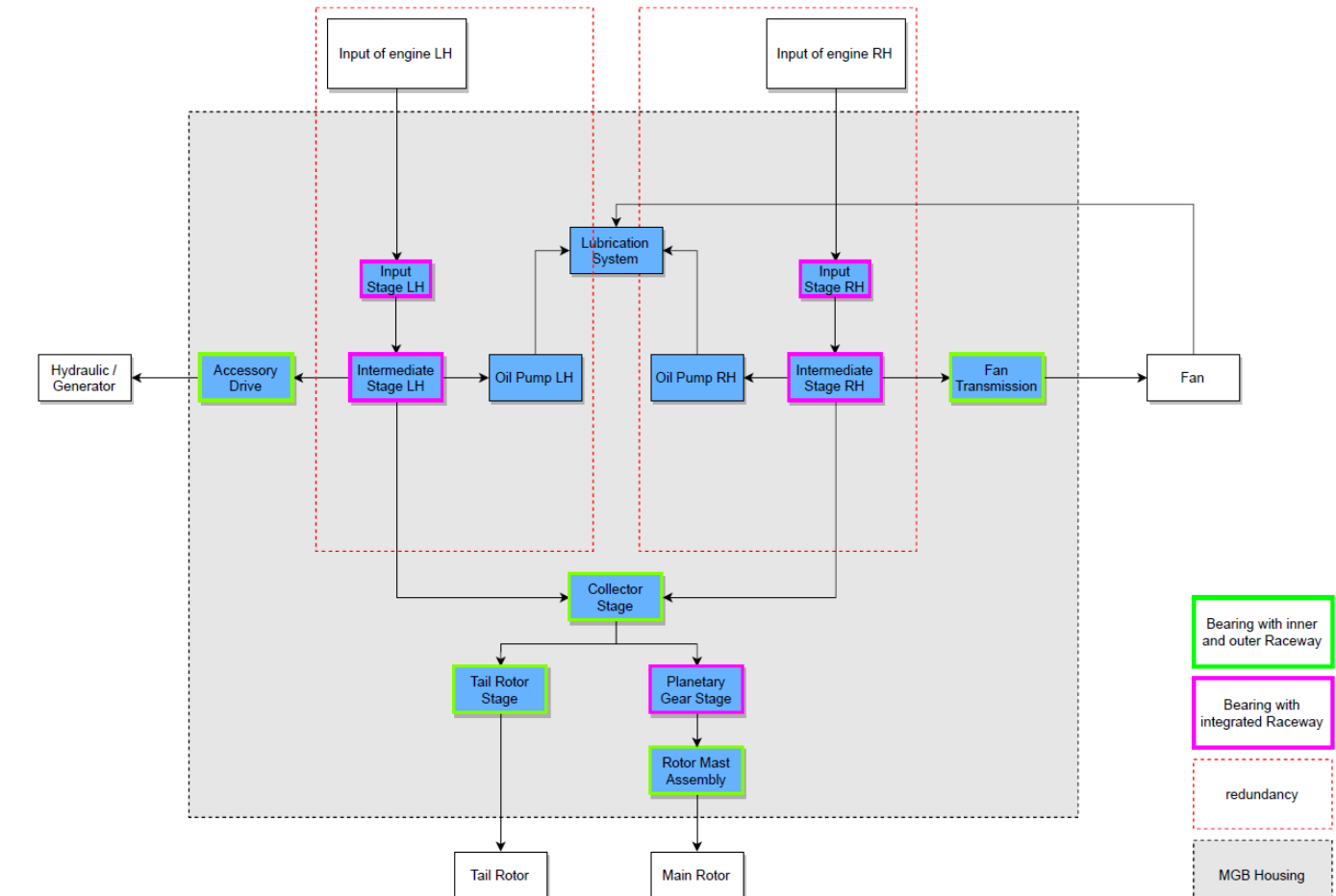


Figure 92: BO105 layout

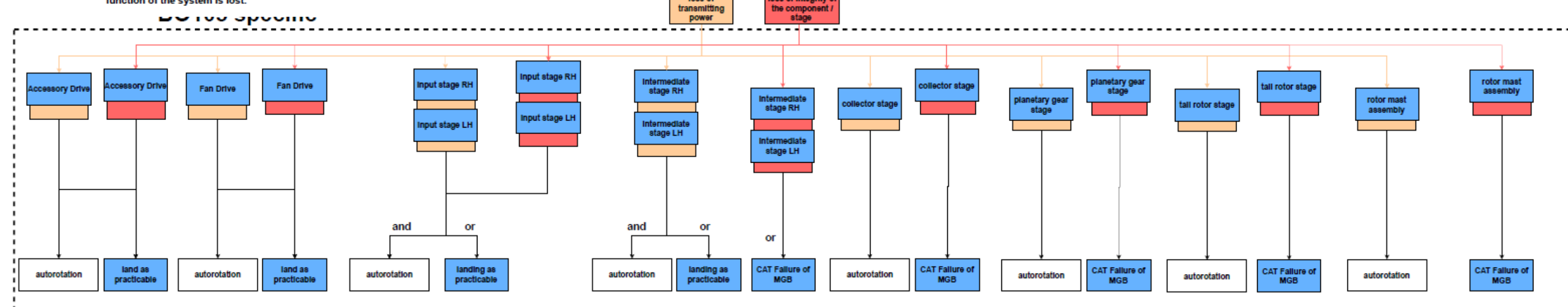


Figure 93: BO 105 specific flow diagram

5.2.4 Example 4: BK117 MGB

The BK117 MGB was chosen due to the good representation of a twin engine MGB with a collector stage and two redundant intermediate and input stages. Based on available information (Figure 16), Figure 94 was created to get an initial overview of the BK117 MGB layout, its redundancies and possible load paths.

The specific failure flow diagram for the BK117 MGB is shown in Figure 95 with the following stages/components that were identified as having the potential for catastrophic failure. The detailed analysis is given in Annex A.4 (Figure 137 to Figure 148).

- Intermediate stage
- Collector stage
- Tail rotor stage
- Rotor mast assembly

loss of transmitting power
disconnect in the load path. No torque can be transmitted, but surrounding components are still free to turn. Rotormast Assembly is mechanically working and able to do autorotation

loss of integrity of the component / stage
jamming and overrolling of fragments lead to breakage of several surrounding components. There is an overload through the whole load path in a way, that integrity of the component is lost and surrounding components are damaged/broken. The autorotation function of the system is lost.

DIVIDE & CONQUER

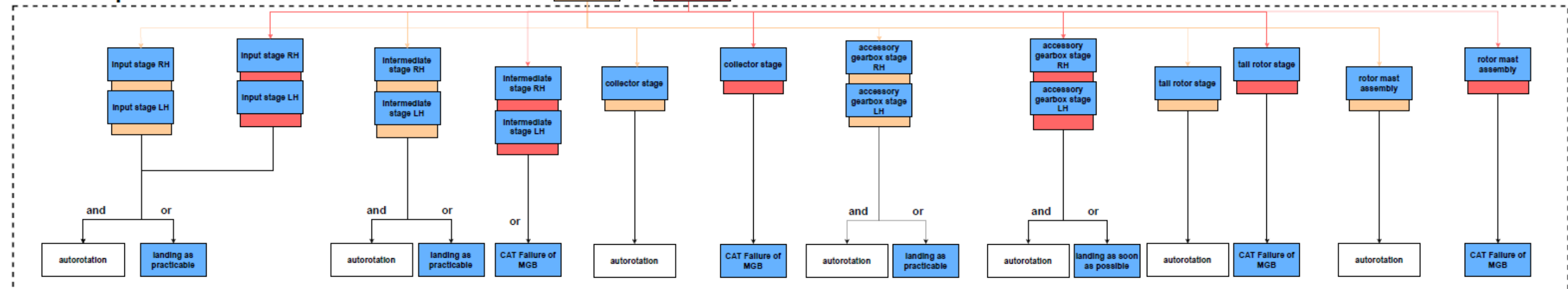


Figure 95 : BK117 specific flow diagram

5.2.5 Example 5: CH53K MGB

The CH53-K was chosen due to the good representation of triple engine MGB with a split-torque load path. Based on available information (Figure 15, [27]), Figure 96 was created to get an initial overview about the CH53-K MGB layout, its redundancies and possible load paths.

The specific failure flow diagram for the CH53K MGB is shown in Figure 97 with the following stages/components that were identified as having the potential for catastrophic failure. The detailed analysis is given in Annex A.5 (Figure 149 to Figure 158).

- First reduction stage
 - Rotor mast assembly

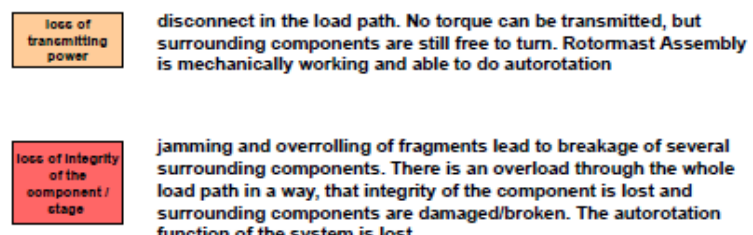
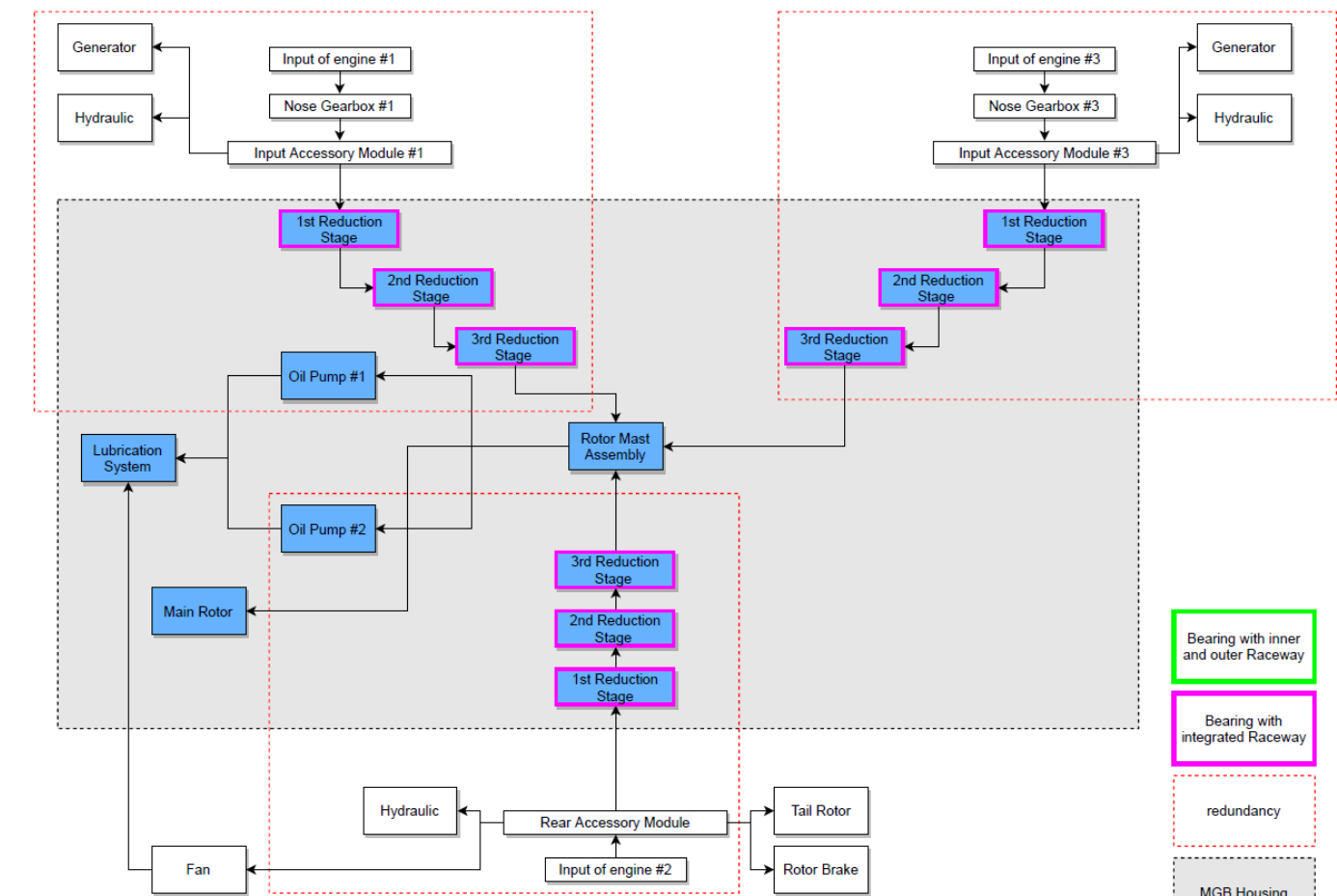


Figure 96 : Sikorsky CH-53K layout



CH53-K specific

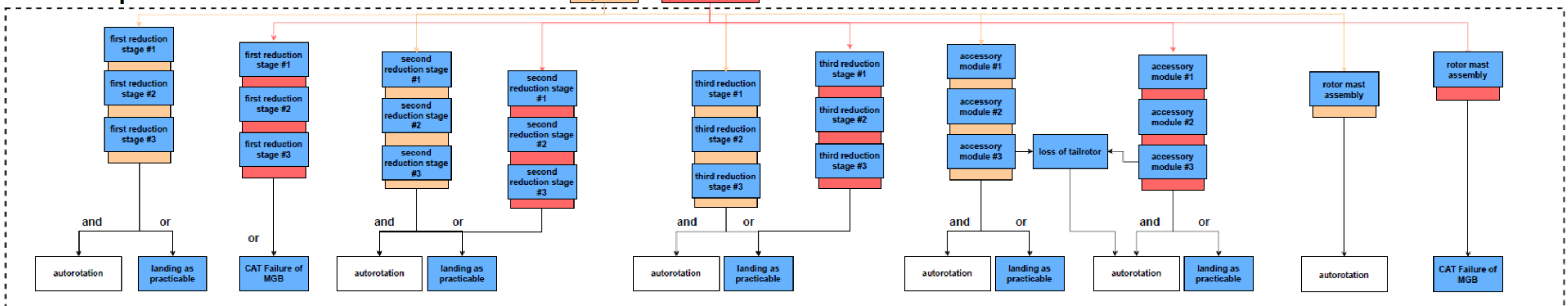


Figure 97 : CH53K – specific flow diagram

5.3 Summary

Table 10 summarizes the catastrophic weaknesses and their positions in the evaluated configurations that can be found in Annex A.1 to A.5. All of the listed cases lead to the loss of the normal distribution of loads from input to output stage, followed by a catastrophic event.

Pos.	Figure	Configuration	Subpart	Weakness	Crack/Wear growth	Breakage/Crack	Additional contributions
1	Figure 98	Epicyclic; 2 Engines with reduction gearboxes	Planetary gear stage outer ring	Loss of transmitting power	Crack growth from tooth root or teeth contact surface into gear ring hub	Circumferential crack through outer ring hub	
2	Figure 98	Epicyclic; 2 Engines with reduction gearboxes	Planetary gear stage outer ring	Jamming of planetary gear stage	Crack growth from tooth root or teeth contact surface into gear ring hub	Circumferential crack through outer ring hub	Deformation of ring No sufficient space for ejection of ring
3	Figure 98	Epicyclic; 2 Engines with reduction gearboxes	Planetary gear stage outer ring	Jamming of planetary gear stage	Crack growth from tooth root or teeth contact surface into gear ring hub	Longitudinal crack	Insufficient stiffness
4	Figure 98	Epicyclic; 2 Engines with reduction gearboxes	Planetary gear stage outer ring	Jamming of planetary gear stage	Crack growth from tooth root or teeth contact surface through single gear tooth	Breakout of larger fragments	Ejection of fragments from gear mesh not possible
5	Figure 98	Epicyclic; 2 Engines with reduction gearboxes	Planetary gear stage outer ring	Jamming due to wrong gear engagement	Crack growth from tooth root or teeth contact surface through single gear tooth/teeth	Breakage of planetary outer gear teeth	Overload due to missing tooth/teeth Contact ratio < 2
6	Figure 99	Epicyclic; 2 Engines with reduction gearboxes	Planetary gear stage carrier	Jamming of planetary gear stage	Crack growth from planetary gear shafts/support	Breakage of gear shaft	Separation of gear shaft
7	Figure 99	Epicyclic; 2 Engines with reduction gearboxes	Planetary gear stage carrier	Loss of transmitting power to rotor mast	Total wear at spline connection	n/a	No release of fragments due to closed design
8	Figure 99	Epicyclic; 2 Engines with reduction gearboxes	Planetary gear stage carrier	Jamming of planetary gear stage	Crack growth from spline connection into hub	Circumferential crack	No sufficient space for ejection Free gear stage fragments

Pos.	Figure	Configuration	Subpart	Weakness	Crack/Wear growth	Breakage/Crack	Additional contributions	
9	Figure 99	Epicyclic; 2 Engines with reduction gearboxes	Planetary gear stage carrier	Jamming of planetary gear stage	Crack growth from spline connection into hub	Longitudinal crack	No sufficient space for ejection	Change of stiffness and gear deflection
10	Figure 99	Epicyclic; 2 Engines with reduction gearboxes	Planetary gear stage carrier	Jamming of planetary gear stage	Crack growth from spline connection through single spline tooth	Breakout of larger fragments	Overrolling of released fragments at gear stage	Damage of gear stage
11	Figure 100	Epicyclic; 2 Engines with reduction gearboxes	Planetary gear stage gear	Jamming of planetary gear stage	Crack growth from tooth root or teeth contact surface through single or multiple gear tooth	Breakage of planetary gear tooth/teeth	No sufficient space for ejecting of fragments	Damage of other surrounding components
12	Figure 100	Epicyclic; 2 Engines with reduction gearboxes	Planetary gear stage gear	Jamming due to wrong gear engagement	Crack growth from tooth root or teeth contact surface through single or multiple gear tooth	Breakage of planetary gear tooth/teeth	Overload due to missing tooth	Contact ratio < 2
13	Figure 100	Epicyclic; 2 Engines with reduction gearboxes	Planetary gear stage gear	Jamming of planetary gear stage	Crack growth from tooth root, teeth contact surface or integrated raceway into gear ring	Radial crack	Change in stiffness and deformation of gear	Gear mesh interference and limited space for ejection of fragments
14	Figure 100	Epicyclic; 2 Engines with reduction gearboxes	Planetary gear stage gear	Jamming of planetary gear stage	Crack growth from tooth root, teeth contact surface or integrated raceway into gear ring	Radial crack	Change in stiffness and deformation of gear	Damage of other surrounding components limited space for ejection of fragments
15	Figure 100	Epicyclic; 2 Engines with reduction gearboxes	Planetary gear stage gear	Jamming of planetary gear stage	Overload of gear	Deformation/breakage of planetary gear	Interference with other gear meshing	Limited space for ejection of fragments
16	Figure 101	Epicyclic; 2 Engines with reduction gearboxes	Collector wheel	Loss of transmitting power to rotor mast	Crack growth from spline connection into upper or bottom area of the wheel	Circumferential crack	Wheel still fixed in position	

Pos.	Figure	Configuration	Subpart	Weakness	Crack/Wear growth	Breakage/Crack	Additional contributions
17	Figure 101	Epicyclic; 2 Engines with reduction gearboxes	Collector wheel	Loss of transmitting power to rotor mast	Crack growth from spline connection into lower area of the wheel	Circumferential crack	Deflection and change of mesh Total wear
18	Figure 101	Epicyclic; 2 Engines with reduction gearboxes	Collector wheel	Loss of transmitting power to rotor mast	Crack growth from oil bore holes into shaft	Circumferential crack	Gear ring is free after disconnection
19	Figure 101	Epicyclic; 2 Engines with reduction gearboxes	Collector wheel	Jamming of collector stage	Crack growth from oil bore holes into shaft	Circumferential crack	Gear ring is free after disconnection
20	Figure 101	Epicyclic; 2 Engines with reduction gearboxes	Collector wheel	Loss of transmitting power to rotor mast	Total wear at spline connection	n/a	No release of fragments due to closed design
21	Figure 102	Epicyclic; 2 Engines with reduction gearboxes	Collector Shaft	Jamming of collector stage	Crack growth from thread upwards to rotor must nut	Circumferential crack	Loss of collector stage integrity
22	Figure 102	Epicyclic; 2 Engines with reduction gearboxes	Collector shaft	Loss of transmitting power to rotor mast	Crack growth from spline connection into shaft	Circumferential crack	Shaft still fixed in position
23	Figure 102	Epicyclic; 2 Engines with reduction gearboxes	Collector shaft	Loss of transmitting power to rotor mast	Total wear at spline connection	n/a	No release of fragments due to closed design
24	Figure 103	Epicyclic; 2 Engines with reduction gearboxes	Collector gear ring	Jamming due to wrong gear engagement	Crack growth from tooth root or tooth contact surface through gear tooth/teeth	Breakage of collector gear ring tooth/teeth	Overload due to missing tooth/teeth Contact ratio < 2
25	Figure 103	Epicyclic; 2 Engines with reduction gearboxes	Collector gear ring	Jamming due to wrong gear engagement	Crack growth from tooth root or tooth contact surface through gear tooth	Fracture of additional teeth	Ejection of fragments from gear mesh not possible
26	Figure 103	Epicyclic; 2 Engines with reduction gearboxes	Collector gear ring	Jamming of collector stage	Crack growth from tooth root, tooth contact surface or bolt/oil holes towards gear shaft/ring	Radial crack	Change of stiffness and gear deflection Gear deformation and breakage

Pos.	Figure	Configuration	Subpart	Weakness	Crack/Wear growth	Breakage/Crack	Additional contributions
27	Figure 103	Epicyclic; 2 Engines with reduction gearboxes	Collector gear ring	Loss of transmitting power to rotor mast	Crack growth from tooth root, tooth contact surface or bolt/oil holes towards gear shaft/ring	Circumferential crack	Free gear ring
28	Figure 103	Epicyclic; 2 Engines with reduction gearboxes	Collector gear ring	Jamming of collector stage	Crack growth from tooth root, tooth contact surface or bolt/oil holes towards gear shaft/ring	Circumferential crack	Free gear ring
29	Figure 104	Epicyclic; 2 Engines with reduction gearboxes	Sun gear	Jamming due to wrong gear engagement	Crack growth from tooth root or tooth contact surface through single or multiple teeth	Breakage of sun gear tooth/teeth	Overload due to missing tooth
30	Figure 104	Epicyclic; 2 Engines with reduction gearboxes	Sun gear	Jamming due to wrong gear engagement	Crack growth from tooth root or tooth contact surface through single or multiple teeth	Fracture of additional teeth	Ejection of fragments from gear mesh not possible
31	Figure 104	Epicyclic; 2 Engines with reduction gearboxes	Sun gear	Loss of transmitting power to rotor mast	Crack growth from tooth root or tooth contact surface into shaft	Circumferential crack	Free collector shaft fragment
32	Figure 104	Epicyclic; 2 Engines with reduction gearboxes	Sun gear	Jamming of collector stage	Crack growth from tooth root or tooth contact surface into shaft	Circumferential crack	Free collector shaft fragment
33	Figure 105	Epicyclic; 2 Engines with reduction gearboxes	Input Pinion	Jamming due to wrong gear engagement	Crack growth from tooth root or tooth contact surface through single or multiple teeth	Breakage of input pinion tooth/teeth	Overload due to missing tooth
34	Figure 105	Epicyclic; 2 Engines with reduction gearboxes	Input Pinion	Jamming due to wrong gear engagement	Crack growth from tooth root or tooth contact surface through single or multiple teeth	Fracture of additional teeth	Ejection of fragments from gear mesh not possible
35	Figure 106	Epicyclic; 2 Engines with reduction gearboxes	Input Pinion	Loss of transmitting power to tail rotor	Crack growth from spline connection into shaft	Circumferential crack	Fragments fixed by bearing support and engine output
36	Figure 106	Epicyclic; 2 Engines with reduction gearboxes	Input Pinion	Loss of transmitting power to TR drive	Total wear at spline connection	n/a	No release of fragments due to closed design

Pos.	Figure	Configuration	Subpart	Weakness	Crack/Wear growth	Breakage/Crack	Additional contributions
37	Figure 107	Epicyclic; 2 Engines with reduction gearboxes	Rotor mast	Loss of transmitting power to rotor mast	Crack growth from spline into shaft	Circumferential crack	Loss of planetary carrier integrity
38	Figure 107	Epicyclic; 2 Engines with reduction gearboxes	Rotor mast	Jamming of rotor mast assembly	Crack growth from spline into shaft	Circumferential crack	Loss of planetary carrier integrity No sufficient space for ejection of components
39	Figure 107	Epicyclic; 2 Engines with reduction gearboxes	Rotor mast	Jamming of rotor mast assembly	Crack growth from spline into shaft	Longitudinal crack	Change of stiffness and high deformation Change of crack growth direction and separation of rotor mast
40	Figure 107	Epicyclic; 2 Engines with reduction gearboxes	Rotor mast	Loss of transmitting power to rotor mast	Total wear at spline connection	n/a	No release of fragments due to closed design
41	Figure 110	Epicyclic; 2 Engines with reduction gearboxes	Spur gear	Jamming due to wrong gear engagement	Crack growth from tooth root or tooth contact surface through single or multiple teeth	Breakage of intermediate shaft tooth/teeth	Overload due to missing tooth contact ratio < 2
42	Figure 111	Epicyclic; 2 Engines with reduction gearboxes	Bevel gear	Jamming due to wrong gear engagement	Crack growth from tooth root or teeth contact surface through single or multiple gear tooth	Breakage of bevel gear tooth/teeth	Overload due to missing tooth contact ratio < 2
43	Figure 111	Epicyclic; 2 Engines with reduction gearboxes	Bevel gear	Jamming due to wrong gear engagement	Crack growth from tooth root or teeth contact surface through single or multiple gear tooth	Fracture of additional teeth	Ejection of fragments from gear mesh not possible
44	Figure 111	Epicyclic; 2 Engines with reduction gearboxes	Bevel gear	Jamming of intermediate stage	Crack growth from tooth root, teeth contact surface or spline connection into gear hub	Radial crack	Change of stiffness and gear deflection Gear deformation
45	Figure 112	Epicyclic; 2 Engines with reduction gearboxes	Intermediate Tail rotor spur gear	Loss of transmitting power to tail rotor	Crack growth from tooth contact surface, tooth root, oil bore holes or spline connection to gear hub	Crack of hub	

Pos.	Figure	Configuration	Subpart	Weakness	Crack/Wear growth	Breakage/Crack	Additional contributions
46	Figure 112	Epicyclic; 2 Engines with reduction gearboxes	Intermediate Tail rotor spur gear	Jamming of TR stage	Crack growth from tooth contact surface, tooth root, oil bore holes or spline connection to gear hub	Radial crack	Change of stiffness and gear deflection
47	Figure 112	Epicyclic; 2 Engines with reduction gearboxes	Intermediate Tail rotor spur gear	Jamming due to wrong gear engagement	Crack growth from tooth root or tooth contact surface through single or multiple gear tooth	Breakage of spur gear tooth/teeth	Overload due to missing tooth
48	Figure 112	Epicyclic; 2 Engines with reduction gearboxes	Intermediate Tail rotor spur gear	Loss of transmitting power to tail rotor	Total wear at spline connection	n/a	No release of fragments due to closed design
49	Figure 113	Epicyclic; 2 Engines with reduction gearboxes	Tail rotor intermediate shaft	Loss of transmitting power to tail rotor	Total wear at spline connection	n/a	No release of fragments due to closed design
50	Figure 114	Epicyclic; 2 Engines with reduction gearboxes	Tail rotor output spur gear	Jamming due to wrong gear engagement	Crack growth from tooth root or tooth contact surface through single or multiple gear tooth	Breakage of TR output spur gear tooth/teeth	Overload due to missing tooth
51	Figure 114	Epicyclic; 2 Engines with reduction gearboxes	Tail rotor output spur gear	Loss of transmitting power to tail rotor	Total wear at spline connection	n/a	No release of fragments due to closed design
52	Figure 114	Epicyclic; 2 Engines with reduction gearboxes	Tail rotor output spur gear	Loss of transmitting power to tail rotor	Crack growth from tooth root, teeth contact surface through, oil bore holes or spline connection into gear hub	Crack of hub	
53	Figure 114	Epicyclic; 2 Engines with reduction gearboxes	Tail rotor output spur gear	Jamming of tail rotor stage	Crack growth from tooth root, teeth contact surface through, oil bore holes or spline connection into gear hub	Radial crack	Change of stiffness and gear deflection
54	Figure 115	Epicyclic; 2 Engines with reduction gearboxes	Tail rotor output shaft	Loss of transmitting power to tail rotor	Crack growth from spline connection into shaft	Circumferential crack	

Pos.	Figure	Configuration	Subpart	Weakness	Crack/Wear growth	Breakage/Crack	Additional contributions
55	Figure 115	Epicyclic; 2 Engines with reduction gearboxes	Tail rotor output shaft	Loss of transmitting power to tail rotor	Total wear at spline connection	n/a	No release of fragments due to closed design
56	Figure 116	Epicyclic; 1 Engine	Input Pinion	Loss of transmitting power	Crack growth from tooth root or teeth contact surface through single or multiple gear teeth	Fracture of additional teeth	Ejection of fragments from gear mesh not possible
57	Figure 116	Epicyclic; 1 Engine	Input Pinion	Jamming due to wrong gear engaging	Crack growth from tooth root or teeth contact surface through single or multiple gear teeth	Breakage of input pinion tooth/teeth	Overload due to missing tooth
58	Figure 116	Epicyclic; 1 Engine	Input Pinion	Loss of transmitting power	Crack growth from tooth root or teeth contact surface into shaft between bearings and gear	Circumferential crack	
59	Figure 117	Epicyclic; 1 Engine	1 st reduction stage bevel Gear Shaft	Jamming of the reduction stage	Crack growth from integrated raceway into shaft	Circumferential crack	Not enough space for ejection of free bevel gear shaft
60	Figure 117	Epicyclic; 1 Engine	1 st reduction stage bevel Gear Shaft	Loss of transmitting power	Crack growth from tooth root or teeth contact surface through single multiple gear tooth	Fracture of additional teeth	Ejection of fragments from gear mesh not possible
61	Figure 117	Epicyclic; 1 Engine	1 st reduction stage bevel Gear Shaft	Jamming due to wrong gear engaging	Crack growth from tooth root or teeth contact surface through single multiple gear tooth	Breakage of bevel gear tooth/teeth	Overload due to missing tooth
62	Figure 117	Epicyclic; 1 Engine	1 st reduction stage bevel Gear Shaft	Loss of transmitting power	Crack growth from tooth root, teeth contact surface or welding area into gear hub	Crack of hub	Free gear ring
63	Figure 117	Epicyclic; 1 Engine	1 st reduction stage bevel Gear Shaft	Jamming	Crack growth from tooth root, teeth contact surface or welding area into gear hub	Crack of hub	Free gear ring
							No sufficient space for loose fragments to engage

Pos.	Figure	Configuration	Subpart	Weakness	Crack/Wear growth	Breakage/Crack	Additional contributions
64	Figure 117	Epicyclic; 1 Engine	1 st reduction stage bevel Gear Shaft	Jamming of 1 st reduction stage	Crack growth from tooth root, teeth contact surface or welding area into gear hub	Radial Crack	Change of stiffness and gear deflection
65	Figure 117	Epicyclic; 1 Engine	1 st reduction stage bevel Gear Shaft	Jamming of reduction stage	Crack growth from spline connection above spline	Circumferential crack	Not enough space for ejection of free bevel gear shaft
66	Figure 117	Epicyclic; 1 Engine	1 st reduction stage bevel Gear Shaft	Loss of transmitting power	Crack growth from spline connection beneath spline	Circumferential crack	Loss of gear meshing
67	Figure 117	Epicyclic; 1 Engine	1 st reduction stage bevel Gear Shaft	Jamming	Crack growth from spline connection beneath spline	Circumferential crack	Not enough space for ejection of free bevel gear shaft
68	Figure 117	Epicyclic; 1 Engine	1 st reduction stage bevel Gear Shaft	Loss of transmitting power to rotor mast	Total wear at spline connection	n/a	No release of fragments due to closed design
69	Figure 118	Epicyclic; 1 Engine	1 st reduction stage sun gear shaft	Jamming due to wrong gear engaging	Crack growth from tooth root or teeth contact surface through gear tooth or multiple teeth	Breakage of sun gear tooth/teeth	Overload due to missing tooth
70	Figure 118	Epicyclic; 1 Engine	1 st reduction stage sun gear shaft	Jamming of collector stage	Crack growth from tooth root or teeth contact surface through gear tooth or multiple teeth	Breakage of sun gear shaft	Ejection of fragments from gear mesh not possible
71	Figure 118	Epicyclic; 1 Engine	1 st reduction stage sun gear shaft	Jamming of sun gear stage	Crack growth from tooth root or teeth contact surface into shaft above sun gear	Circumferential crack	Not enough space for ejection of fragments
72	Figure 118	Epicyclic; 1 Engine	1 st reduction stage sun gear shaft	Jamming of reduction stage	Crack growth from tooth root or teeth contact surface into shaft beneath sun gear	Circumferential crack	Not enough space for ejection of free bevel gear shaft
73	Figure 118	Epicyclic; 1 Engine	1 st reduction stage sun gear shaft	Loss of transmitting power	Crack growth from tooth root or teeth contact surface into shaft beneath sun gear	Circumferential crack	

Pos.	Figure	Configuration	Subpart	Weakness	Crack/Wear growth	Breakage/Crack	Additional contributions
74	Figure 118	Epicyclic; 1 Engine	1 st reduction stage sun gear shaft	Jamming of reduction stage	Crack growth from spline connection above spline	Circumferential crack	Not enough space for ejection of free sun gear shaft
75	Figure 118	Epicyclic; 1 Engine	1 st reduction stage sun gear shaft	Loss of transmitting power	Crack growth from spline connection beneath spline	Circumferential crack	Loss of gear meshing
76	Figure 118	Epicyclic; 1 Engine	1 st reduction stage sun gear shaft	Jamming	Crack growth from spline connection beneath spline	Circumferential crack	Not enough space for ejection of free sun gear shaft
77	Figure 118	Epicyclic; 1 Engine	1 st reduction stage sun gear shaft	Loss of transmitting power to rotor mast	Total wear at spline connection	n/a	No release of fragments due to closed design
78	Figure 119	Epicyclic; 1 Engine	2 nd reduction stage planetary outer ring	Jamming due to wrong gear engaging	Crack growth from tooth root or teeth contact surface through single or multiple gear teeth	Breakage of outer ring tooth/teeth	Overload due to missing tooth
79	Figure 119	Epicyclic; 1 Engine	2 nd reduction stage planetary outer ring	Jamming of planetary gear stage	Crack growth from tooth root or teeth contact surface through single or multiple gear teeth	Breakout of larger fragments	Ejection of fragments from gear mesh not possible
80	Figure 119	Epicyclic; 1 Engine	2 nd reduction stage planetary outer ring	Loss of transmitting power	Crack growth from tooth root or teeth contact surface into gear hub	Circumferential crack	Free gear ring
81	Figure 119	Epicyclic; 1 Engine	2 nd reduction stage planetary outer ring	Jamming of planetary gear stage	Crack growth from tooth root or teeth contact surface into gear hub	Circumferential crack	No sufficient space for ejection of gear ring
82	Figure 120	Epicyclic; 1 Engine	2 nd reduction stage planetary carrier	Jamming of intermediate shaft	Crack growth from spline connection or planetary gear shaft/support	Circumferential crack	No sufficient space for ejection
83	Figure 120	Epicyclic; 1 Engine	2 nd reduction stage planetary carrier	Jamming of intermediate shaft	Crack growth from spline connection or planetary gear shaft/support	Longitudinal crack	Change of stiffness, carrier deflection, gear interference
							Limited space to eject broken fragments

Pos.	Figure	Configuration	Subpart	Weakness	Crack/Wear growth	Breakage/Crack	Additional contributions	
84	Figure 120	Epicyclic; 1 Engine	2 nd reduction stage planetary carrier	Loss of transmitting power to rotor mast	Total wear at spline connection	n/a	No release of fragments due to closed design	
85	Figure 121	Epicyclic; 1 Engine	2 nd reduction stage planetary gear	Jamming of planetary gear stage	Deformation of planetary gear	Breakout of planetary gear fragments	Interference with other gear meshing	Limited space to eject broken fragments
86	Figure 121	Epicyclic; 1 Engine	2 nd reduction stage planetary gear	Jamming of planetary gear stage	Crack growth from tooth root or teeth contact surface through single gear tooth	Breakage of planetary gear	Ejection of fragments from gear mesh not possible	Damage of other surrounding components
87	Figure 121	Epicyclic; 1 Engine	2 nd reduction stage planetary gear	Jamming due to wrong gear engaging	Crack growth from tooth root or teeth contact surface through single gear tooth	Breakage of planetary ring tooth/teeth	Overload due to missing tooth	contact ratio < 2
88	Figure 121	Epicyclic; 1 Engine	2 nd reduction stage planetary gear	Jamming of planetary gear stage	Crack growth from tooth root, teeth contact surface or integrated raceway into gear ring	Radial crack	Change in stiffness, deformation and breakage of planetary gear	Damage of surrounding components without space for ejection
89	Figure 122	Epicyclic; 1 Engine	Rotor mast	Loss of rotor mast	Crack growth from spline into upper area of rotor mast	Circumferential crack	Loss of integrity of rotor mast	
90	Figure 122	Epicyclic; 1 Engine	Rotor mast	Loss of rotor mast	Crack growth from integrated raceway into lower area of rotor mast	Circumferential crack	Loss of integrity of rotor mast	
91	Figure 122	Epicyclic; 1 Engine	Rotor mast	Loss of transmitting power to rotor mast	Total wear at spline connection	n/a	No release of fragments due to closed design	
92	Figure 123	Epicyclic; 2 Engines	Intermediate shaft	Jamming of intermediate shaft	Crack growth from integrated raceway towards spur gear	Circumferential crack	No sufficient bearing support	
93	Figure 124	Epicyclic; 2 Engines	Intermediate shaft spur gear	Jamming of intermediate shaft	Crack growth from tooth root or teeth contact surface into shaft	Circumferential crack	Shaft deflection	No sufficient bearing support

Pos.	Figure	Configuration	Subpart	Weakness	Crack/Wear growth	Breakage/Crack	Additional contributions
94	Figure 124	Epicyclic; 2 Engines	Intermediate shaft spur gear	Jamming due to wrong gear engaging	Crack growth from tooth root or teeth contact surface through single tooth or multiple teeth	Fracture of additional teeth	Ejection of fragments from gear mesh not possible
95	Figure 124	Epicyclic; 2 Engines	Intermediate shaft spur gear	Jamming due to wrong gear engaging	Crack growth from tooth root or teeth contact surface through single tooth or multiple teeth	Breakage of spur gear tooth/teeth	Overload due to missing tooth
96	Figure 125	Epicyclic; 2 Engines	Intermediate shaft bevel gear	Jamming due to wrong gear engaging	Crack growth from tooth root or teeth contact surface through single tooth or multiple teeth	Fracture of additional teeth	Ejection of fragments from gear mesh not possible
97	Figure 125	Epicyclic; 2 Engines	Intermediate shaft bevel gear	Jamming due to wrong gear engaging	Crack growth from tooth root or teeth contact surface through single tooth or multiple teeth	Breakage of bevel gear tooth/teeth	Overload due to missing tooth
98	Figure 125	Epicyclic; 2 Engines	Intermediate shaft bevel gear	Jamming of intermediate shaft stage	Crack growth from tooth root, teeth contact surface or spline connection into gear hub	Radial crack	Change of stiffness and gear deflection
99	Figure 126	Epicyclic; 2 Engines	Intermediate shaft	Jamming of intermediate shaft	Crack growth from spline connection into shaft beneath or above spline	Circumferential crack	Shaft deflection
100	Figure 127	Epicyclic; 2 Engines	Collector shaft	Loss of transmitting power to rotor mast	Crack growth from upper spline connection of sun gear into shaft	Circumferential crack	Crack propagation on shaft
101	Figure 127	Epicyclic; 2 Engines	Collector shaft	Loss of transmitting power to main rotor	Crack growth from bottom spline connection of bevel gear up- or downwards into shaft	Circumferential crack	Crack propagation on shaft
102	Figure 127	Epicyclic; 2 Engines	Collector shaft	Loss of transmitting power to rotor mast	Total wear at spline connection	n/a	No release of fragments due to closed design
103	Figure 128	Epicyclic; 2 Engines	Collector gear ring	Jamming of collector stage	Crack growth from tooth root or teeth contact surface towards gear ring	Radial crack	Change of stiffness and gear deflection

Pos.	Figure	Configuration	Subpart	Weakness	Crack/Wear growth	Breakage/Crack	Additional contributions
104	Figure 128	Epicyclic; 2 Engines	Collector gear ring	Loss of transmitting power to collect. stage	Crack growth from tooth root or teeth contact surface towards gear ring	Circumferential crack	Free gear ring
105	Figure 128	Epicyclic; 2 Engines	Collector gear ring	Jamming of collector stage	Crack growth from tooth root or teeth contact surface towards gear ring	Circumferential crack	Free gear ring No sufficient space for gear ring ejection
106	Figure 128	Epicyclic; 2 Engines	Collector gear ring	Jamming due to wrong gear engaging	Crack growth from tooth root or teeth contact surface through single or multiple teeth	Fracture of additional teeth	Ejection of fragments from gear mesh not possible
107	Figure 128	Epicyclic; 2 Engines	Collector gear ring	Jamming due to wrong gear engaging	Crack growth from tooth root or teeth contact surface through single or multiple teeth	Breakage of gear ring tooth/teeth	Overload due to missing tooth contact ratio < 2
108	Figure 129	Epicyclic; 2 Engines	Collector shaft bevel gear	Jamming due to wrong gear engaging	Crack growth from tooth root or teeth contact surface through single or multiple teeth	Fracture of additional teeth	Ejection of fragments from gear mesh not possible
109	Figure 129	Epicyclic; 2 Engines	Collector shaft bevel gear	Jamming due to wrong gear engaging	Crack growth from tooth root or teeth contact surface through single or multiple teeth	Breakage of bevel gear tooth/teeth	Overload due to missing tooth contact ratio < 2
110	Figure 129	Epicyclic; 2 Engines	Collector shaft bevel gear	Jamming of collector stage	Crack growth from tooth root, teeth contact surface, oil bore holes or spline into gear hub	Crack of hub	Free gear ring
111	Figure 129	Epicyclic; 2 Engines	Collector shaft bevel gear	Loss of transmitting power to tail rotor	Crack growth from tooth root, teeth contact surface, oil bore holes or spline into gear hub	Radial crack	Change of stiffness and gear deflection Gear deformation and breakage
112	Figure 129	Epicyclic; 2 Engines	Collector shaft bevel gear	Loss of transmitting power to rotor mast	Total wear at spline connection	n/a	No release of fragments due to closed design
113	Figure 130	Epicyclic; 2 Engines	Collector stage sun gear	Jamming of collector stage	Crack growth from tooth root or teeth contact surface through single or multiple teeth	Breakage of sun gear ring	Ejection of fragments from gear mesh not possible No sufficient space for ejection of add. fragments

Pos.	Figure	Configuration	Subpart	Weakness	Crack/Wear growth	Breakage/Crack	Additional contributions
114	Figure 130	Epicyclic; 2 Engines	Collector stage sun gear	Jamming due to wrong gear engaging	Crack growth from tooth root or teeth contact surface through single or multiple teeth	Breakage of sun gear tooth/teeth	Overload due to missing tooth contact ratio < 2
115	Figure 130	Epicyclic; 2 Engines	Collector stage sun gear	Loss of transmitting power to rotor mast	Total wear at spline connection	n/a	No release of fragments due to closed design
116	Figure 130	Epicyclic; 2 Engines	Collector stage sun gear	Jamming of collector stage	Crack growth from tooth root, teeth contact surface or spline connection into gear hub	Radial crack	Change in stiffness, deformation, sun gear breakage
117	Figure 130	Epicyclic; 2 Engines	Collector stage sun gear	Loss of transmitting power to rotor mast	Crack growth from tooth root, teeth contact surface or spline connection into gear hub	Crack of hub	Free gear ring
118	Figure 131	Epicyclic; 2 Engines	Tail rotor pinion shaft	Loss of transmitting power to tail rotor	Crack growth from tooth root or teeth contact surface into shaft	Circumferential crack	
119	Figure 131	Epicyclic; 2 Engines	Tail rotor pinion shaft	Loss of transmitting power to tail rotor	Crack growth from spline into shaft	Circumferential crack	No sufficient space for ejection of fragments
120	Figure 131	Epicyclic; 2 Engines	Tail rotor pinion shaft	Jamming due to wrong gear engaging	Crack growth from tooth root or teeth contact surface through single gear tooth	Breakage of pinion tooth/teeth	No sufficient space for ejection of fragments
121	Figure 131	Epicyclic; 2 Engines	Tail rotor pinion shaft	Loss of transmitting power to tail rotor	Total wear at spline connection	n/a	No release of fragments due to closed design
122	Figure 132	Epicyclic; 2 Engines	Tail rotor input pinion	Jamming due to wrong gear engaging	Crack growth from tooth root or teeth contact surface through single tooth or multiple teeth	Breakage of pinion tooth/teeth	Overload due to missing tooth
123	Figure 133	Epicyclic; 2 Engines	Rotor mast	Loss of transmitting power	Crack growth from spline into shaft	Circumferential crack	Shaft deflection

Pos.	Figure	Configuration	Subpart	Weakness	Crack/Wear growth	Breakage/Crack	Additional contributions
124	Figure 133	Epicyclic; 2 Engines	Rotor mast	Loss of rotor mast assembly	Crack growth from spline into shaft	Circumferential crack	Shaft deflection
125	Figure 133	Epicyclic; 2 Engines	Rotor mast	Loss of rotor mast assembly	Crack growth at thread at rotor mast nut	Circumferential crack	Loss of integrity of rotor mast
126	Figure 133	Epicyclic; 2 Engines	Rotor mast	Loss of transmitting power to rotor mast	Total wear at spline connection	n/a	No release of fragments due to closed design
127	Figure 134	Epicyclic; 2 Engines	Planetary outer ring	Jamming of planetary gear stage	Crack growth from tooth root or teeth contact surface through single gear tooth	Breakout of larger fragments	Ejection of fragments from gear mesh not possible
128	Figure 134	Epicyclic; 2 Engines	Planetary outer ring	Loss of transmitting power	Crack growth from tooth root or teeth contact surface into hub	Circumferential crack	Free gear ring
129	Figure 134	Epicyclic; 2 Engines	Planetary outer ring	Jamming of planetary gear stage	Crack growth from tooth root or teeth contact surface into hub	Circumferential crack	Free gear ring
130	Figure 134	Epicyclic; 2 Engines	Planetary outer ring	Jamming due to wrong gear engaging	Crack growth from tooth root or teeth through single tooth or multiple teeth	Breakage of outer ring tooth/teeth	Overload due to missing tooth
131	Figure 135	Epicyclic; 2 Engines	Planetary carrier	Jamming of intermediate shaft	Crack growth from spline connection or planetary gear shafts/support into hub	Circumferential crack	Free planetary gear stage fragments
132	Figure 135	Epicyclic; 2 Engines	Planetary carrier	Jamming of intermediate shaft	Crack growth from spline connection or planetary gear shafts/support into hub	Longitudinal crack	Change in stiffness, carrier deflection, gear interference
133	Figure 135	Epicyclic; 2 Engines	Planetary carrier	Loss of transmitting power to rotor mast	Total wear at spline connection	n/a	No release of fragments due to closed design
134	Figure 136	Epicyclic; 2 Engines	Planetary gear	Jamming of planetary gear stage	Crack growth from tooth root or teeth contact surface through single gear tooth	Breakage of planetary gear	Ejection of fragments from gear mesh not possible
							Limited space to eject damaged surrounding parts

Pos.	Figure	Configuration	Subpart	Weakness	Crack/Wear growth	Breakage/Crack	Additional contributions
135	Figure 136	Epicyclic; 2 Engines	Planetary gear	Jamming due to wrong gear engaging	Crack growth from tooth root or teeth contact surface through single gear tooth	Breakage of planetary gear tooth/teeth	Overload due to missing tooth contact ratio < 2
136	Figure 136	Epicyclic; 2 Engines	Planetary gear	Jamming of planetary gear stage	Crack growth from tooth root, teeth contact surface or integrated raceway into gear ring	Radial crack	Change in stiffness, deformation and breakage of planetary gear Damage of surrounding components without sufficient space for ejection
137	Figure 136	Epicyclic; 2 Engines	Planetary gear	Jamming of planetary gear stage	Deformation of planetary gear	Breakout of planetary gear fragments	Interference with other gear meshing Limited space to eject broken fragments
138	Figure 137	Collector; 2 Engines Fenestron Tail Rotor	Collector gear ring	Jamming at collector stage	Crack growth from tooth root, teeth contact surface or bolt holes towards gear ring	Circumferential crack	Free gear ring
139	Figure 137	Collector; 2 Engines Fenestron Tail Rotor	Collector gear ring	Loss of transmitting power to Rotor Mast	Crack growth from tooth root, teeth contact surface or bolt holes towards gear ring	Circumferential crack	Free gear ring
140	Figure 137	Collector; 2 Engines Fenestron Tail Rotor	Collector gear ring	Jamming at collector stage	Crack growth from tooth root, teeth contact surface or bolt holes towards gear ring	Radial crack	Change in stiffness Gear deformation and breakage
141	Figure 137	Collector; 2 Engines Fenestron Tail Rotor	Collector gear ring	Jamming due to wrong gear engaging	Crack growth from tooth root or teeth contact surface through single tooth or multiple teeth	Fracture of additional teeth	Ejection of fragments from gear mesh not possible
142	Figure 137	Collector; 2 Engines Fenestron Tail Rotor	Collector gear ring	Jamming due to wrong gear engaging	Crack growth from tooth root or teeth contact surface through single tooth or multiple teeth	Breakage of gear ring tooth/teeth	Overload due to missing tooth contact ratio < 2
143	Figure 138	Collector; 2 Engines Fenestron Tail Rotor	Collector wheel	Loss of transmitting power	Crack growth from spline connection into wheel	Circumferential crack	

Pos.	Figure	Configuration	Subpart	Weakness	Crack/Wear growth	Breakage/Crack	Additional contributions
144	Figure 138	Collector; 2 Engines Fenestron Tail Rotor	Collector wheel	Loss of transmitting power to rotor mast	Total wear at spline connection	n/a	No release of fragments due to closed design
145	Figure 138	Collector; 2 Engines Fenestron Tail Rotor	Collector wheel	Loss of transmitting power to rotor mast	Crack growth from oil bore holes into shaft	Circumferential crack	Free gear ring
146	Figure 138	Collector; 2 Engines Fenestron Tail Rotor	Collector wheel	Jamming of collector stage	Crack growth from oil bore holes into shaft	Circumferential crack	Free gear ring
147	Figure 139	Collector; 2 Engines Fenestron Tail Rotor	Rotor mast	Jamming of rotor mast assembly	Crack growth from thread upwards rotor mast nut	Circumferential crack	Loss of rotor mast integrity
148	Figure 139	Collector; 2 Engines Fenestron Tail Rotor	Rotor mast	Jamming of rotor mast assembly	Crack growth from spline beneath it into shaft	Circumferential crack	Shaft deflection
149	Figure 139	Collector; 2 Engines Fenestron Tail Rotor	Rotor mast	Loss of rotor mast assembly	Crack growth from spline beneath it into shaft	Circumferential crack	Shaft deflection
150	Figure 139	Collector; 2 Engines Fenestron Tail Rotor	Rotor mast	Loss of rotor mast assembly	Crack growth from spline above it into shaft	Circumferential crack	Loss of rotor mast integrity
151	Figure 139	Collector; 2 Engines Fenestron Tail Rotor	Rotor mast	Loss of transmitting power to rotor mast	Total wear at spline connection	n/a	No release of fragments due to closed design
152	Figure 140	Collector; 2 Engines Fenestron Tail Rotor	Input pinion	Jamming due to wrong gear engaging	Crack growth from tooth root or teeth contact surface through single tooth or multiple teeth	Fracture of additional teeth	Ejection of fragments from gear mesh not possible
153	Figure 140	Collector; 2 Engines Fenestron Tail Rotor	Input pinion	Jamming due to wrong gear engaging	Crack growth from tooth root or teeth contact surface through single tooth or multiple teeth	Breakage of pinion tooth/teeth	Overload due to missing tooth
154	Figure 141	Collector; 2 Engines Fenestron Tail Rotor	Intermediate shaft	Jamming of intermediate shaft	Crack growth at upper integrated raceway between bearing and spur gear	Circumferential crack	No sufficient bearing support

Pos.	Figure	Configuration	Subpart	Weakness	Crack/Wear growth	Breakage/Crack	Additional contributions
155	Figure 143	Collector; 2 Engines Fenestron Tail Rotor	Spur gear	Jamming due to wrong gear engaging	Crack growth from tooth root or teeth contact surface through single tooth or multiple teeth	Fracture of additional teeth	Ejection of fragments from gear mesh not possible
156	Figure 143	Collector; 2 Engines Fenestron Tail Rotor	Spur gear	Jamming due to wrong gear engaging	Crack growth from tooth root or teeth contact surface through single tooth or multiple teeth	Breakage of gear ring tooth/teeth	Overload due to missing tooth contact ratio < 2
157	Figure 143	Collector; 2 Engines Fenestron Tail Rotor	Spur gear	Jamming of intermediate shaft	Crack growth from tooth root or teeth contact surface into shaft between upper bearing and spur gear	Circumferential crack	Shaft deflection No sufficient bearing support
158	Figure 144	Collector; 2 Engines Fenestron Tail Rotor	Intermediate stage bevel gear	Jamming of intermediate shaft	Crack growth from tooth root, teeth contact surface or oil bore holes into gear hub	Radial crack	Change in stiffness and deflection of gear Gear deformation and breakage
159	Figure 144	Collector; 2 Engines Fenestron Tail Rotor	Intermediate stage bevel gear	Jamming due to wrong gear engaging	Crack growth from tooth root or teeth contact surface through single tooth or multiple teeth	Fracture of additional teeth	Ejection of fragments from gear mesh not possible
160	Figure 144	Collector; 2 Engines Fenestron Tail Rotor	Intermediate stage bevel gear	Jamming due to wrong gear engaging	Crack growth from tooth root or teeth contact surface through single tooth or multiple teeth	Breakage of bevel gear tooth/teeth	Overload due to missing tooth contact ratio < 2
161	Figure 145	Collector; 2 Engines Fenestron Tail Rotor	Intermediate tail rotor shaft bevel gear	Jamming of tail rotor stage	Crack growth from tooth root, teeth contact surface or spline connection into gear hub	Radial crack	Change in stiffness and deflection of gear Gear deformation and breakage
162	Figure 145	Collector; 2 Engines Fenestron Tail Rotor	Intermediate tail rotor shaft bevel gear	Loss of transmitting power	Crack growth from tooth root, teeth contact surface or spline connection into gear hub	Crack of hub	Free gear ring No sufficient space for engaging of fragments
163	Figure 145	Collector; 2 Engines Fenestron Tail Rotor	Intermediate tail rotor shaft bevel gear	Jamming of tail rotor stage	Crack growth from tooth root, teeth contact surface or spline connection into gear hub	Crack of hub	Free gear ring

Pos.	Figure	Configuration	Subpart	Weakness	Crack/Wear growth	Breakage/Crack	Additional contributions
164	Figure 145	Collector; 2 Engines Fenestron Tail Rotor	Intermediate tail rotor shaft bevel gear	Loss of transmitting power	Crack growth from tooth root, teeth contact surface through single tooth or multiple teeth	Fracture of additional teeth	Ejection of fragments from gear mesh not possible
165	Figure 145	Collector; 2 Engines Fenestron Tail Rotor	Intermediate tail rotor shaft bevel gear	Jamming due to wrong gear engaging	Crack growth from tooth root, teeth contact surface through single tooth or multiple teeth	Fracture of additional teeth	Ejection of fragments from gear mesh not possible
166	Figure 145	Collector; 2 Engines Fenestron Tail Rotor	Intermediate tail rotor shaft bevel gear	Jamming due to wrong gear engaging	Crack growth from tooth root, teeth contact surface through single tooth or multiple teeth	Breakage of bevel gear tooth/teeth	Overload due to missing tooth contact ratio < 2
167	Figure 145	Collector; 2 Engines Fenestron Tail Rotor	Intermediate tail rotor shaft bevel gear	Loss of transmitting power to tail rotor	Total wear at spline connection	n/a	No release of fragments due to closed design
168	Figure 146	Collector; 2 Engines Fenestron Tail Rotor	Intermediate tail rotor shaft spur gear	Jamming of intermediate shaft	Crack growth from tooth root or teeth contact surface into shaft above spur gear	Circumferential crack	Shaft deflection No sufficient bearing support
169	Figure 146	Collector; 2 Engines Fenestron Tail Rotor	Intermediate tail rotor shaft spur gear	Jamming due to wrong gear engaging	Crack growth from tooth root, teeth contact surface through single tooth or multiple teeth	Fracture of additional teeth	Ejection of fragments from gear mesh not possible
170	Figure 146	Collector; 2 Engines Fenestron Tail Rotor	Intermediate tail rotor shaft spur gear	Jamming due to wrong gear engaging	Crack growth from tooth root, teeth contact surface through single tooth or multiple teeth	Breakage of spur gear tooth/teeth	Overload due to missing tooth contact ratio < 2
171	Figure 146	Collector; 2 Engines Fenestron Tail Rotor	Intermediate tail rotor shaft spur gear	Loss of transmitting power to tail rotor	Crack growth from tooth root or teeth contact surface into shaft beneath spur gear	Circumferential crack	Bearings hold shaft in position
172	Figure 147	Collector; 2 Engines Fenestron Tail Rotor	Intermediate tail rotor shaft	Jamming of tail rotor intermediate shaft	Crack growth from spline connection into shaft	Circumferential crack	Shaft deflection No sufficient bearing support
173	Figure 147	Collector; 2 Engines Fenestron Tail Rotor	Intermediate tail rotor shaft	Loss of transmitting power to tail rotor	Total wear at spline connection	n/a	No release of fragments due to closed design

Pos.	Figure	Configuration	Subpart	Weakness	Crack/Wear growth	Breakage/Crack	Additional contributions
174	Figure 148	Collector; 2 Engines Fenestron Tail Rotor	Tail rotor output pinion	Jamming due to wrong gear engaging	Crack growth from tooth root, teeth contact surface through single tooth or multiple teeth	Breakage of pinion tooth/teeth	Overload due to missing tooth contact ratio < 2
175	Figure 148	Collector; 2 Engines Fenestron Tail Rotor	Tail rotor output pinion	Loss of transmitting power to tail rotor	Crack growth from tooth root or teeth contact surface into shaft between bevel gear and bearing	Circumferential crack	Free gear ring No sufficient space for engaging of fragments
176	Figure 148	Collector; 2 Engines Fenestron Tail Rotor	Tail rotor output pinion	Jamming of tail rotor stage	Crack growth from tooth root or teeth contact surface through single tooth or multiple teeth	Circumferential crack	Free gear ring No sufficient space for engaging of fragments
177	Figure 148	Collector; 2 Engines Fenestron Tail Rotor	Tail rotor output pinion	Loss of transmitting power to tail rotor	Crack growth from tooth root or teeth contact surface into shaft between input spline and bearing	Circumferential crack	Output flange fixed in position
178	Figure 150	Collector; 3 Engines Split torque variant	Input pinion	Jamming due to wrong gear engaging	Crack growth from tooth root, teeth contact surface through single tooth or multiple teeth	Fracture of additional teeth	Ejection of fragments from gear mesh not possible
179	Figure 150	Collector; 3 Engines Split torque variant	Input pinion	Jamming due to wrong gear engaging	Crack growth from tooth root, teeth contact surface through single tooth or multiple teeth	Breakage of pinion tooth/teeth	Overload due to missing tooth contact ratio < 2
180	Figure 151	Collector; 3 Engines Split torque variant	Reduction stage shaft	Jamming of one of the 1 st reduction stages	Crack growth between upper integrated raceway and bevel gear	Circumferential crack	Shaft deflection No sufficient bearing support
181	Figure 152	Collector; 3 Engines Split torque variant	Reduction stage upper / lower spur gear	Jamming due to wrong gear engaging	Crack growth from tooth root, teeth contact surface through single tooth or multiple teeth	Fracture of additional teeth	Ejection of fragments from gear mesh not possible
182	Figure 152	Collector; 3 Engines Split torque variant	Reduction stage upper / lower spur gear	Jamming due to wrong gear engaging	Crack growth from tooth root, teeth contact surface through single tooth or multiple teeth	Breakage of spur gear tooth/teeth	Overload due to missing tooth contact ratio < 2

Pos.	Figure	Configuration	Subpart	Weakness	Crack/Wear growth	Breakage/Crack	Additional contributions
183	Figure 153	Collector; 3 Engines Split torque variant	Reduction stage shaft bevel gear	Jamming due to wrong gear engaging	Crack growth from tooth root, teeth contact surface through single tooth or multiple teeth	Fracture of additional teeth	Ejection of fragments from gear mesh not possible
184	Figure 153	Collector; 3 Engines Split torque variant	Reduction stage shaft bevel gear	Jamming due to wrong gear engaging	Crack growth from tooth root, teeth contact surface through single tooth or multiple teeth	Breakage of bevel gear tooth/teeth	Overload due to missing tooth contact ratio < 2
185	Figure 153	Collector; 3 Engines Split torque variant	Reduction stage shaft bevel gear	Jamming of reduction stage	Crack growth from tooth root, teeth contact surface or spline connection into gear hub	Crack of hub	Free ring gear No release of ring
186	Figure 153	Collector; 3 Engines Split torque variant	Reduction stage shaft bevel gear	Jamming of reduction stage	Crack growth from tooth root, teeth contact surface or spline connection into gear hub	Radial crack	Change in stiffness and deflection of gear Gear deformation and breakage
187	Figure 153	Collector; 3 Engines Split torque variant	Reduction stage shaft bevel gear	Jamming due to wrong gear engaging	Crack growth from tooth root, teeth contact surface or spline connection through spline tooth	Fracture of additional teeth	Overload due to missing tooth contact ratio < 2 due to teeth fracture at bull gear
188	Figure 154	Collector; 3 Engines Split torque variant	Quill shaft	Jamming due to wrong gear engaging	Crack growth from spline connection through single spline tooth	Fracture of additional teeth	Overload due to missing tooth contact ratio < 2 due to teeth fracture at bull gear
189	Figure 155	Collector; 3 Engines Split torque variant	Reduction stage large/small spur gear	Jamming of 2nd reduction stage	Crack growth from spur gear through single spline tooth	Fracture of additional teeth	Overload due to missing tooth contact ratio < 2 due to teeth fracture at bull gear
190	Figure 155	Collector; 3 Engines Split torque variant	Reduction stage large/small spur gear	Jamming of 2nd reduction stage	Crack growth from tooth root or contact surface through gear hub/body	Radial crack	Change in stiffness and deflection of gear Gear deformation and breakage
191	Figure 155	Collector; 3 Engines Split torque variant	Reduction stage large/small spur gear	Jamming due to wrong gear engaging	Crack growth from tooth root or contact surface through single gear tooth	Fracture of additional teeth	Ejection of fragments from gear mesh not possible
192	Figure 155	Collector; 3 Engines Split torque variant	Reduction stage large/small spur gear	Jamming due to wrong gear engaging	Crack growth from tooth root or contact surface through single gear tooth	Breakage of spur gear tooth/teeth	Overload due to missing tooth contact ratio < 2

Pos.	Figure	Configuration	Subpart	Weakness	Crack/Wear growth	Breakage/Crack	Additional contributions
193	Figure 156	Collector; 3 Engines Split torque variant	Double helical gear	Jamming of 3rd reduction stage	Crack growth from tooth root or teeth contact surface through single tooth or multiple teeth	Fracture of additional teeth	Ejection of fragments from gear mesh not possible
194	Figure 156	Collector; 3 Engines Split torque variant	Double helical gear	Jamming of 3rd reduction stage	Crack growth from tooth root or teeth contact surface through single tooth or multiple teeth	Breakage of helical gear tooth/teeth	Overload due to missing tooth
195	Figure 157	Collector; 3 Engines Split torque variant	Helical bull gear	Jamming due to wrong gear engaging	Crack growth from tooth root, tooth contact surface or spline connection through gear tooth	Fracture of additional teeth	Ejection of fragments from gear mesh not possible
196	Figure 157	Collector; 3 Engines Split torque variant	Helical bull gear	Jamming due to wrong gear engaging	Crack growth from tooth root, tooth contact surface or spline connection through gear tooth	Breakage of bull gear tooth/teeth	Overload due to missing tooth
197	Figure 157	Collector; 3 Engines Split torque variant	Helical bull gear	Jamming of 3rd reduction stage	Crack growth from tooth root, tooth contact surface, spline or oil bore holes toward gear hub	Radial crack	Change in stiffness and deflection of gear
198	Figure 157	Collector; 3 Engines Split torque variant	Helical bull gear	Loss of transmitting power to rotor mast	Crack growth from tooth root, tooth contact surface, spline or oil bore holes toward gear hub	Circumferential crack	Free bull gear ring
199	Figure 157	Collector; 3 Engines Split torque variant	Helical bull gear	Jamming of 3rd reduction stage	Crack growth from tooth root, tooth contact surface, spline or oil bore holes toward gear hub	Circumferential crack	Free bull gear ring
200	Figure 157	Collector; 3 Engines Split torque variant	Helical bull gear	Loss of transmitting power to rotor mast	Total wear at spline connection	n/a	No release of fragments due to closed design
201	Figure 158	Collector; 3 Engines Split torque variant	Rotor mast	Loss of transmitting power	Crack growth from integrated raceway into rotor mast	Circumferential crack	
202	Figure 158	Collector; 3 Engines Split torque variant	Rotor mast	Loss of transmitting power	Crack growth from integrated raceway into rotor mast	Longitudinal crack	Change in stiffness and shaft deformation
							Change of crack growth direction

Pos.	Figure	Configuration	Subpart	Weakness	Crack/Wear growth	Breakage/Crack	Additional contributions
203	Figure 158	Collector; 3 Engines Split torque variant	Rotor mast	Loss of rotor mast assembly	Crack growth from spline into shaft	Circumferential crack	Shaft deflection Change in stiffness and shaft deformation
204	Figure 158	Collector; 3 Engines Split torque variant	Rotor mast	Loss of rotor mast assembly	Crack growth from spline into shaft	Longitudinal crack	Change of crack growth direction
205	Figure 158	Collector; 3 Engines Split torque variant	Rotor mast	Loss of rotor mast assembly	Crack growth from thread upwards rotor mast nut	Circumferential crack	Loss of integrity of rotor mast
206	Figure 158	Collector; 3 Engines Split torque variant	Rotor mast	Loss transmitting power to rotor mast	Total wear at spline connection	n/a	No release of fragments due to closed design

Table 10: Overview of weaknesses and their criticality

6. Conclusion

Based on the aforementioned MGB configurations, two concepts have prevailed, by focusing on the concept for the final drive stage. One concept is the planetary gear train using one or more planetary gear stages. It provides high torque density in a lightweight and compact gear reduction configuration. A possible configuration, common in older helicopter designs, involves a 2-stage planetary gearbox.

The other typical design variant is the collector architecture, which has a combining gear at the axis of the rotor shaft, which can be powered in several different ways. A common variant of this is the split torque configuration, where the power of the engines is split in at least 2 load paths, which also offers great potential for weight and design space savings. This variant can be found with up to three engines. Table 2 summarizes the different concepts as far as data is available.

Furthermore, a general description of main failure modes was performed. This was done based on the information available in different public literature, as well as based on experience from ZF and SKF. Within this description a wide range of failure modes and their different mechanisms are described. The principal causes of a crack or breakage are summarized in Table 3 to Table 6. With the help of suitable illustrations and the mentioned evaluations, it is assumed that all damages can be analyzed accurately to be used as a basis for the failure analysis.

During further literature survey and analysis of public available data and documentation, some relevant examples of incidents concerning epicyclic architectures and publicly available assessment of catastrophic failures on MGB were found. In this context, no catastrophic failures were identified within the MGBs using collector architecture designs. All the presented events and assessments are only taken over from above mentioned public sources. No additional rating or judgement of these events was done by ZFL. It is just a summary of information, which are publicly available. This information and the internal experience have been taken into account and used as valuable input for the failure analysis in chapter 5. The detailed design of each drive system section, affected by a certain failure mechanism, plays a fundamental role for the consequences and severity of the failure. Relevant for this are in general the following points, which could even work as a safety barrier:

- Component dimensioning and design
- Bearing dimensioning and design
- Redundancies
- Installation space
- Design of interfaces/connection points
- Gearbox type/architecture

For a deeper understanding of the single drive system sections and their severity to failures, the generic failure flow diagrams and the corresponding MGB layouts were created (see chapter 5.2.1 to chapter 5.2.5). Based on this, specific failure flow diagrams for each section were developed, with focus on sections contributing to the main load path to the main rotor. Accessory or hydraulic drives were not part of the investigations.

By the elaboration of the failure flow diagrams and the review of the described cases in Table 10 of chapter 5 regarding the identified design weaknesses, causes can be highlighted leading to jamming, loss of transmitting power or loss of the rotor mast itself. The contributing factors in designs experiencing catastrophic breakage and/or cracking can be summarized by the following issues:

- Ejection of fragments from gear mesh not possible, which could further lead to additional damage
- Release of fragments and damaging of other gear stages by overrolling
- No sufficient support from e.g. bearing and hub of parts after breakage, which further contributes noises, high vibrations, and jamming due to deflection/movement of fragments/parts.
- Incorrect gear reengaging due to loss of single tooth or multiple teeth leading to jamming of the gear or the loss of transmitting power
- Total wear of spline leading to loss of transmitting power to the main rotor or tail rotor
- Radial, circumferential or longitudinal cracks leading to a disconnect in the power transmission path or a jamming due to increased deflection or deformation of the components

As a result of the assessment, it was shown that circumferential and radial cracks or tooth breakages could lead to jamming or disconnection within the load path. Mainly for shafts, longitudinal cracks lead to a stiffness reduction rather than a disconnection or jamming and therefore, they do not lead to catastrophic events as often as circumferential or radial cracks. Longitudinal cracks at the rotor mast are an exception by consideration of catastrophic events. It is also assumed, that a stiff bolted connection could reduce the risk of catastrophic failures due to radial cracks (e.g. bolted connection at collector gear or intermediate shaft gear). Additionally, it is shown that tooth breakage does not automatically lead to a disconnection of load transmission but rather contributes to jamming if the broken parts cannot be ejected.

Finally, it is important to explain, that this evaluation is restricted by limitations of data and assumptions:

- Assumptions on the design solutions due to limited access on original design data
- Simplification of failure mechanism (e.g. radial, circumferential and longitudinal crack as representation for all crack types)
- Assumptions on failure behavior and the consequences for the power transmission or component integrity
- Failure modes and mechanisms based on and limited to ZF experience as well as public data

This report is therefore not capable of identifying all possible catastrophic failure modes for all of the presented gearbox examples, but to identify potential design weaknesses that can be improved and/or avoided by general design solutions and modifications to the MGB architectures in the frame of this research project.

Nevertheless, there are other cases which could potentially lead to catastrophic events, which were not part of the evaluation of the failure flow diagrams as they are not part of the main transmission path from input stages to output stages of a MGB. Moreover, the analysis was based on several assumptions (e.g. no bearing seizure, origin of failures considered only based on individual component failures, instead of system failures and lack of design information, that lead to assumptions), which potentially could lead to a missing catastrophic failure mode within this analysis. Some public examples of this kind are part of the collection in Table 8.

However, the evaluated results will be used as a basis for the following Report D1-2.

7. References

References for which the revision status is not provided refer to the last completely signed and therefore approved version.

- [1] EASA, Procurement Document "Integrity improvement of rotorcraft main gear box (MGB)", EASA.2019.HVP.17, 09/2019
- [2] EASA/ZFL, Contract "Direct service contract for H2020 Project: Integrity improvement of rotorcraft main gear box (MGB)", EASA.2019.C15, 16/06/2020
- [3] Campbell Helicopters, "Bell 212 Pilot Training Manual", Chapter 8 Rev. No. 00
- [4] IJERA, "Design and Power Transmission of Advanced Light Helicopter", Vol.3 Issue 4, Jul.-Aug. 2013
- [5] A. T. Bellocchino, "Drive System Design Methodology for a Single Main Rotor Heavy Lift Helicopter", December 2015
- [6] A. Doleschel, S. Emmerling, "The EC135 Drive Train Analysis and Improvement of the Fatigue Strength", ECD-0159-07-PUB
- [7] S. Augustyn, Scientific Paper "Capabilities of the FAM-C Method to diagnose the accessory gearboxes and transmission-train assemblies of the MI-24 Helicopters" DOI 10.2478/v10041-012-0012-2, 2012
- [8] Technical Definition BO105 CB/CBS, Edition DB 341-1/84
- [9] NASA, Technical Memorandum "Review of the Transmissions of the Soviet Helicopters", 90-C-015, December 1990
- [10] Russianpatents.com, "The main gearbox of the helicopter coaxial configuration", No. 2059535, <https://russianpatents.com/patent/205/2059535.html>
- [11] NASA, "Summary of Drive-Train Component Technology in Helicopter", 84-C-10, October 8-12.1984
- [12] E. V. Zaretsky, "NASA Helicopter Transmission System Technology Program"
- [13] XTEK, Scientific Paper "Gear Failures", December 7, 1967
- [14] Barden Precision Bearings, "Bearing Failure: Causes and Cures"
- [15] Sikorsky, "Design and Development of a Modern Transmission: Baseline Configuration of the CH-53K Drive System"
- [16] ZF, Technical Manual "Damage and Wear Assessment", 000 754 702a, Edition 2008
- [17] SKF Aerospace, Technical Report "ZF GIFT MGB – HAP100", AV200142, 26/11/2020
- [18] Department for Transport (UK), Accident Report "The accident with G-REDL", EW/C2009/04/01, 2/2011
- [19] AIBN, Accident Report "The accident with LN-OJF", SL 2018/04, July 2018
- [20] RAS, ERF, Technical Paper "Gearbox Loss of Lubrication Performance: Myth, Art or Science"
- [21] Scope, Kawasaki Heavy Industries Quarterly Newsletter, "High-Performance, Twin-Engine, Multi-Purpose Helicopter BK117 D-2", Winter 2017
- [22] KHI, 2Unrivaled Reliability of Kawasaki Gear Products", <https://global.kawasaki.com/en/stories/articles/vol80/>"

- [23] Wikipedia.org
- [24] Scott Poster, "Safety Consideration of the 525 Relentless Drive System", December 2016
- [25] FAG, "Wälzlagerschäden", Publ.-Nr. WL 82 102/2 DA, Stand 2000
- [26] ZF Luftfahrttechnik: "Drawing BO105", TKZ 4639 001 007, 2020
- [27] Sikorsky, European Patent Specification "Multi-path rotary wing aircraft gearbox", EP 2 005 030 B1, 22.05.2013
- [28] ISO, International Standard "Rolling bearings – Damage and failures – Terms, characteristics and causes", ISO 15243, 2004-02.15
- [29] SKF, Technical Note "Bearing damage and failure analysis" PUB BU/I3 14219/2 EN, June 2017
- [30] SKF, Annex to [17] "FTA Rolling Bearing to critical failure"
- [31] Aeroenginesafety.tugraz.at, Technical Note "Lightning", <https://aeroenginesafety.tugraz.at/doku.php?id=5:51:513:513>
- [32] McFadden, Technical Report "Analysis of the vibration of the input bevel pinion in RAN WESSEX Helicopter main rotor gearbox WAK143 prior to failure", AD-A173 851, September 1985
- [33] Investigation Report "Accident Investigation BO 105 CB S-781", June 1, 2005
- [34] Investigation Report "Accident Investigation BO 105 CBS 5 S/N S-573", 14. Aug. 1996
- [35] Investigation Report "Results of the ECD Accident Investigation BO 105 CBS 5 S/N S-86 'LV-WJX'", Sep. 30, 2010
- [36] BFU, "Untersuchungsbericht", BFU 4x041-11 and BFU 4x042-11, 17. December 2011
- [37] BFU, "Untersuchungsbericht", BFU 3X006-14, 28. Februar 2014
- [38] BFU, "Untersuchungsbericht", BFU16-0185-3X, 25. Februar 2016
- [39] AAIB, Accident Report "EC225 LP Super Puma G-REDW and G-CHCN", 2/2014
- [40] Transportation Safety Board of Canada, Aviation Investigation Report "Main gearbox malfunction / collision with water", A09A0016, 12 March 2009
- [41] ZF, Schadensanalyse "Zwischenwelle", F00027198 / FAN180414_v5, 2018-10-12
- [42] ZF, Metal failure analysis "BO105 planet gear", F00037474 / FAN190355_v3, 2019-09-17
- [43] EASA/Crafield University, Technical Report "Vibration Health or Alternative Monitoring Technologies for Helicopters", EASA_REP_RESEA_2012_6, 2012

Bibliography

Project reports

n/a

Annex A Flow diagram of examples

A.1 Flow diagram of Example 1

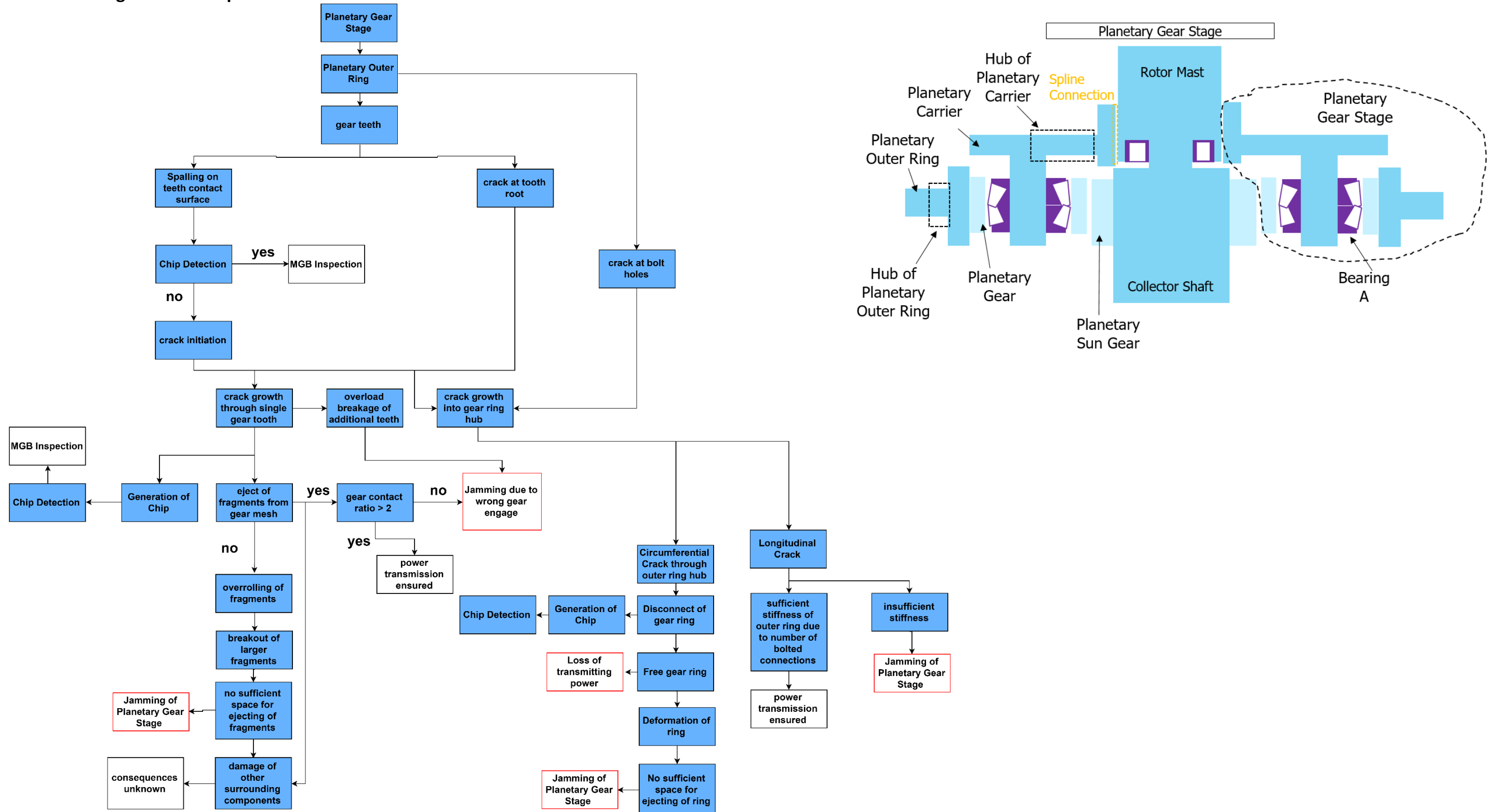


Figure 98: Bell 525 – Planetary Gear Stage

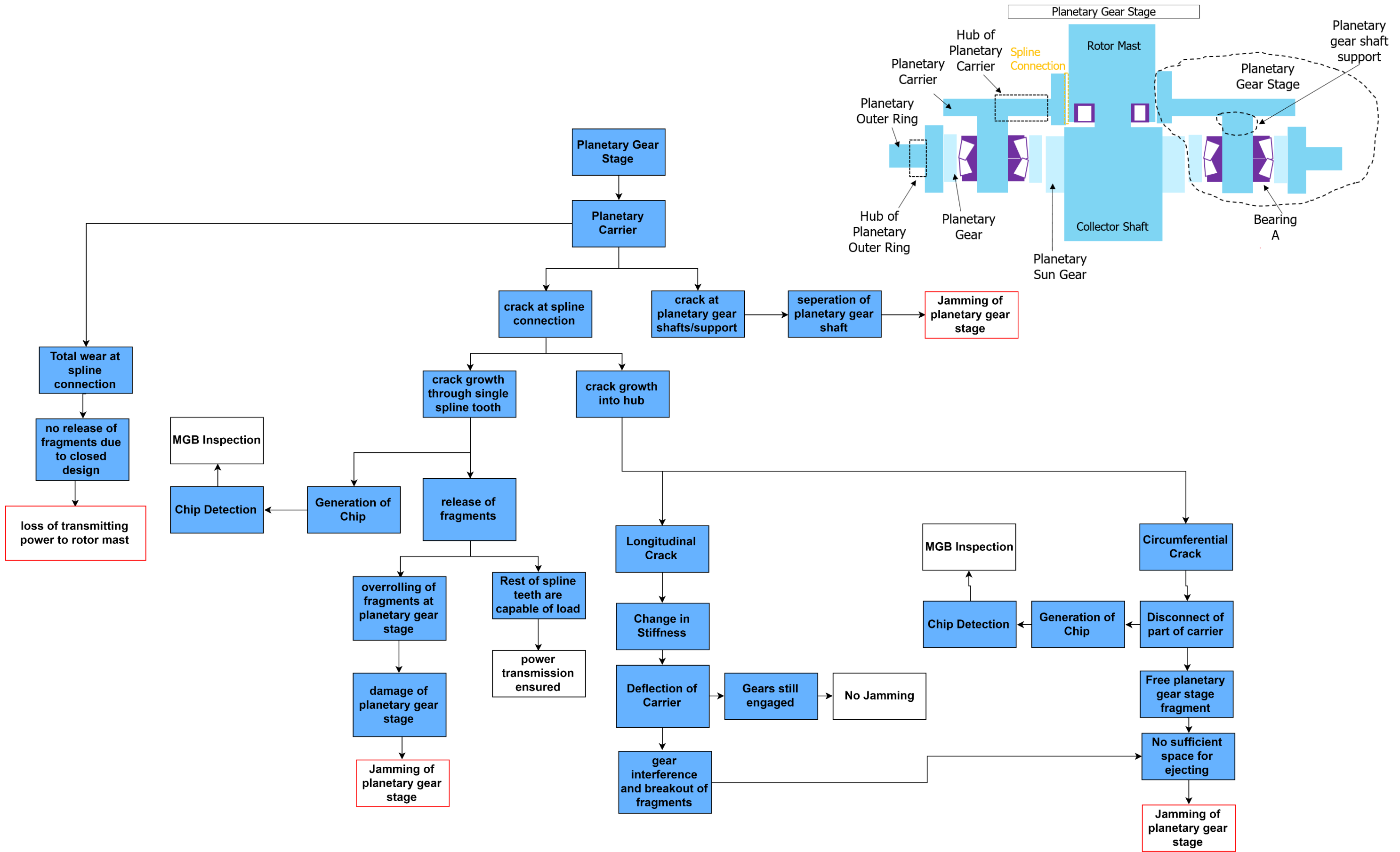


Figure 99: Bell 525 – Planetary Gear Stage

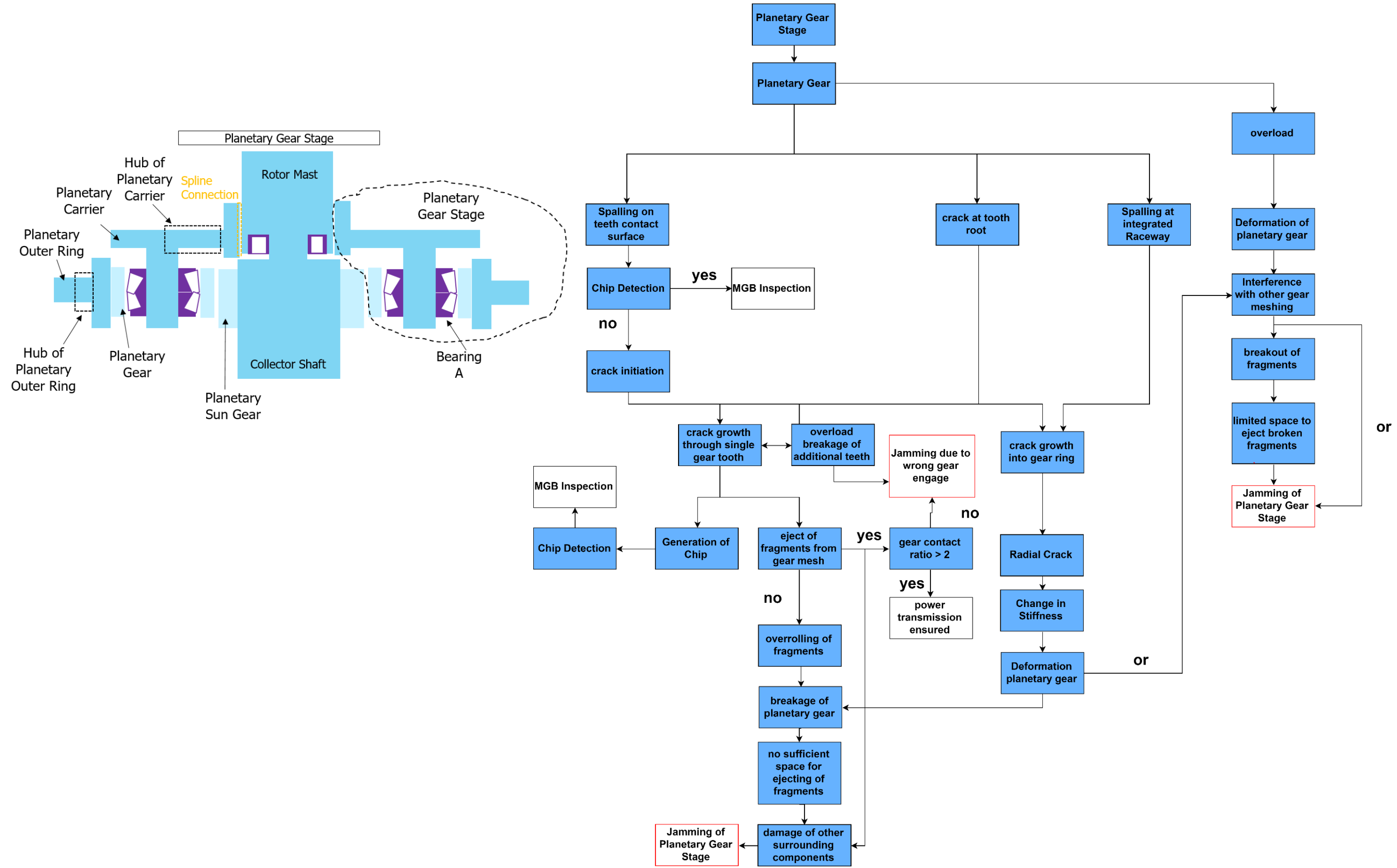


Figure 100: Bell 525 – Planetary Gear Stage

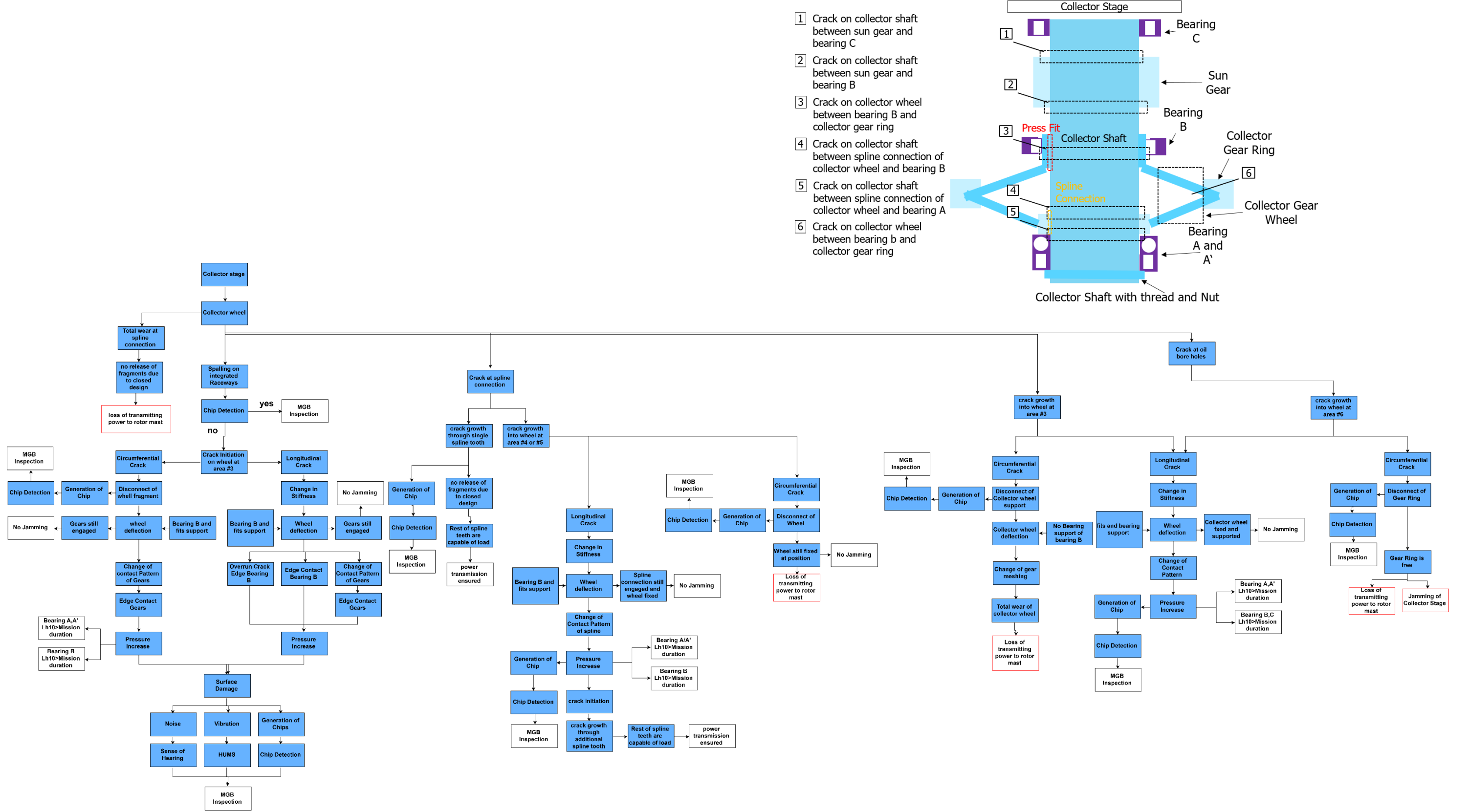


Figure 101: Bell 525 – Collector Wheel

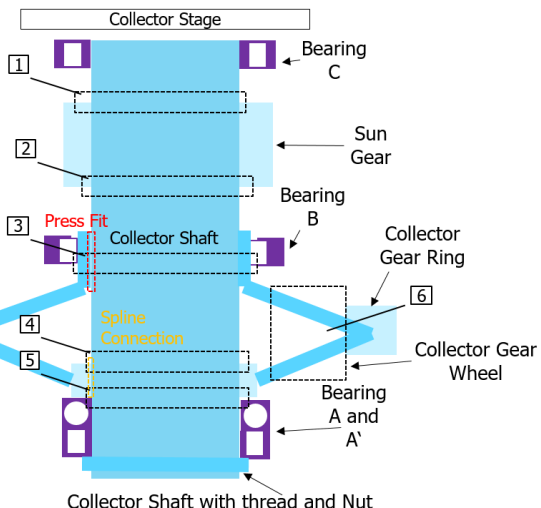
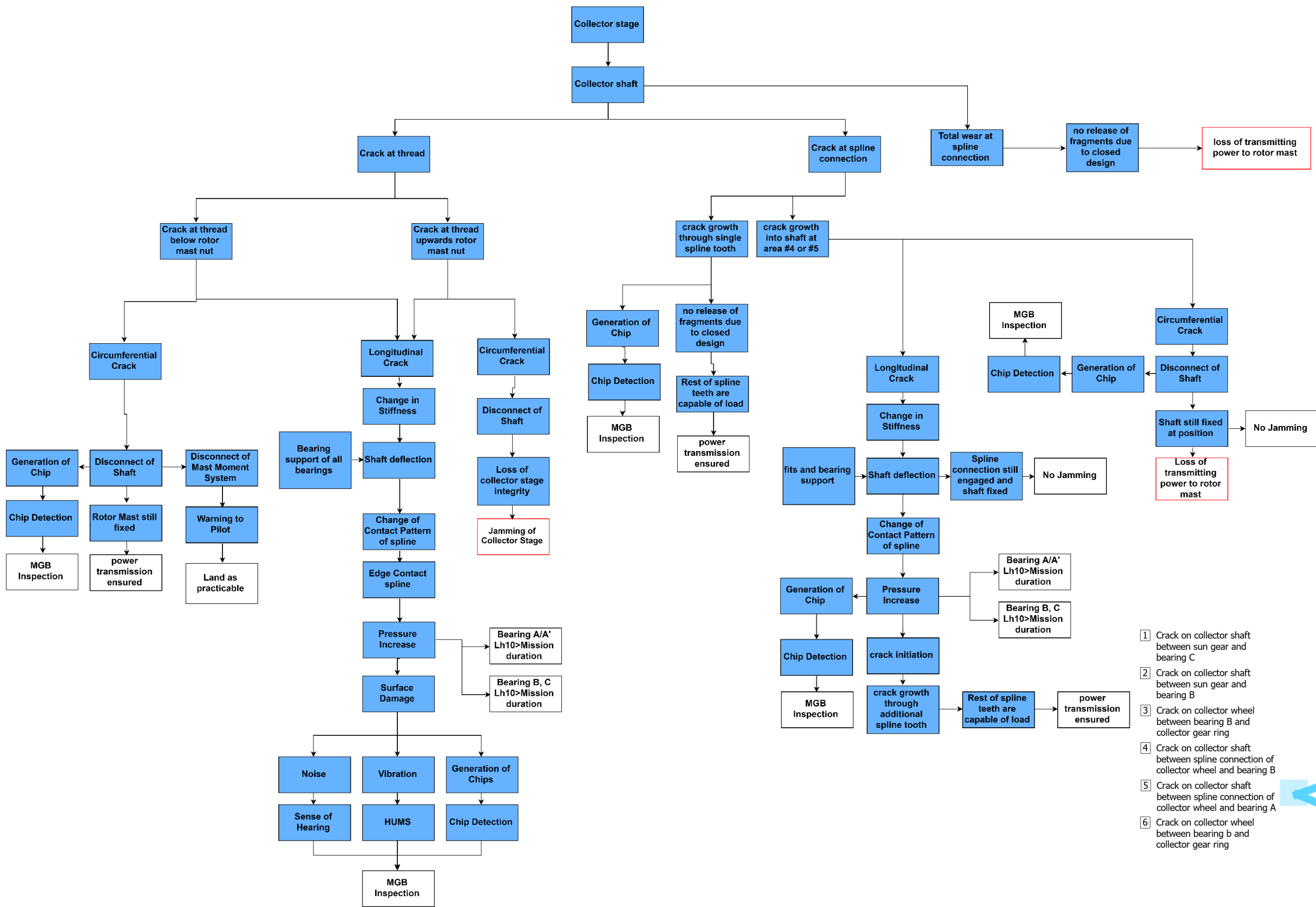
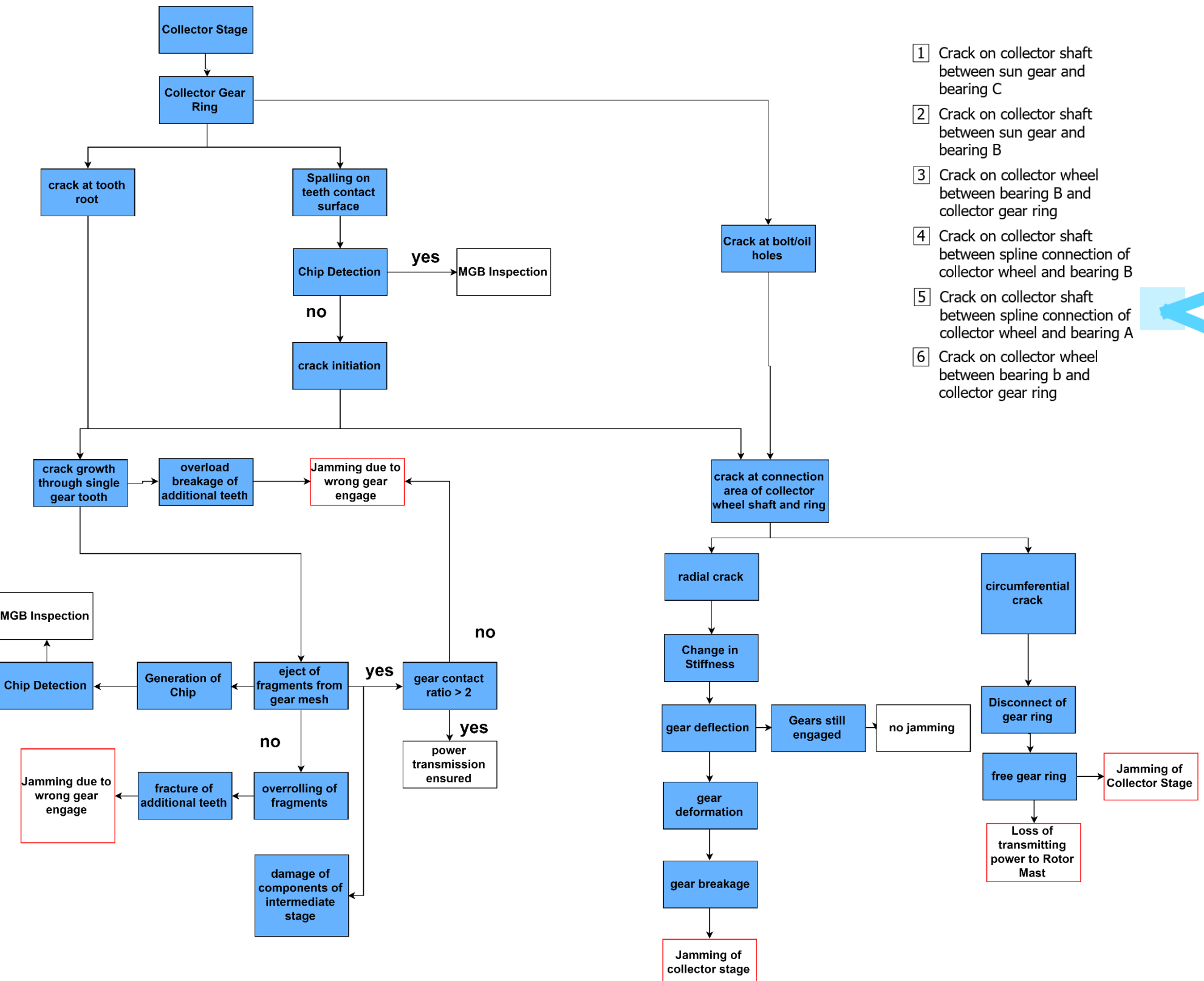


Figure 102: Bell 525 – Collector Shaft



- 1 Crack on collector shaft between sun gear and bearing C
- 2 Crack on collector shaft between sun gear and bearing B
- 3 Crack on collector wheel between bearing B and collector gear ring
- 4 Crack on collector shaft between spline connection of collector wheel and bearing B
- 5 Crack on collector shaft between spline connection of collector wheel and bearing A
- 6 Crack on collector wheel between bearing b and collector gear ring

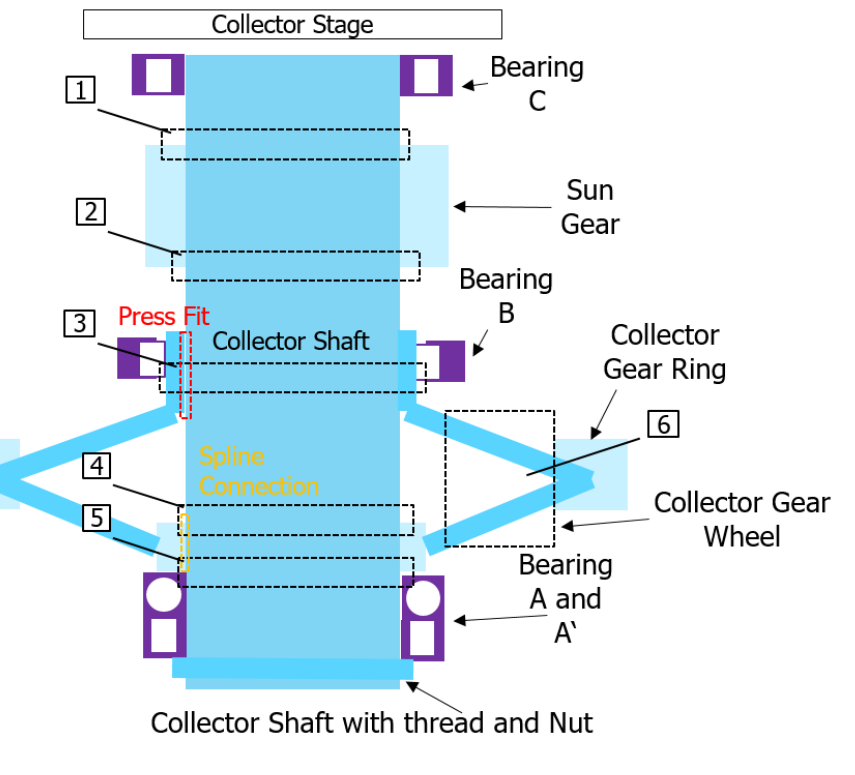


Figure 103: Bell 525 – Collector Gear Ring

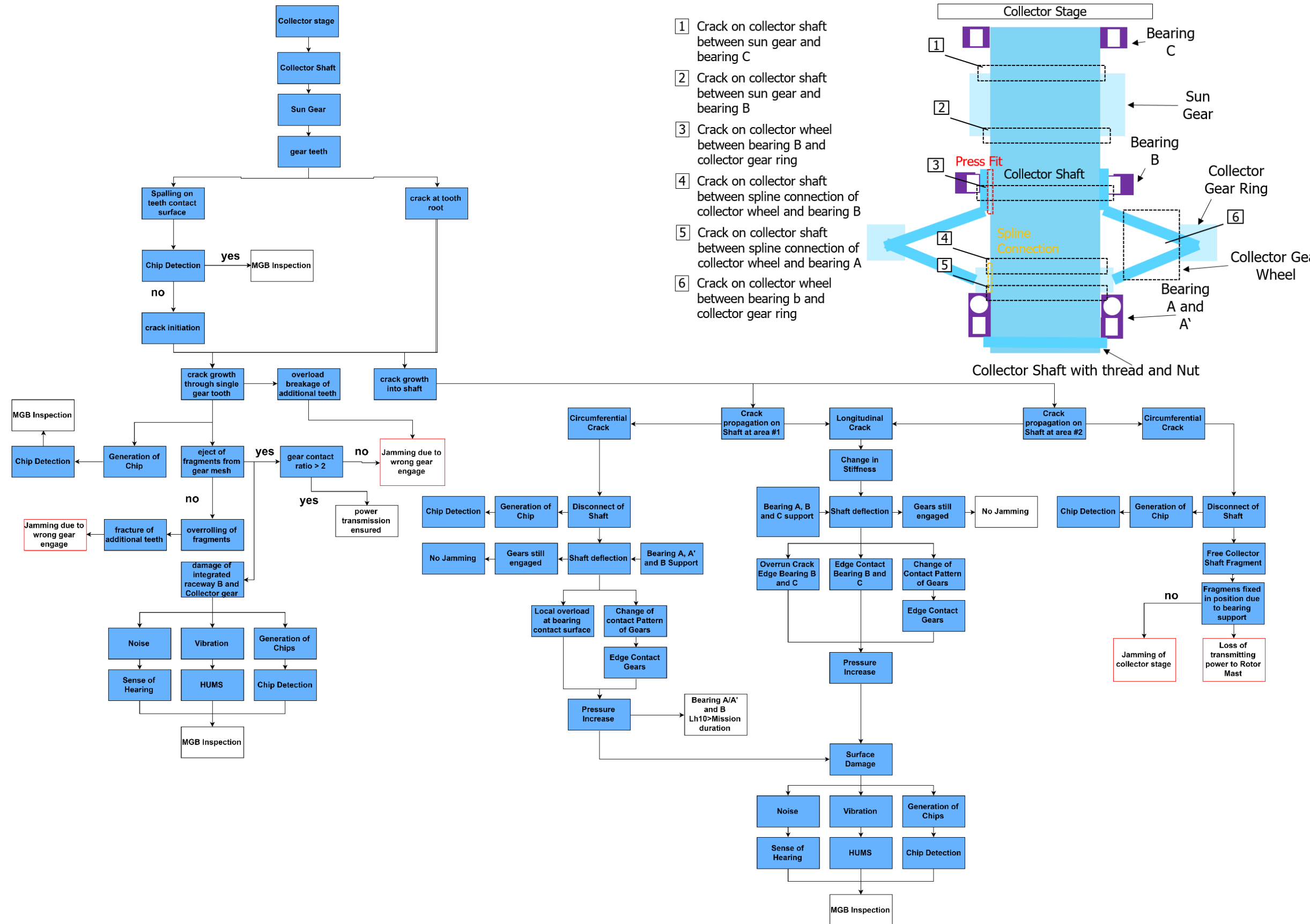


Figure 104: Bell 525 – Collector Shaft Sun Gear

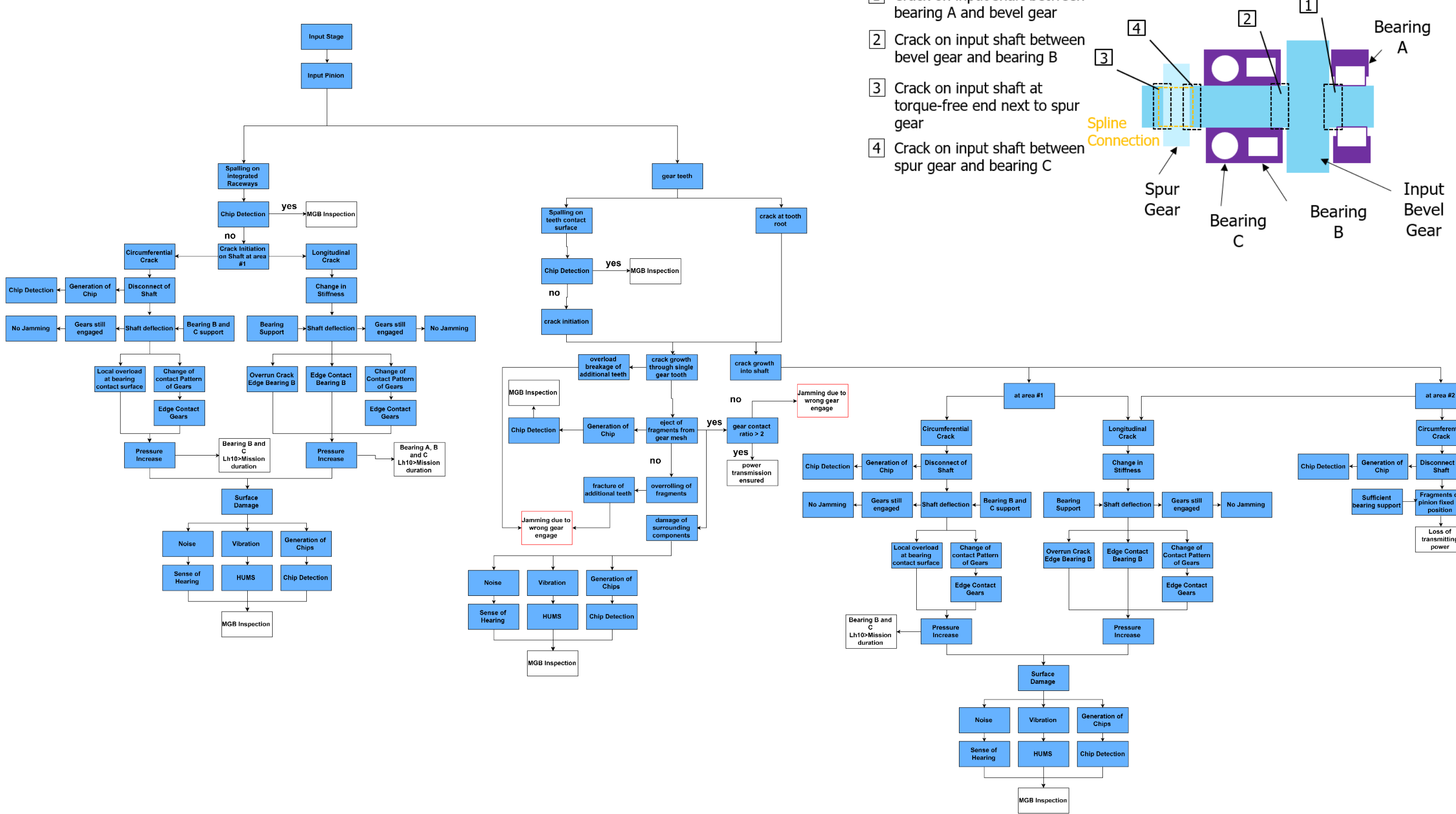


Figure 105: Bell 525 – Input Pinion

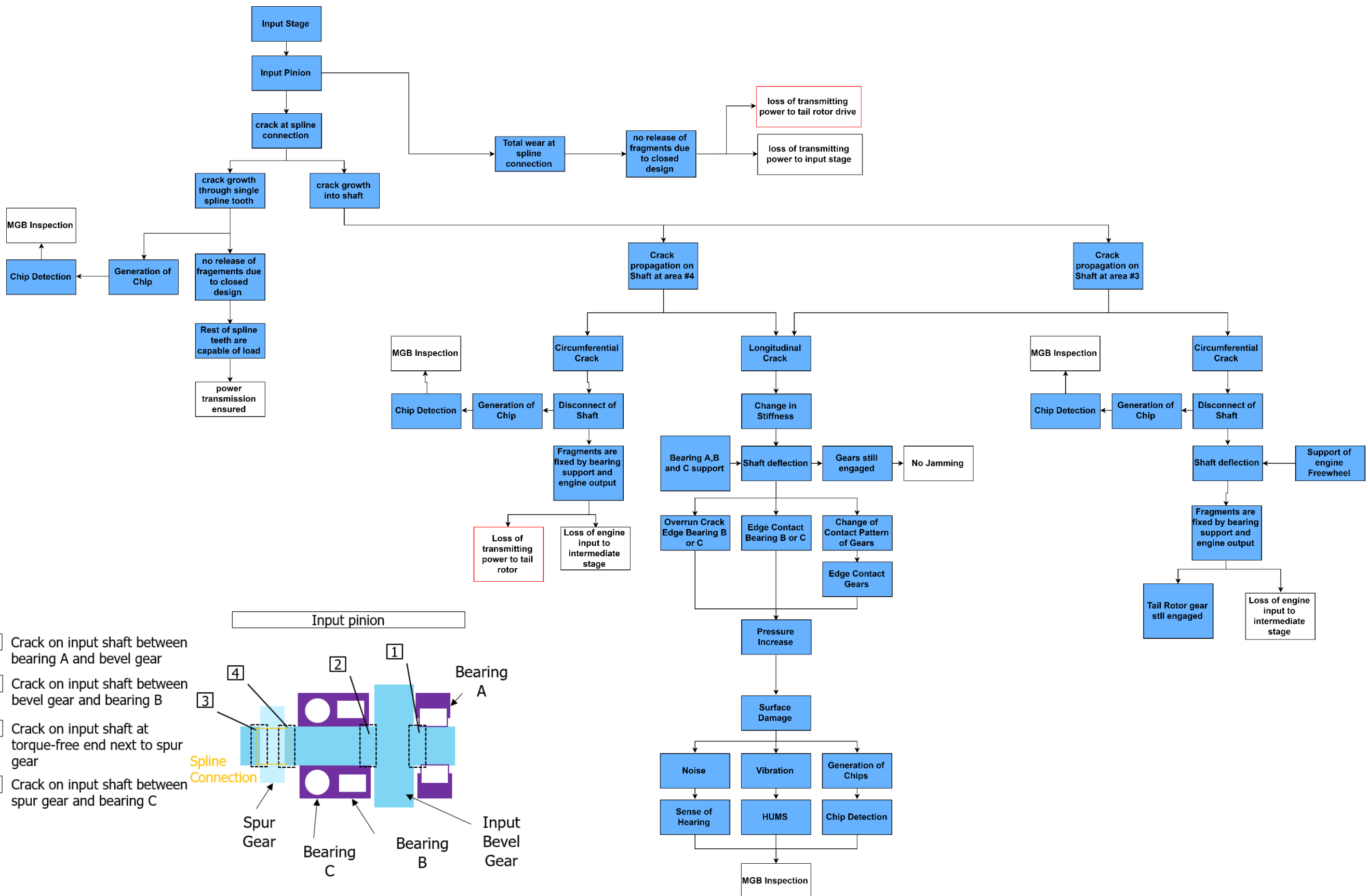


Figure 106: Bell 525 – Input Pinion

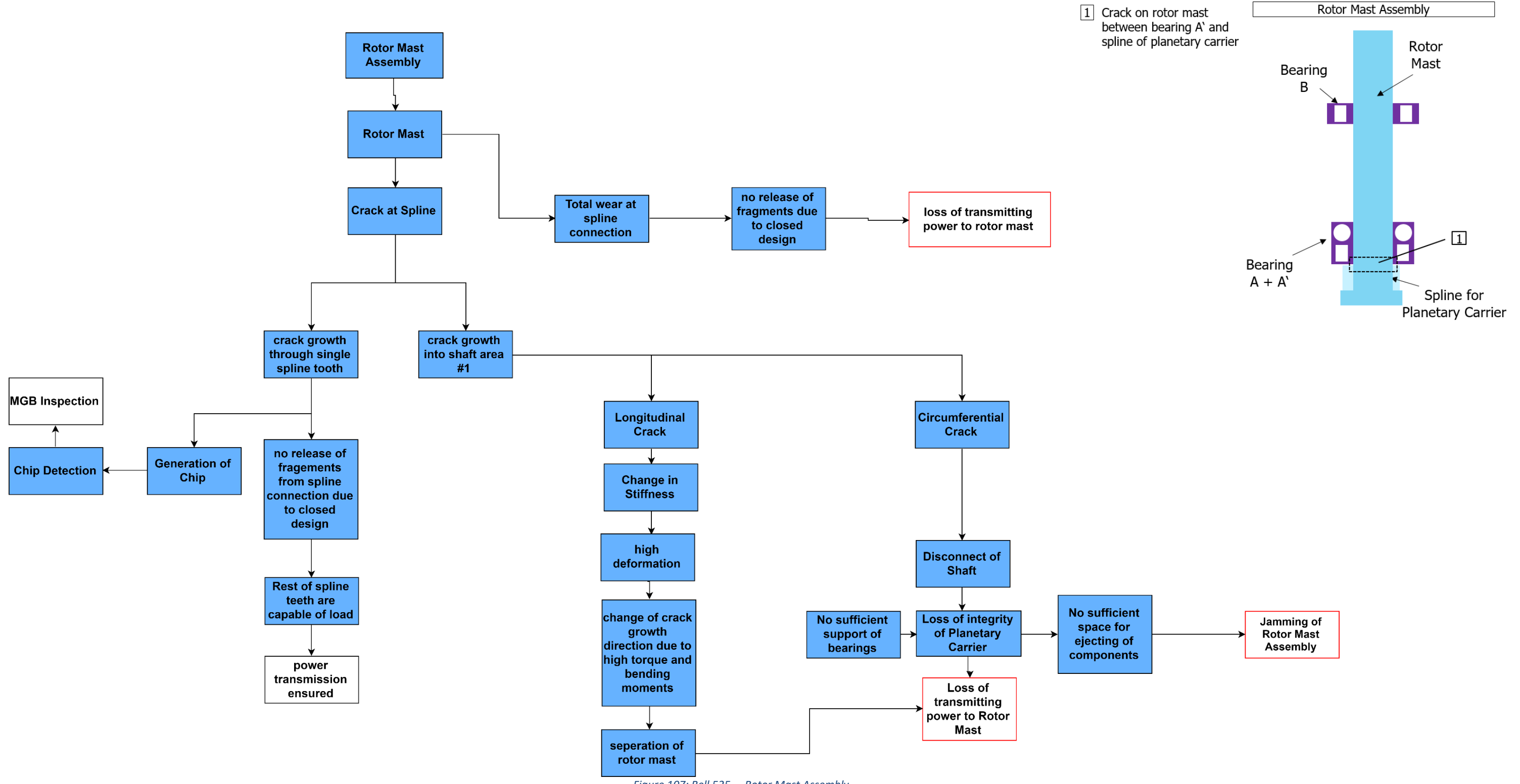


Figure 107: Bell 525 – Rotor Mast Assembly

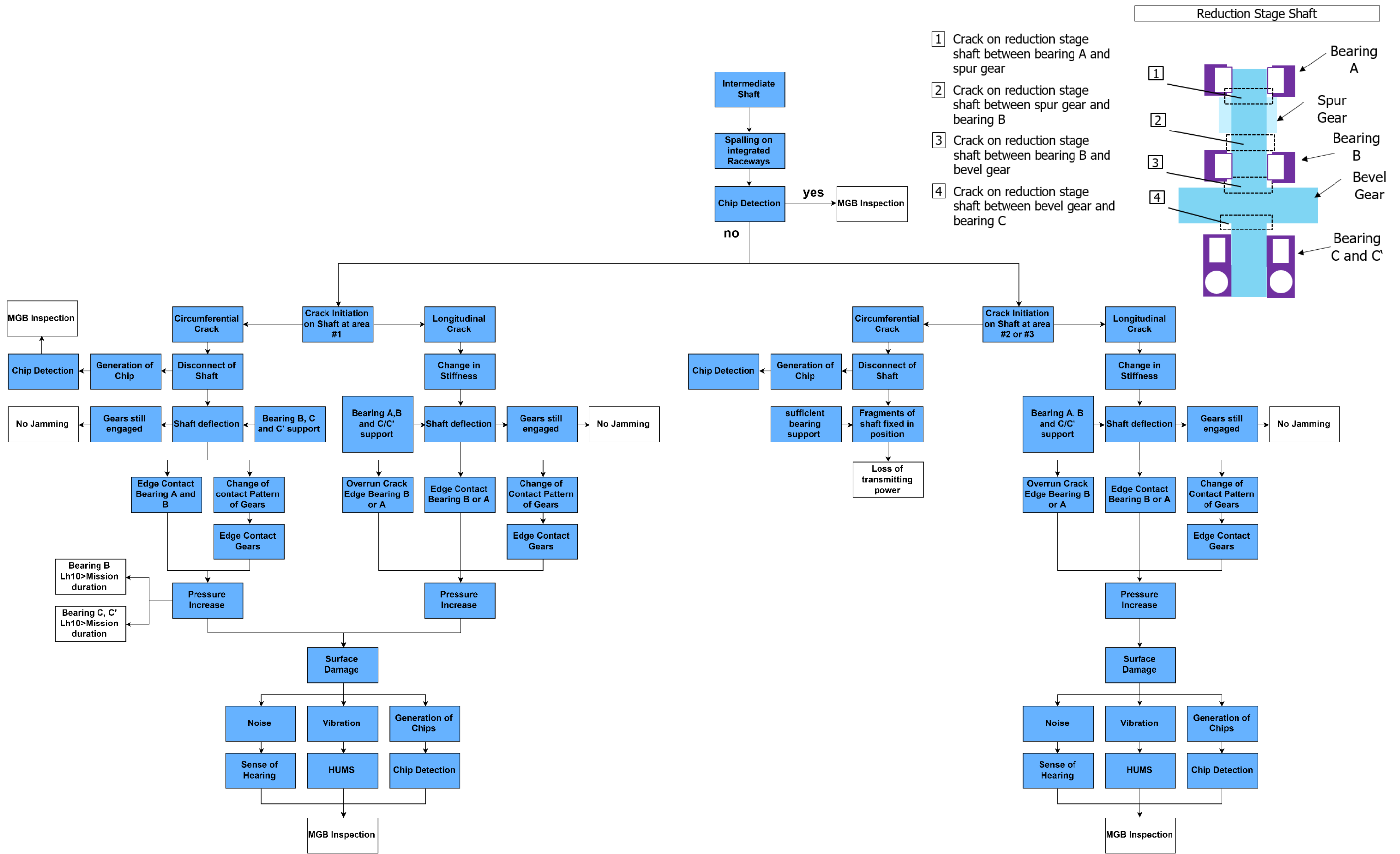


Figure 108: Bell 525 – Intermediate Shaft

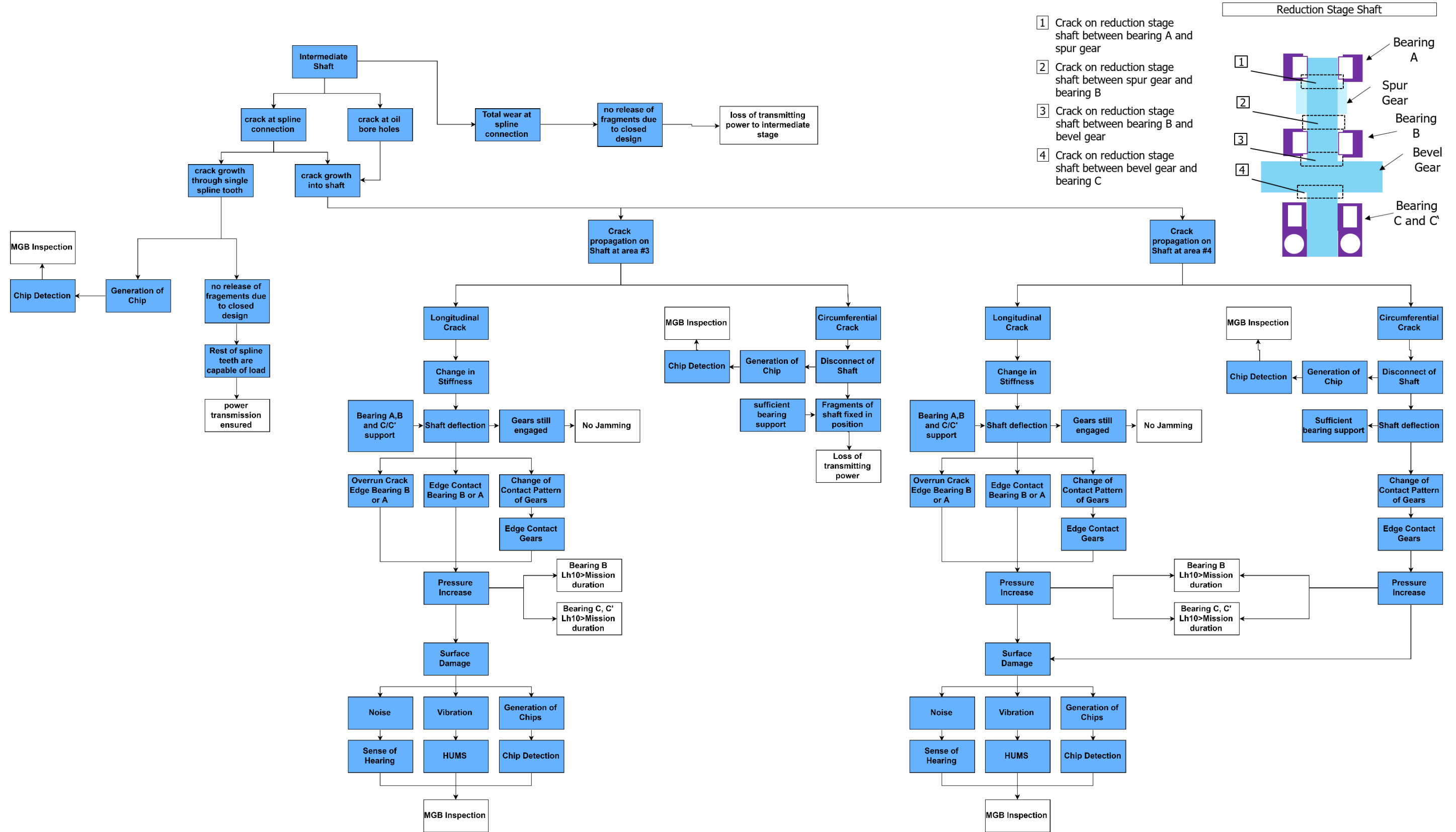


Figure 109: Bell 525 – Intermediate Shaft

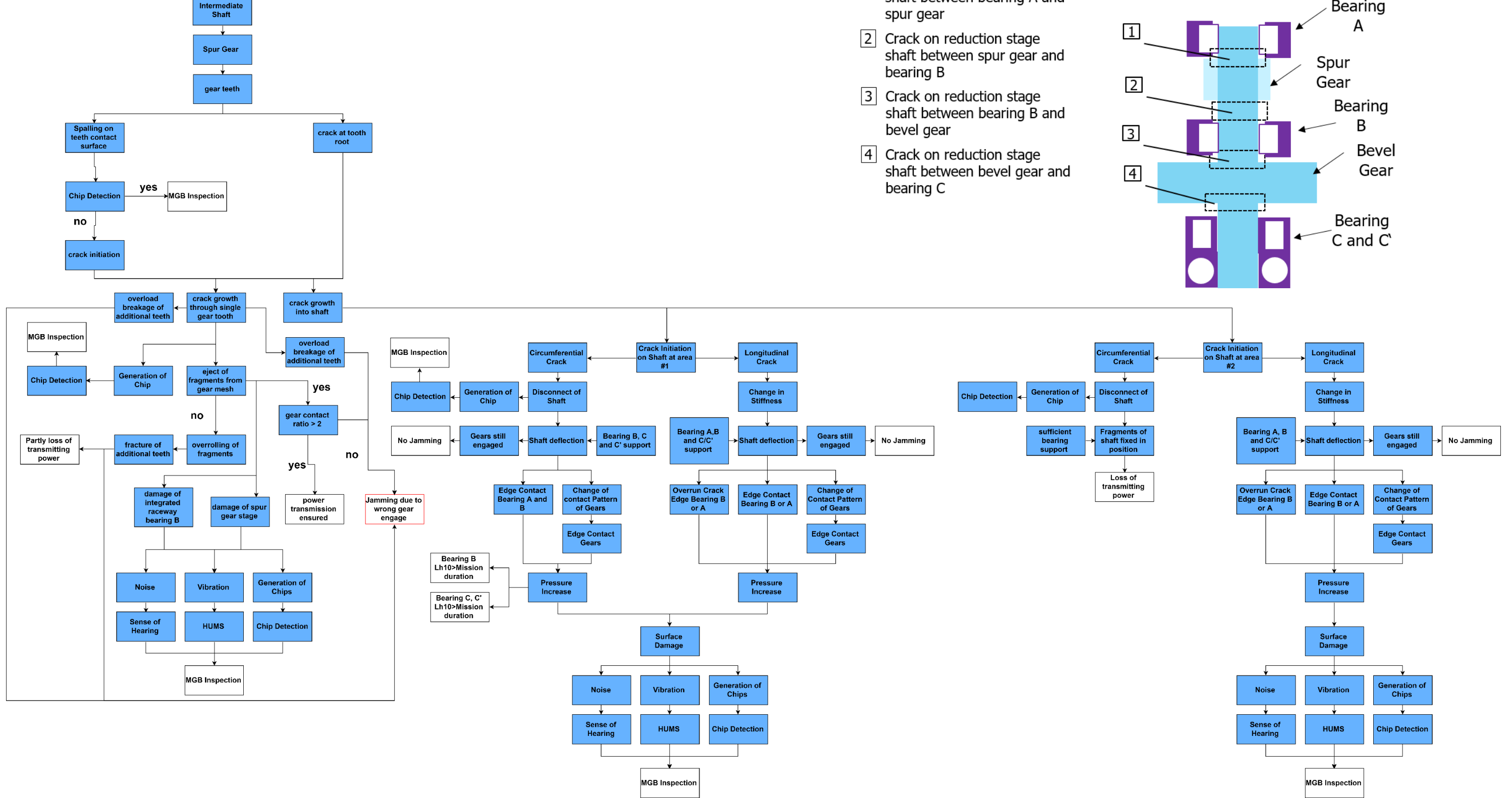


Figure 110: Bell 525 – Intermediate Shaft

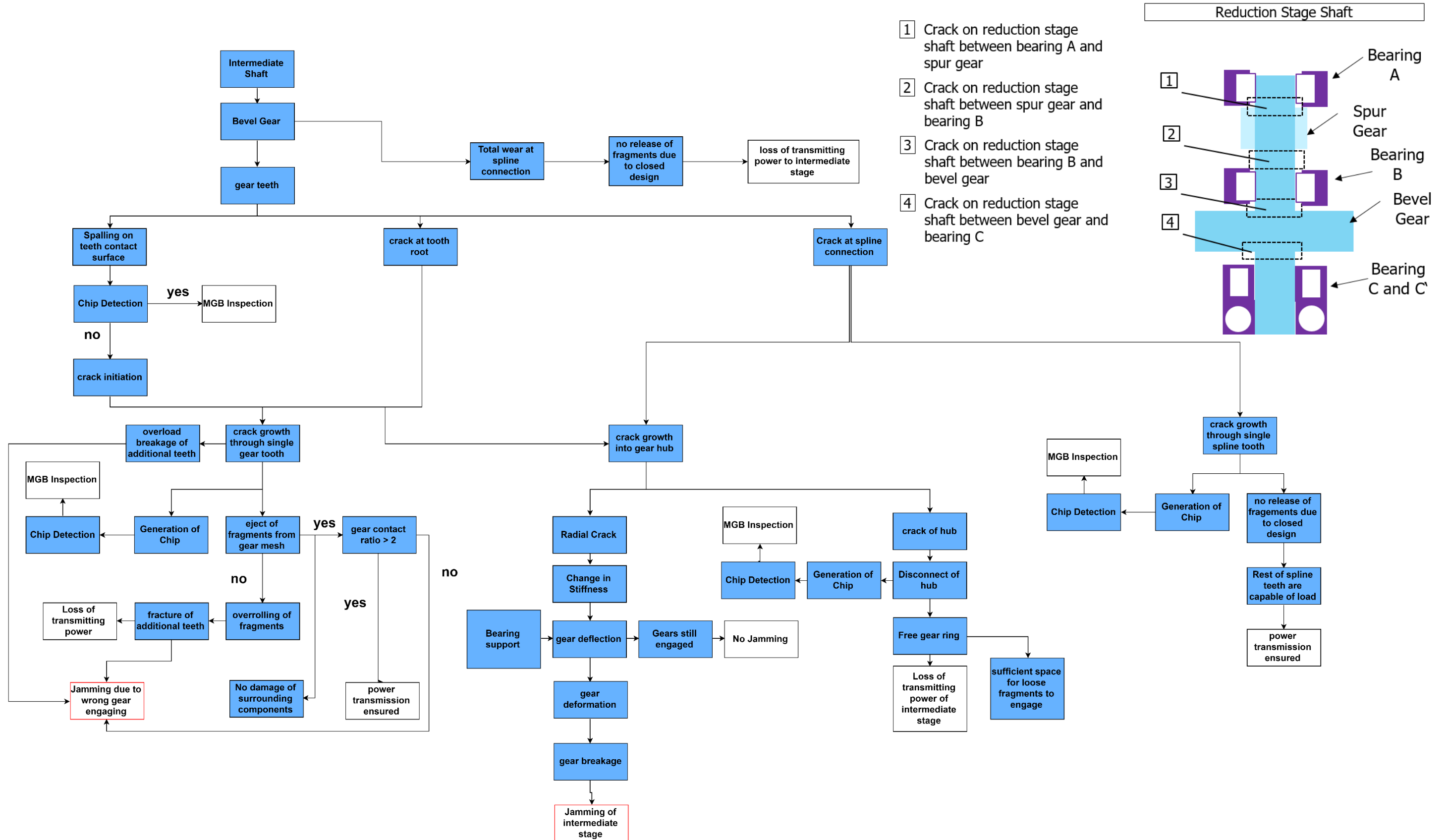


Figure 111: Bell 525 – Intermediate Shaft

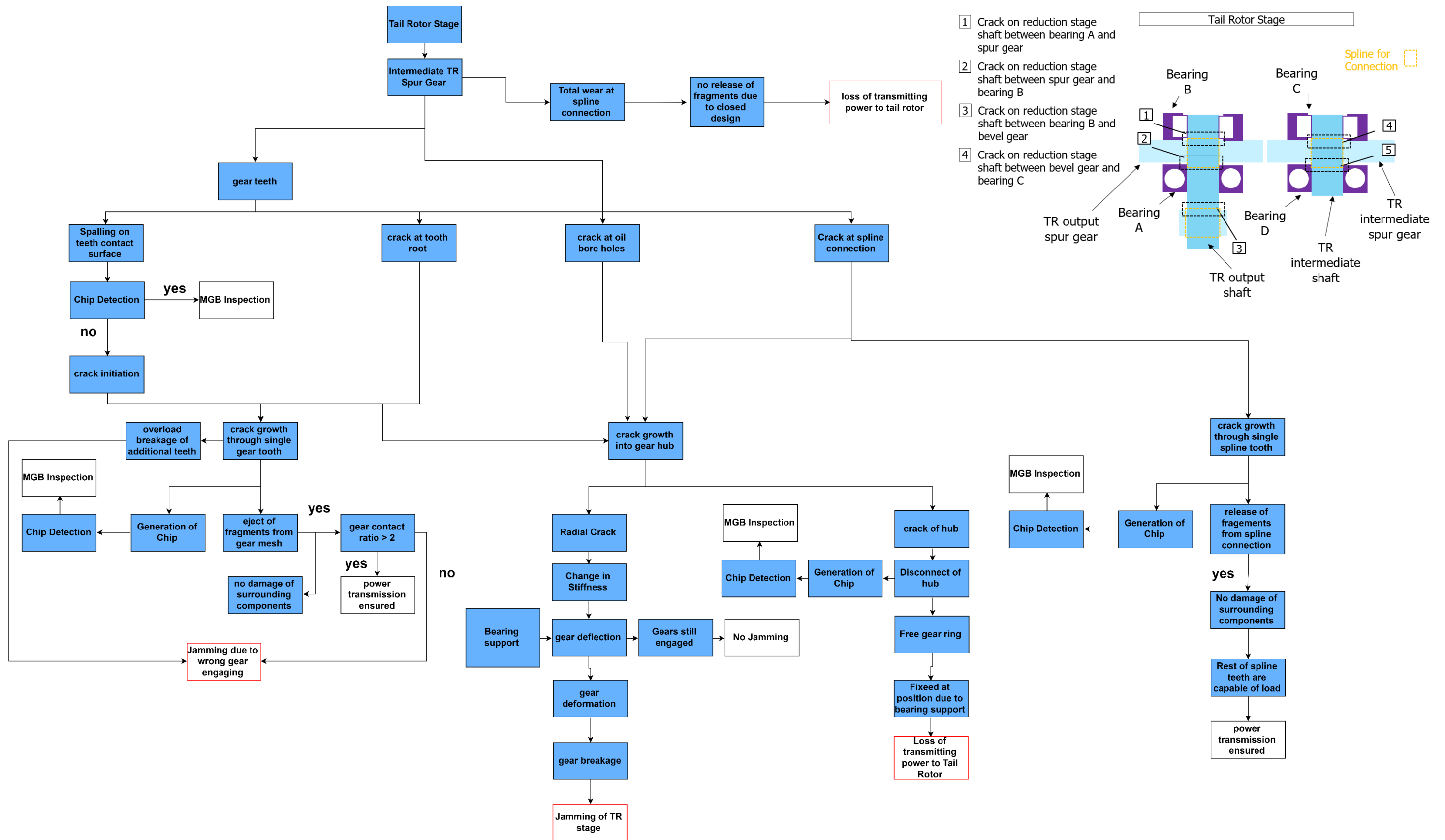


Figure 112: Bell 525 – Tail Rotor Stage

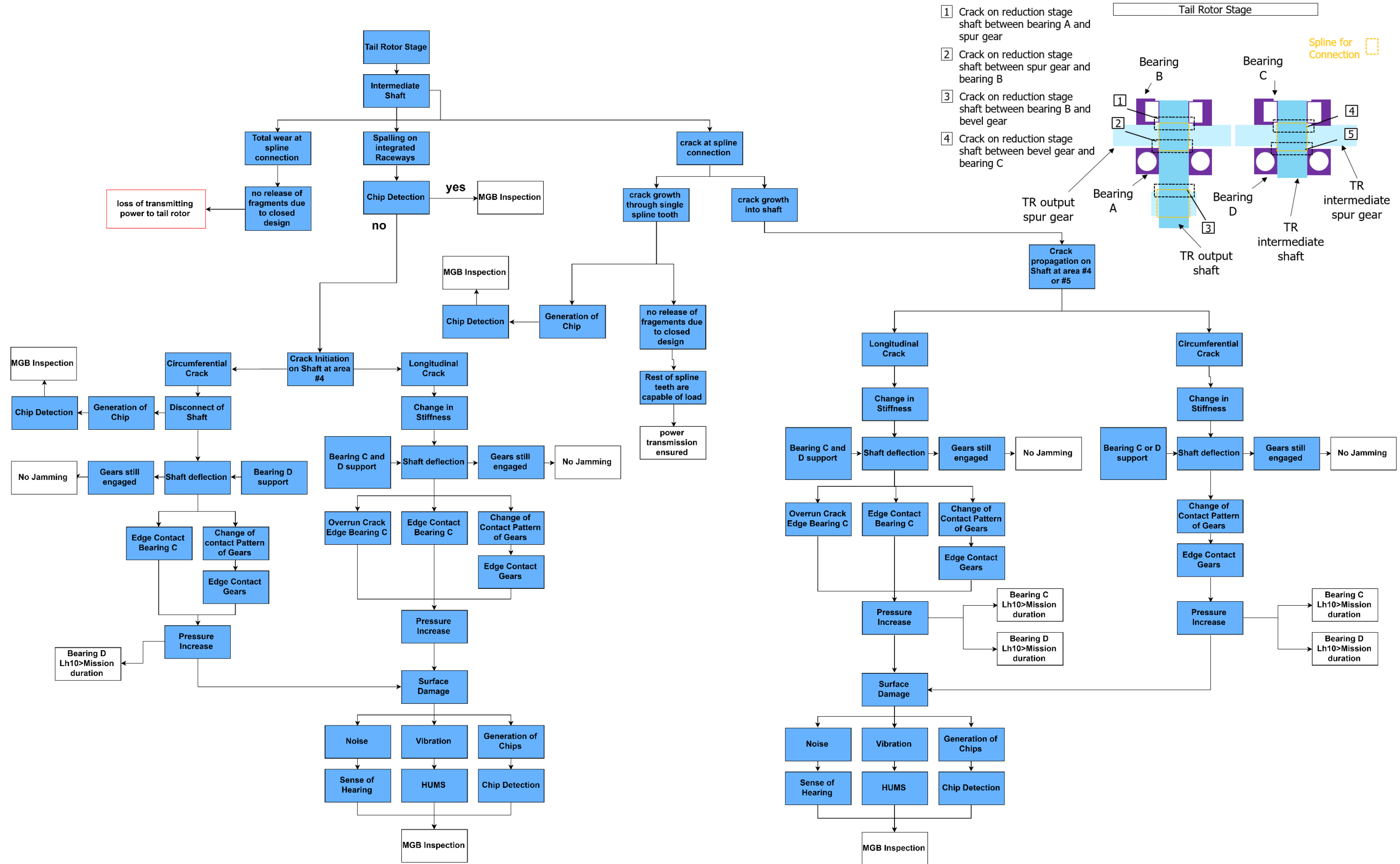


Figure 113: Bell 525 – Tail Rotor Stage

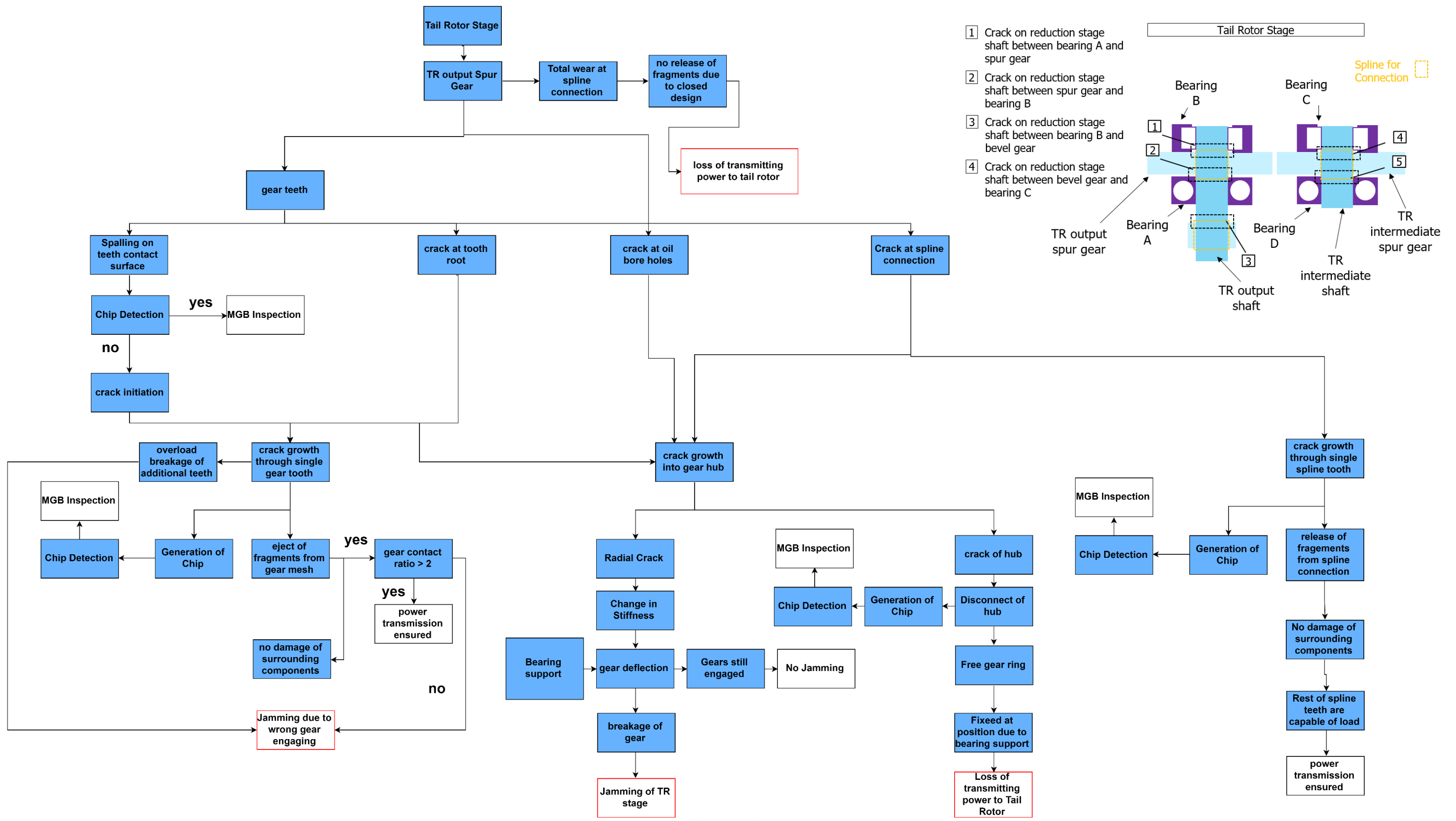


Figure 114: Bell 525 – Tail Rotor Stage

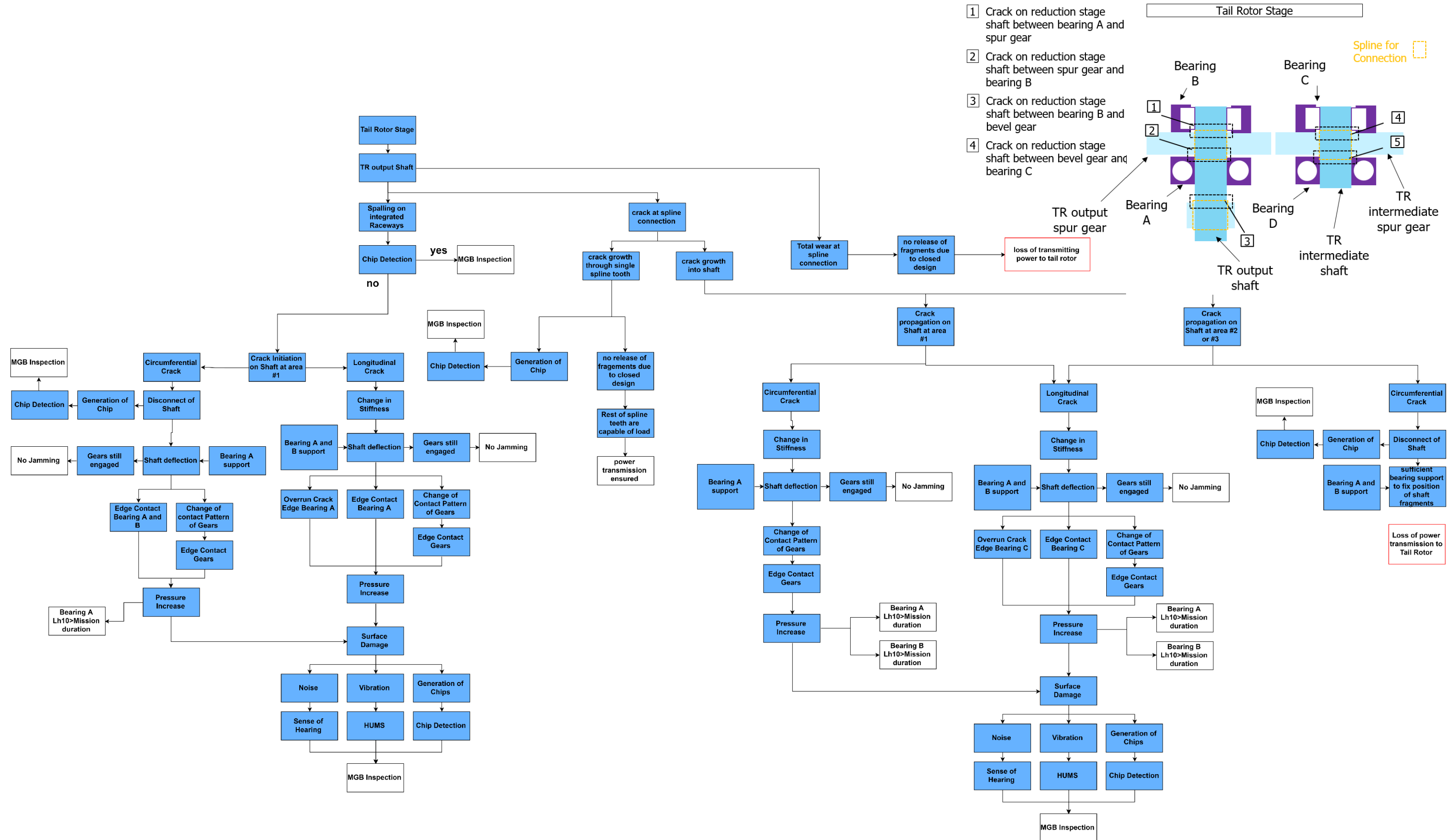


Figure 115: Bell 525 – Tail Rotor Stage

A.2 Flow diagram of Example 2

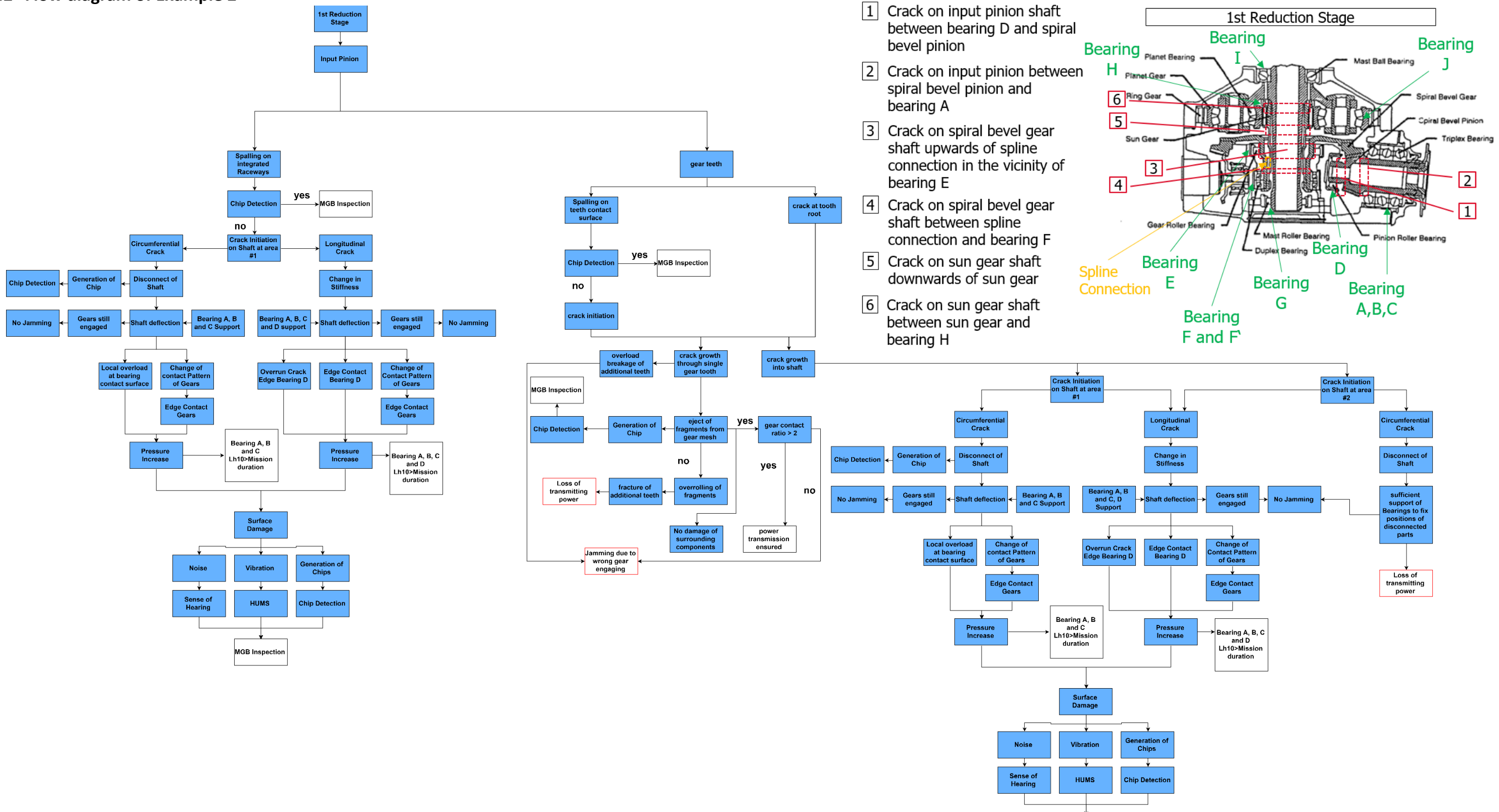
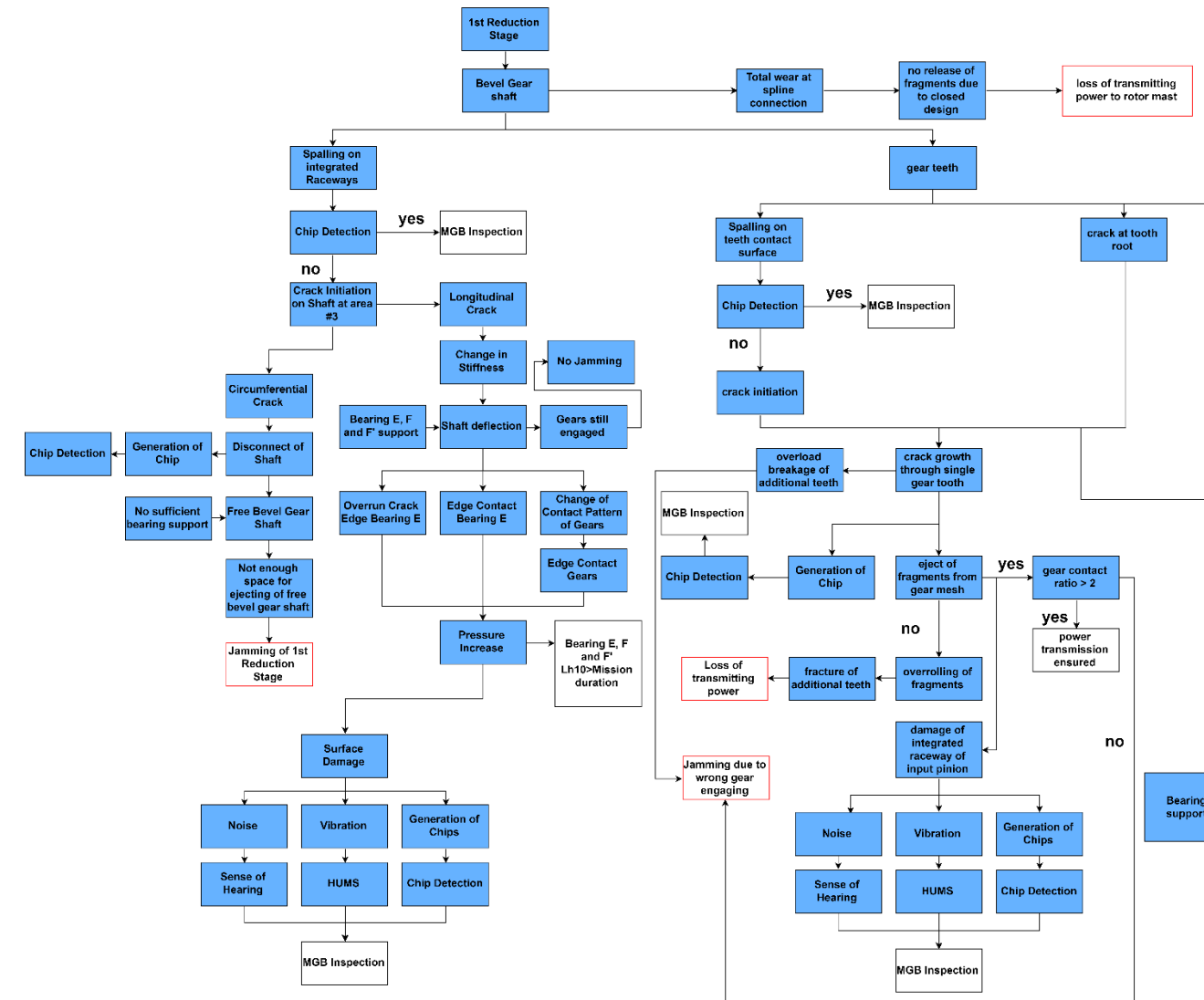


Figure 116: Bell OH58 – Input Pinion



- 1 Crack on input pinion shaft between bearing D and spiral bevel pinion
 - 2 Crack on input pinion between spiral bevel pinion and bearing A
 - 3 Crack on spiral bevel gear shaft upwards of spline connection in the vicinity of bearing E
 - 4 Crack on spiral bevel gear shaft between spline connection and bearing F
 - 5 Crack on sun gear shaft downwards of sun gear
 - 6 Crack on sun gear shaft between sun gear and bearing H

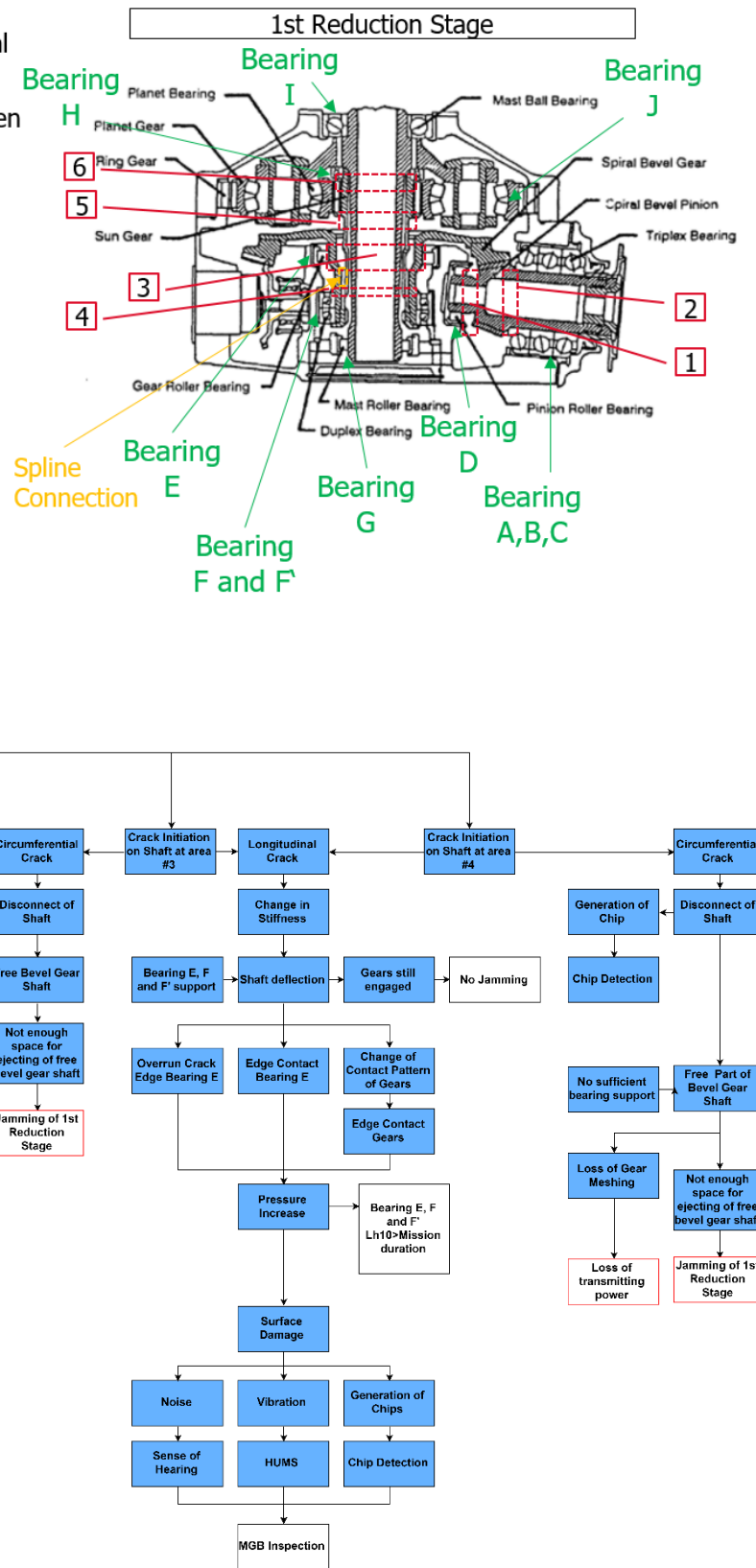
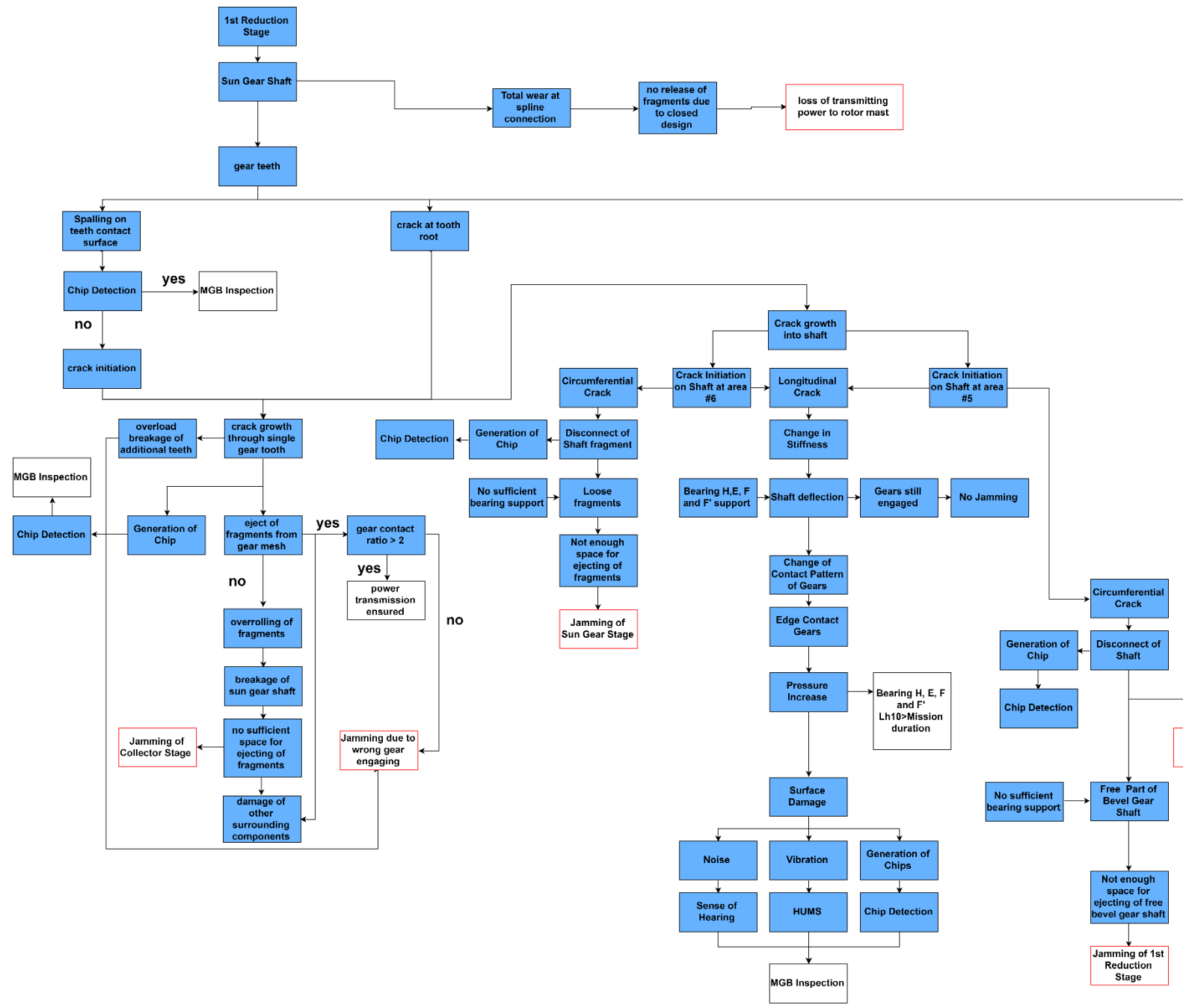


Figure 117: Bell OH58 – 1st Reduction Stage



- 1 Crack on input pinion shaft between bearing D and spiral bevel pinion
- 2 Crack on input pinion between spiral bevel pinion and bearing A
- 3 Crack on spiral bevel gear shaft upwards of spline connection in the vicinity of bearing E
- 4 Crack on spiral bevel gear shaft between spline connection and bearing F
- 5 Crack on sun gear shaft downwards of sun gear
- 6 Crack on sun gear shaft between sun gear and bearing H

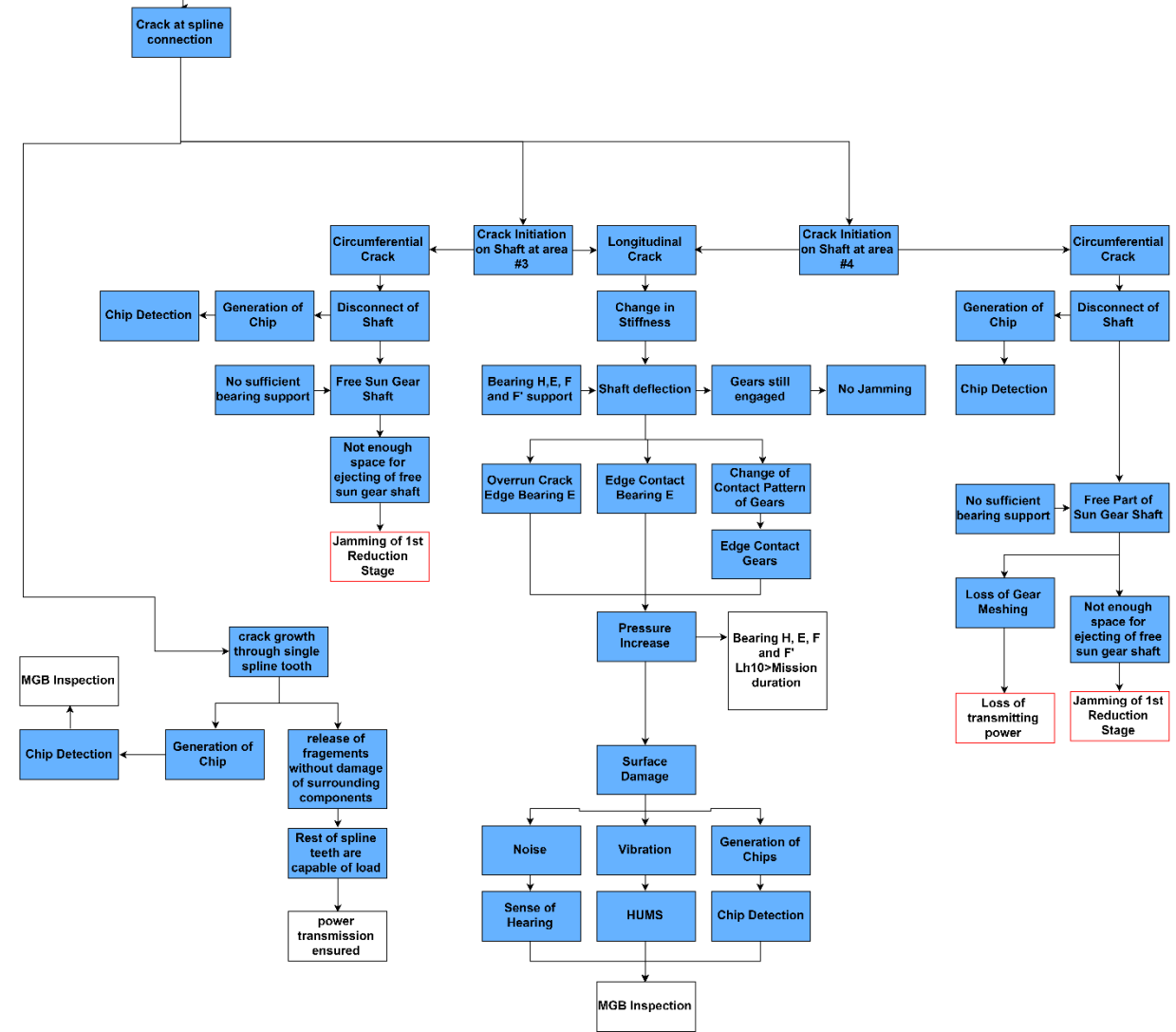
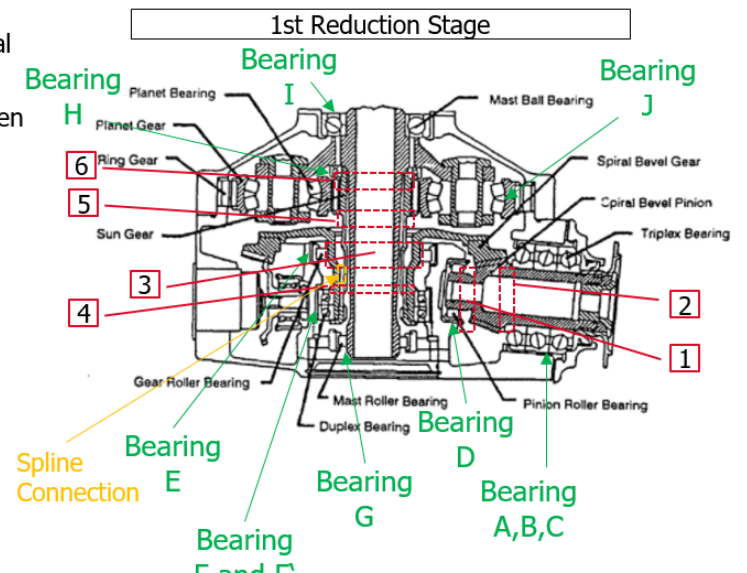


Figure 118: Bell OH58 – 1st Reduction Stage

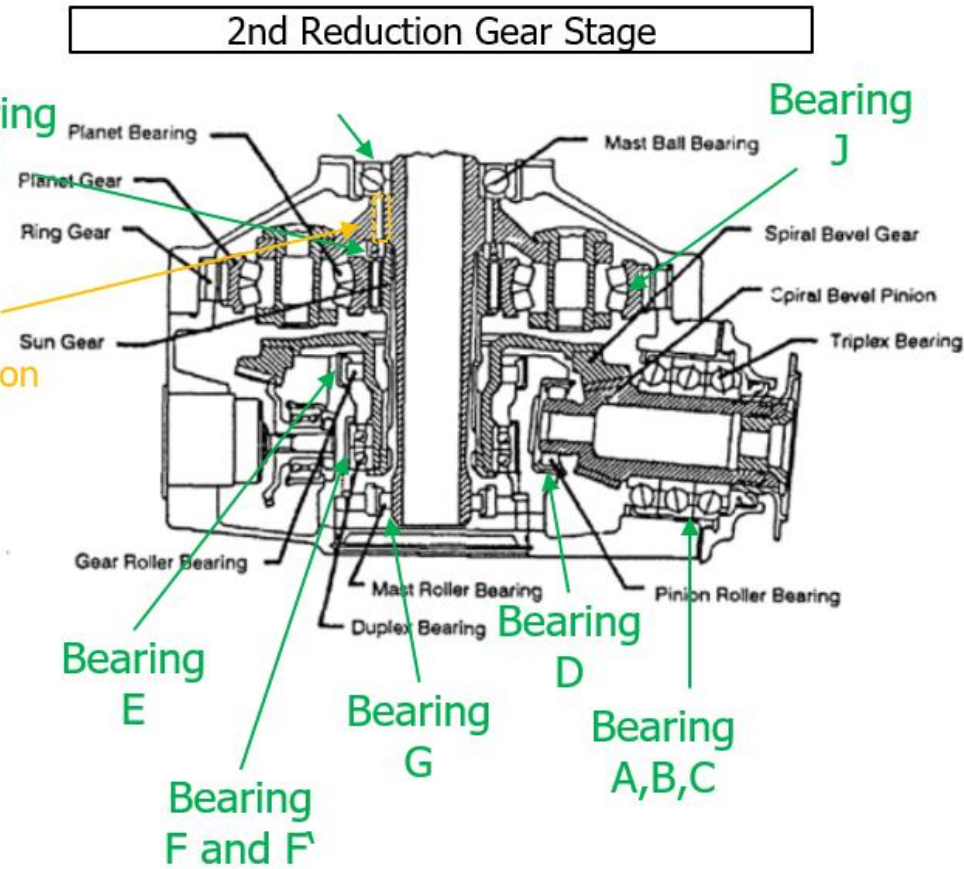
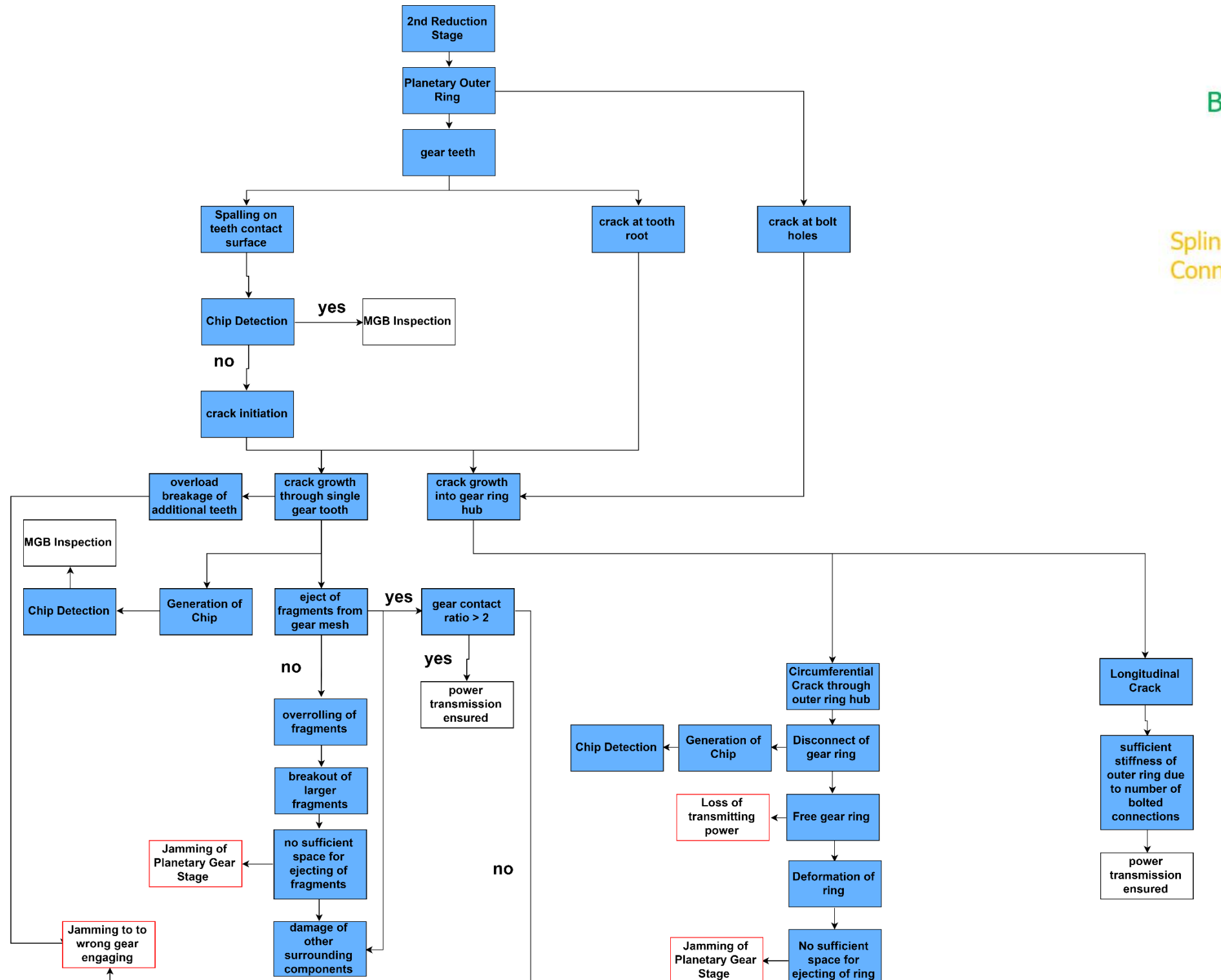


Figure 119: Bell OH58 – 2nd Reduction Stage

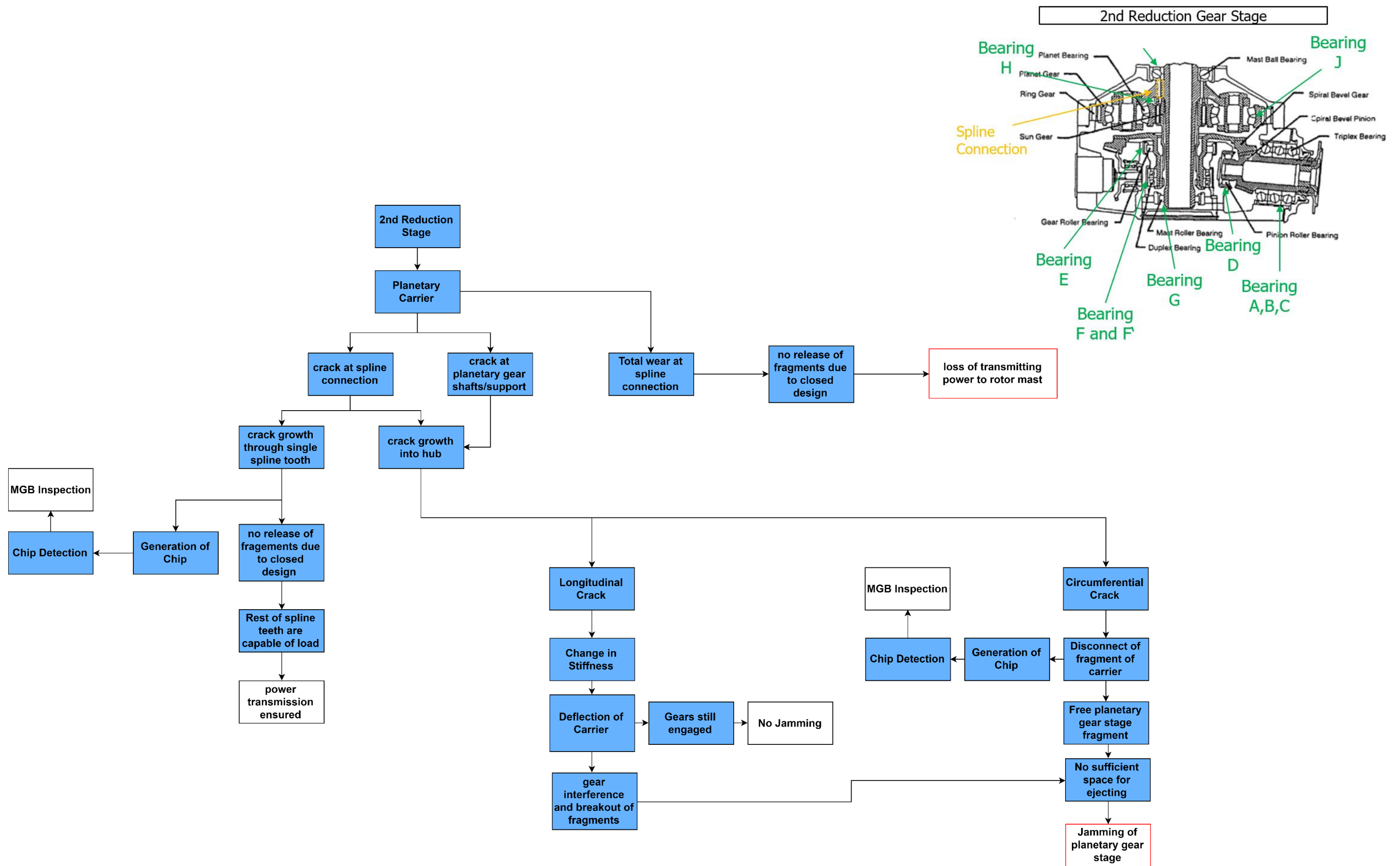


Figure 120: Bell OH58 – 2nd Reduction Stage

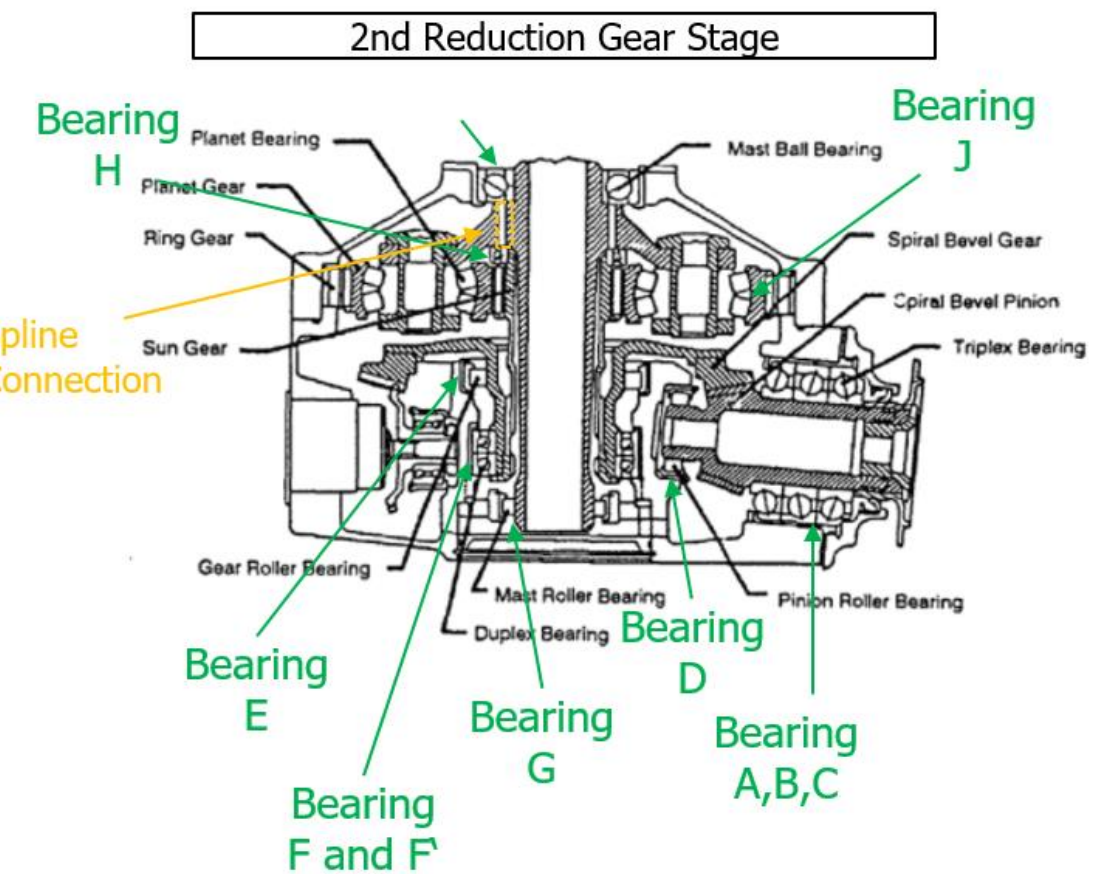
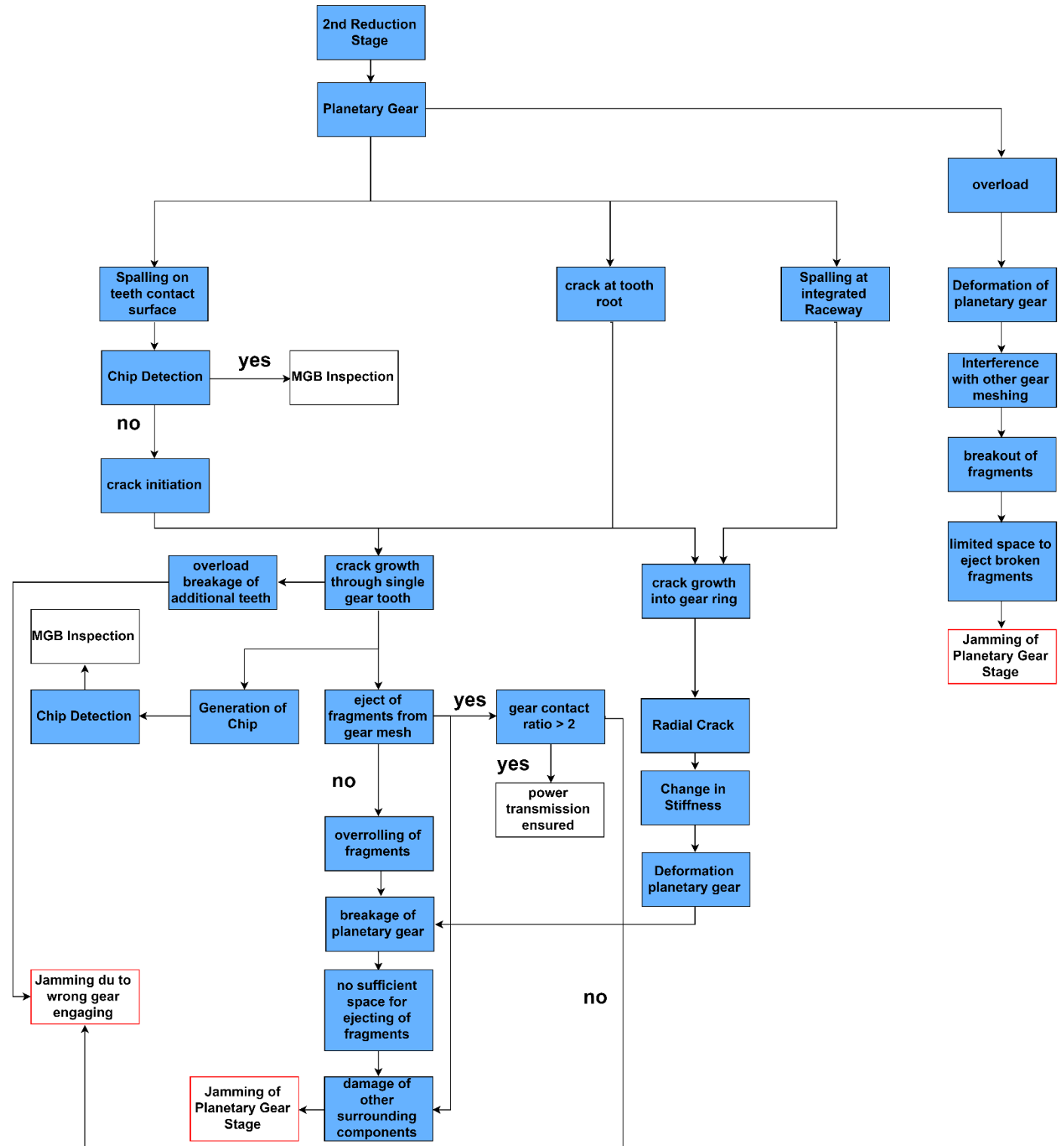


Figure 121: Bell OH58 – 2nd Reduction Stage

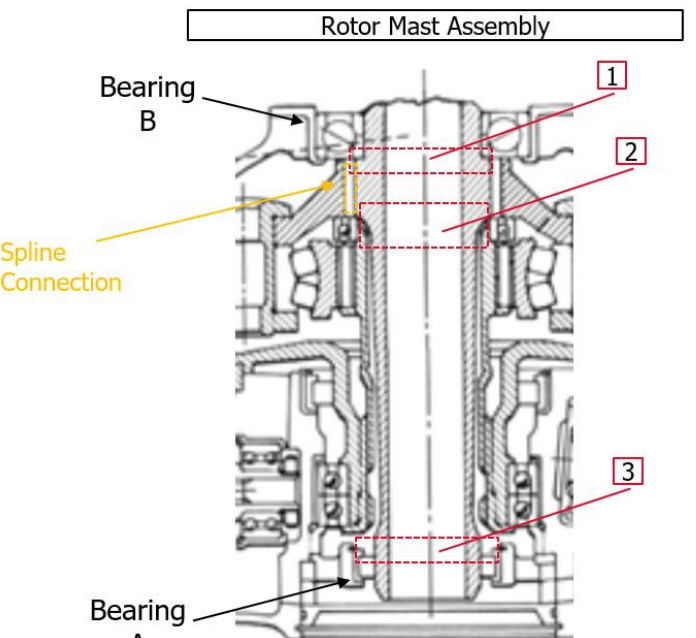
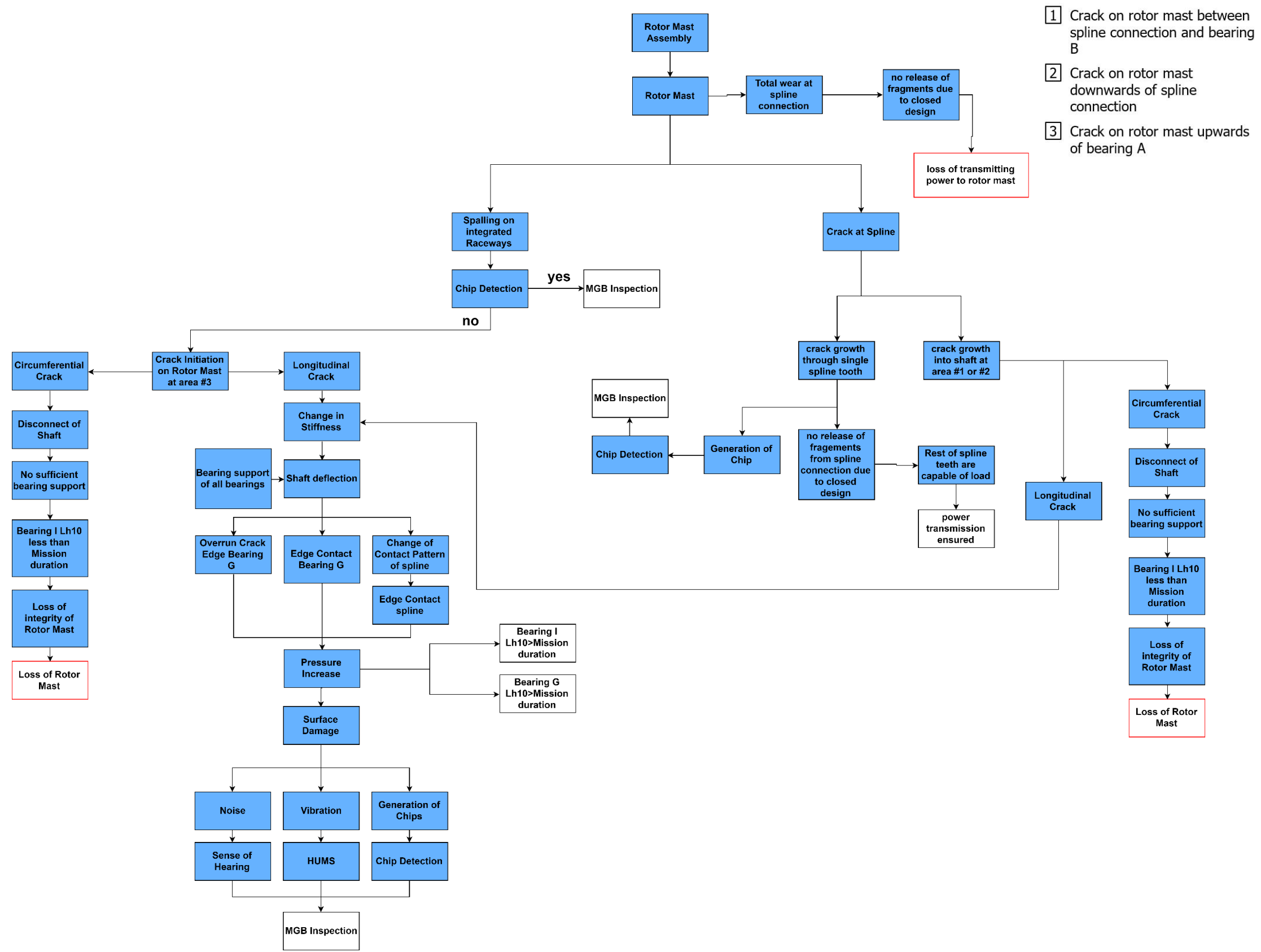
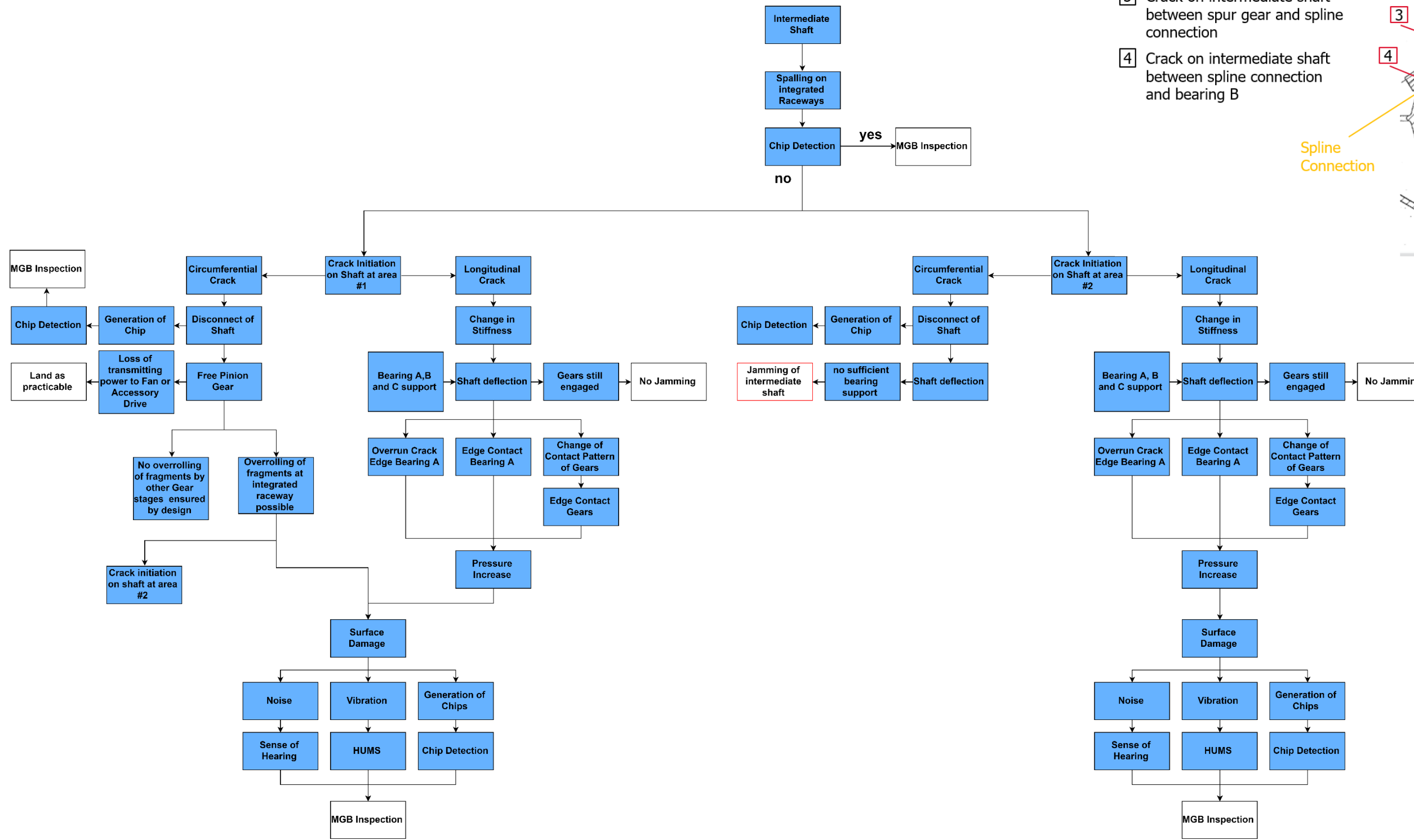


Figure 122: Bell OH58 – Rotor Mast Assembly

A.3 Flow diagram of Example 3



- 1 Crack on intermediate shaft between bearing A and fan drive bevel pinion
- 2 Crack on intermediate shaft between bearing A and spur gear
- 3 Crack on intermediate shaft between spur gear and spline connection
- 4 Crack on intermediate shaft between spline connection and bearing B

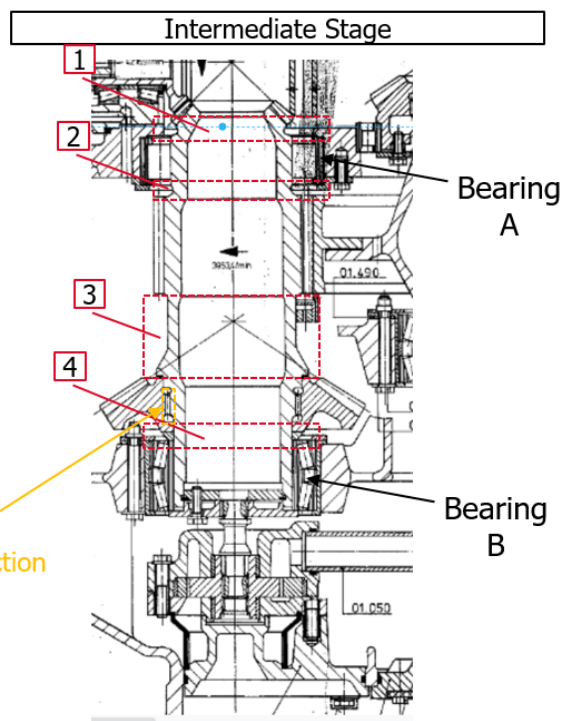
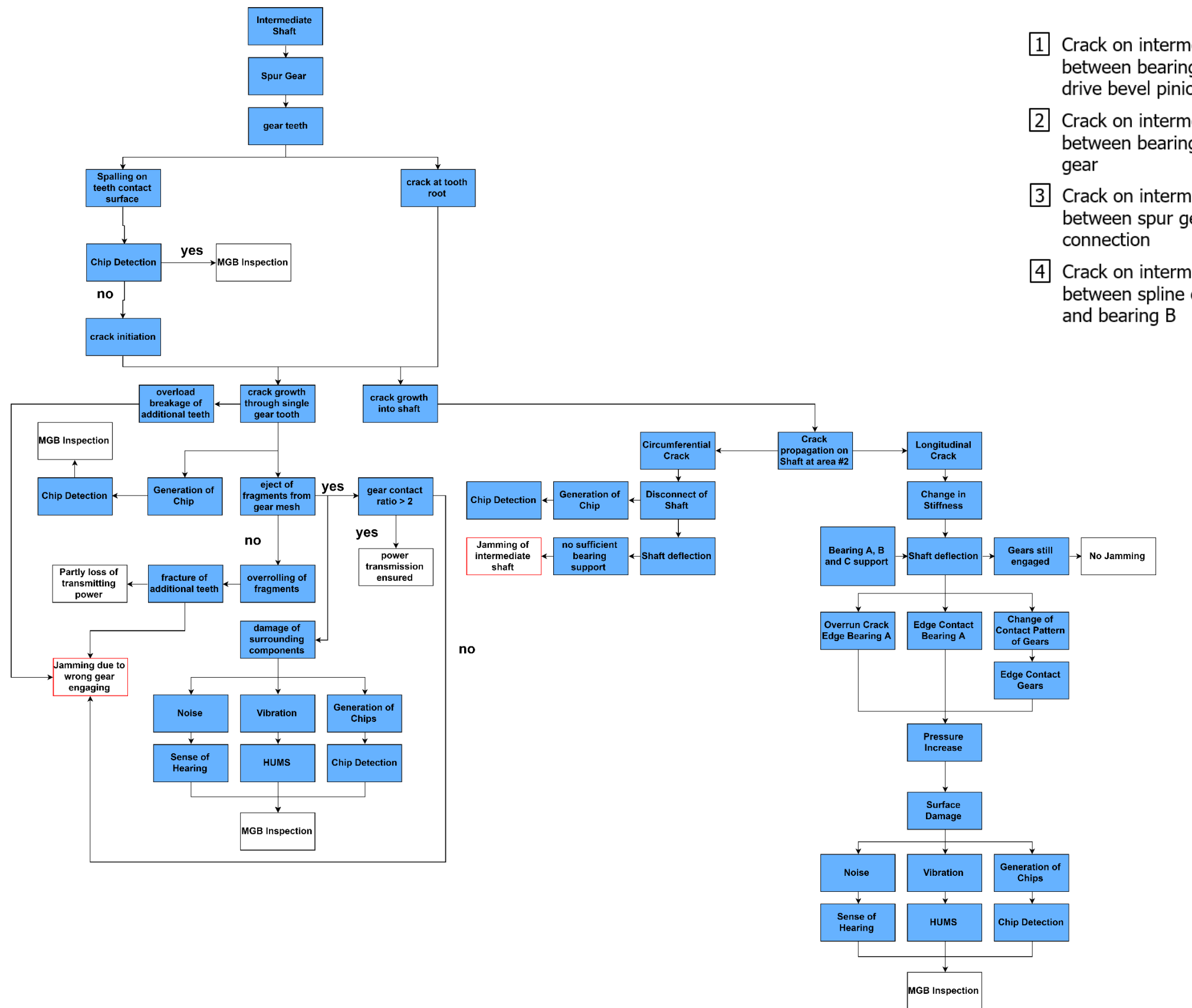


Figure 123: BO105 – Intermediate Shaft



- 1 Crack on intermediate shaft between bearing A and fan drive bevel pinion
- 2 Crack on intermediate shaft between bearing A and spur gear
- 3 Crack on intermediate shaft between spur gear and spline connection
- 4 Crack on intermediate shaft between spline connection and bearing B

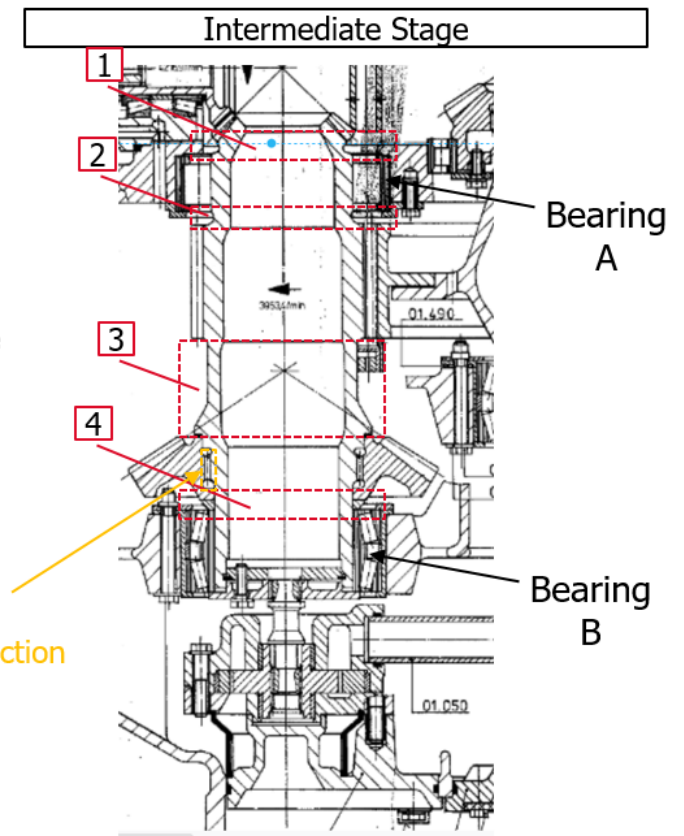


Figure 124: BO105 – Intermediate Shaft

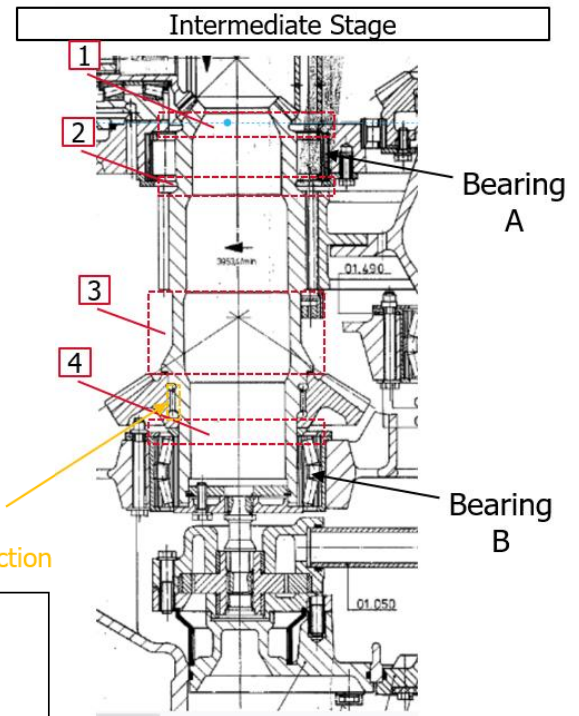
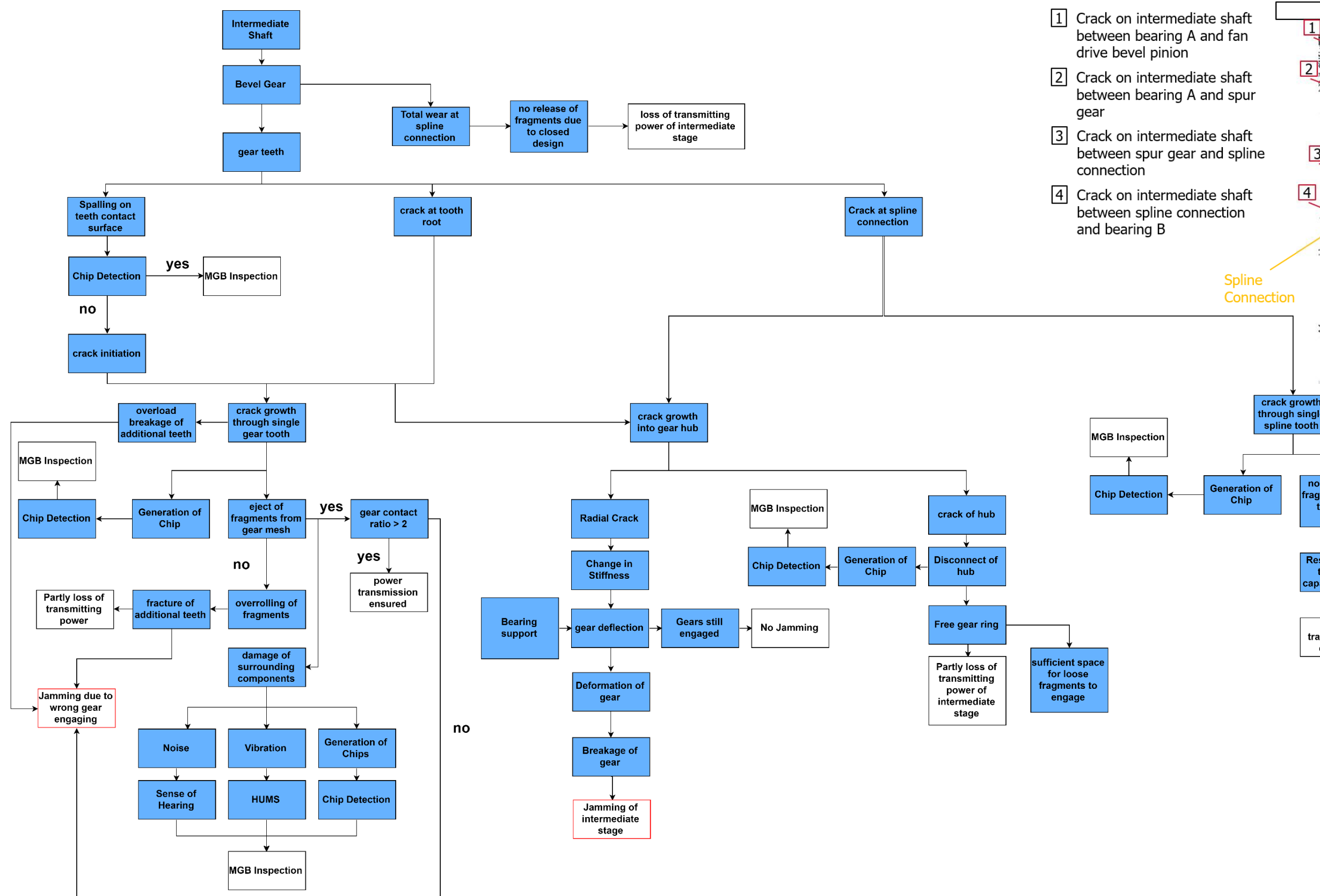


Figure 125: BO105 – Intermediate Shaft

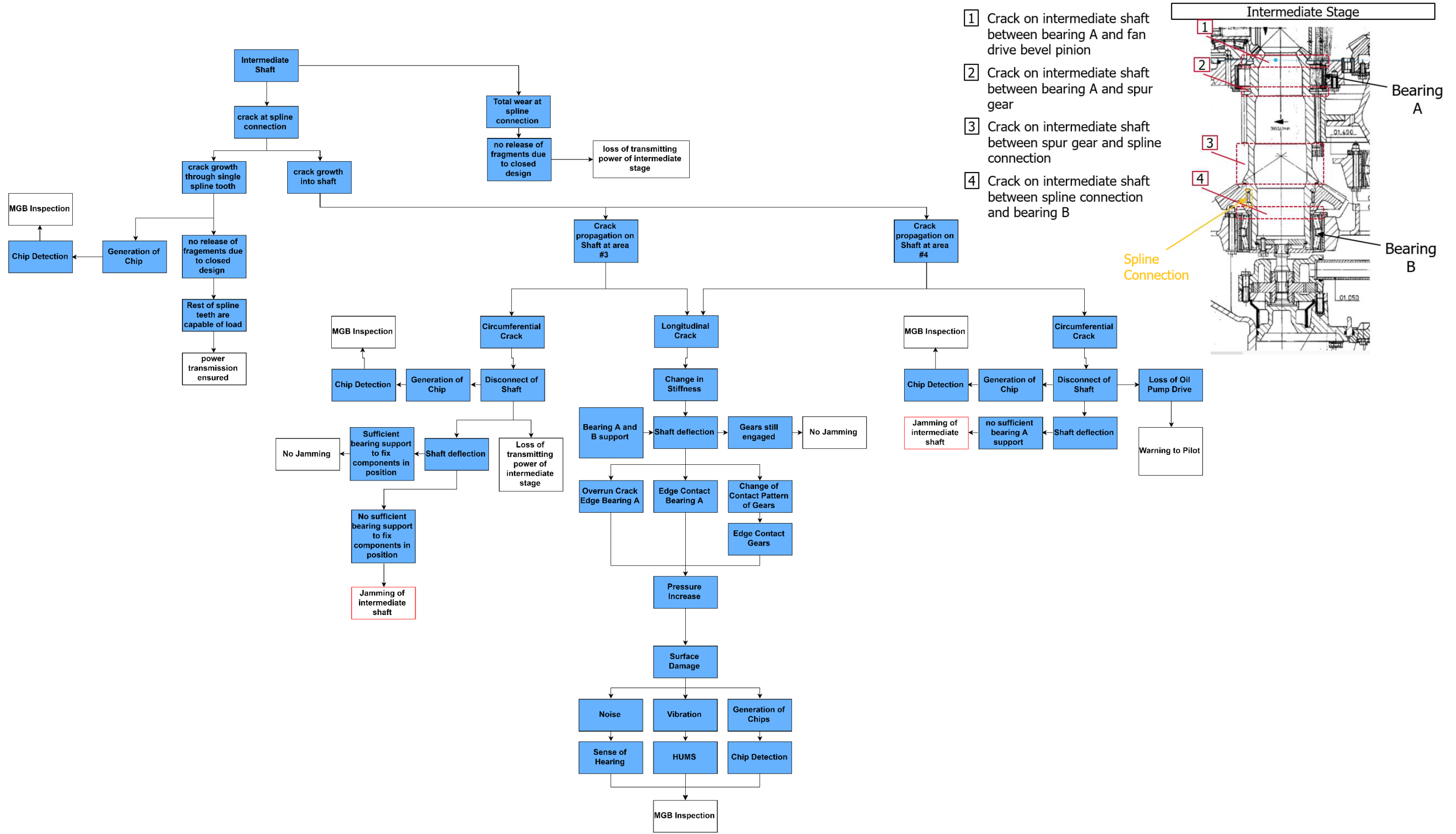


Figure 126: BO105 – Intermediate Shaft

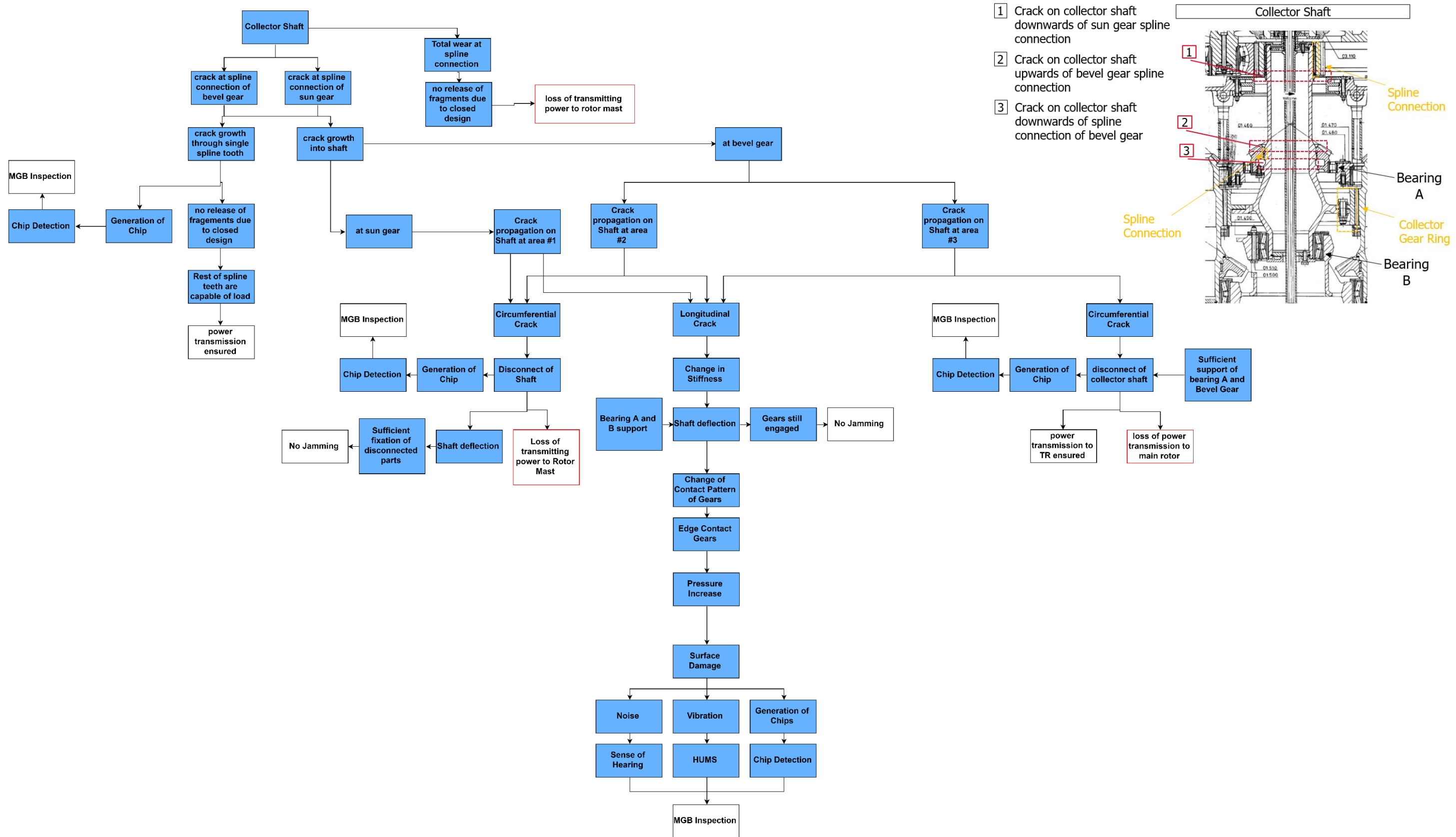


Figure 127: BO105 – Collector Shaft

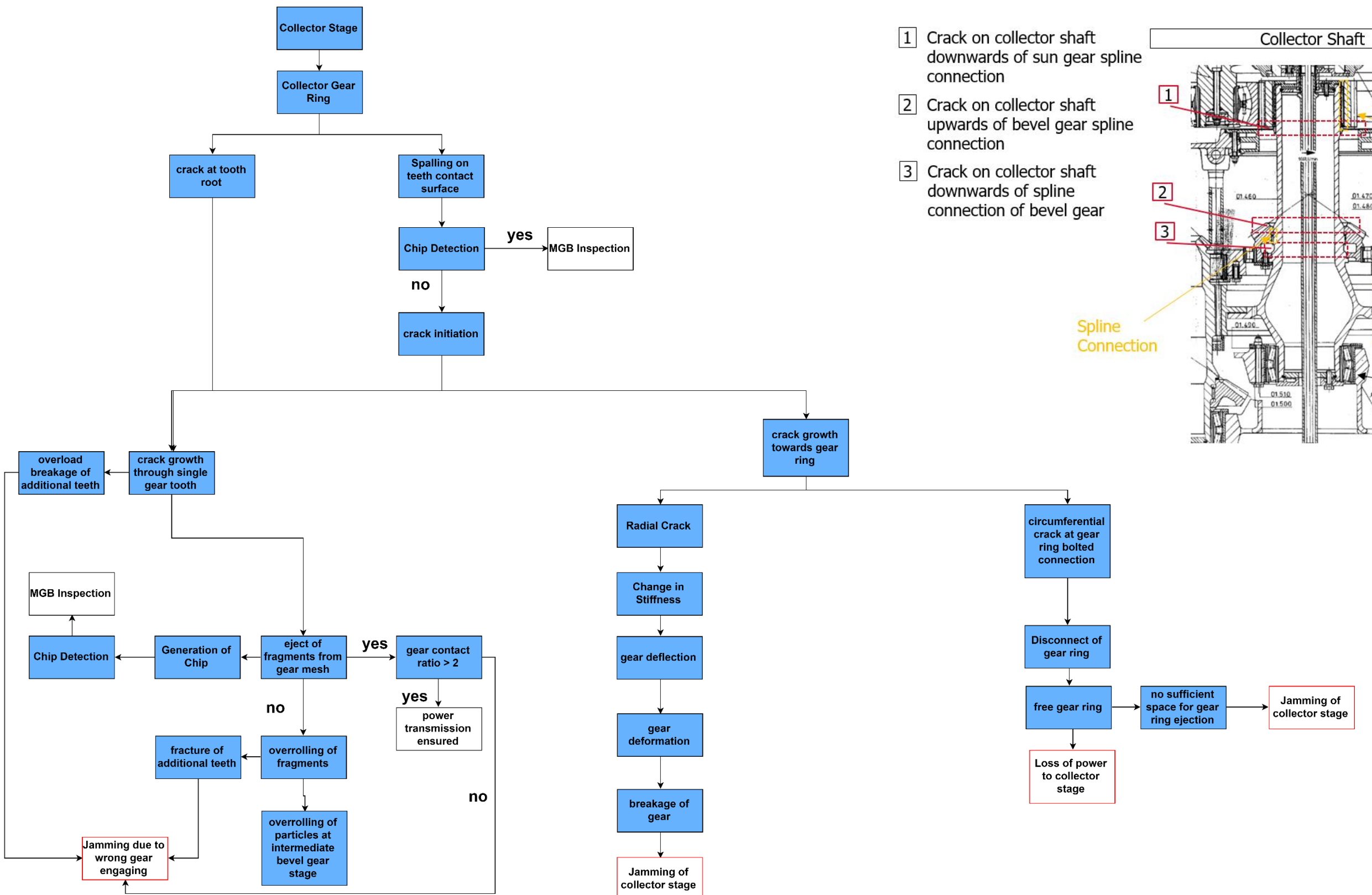


Figure 128: BO105 – Collector Gear Ring

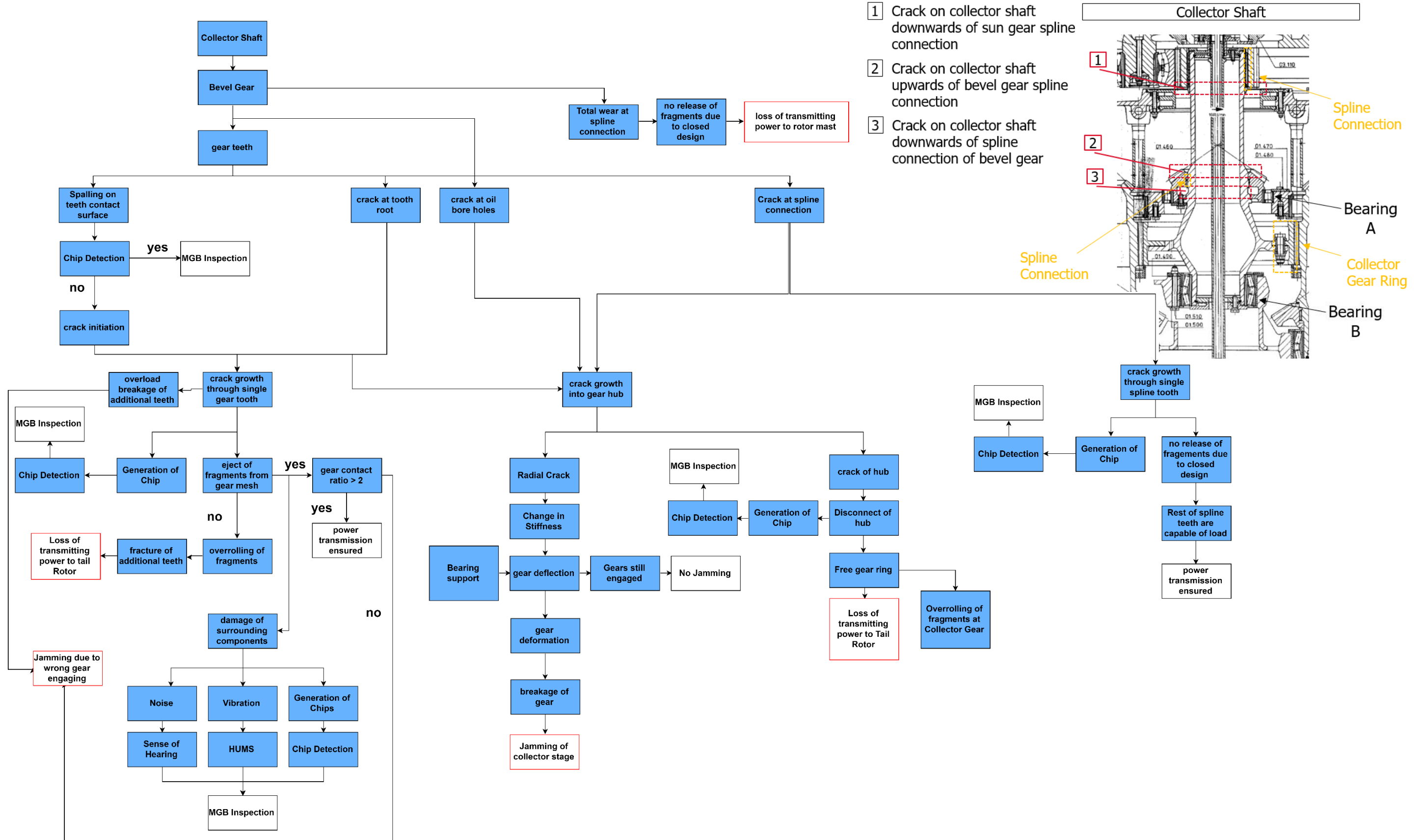


Figure 129: BO105 – Collector Shaft

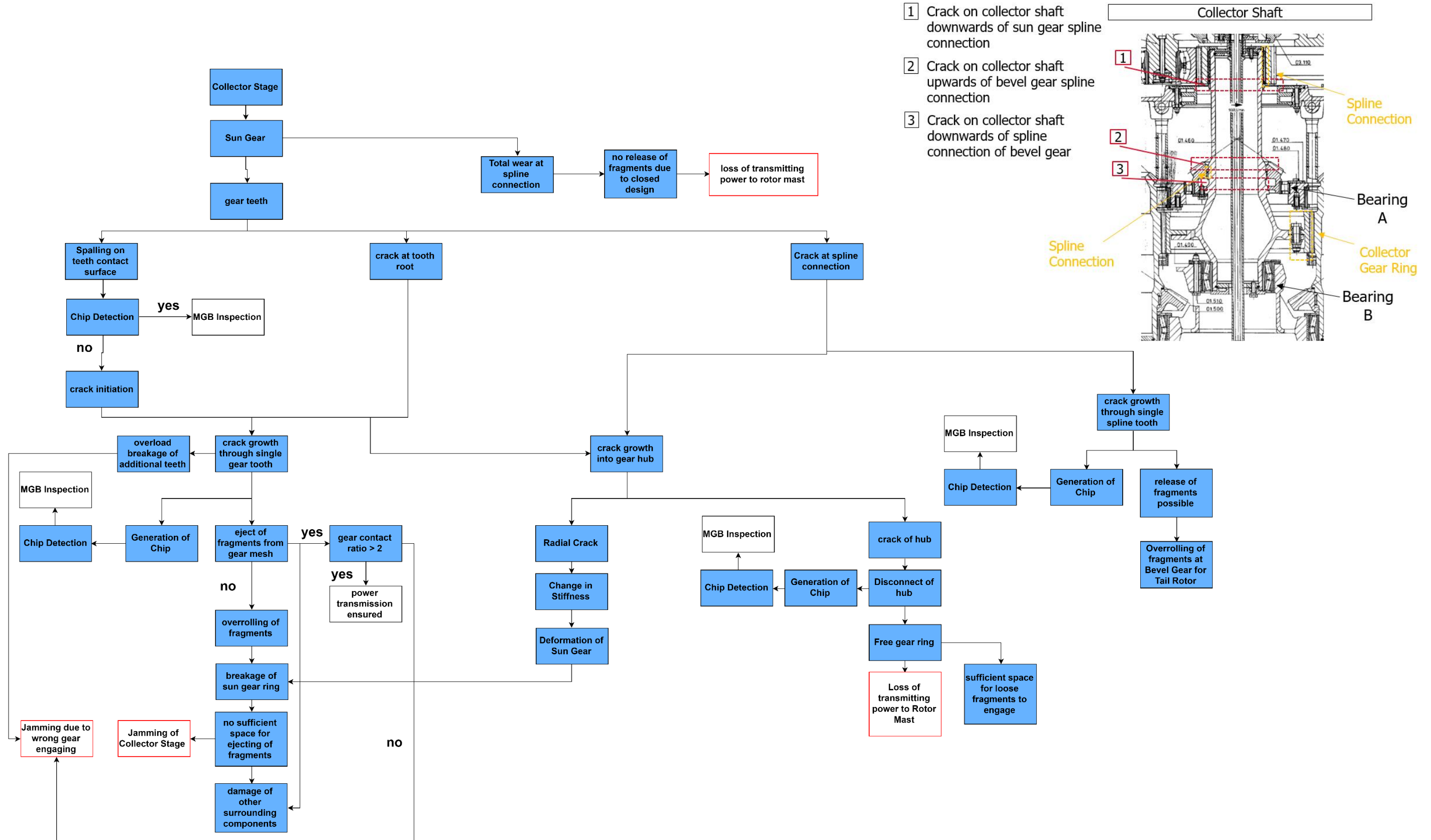
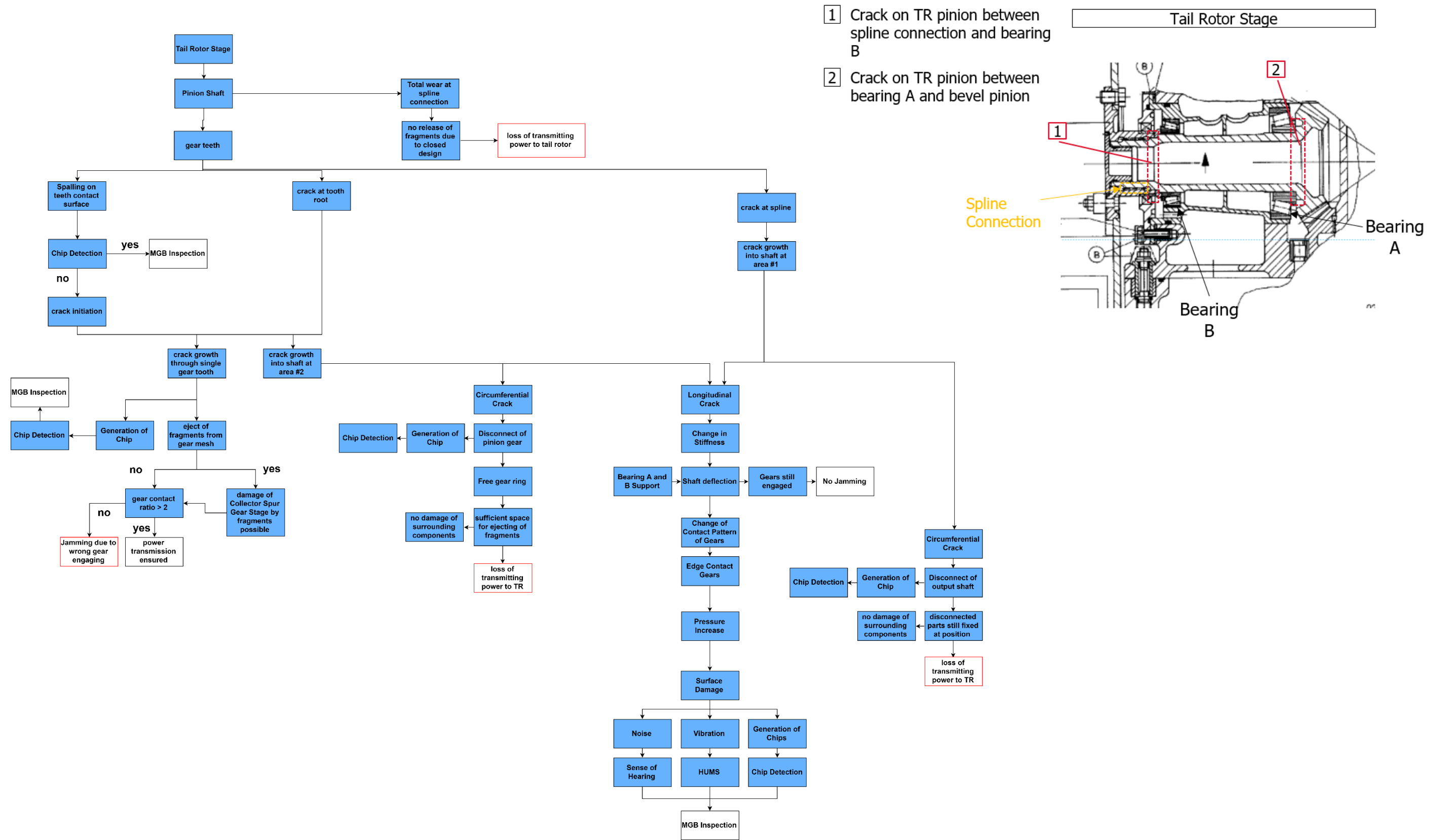


Figure 130: BO105 – Collector Shaft



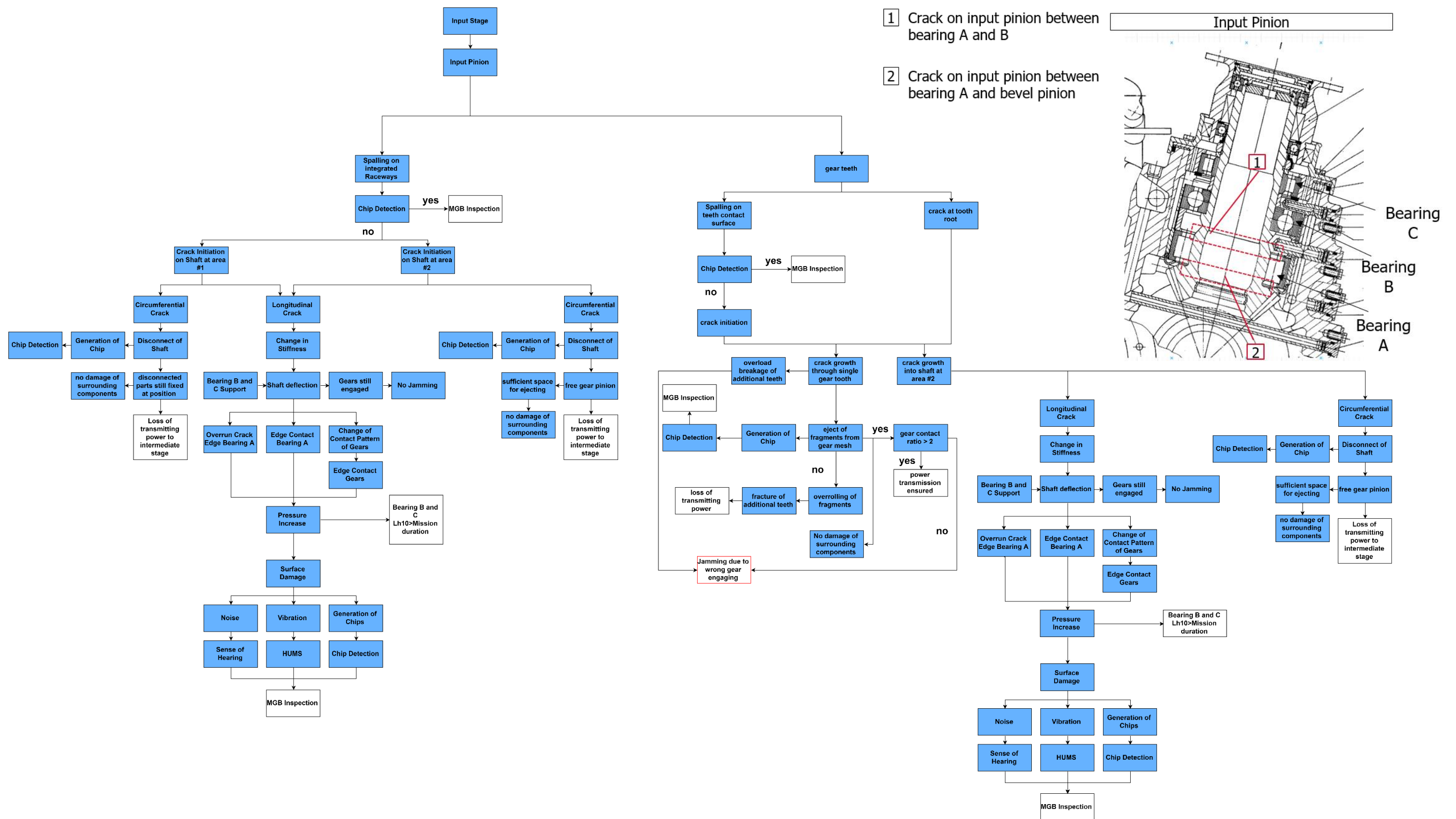


Figure 132: BO105 – Input Pinion

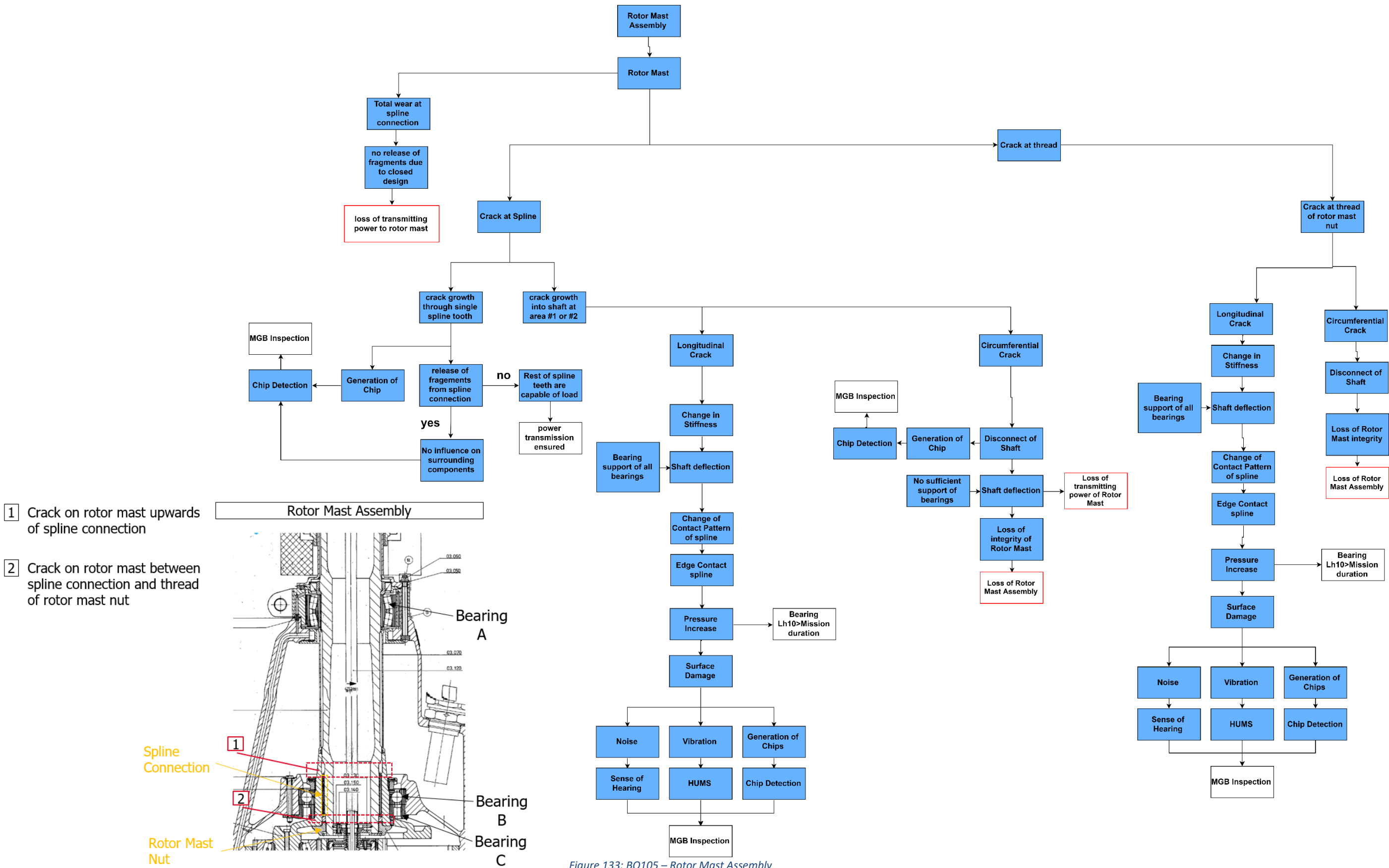
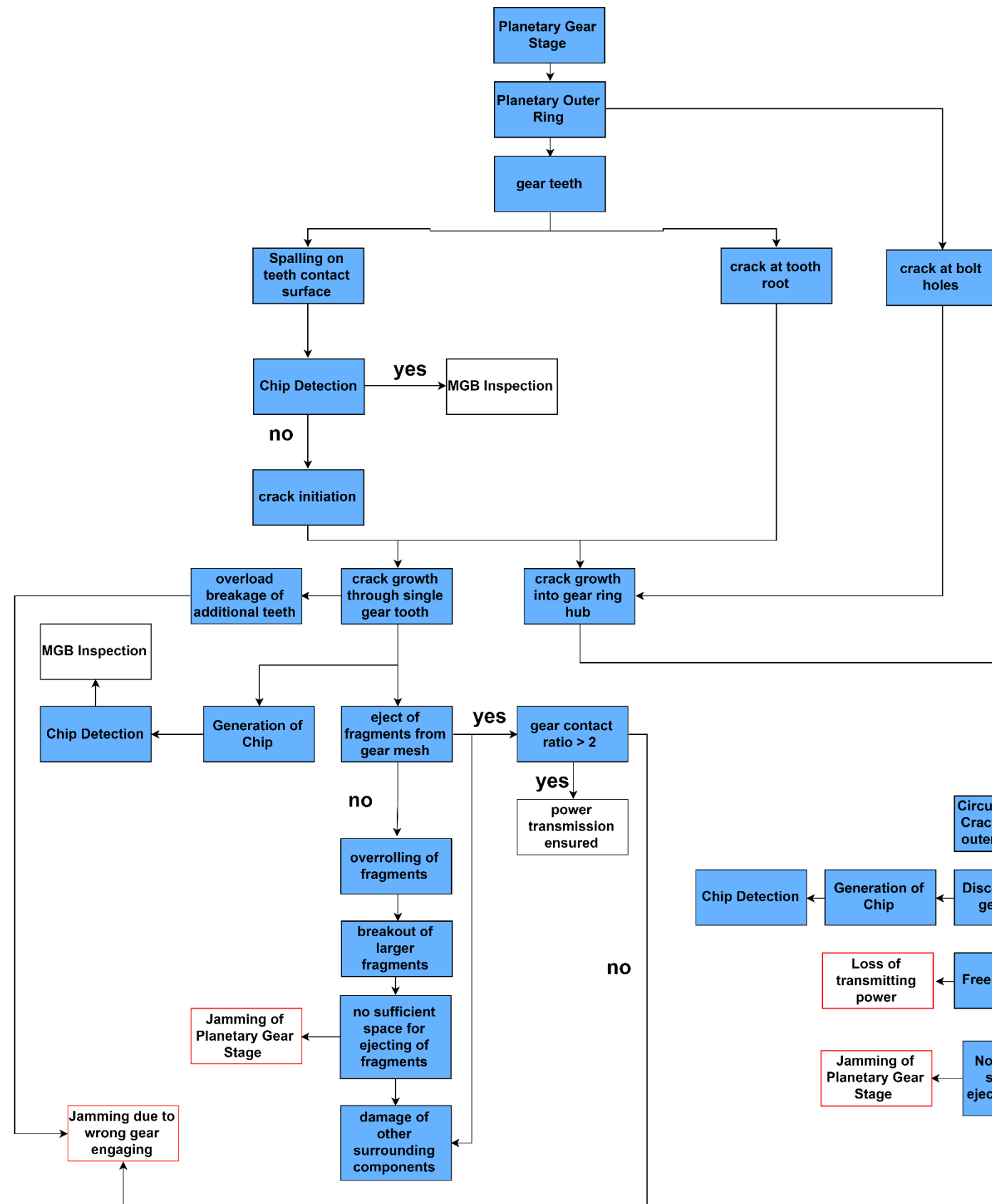


Figure 133: BO105 – Rotor Mast Assembly



1 Crack on planetary carrier downwards of spline connection

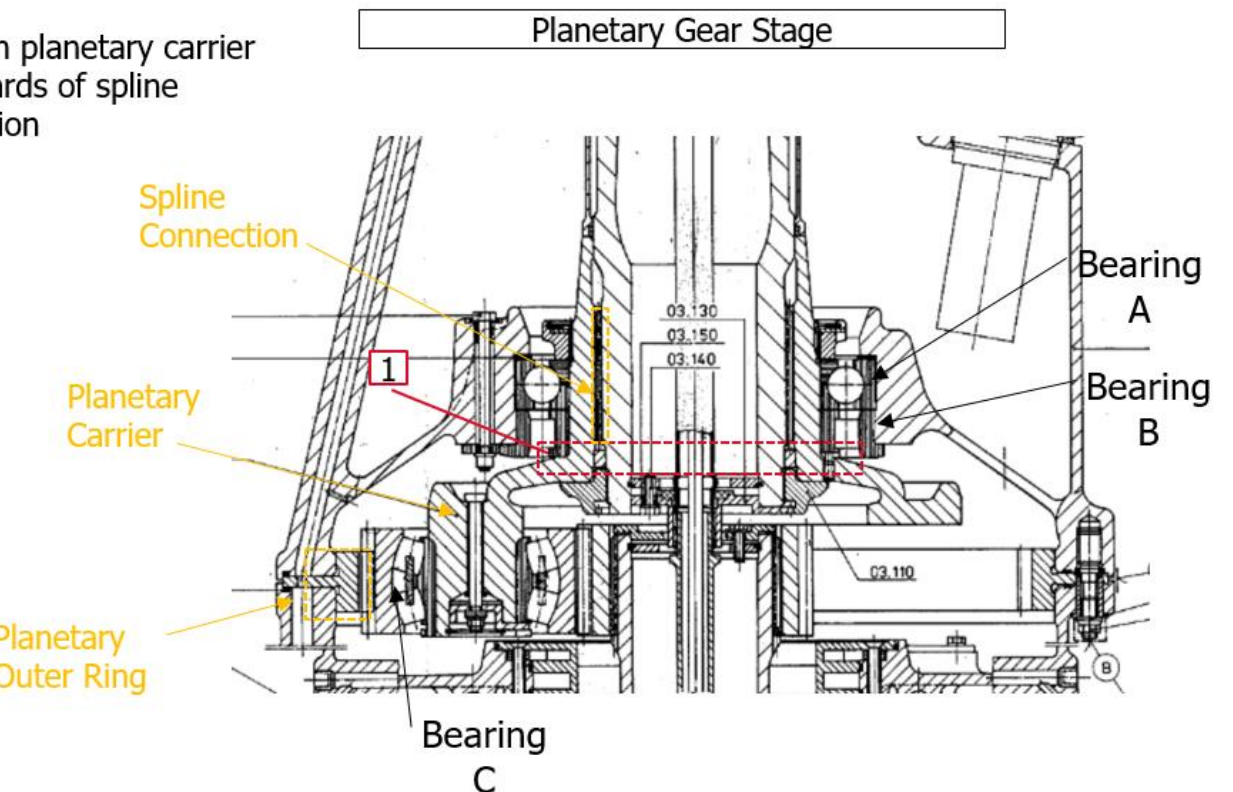


Figure 134: BO105 – Planetary Gear Stage

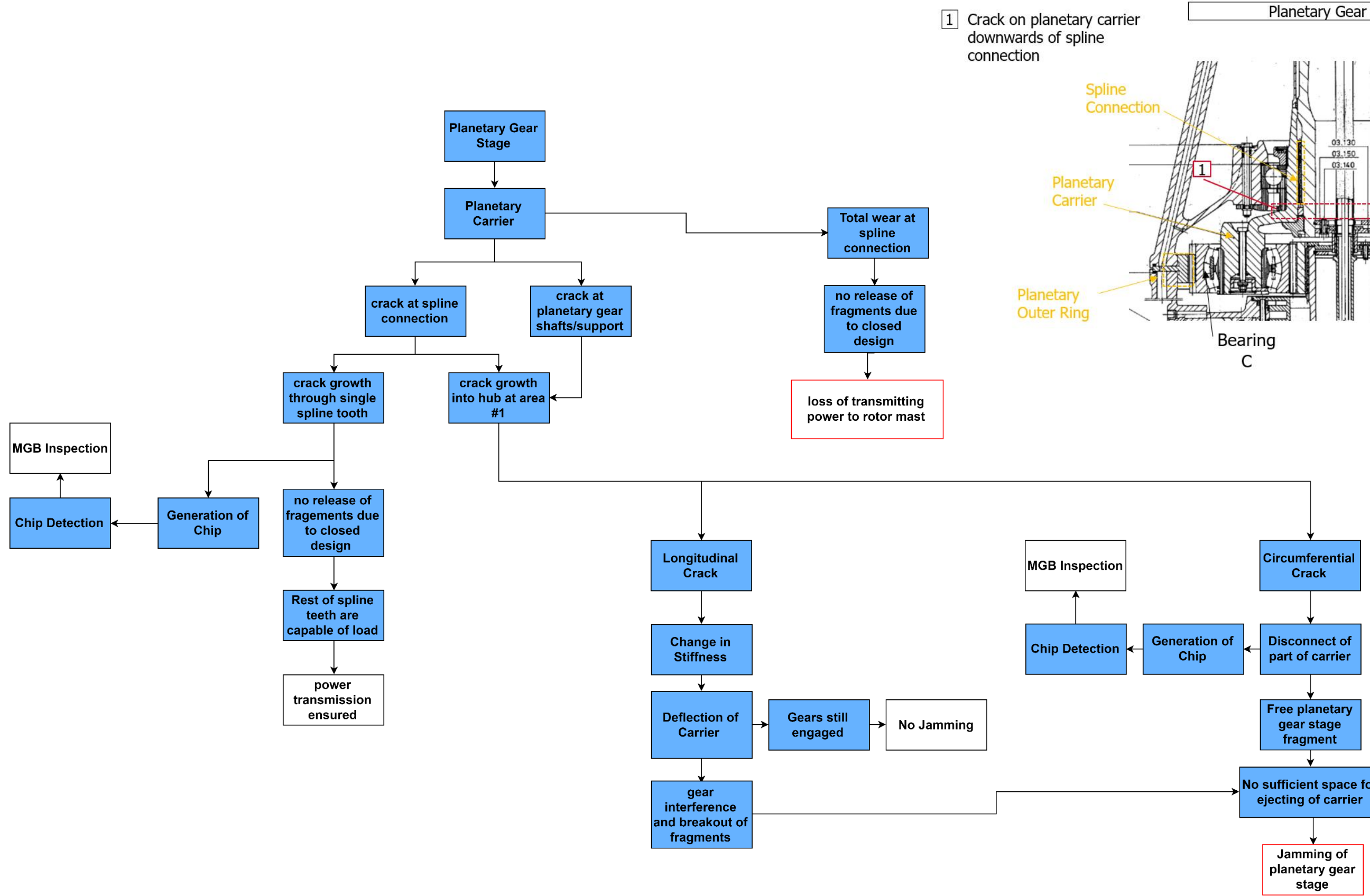
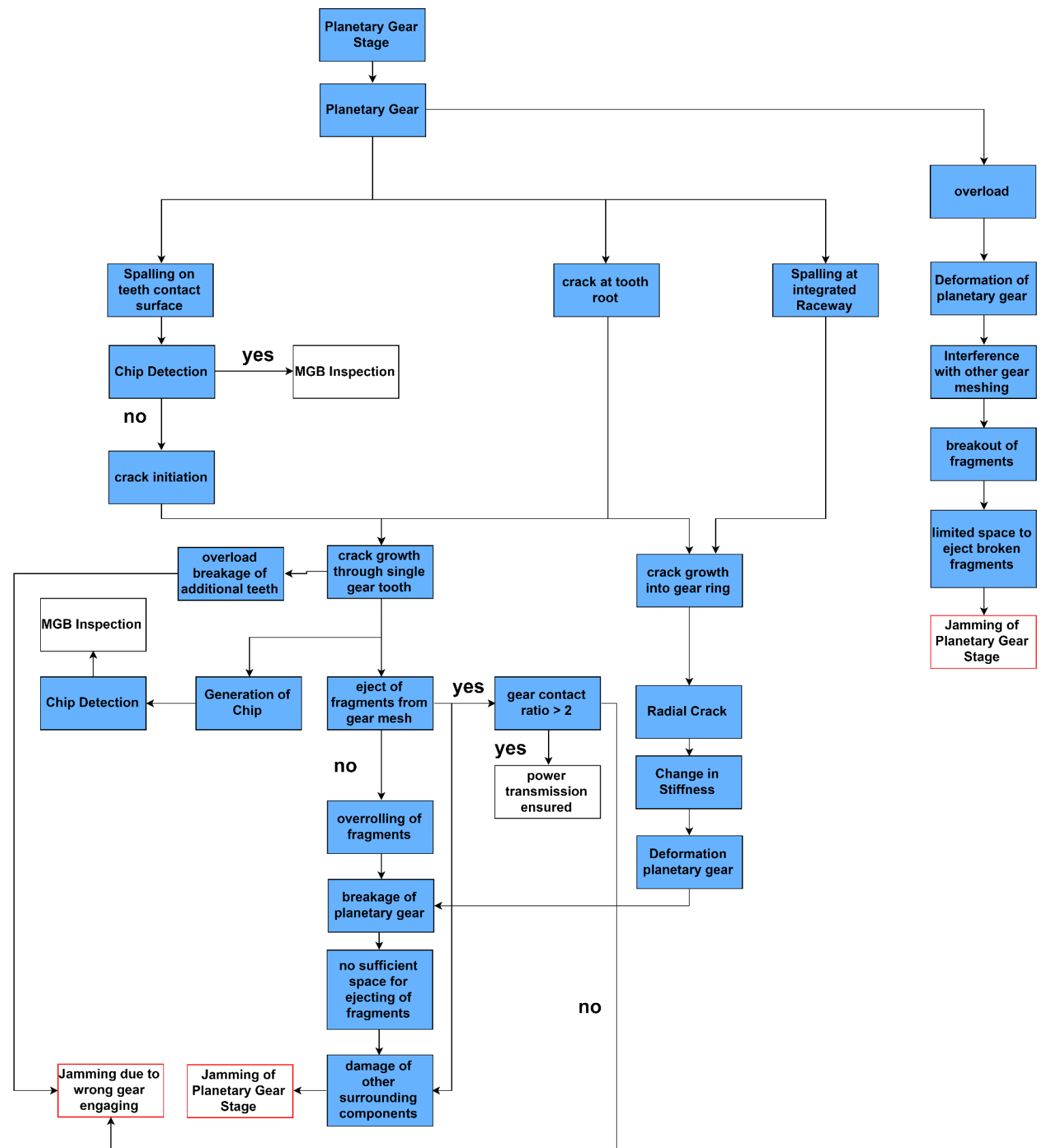


Figure 135: BO105 – Planetary Gear Stage



1 Crack on planetary carrier downwards of spline connection

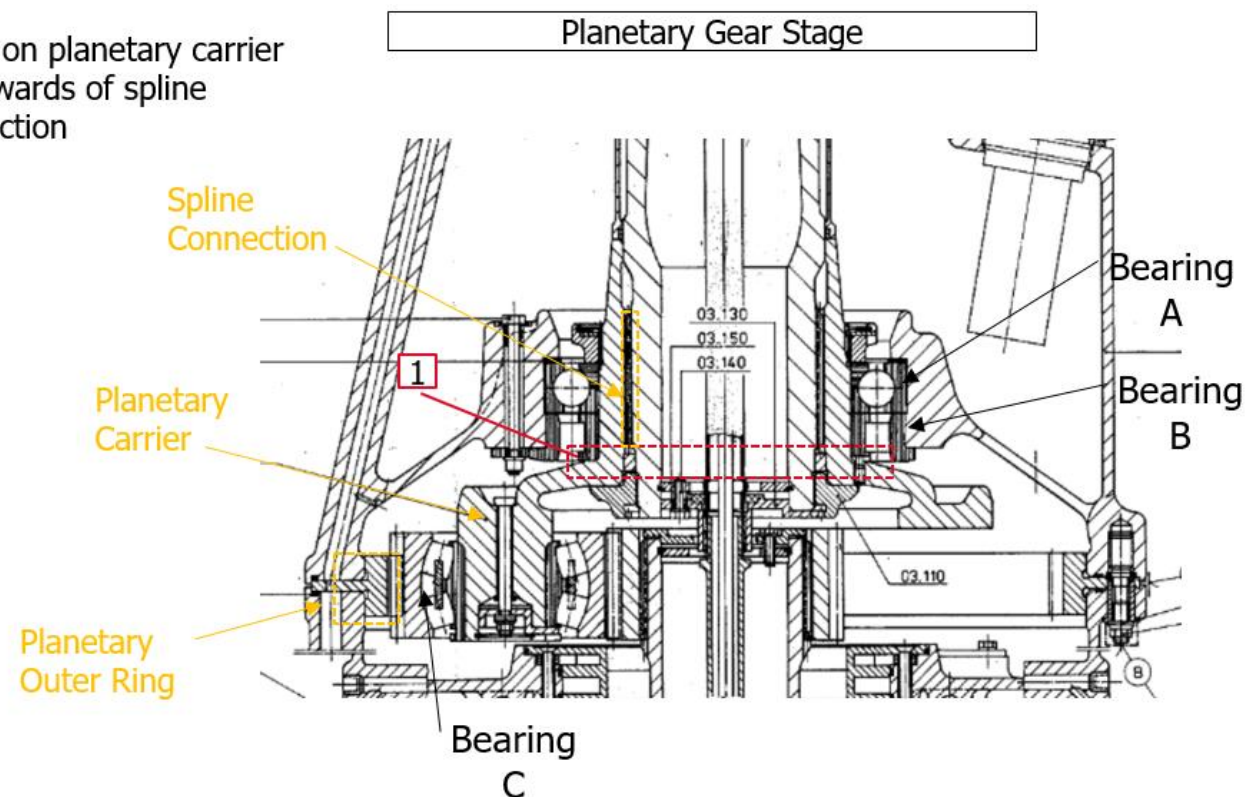
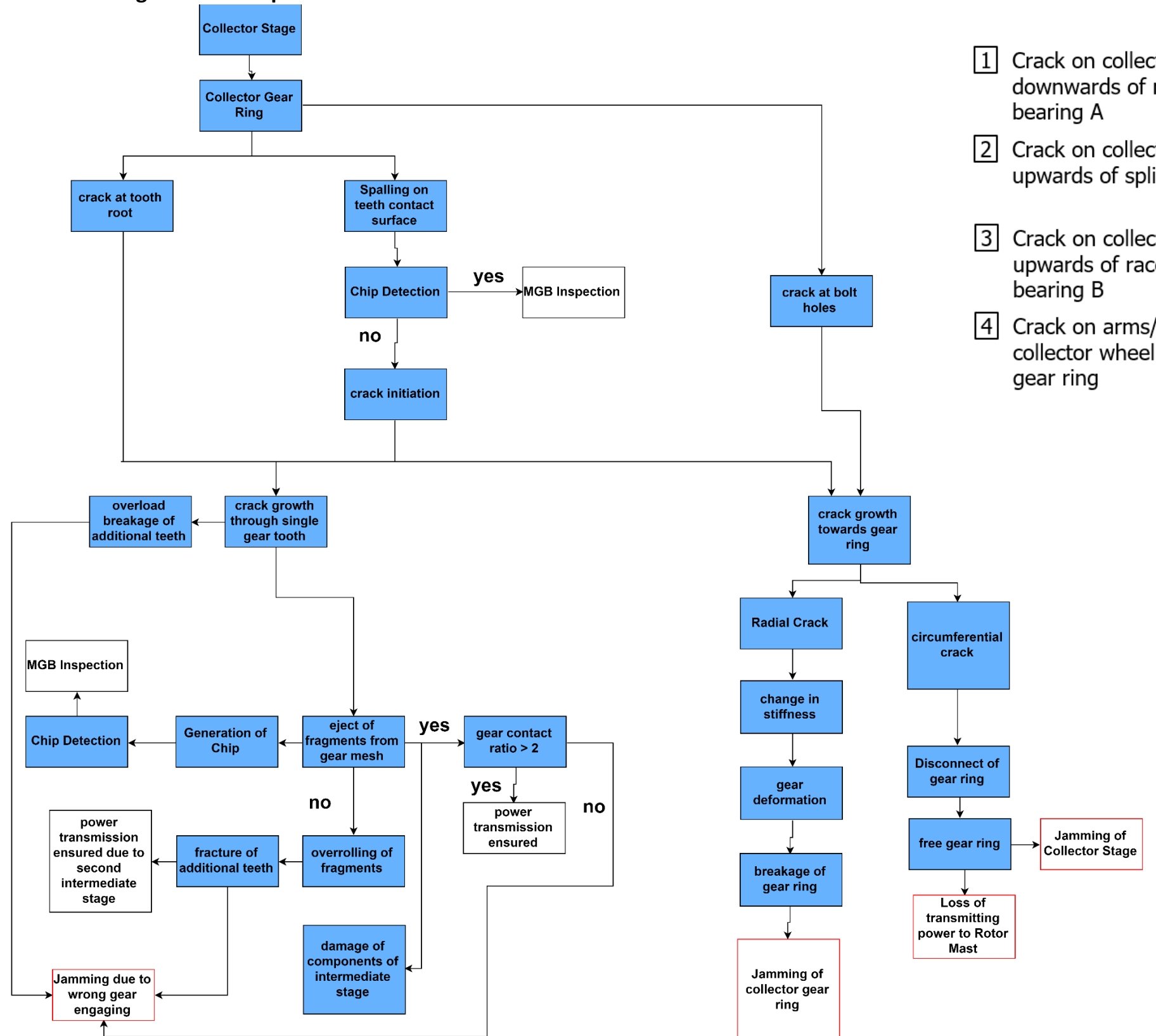


Figure 136: BO105 – Planetary Gear Stage

A.4 Flow diagram of Example 4



- [1] Crack on collector wheel downwards of raceway of bearing A
- [2] Crack on collector shaft upwards of spline connection
- [3] Crack on collector wheel upwards of raceway of bearing B
- [4] Crack on arms/connection of collector wheel to collector gear ring

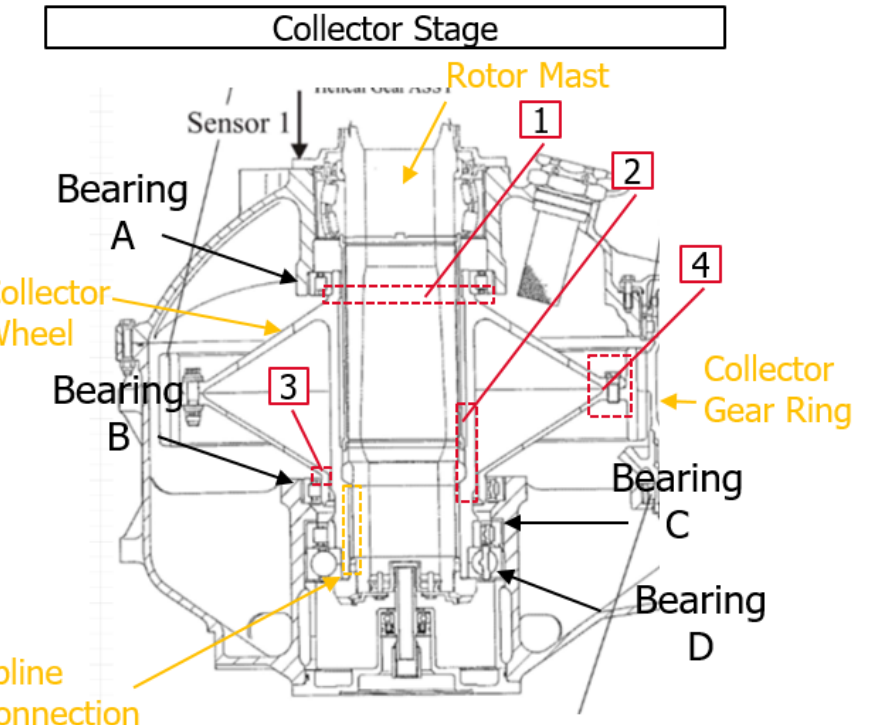


Figure 137: BK117 – Collector Shaft Ring

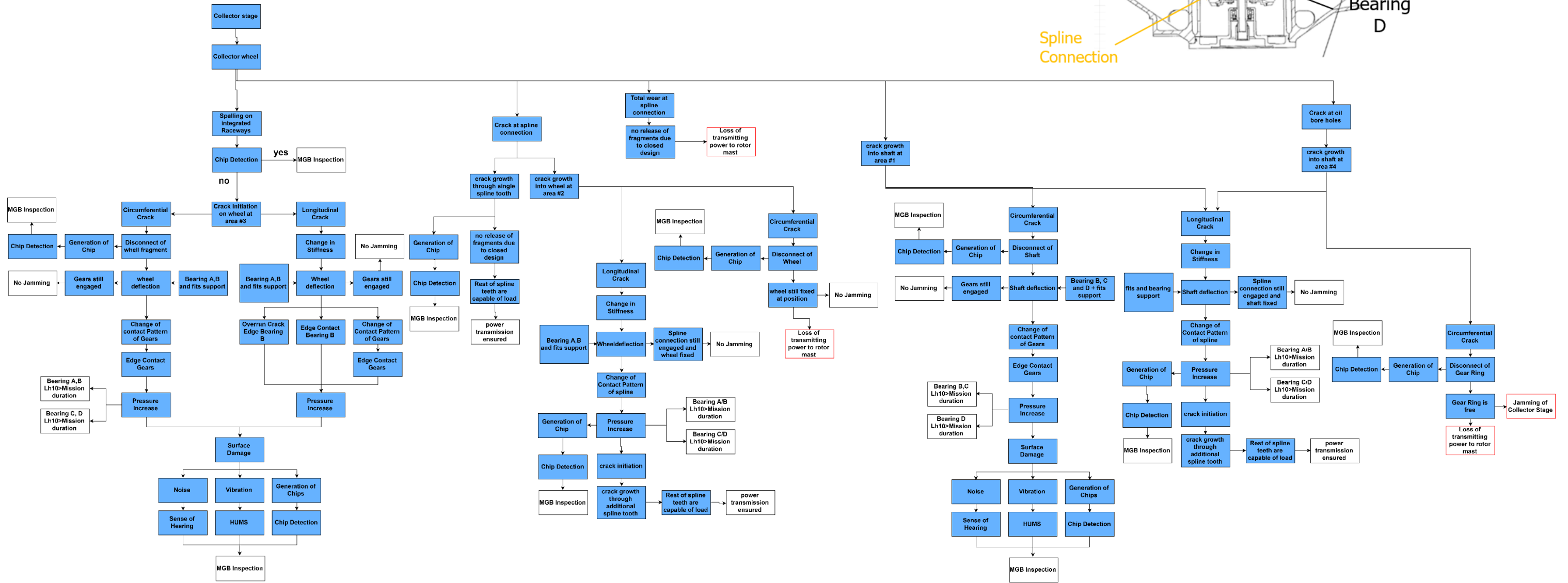


Figure 138: BK117 – Collector Wheel

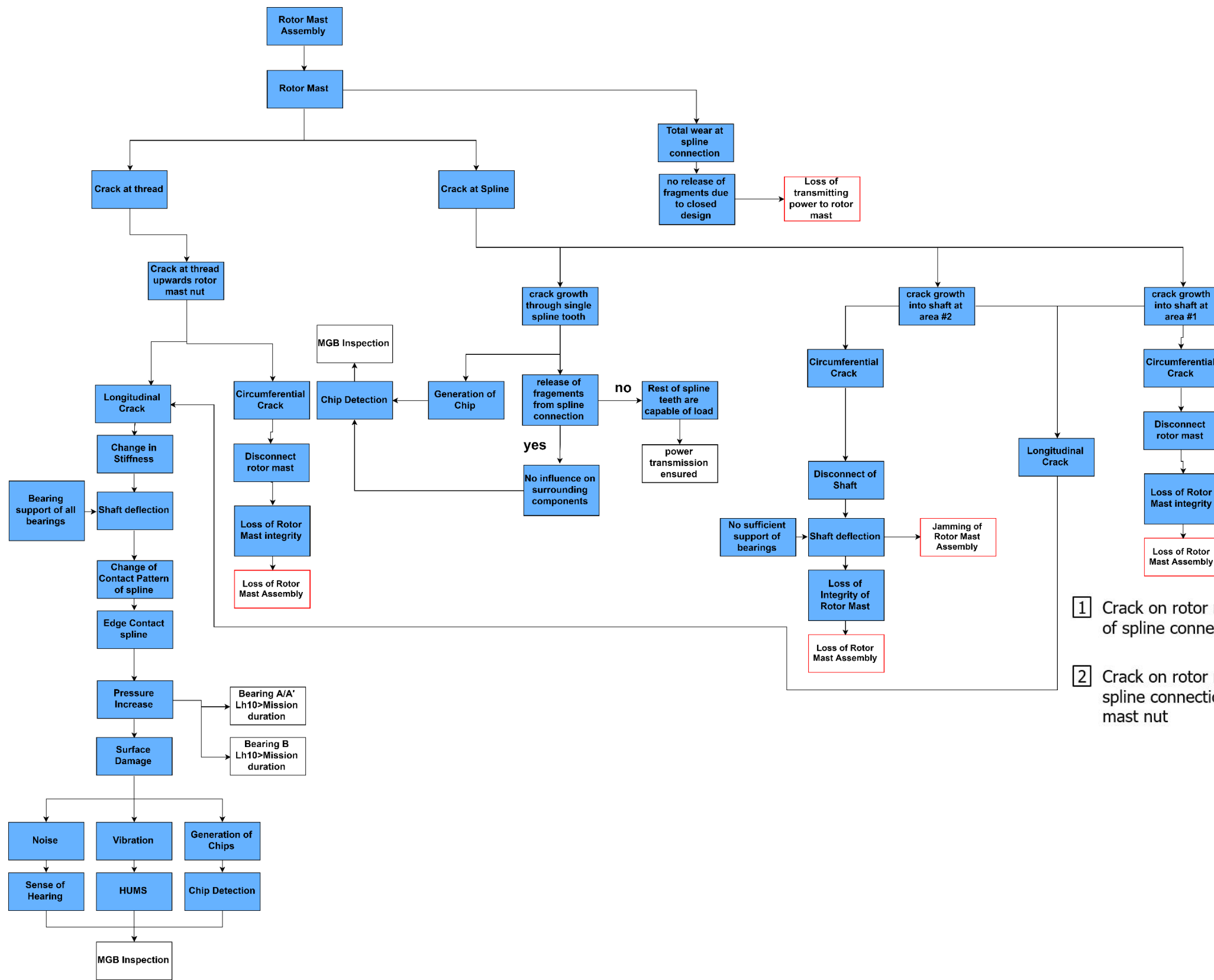
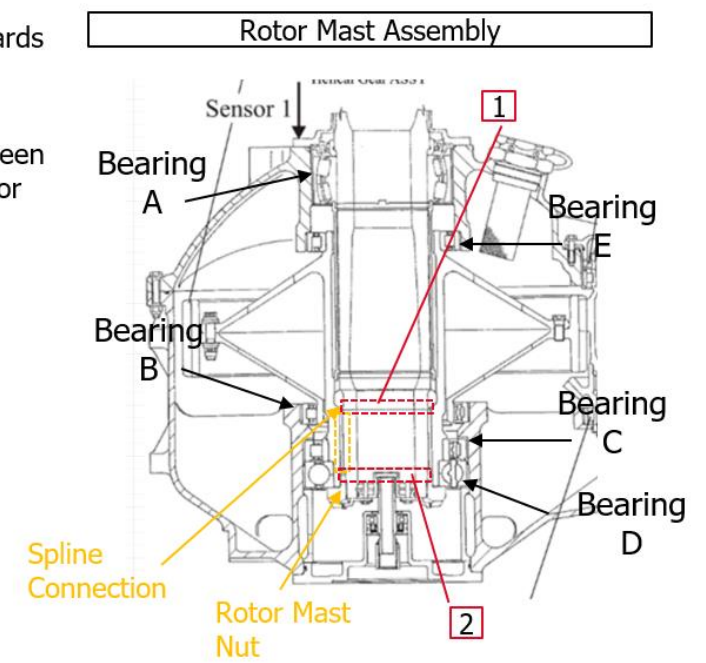


Figure 139: BK117 – Rotor Mast Assembly



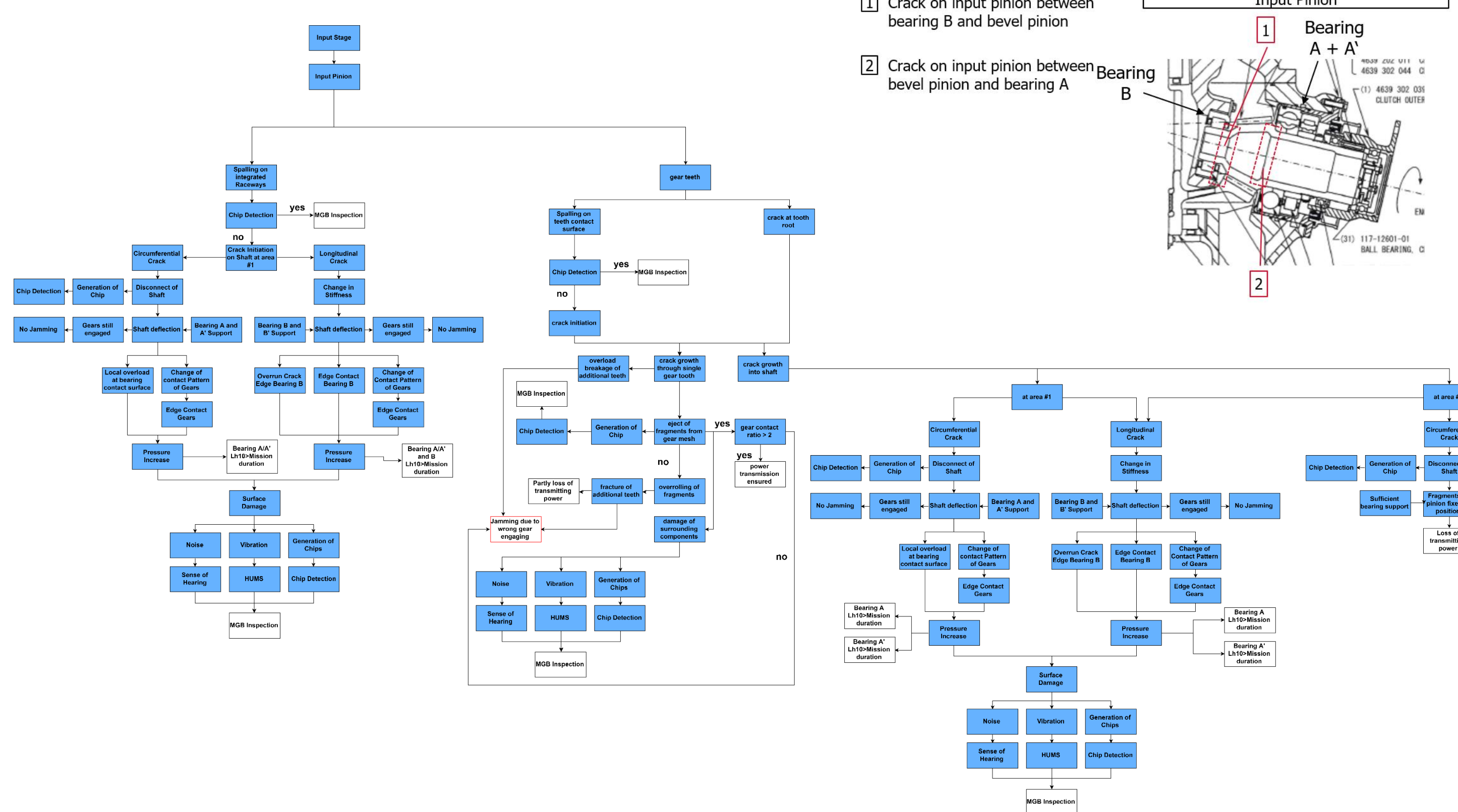


Figure 140: BK117 – Input Pinion

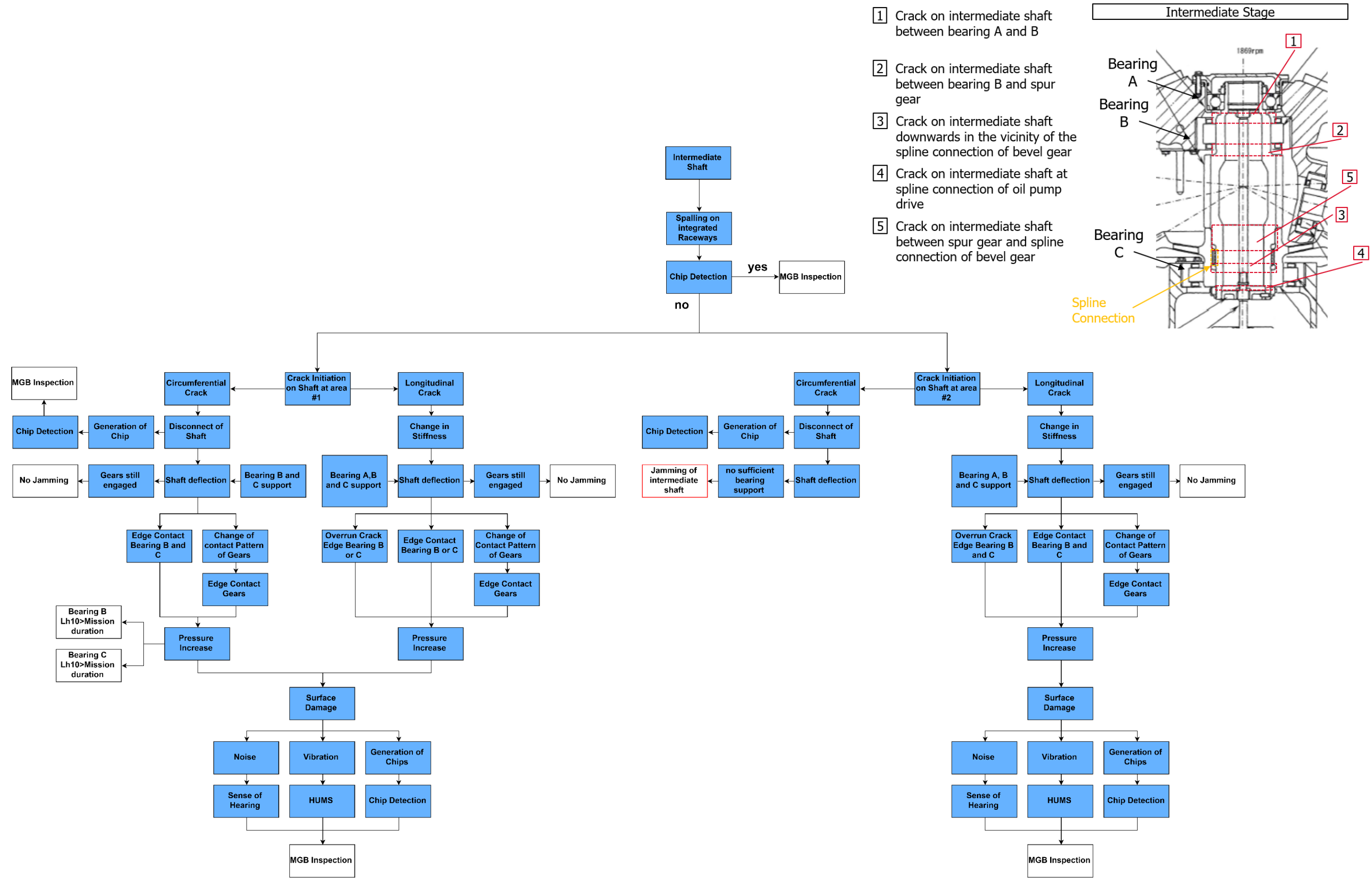
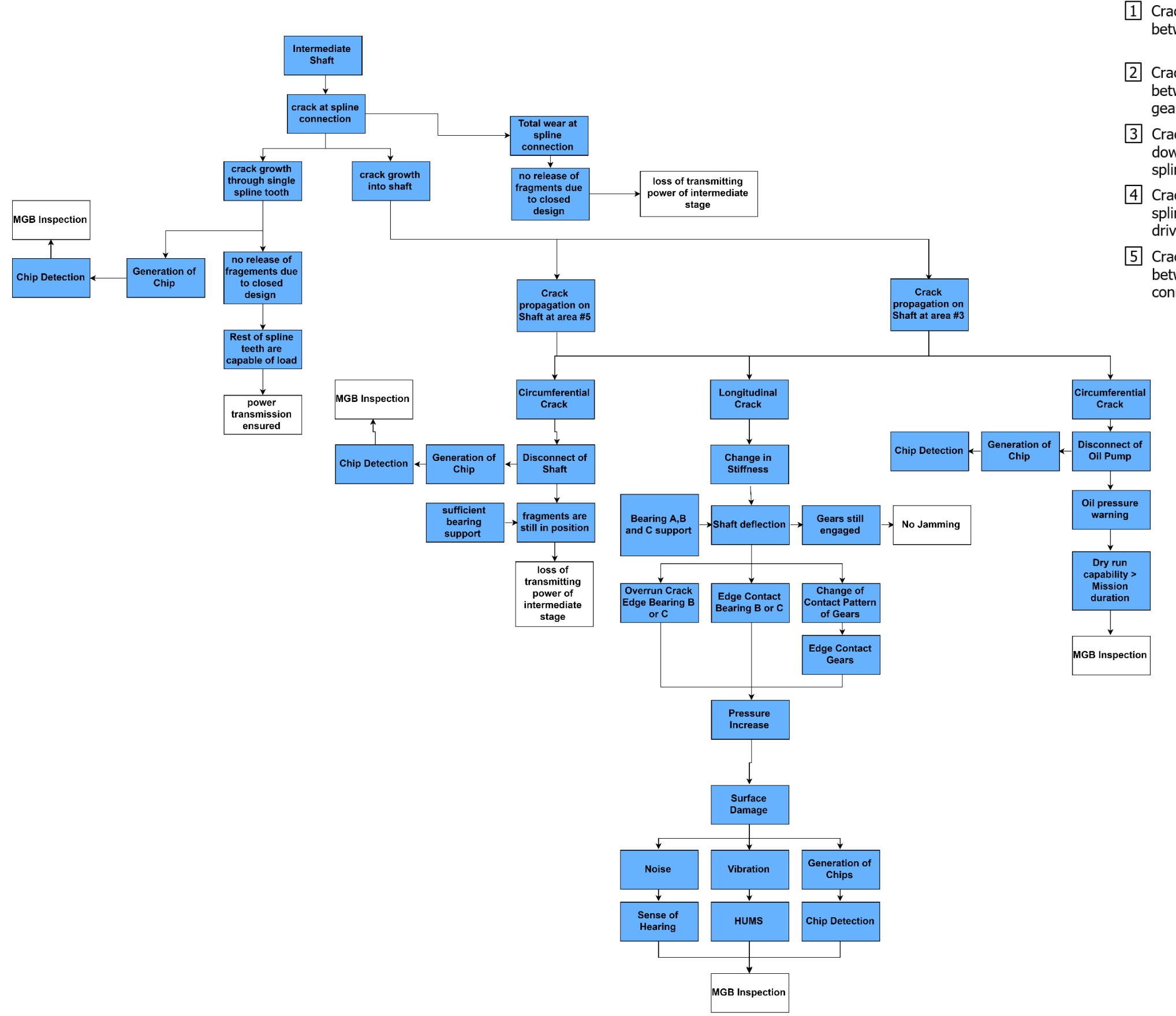


Figure 141: BK117 – Intermediate Shaft



① Crack on intermediate shaft between bearing A and B

② Crack on intermediate shaft between bearing B and spur gear

③ Crack on intermediate shaft downwards in the vicinity of the spline connection of bevel gear

④ Crack on intermediate shaft at spline connection of oil pump drive

⑤ Crack on intermediate shaft between spur gear and spline connection of bevel gear

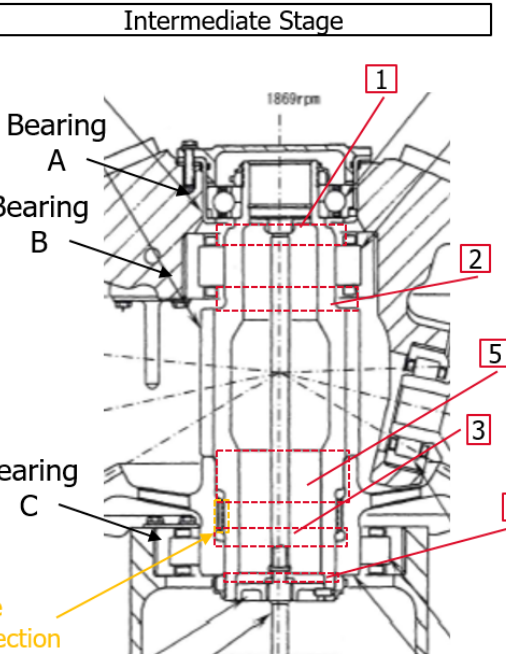


Figure 142: BK117 – Intermediate Shaft

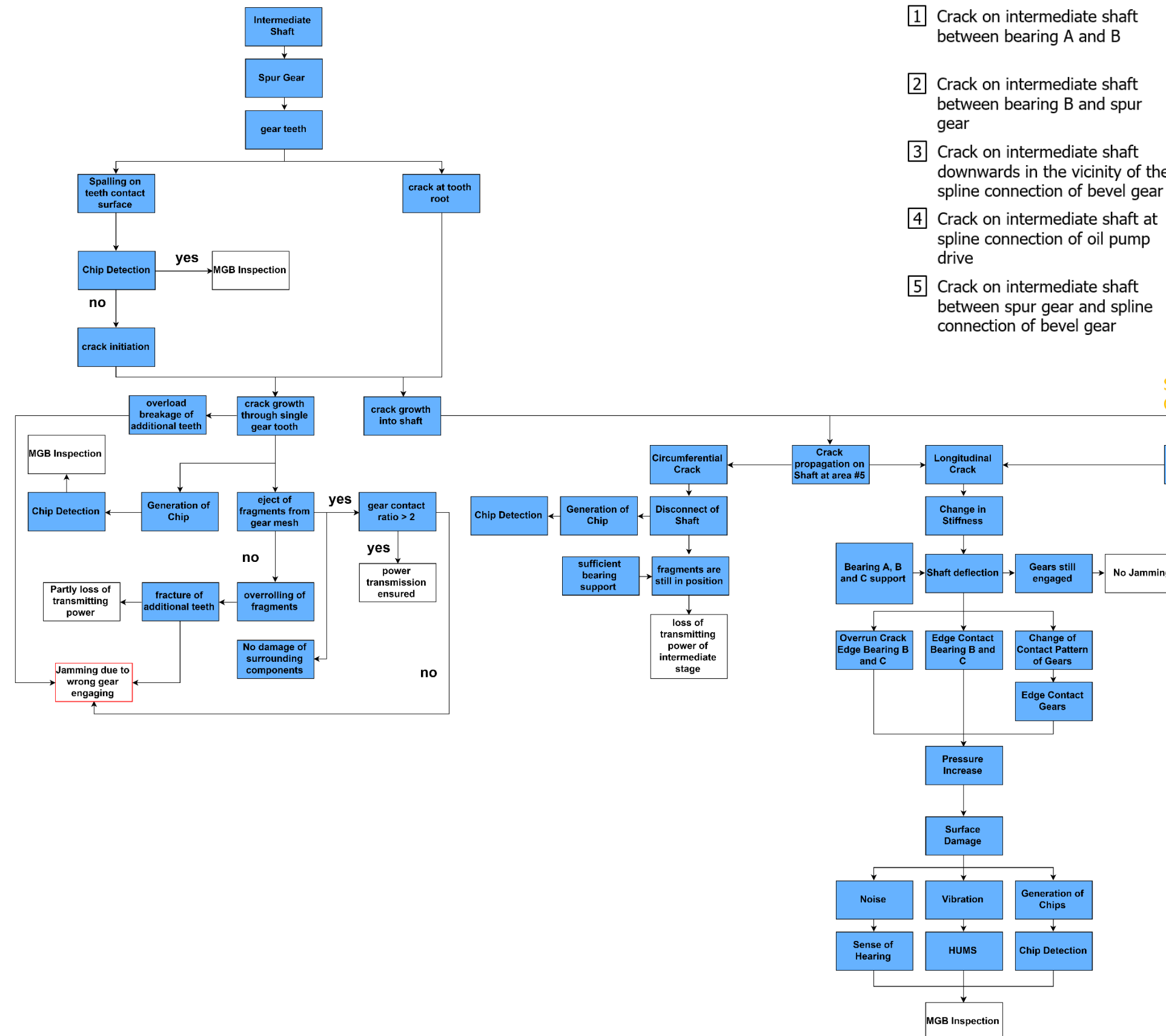


Figure 143: BK117 – Intermediate Shaft

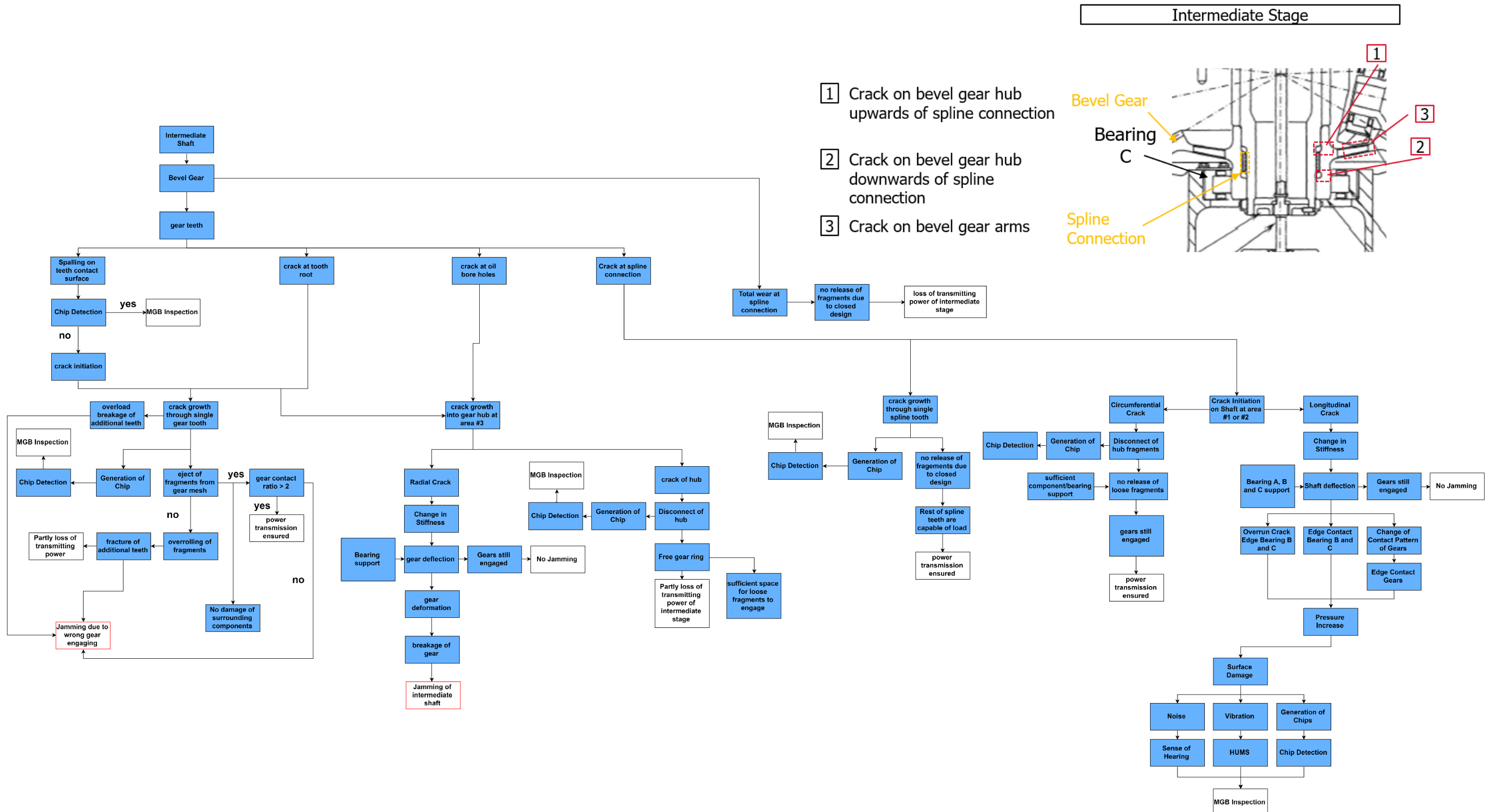


Figure 144: BK117 – Intermediate Shaft

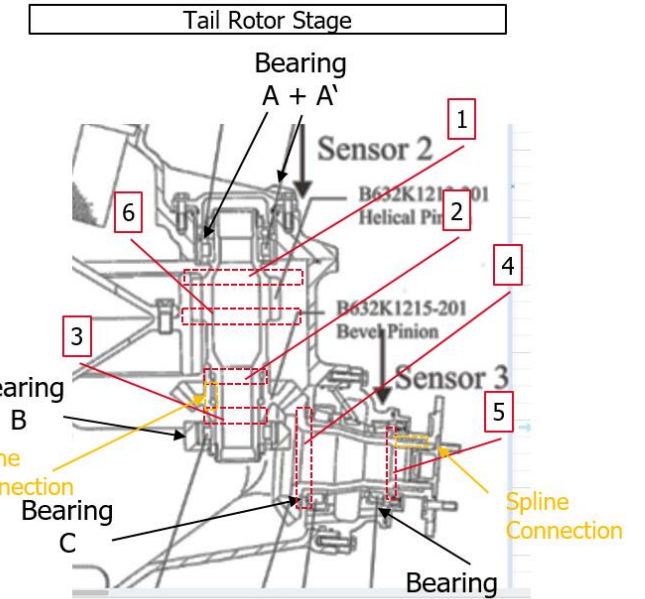
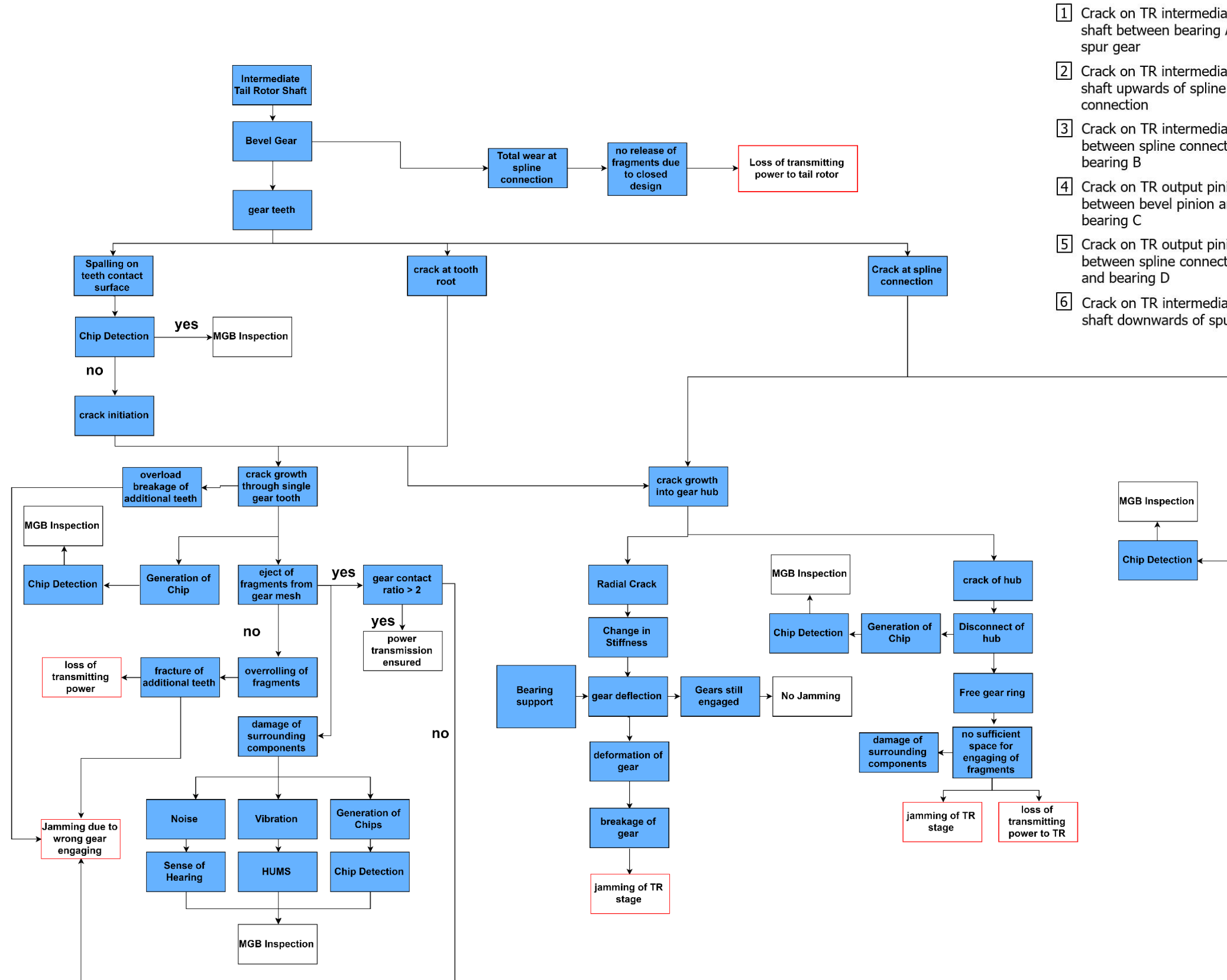


Figure 145: BK117 – Intermediate Tail Rotor Shaft

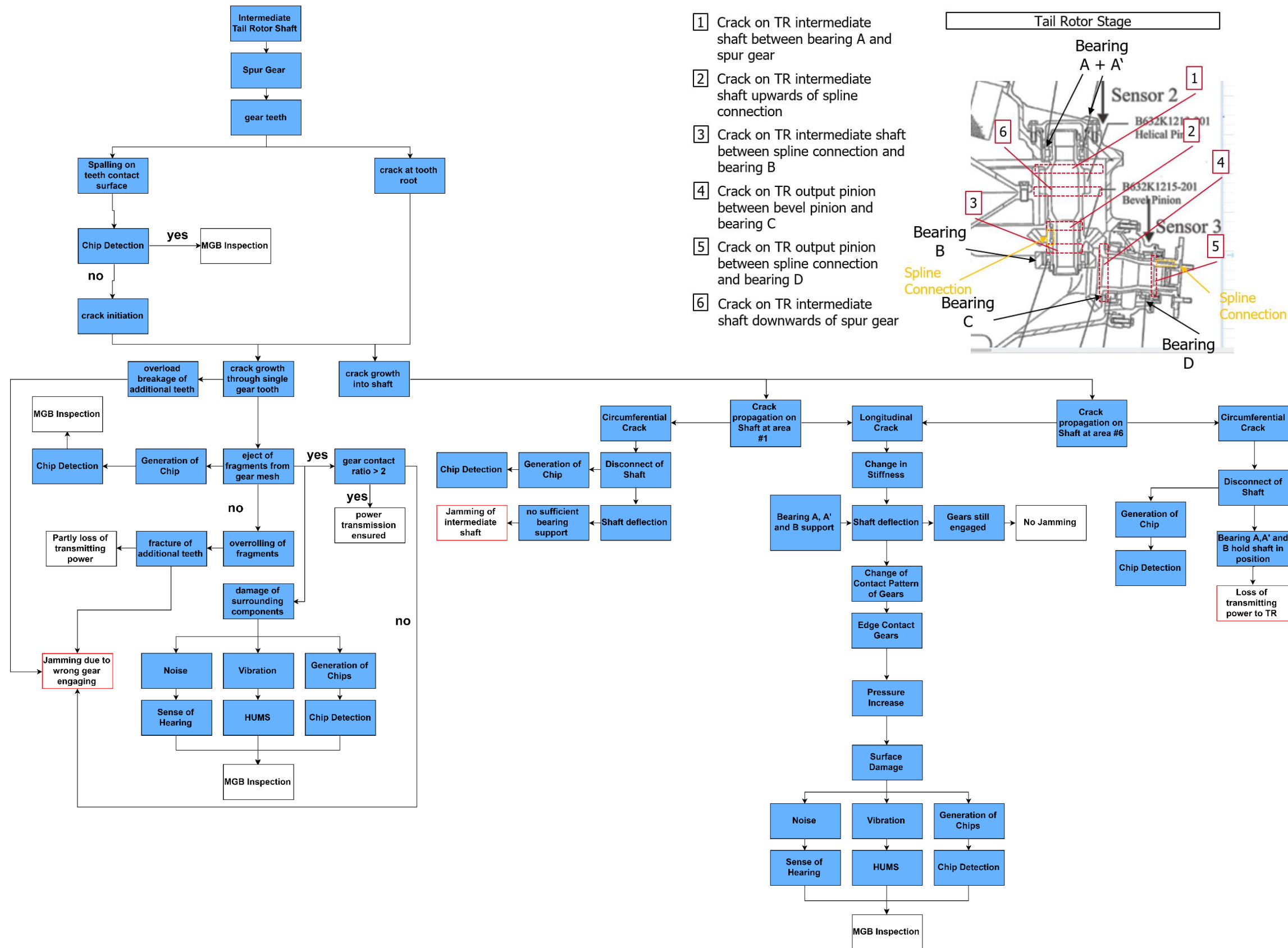
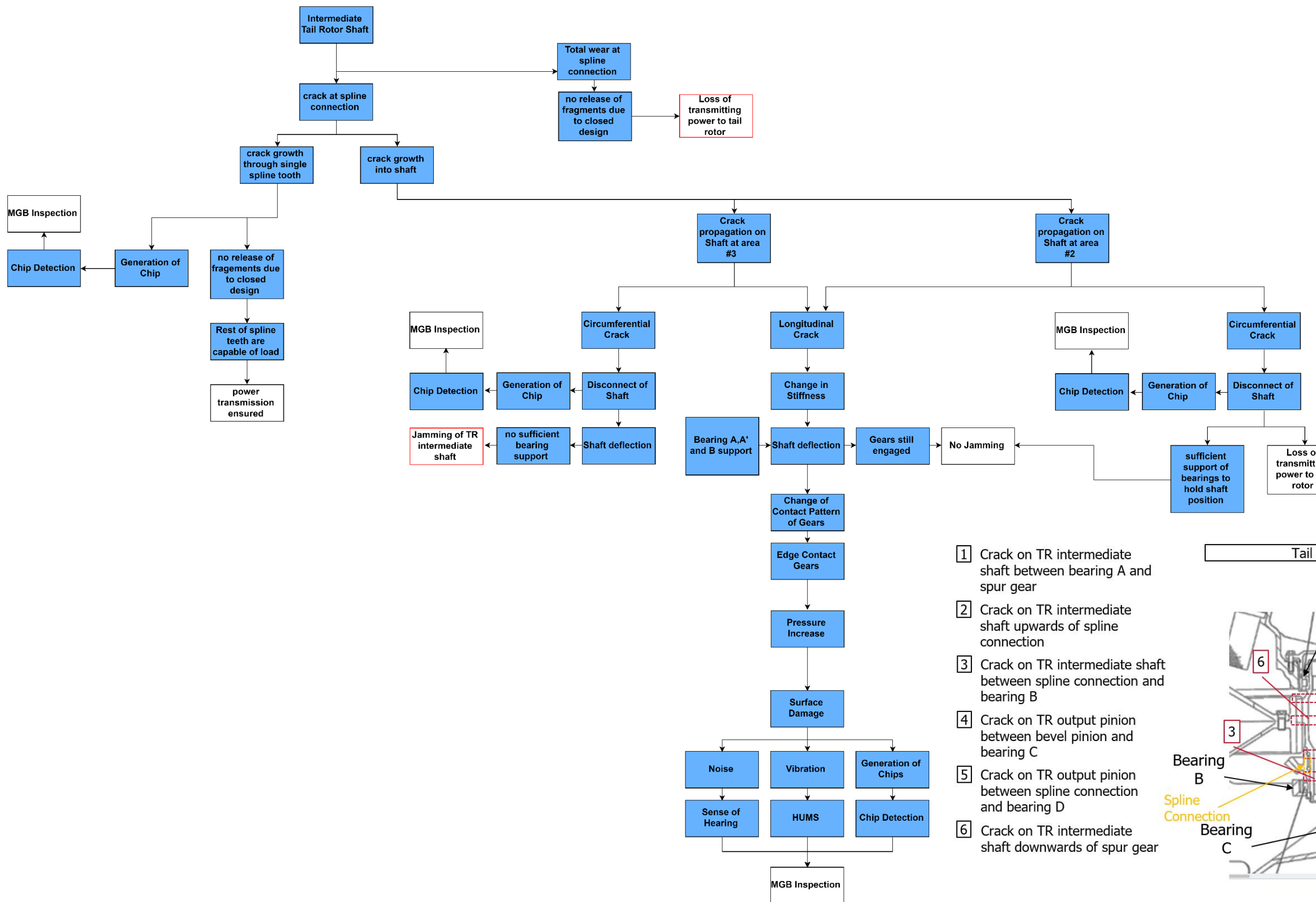


Figure 146: BK117 - Intermediate Tail Rotor Shaft



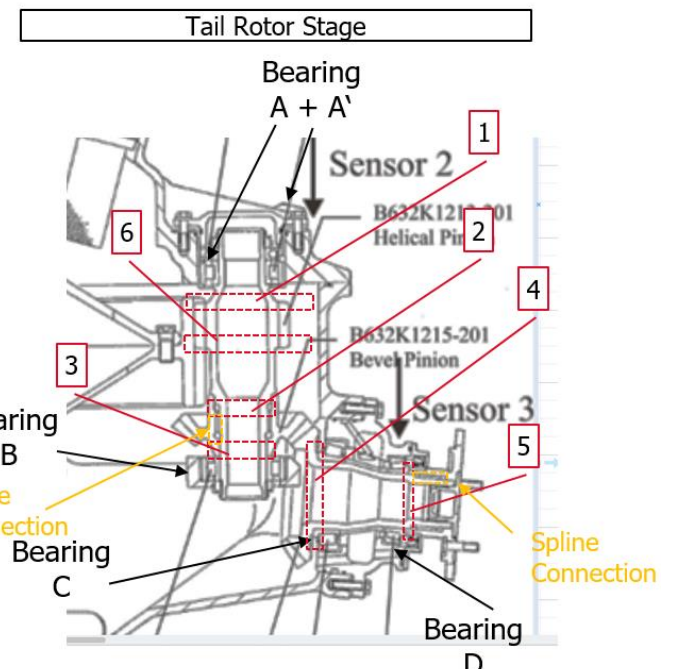
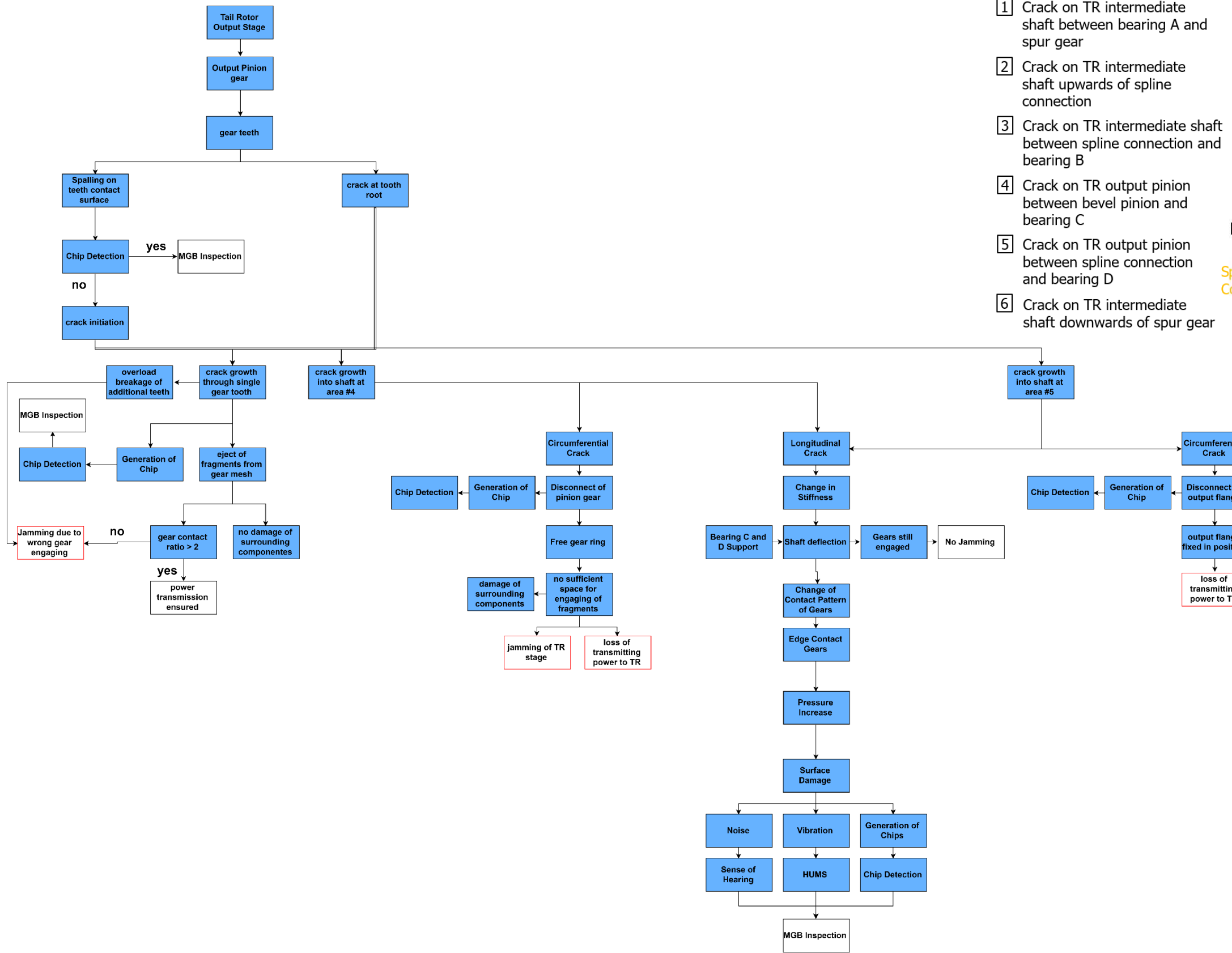


Figure 148: BK117 – Tail Rotor Output Pinion

A.5 Flow diagram of Example 5

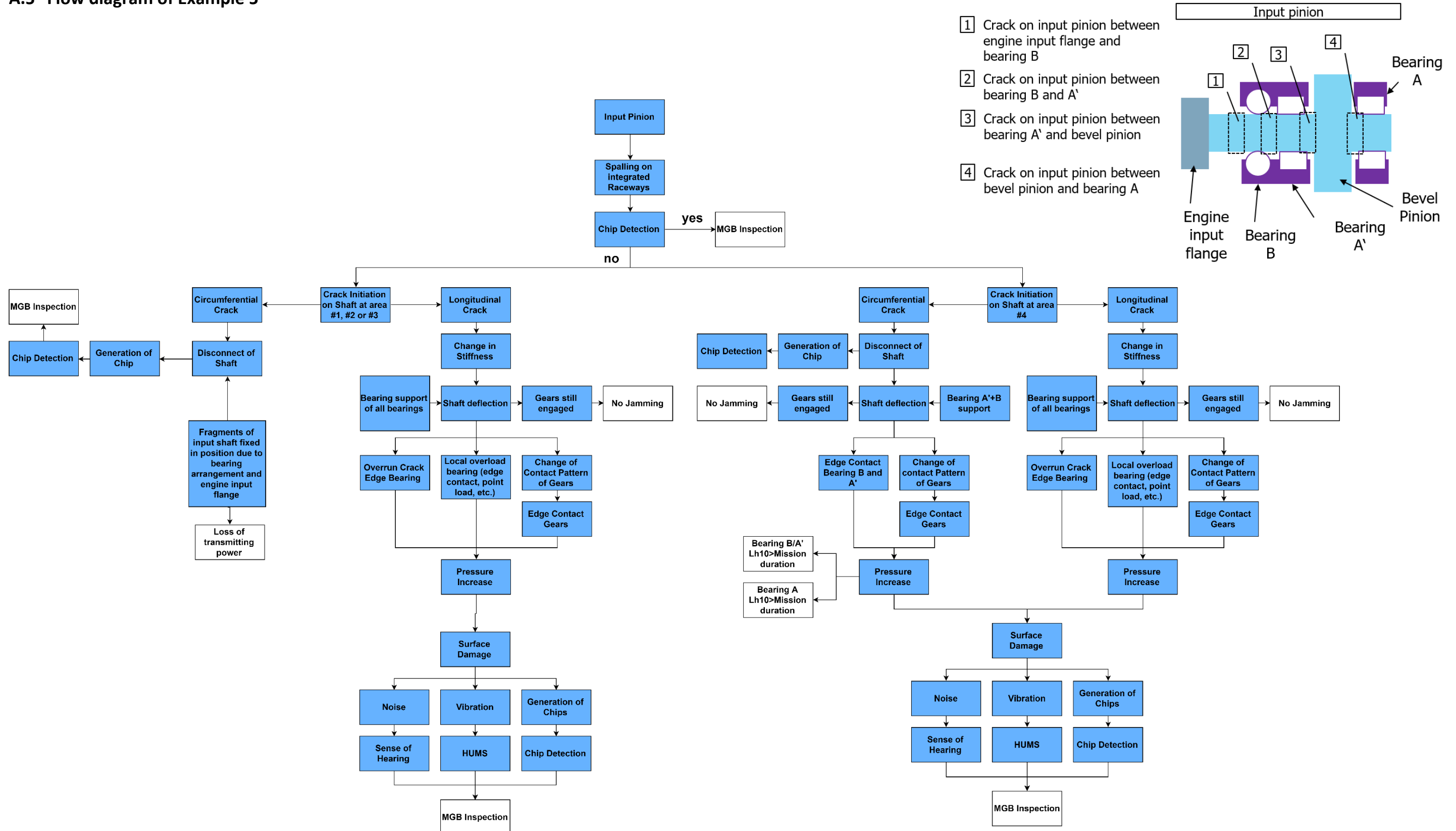
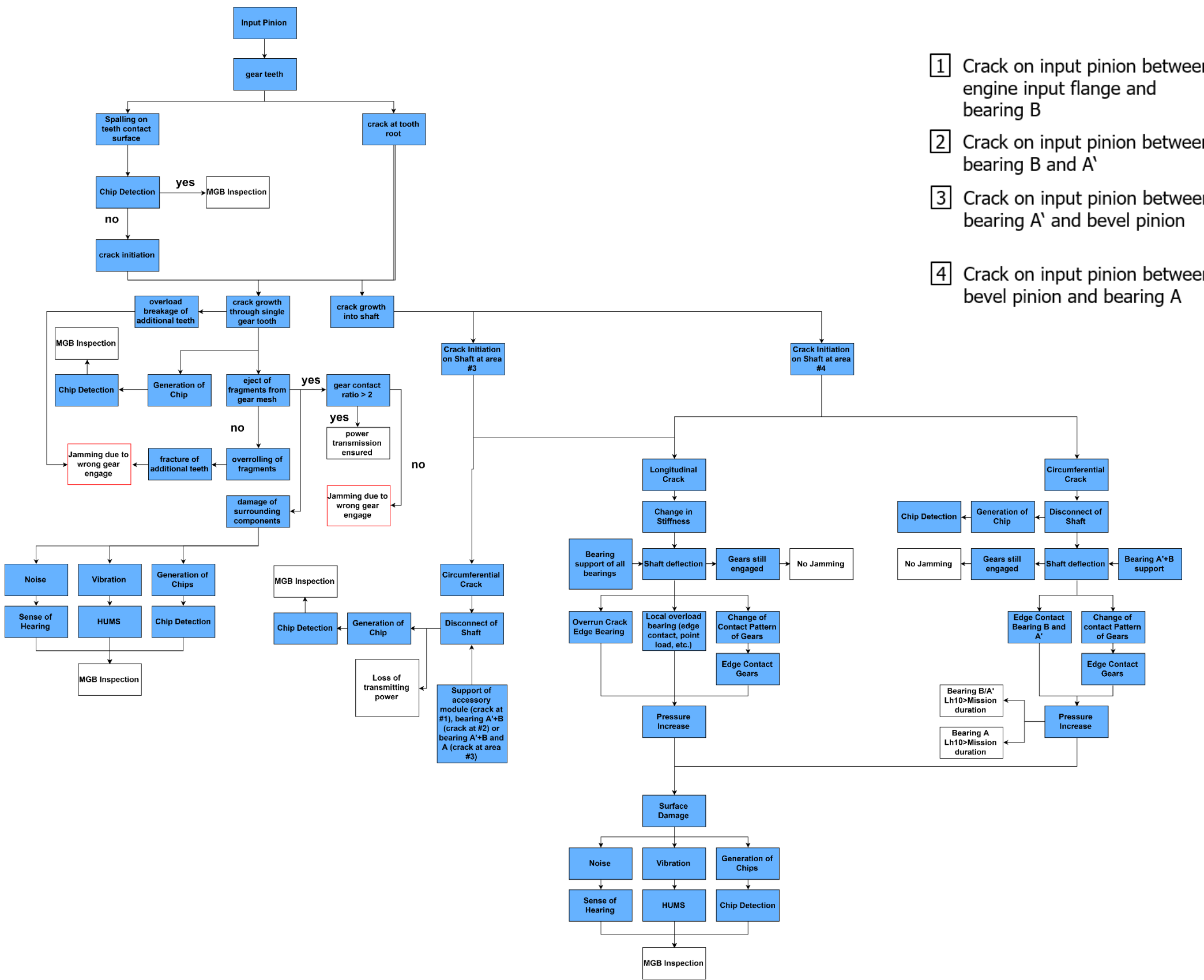


Figure 149: CH53-K – Input Pinion



- [1] Crack on input pinion between engine input flange and bearing B
- [2] Crack on input pinion between bearing B and A'
- [3] Crack on input pinion between bearing A' and bevel pinion
- [4] Crack on input pinion between bevel pinion and bearing A

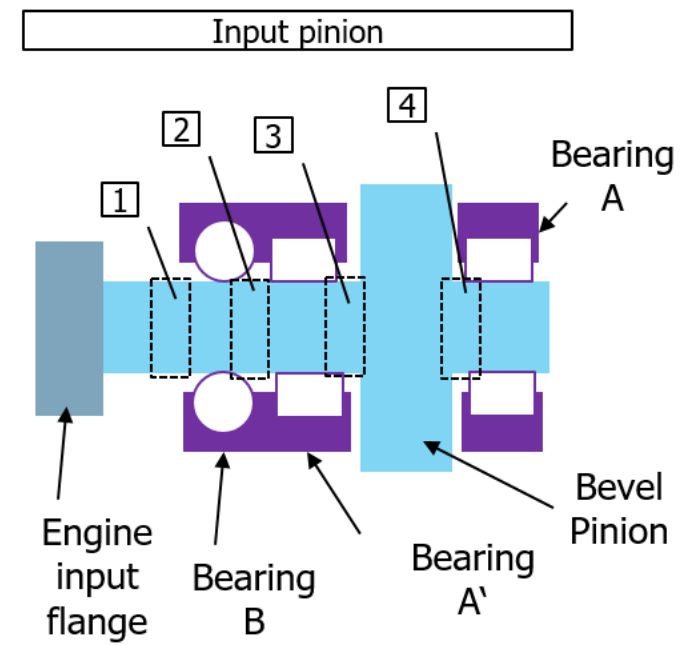
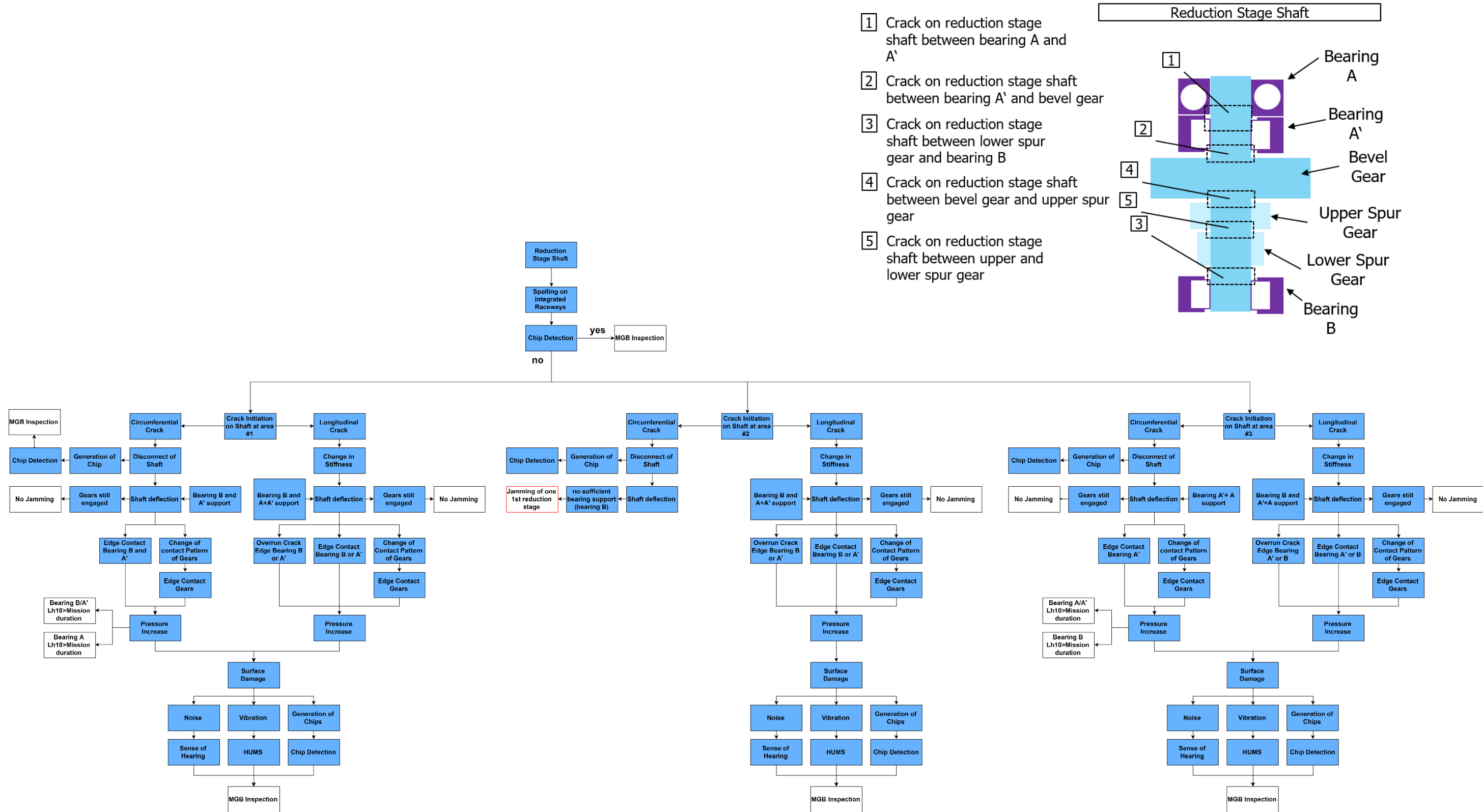


Figure 150: CH53-K – Input Pinion



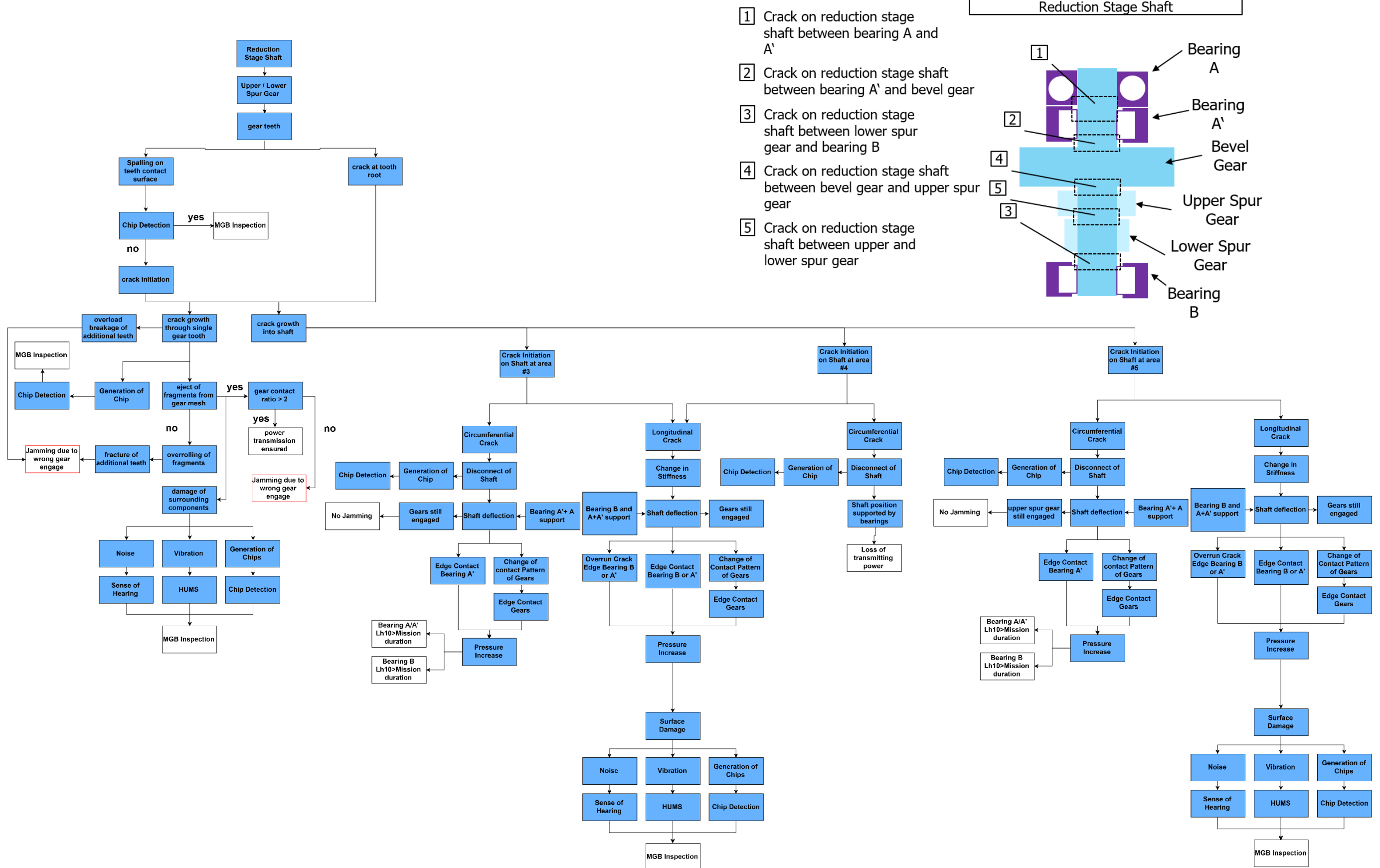


Figure 152: CH53-K – Reduction Stage Shaft

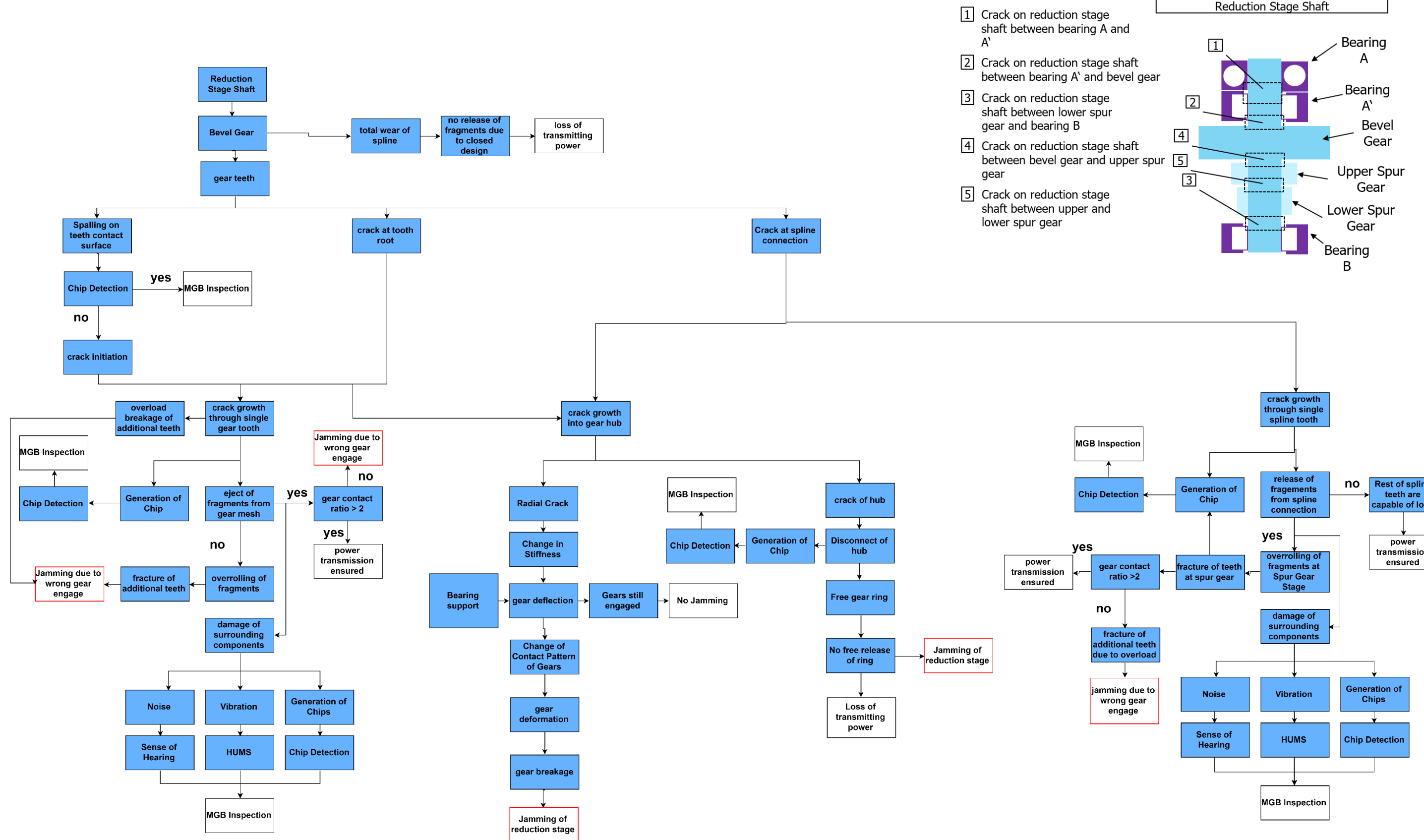


Figure 153: CH53-K – Reduction Stage Shaft

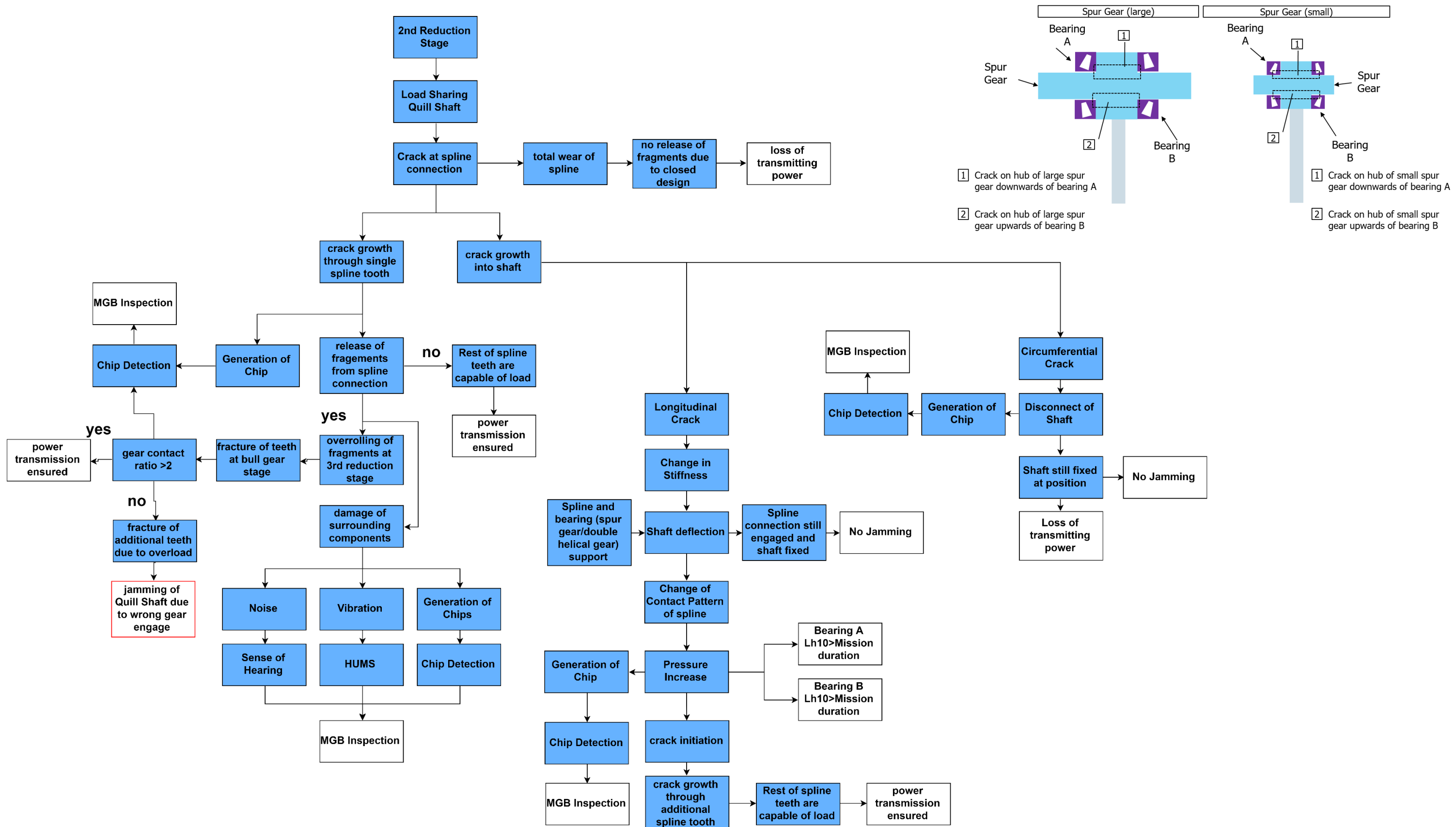


Figure 154: CH53-K – Load Sharing Quill Shaft

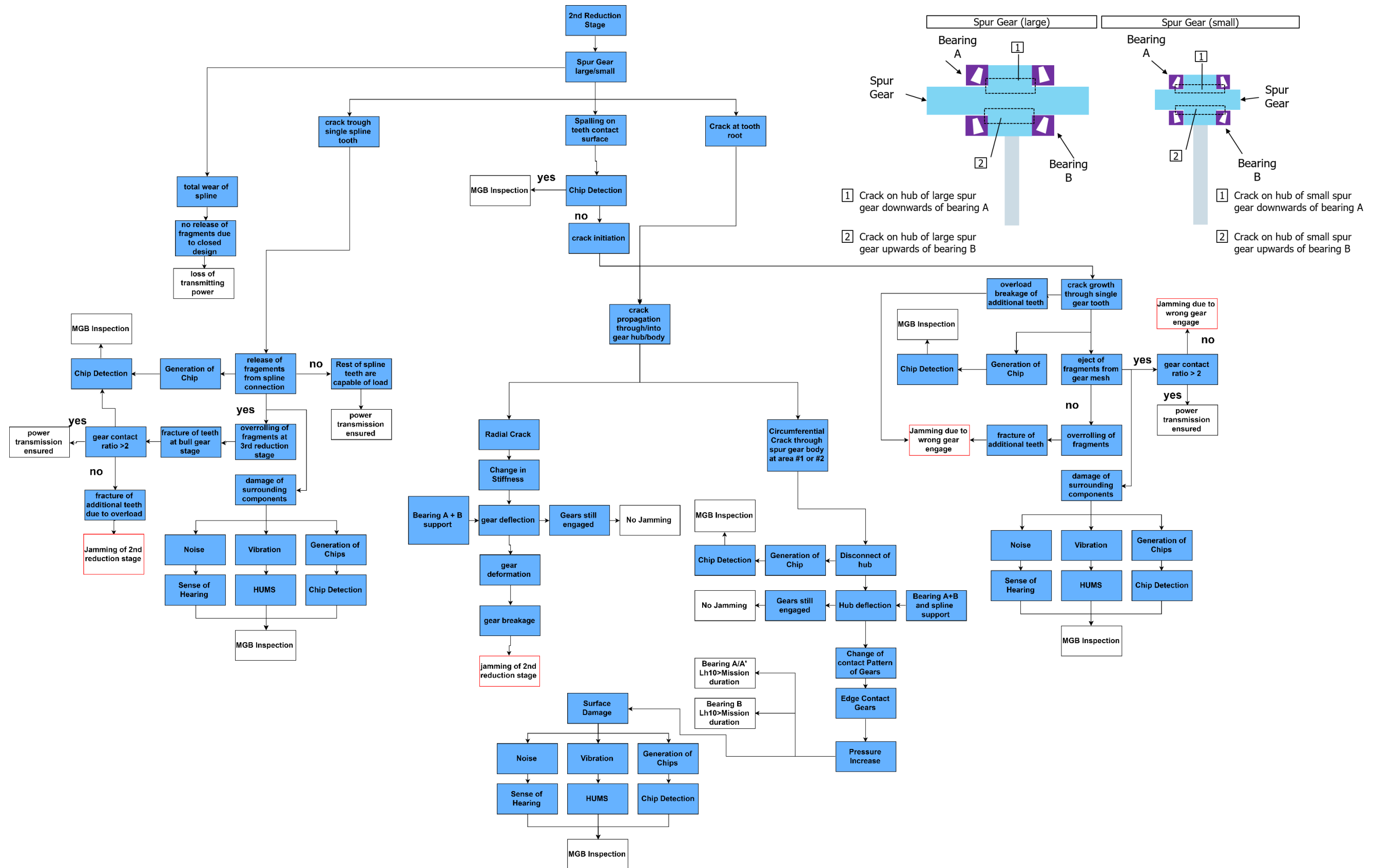


Figure 155: CH53-K – Spur Gear small/large

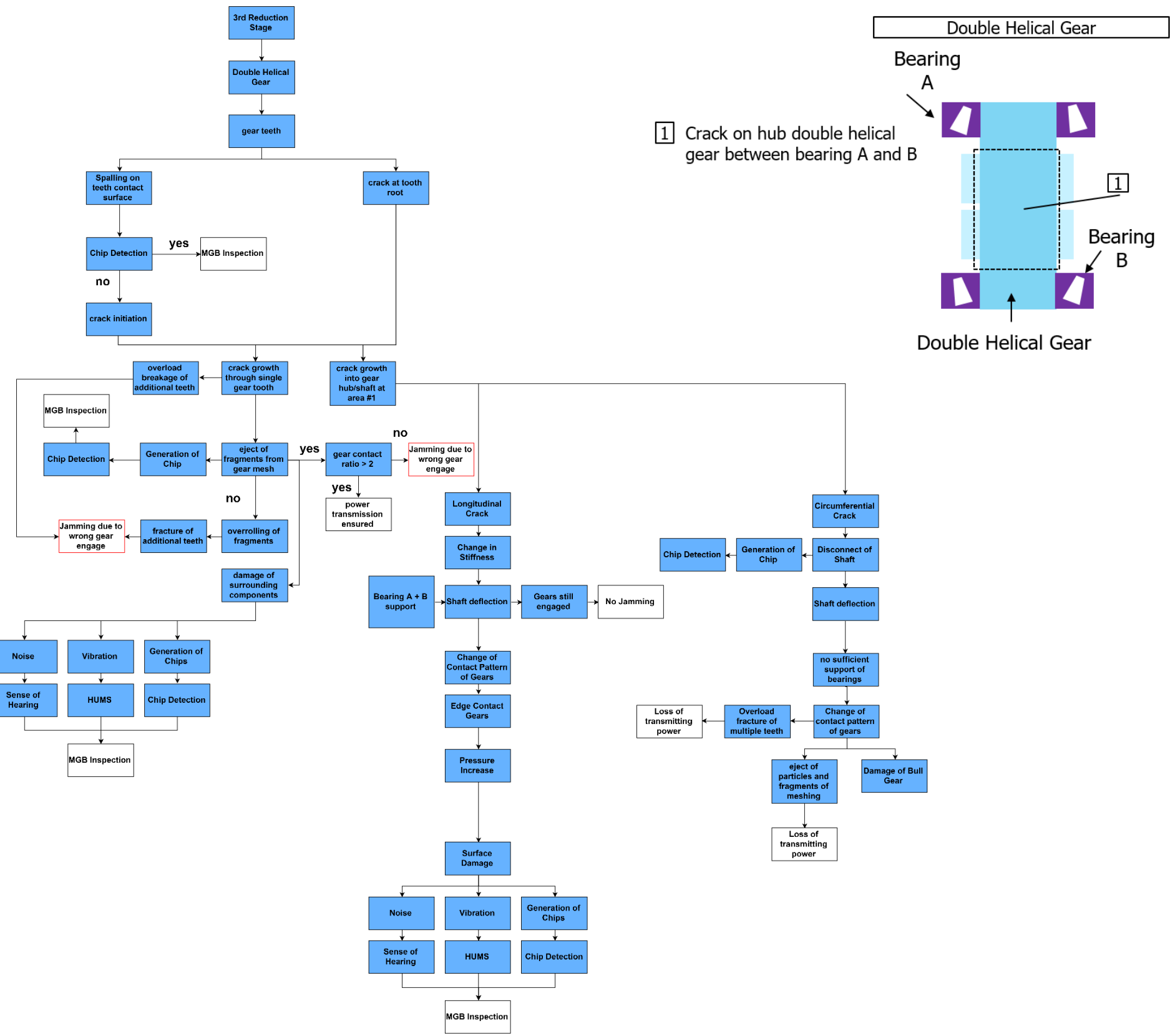


Figure 156: CH53-K – Double Helical Gear

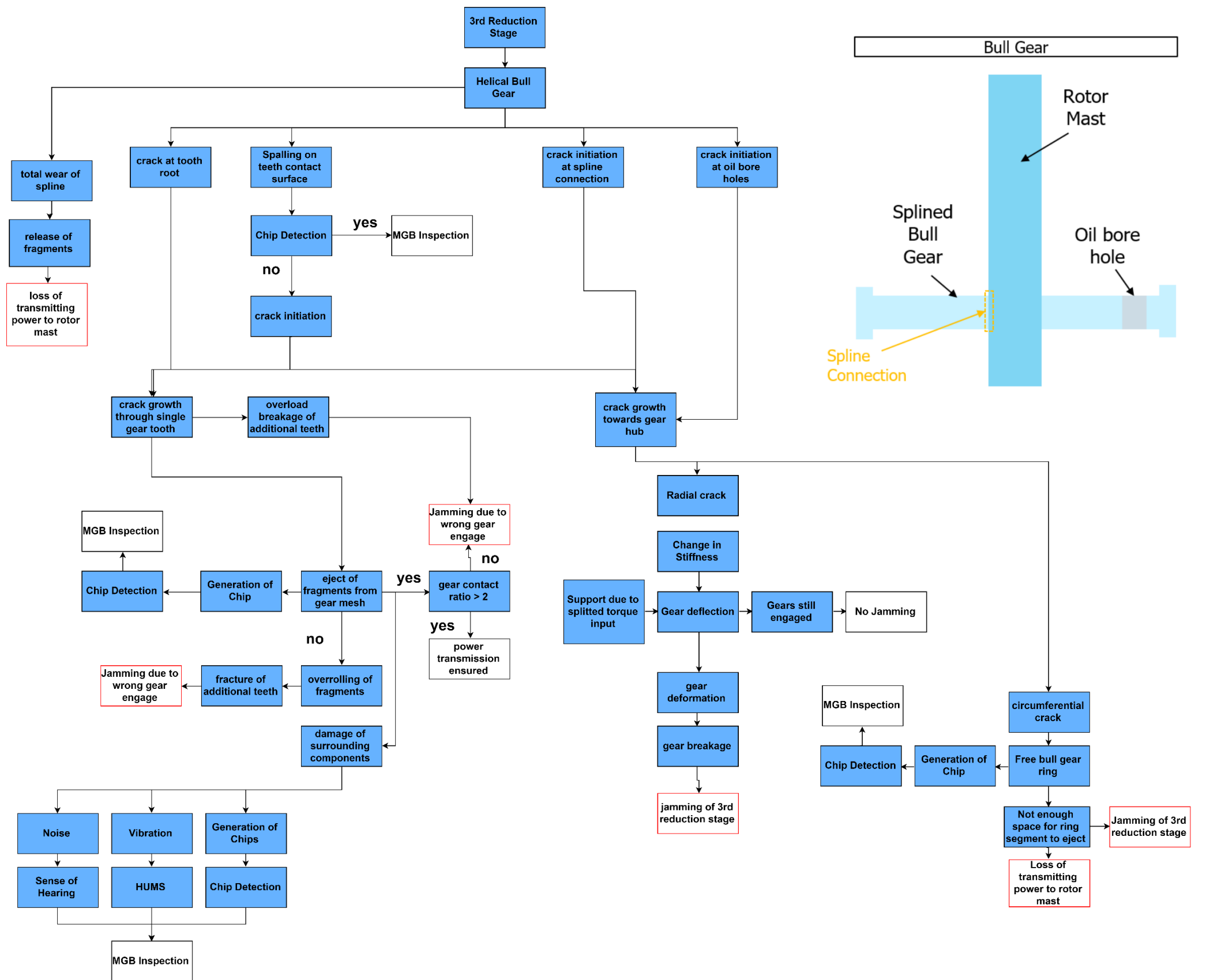


Figure 157: CH53-K – Helical Bull Gear

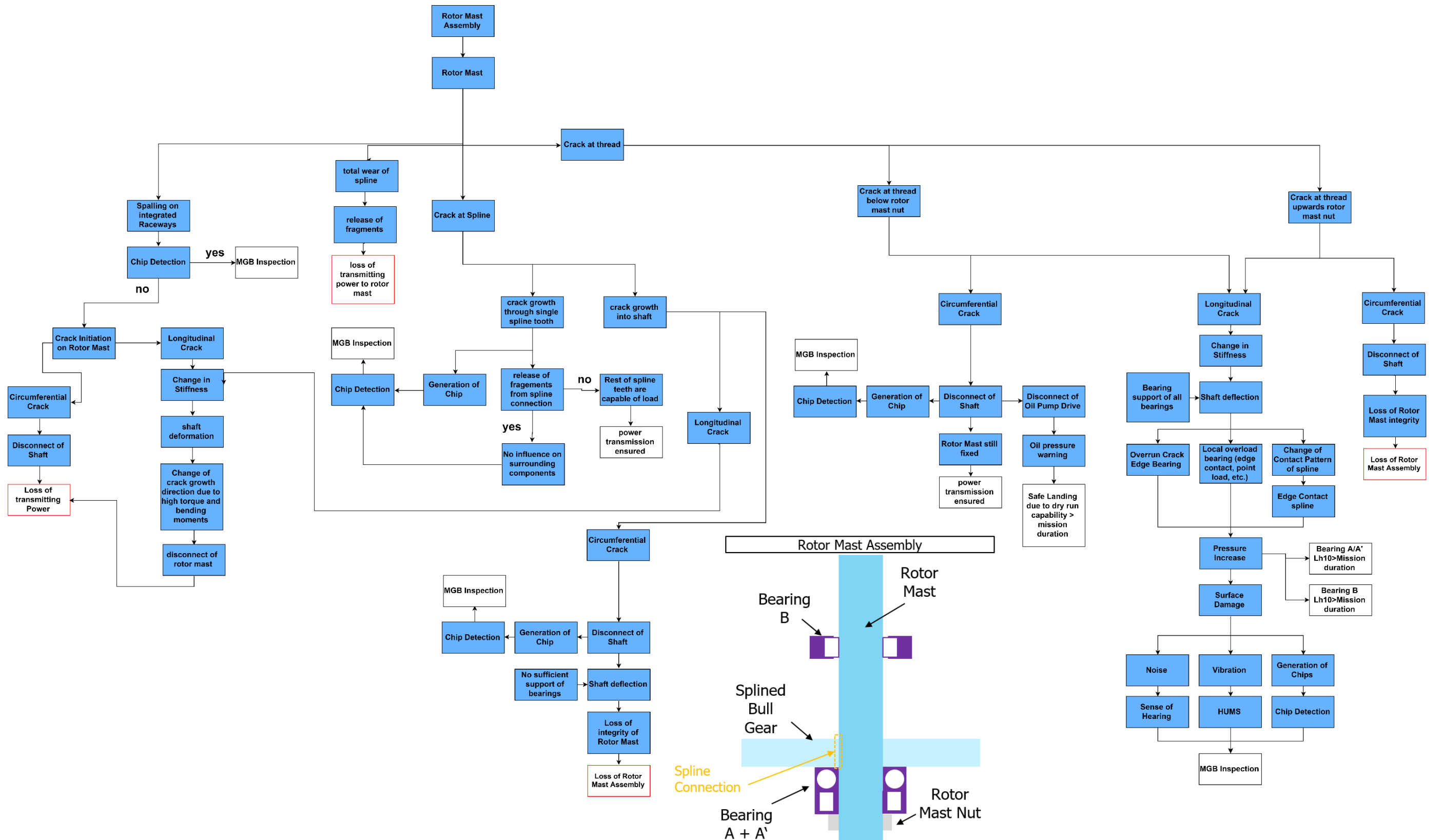


Figure 158: CH53-K – Rotor Mast Assembly



European Union Aviation Safety Agency

European Union Aviation Safety Agency

Konrad-Adenauer-Ufer 3
50668 Cologne
Germany

Project website <https://www.easa.europa.eu/research-projects/integrity-improvement-rotorcraft-main-gear-box-mgb>

Tel. +49 221 89990- 000
Mail research@easa.europa.eu
Web www.easa.europa.eu

An Agency of the European Union

